Development of in vitro dissolution tests for orally inhaled products

Hassoun, Mireille

Awarding institution:
King's College London

Development of *in vitro* dissolution tests for orally inhaled products

Mireille Abdallah Hassoun

Institute of Pharmaceutical Science
Faculty of Life Sciences and Medicine
King's College London

A thesis submitted to the King's College of London
in fulfilment of the requirements for the
degree of Doctor of Philosophy

October 2018

Abstract

Background: Dissolution testing has been proposed as a sensitive and discriminatory *in vitro* test for evaluating the quality or similarity of inhaled pharmaceuticals. This has led to a number of bespoke respirable particle collection and dissolution techniques being developed by academic and industrial pharmaceutical scientists. However, each comes with limitations and there is no standard or universal dissolution system for orally inhaled products. A dissolution test system would ideally reproduce conditions that represent the *in vivo* lung environment and would have the potential to be used for both quality control purposes and as a predictive *in vitro-in vivo* correlation tool. However, test systems proposed to date do not meet these criteria fully, for example many have not utilised media designed to simulate respiratory tract lung fluid (RTLF). Dissolution methodology should fulfil requirements such as simplicity, reproducibility, ease of handling, robustness and be able to discriminate differences between inhaler batch, product and formulation types.

Aim: The aim of this thesis was to develop dissolution methods for OIPs by identifying the critical attributes and shortcomings of current systems and designing and evaluating improved systems using fluticasone propionate (FP) as the model drug.

Methods: Two dissolution systems were evaluated: a Next Generation Impactor/Rotating paddle system and a Twin stage Impinger/Transwell® system. A novel simulated lung fluid (SLF) based on the major components of human RTLF was manufactured and characterised in terms of its physicochemical properties and stability in solution and after freeze-drying. The solubility and dissolution of inhaled drugs, including FP, were evaluated in the SLF and compared to other media. The impact of using SLF as a dissolution media was evaluated in a biorelevant dissolution system, the novel Dissolv*It*® system, and an *in-silico* PBPK model was developed and applied to evaluate the impact of *in vitro* data on drug pharmacokinetics and enable comparison with *in vivo* data. To develop the TSI/Transwell system as a biorelevant system, a Design of Experiments (DOE) approach was used to identify the influence of temperature, stirring and the solubilising capacity of dissolution media on dissolution profiles of FP. Finally, a biorelevant methodology was used to compare the dissolution of nebulised suspension and microemulsion formulations to other inhaled formulations.

Results: Both dissolution systems were simple and easy to handle, producing reproducible data. Although the novel NGI/rotating paddle system was a convenient starting point for quality control purposes, the TSI/Transwell system was more amenable to development as a biorelevant technique as it was able to mimic the low fluid volume of RTLF and could be used with lung fluid simulants that are expensive and only available in limited volume. A SLF of biorelevant composition, consisting of proteins (albumin, transferrin and IgG), lipids (DPPC, DPPG and cholesterol) and antioxidants, was characterised. It was shown to possess physiochemical properties comparable to those of RTLF, such as being an isotonic solution with a physiological pH of 7.2, viscosity of 1.138×10^{-3} Pa s, conductivity of 14.5 mS/m, surface tension of 54.9 mN/m and density of 0.999 g/cm^3.The simulant was stable for 24 and 48 h at 37 and 20°C and for 14 days at 4°C and when freeze-dried. A novel and sensitive solid phase extraction and LC-MS/MS technique for the assay of FP was established and validated successfully to quantify the drug in low concentrations in biological matrices, in picogram concentrations. In the *DissolvIt* system the use of SLF as a dissolution medium did not impact on dissolution profiles compared to the standard polymer solution ($P>0.05$), but DOE using the TSI/Transwell system found solubilising capacity of the medium to be a major factor. Biorelevant conditions assigned as a dissolution medium of 0.1% w/v SDS in PBS (providing the same solubilising capacity as SLF), temperature 37°C and stirring rate 15 rpm. These biorelevant dissolution test conditions indicated that the dissolution of FP from a novel microemulsion formulation reached approximately 70% (almost double) over the 8 h experiment, compared to the dissolution of FP from the Flixotide suspension formulation ($P< 0.05$).

Conclusion: A simulated lung fluid has been developed for use in a dissolution system tailored to orally inhaled products. The dissolution technique is sensitive to temperature, stirring and the solubilising capacity of the dissolution medium and in preliminary tests has shown promise in discriminating between different fluticasone inhaler products and formulations.

Table of Contents

List of Figures

List of Tables

Acknowledgements

First and foremost, I would like to express gratitude to my supervisor, Professor Ben Forbes, for his immense knowledge, guidance, patience and time, without whom, this thesis would not have been possible to complete. I would also like to thank my secondary supervisor, Dr Paul Royall for continuing to encourage and support me throughout my PhD. Similarly, I would like to thank Professor Khuloud Al-Jamal for being a friend and for her general loveliness and care in all matters from the beginning. I would like to acknowledge Dr Norman Smith, Steve Ingham and Dan Asker for trusting me to keep hold of their equipment and for always providing me with the help I've requested.

It would be impossible to name everyone at King's who have supported me throughout the past four years, but I thank them all and I am sure they know who they are! I appreciate their advice, whether it was scientific or personal, and thank them for being there to listen. My friends and colleagues have been awesome and an absolute pleasure to sit beside and work with.

I would also like to thank my sponsors, BBSRC and Intertek Melbourn, for providing me with the opportunity to complete a PhD degree and undergo a short industrial placement there. Also, a thank you to Inhalation Sciences in Sweden for providing me with the opportunity to work in their labs and use their equipment, and for being very approachable and welcoming. I would like to acknowledge Sumit Arora and collaborators at University of Graz in Austria, for their help in the development and application of *in silico* modelling to my data.

Finally, to my amazing family, my mum, my dad and my four sisters who have always had to put up with me, for loving me unconditionally, and supporting me constantly. To you guys, I really cannot thank you enough! A huge thank you to my loving parents in law who have encouraged me immensely and allowed me to use their home as my own throughout the completion of my write-up. A special thank you to my fiancé Haitham Hajj Shehade who stood by me throughout this entire academic journey, kept me company, was my shoulder to cry on or to laugh with, who made my studying bearable and for always checking on me, motivating me and keeping me smiling. I truly love you and value going through this period with you by my side.

Abbreviations

A1AT	Alpha 1-antitrypsin
ACI	Anderson Cascade Impactor
ADME	Absorption, Distribution, Metabolism and Excretion
API	Active Pharmaceutical Ingredient
APSD	Aerodynamic particle size distribution
BCS	Biopharmaceutics Classification system
CMC	Critical Micellar Concentration
COPD	Chronic Obstructive Pulmonary Disease
Cryo-TEM	Cryogenic Transmission Electron Microscopy
DLS	Dynamic Light Scattering
Dmix	Drug mix
DOE	Design of Experiment
DPI	Dry Powder Inhaler
DPPC	1,2-dipalmitoyl-sn-glycero-3-phosphocholine
DPPG	1,2-dipalmitoyl-sn-glycero-3-phosphorylglycerol sodium
Dv90	Volume diameter of 90% of aerosol droplets
Dv50	Volume diameter of 50% of aerosol droplets
Dv10	Volume diameter of 10% of aerosol droplets
FaSSIF	Fasted State Simulated Intestinal Fluid
FBS	Fetal Bovine Serum
FeSSIF	Fed State Simulated Intestinal Fluid
FP	Fluticasone Propionate
FPF	Fine Particle Fraction
GSD	Geometric Standard Deviation
HBSS	Hanks' Balanced Salt Solution
IgA	Immunoglobulin A
IgG	Immunoglobulin G

IPL	Isolated Perfused Lung
IS	Internal Standard
IVIVC	In vitro – In vivo correlation
LC-MS/MS	Liquid Chromatography with tandem Mass Spectrometric detection
ME	Microemulsion
MeOH	Methanol
MMAD	Mass Median Aerodynamic Diameter
MTT	(3-(4,5-Dimethylthiazol-2-yl)-2,5-Diphenyltetrazolium Bromide)
NGI	Next Generation Impactor
OIPs	Orally Inhaled Products
PBPK	Physiologically based pharmacokinetic modelling
PBS	Phosphate Buffered Saline
PDI	Polydispersity Index
PEO	Polyethylene Oxide
pMDI	Pressurised Metered Dose Inhaler
QC	Quality Control
R&D	Research and Development
RP-HPLC-UV	Reverse phase - High Performance Liquid Chromatography-Ultraviolet Spectroscopy
RTLF	Respiratory Tract Lining Fluid
SDS	Sodium Dodecyl Sulphate Lauryl
SLF	Simulated Lung Lining Fluid
Smix	Surfactant mix
SPE	Solid Phase Extraction
TGA	Thermogravimetric Analysis
TLC	Thin Layer Chromatography
TSI	Twin Stage Impinger
V_{LF}	Volume of lung fluid

Chapter 1

Introduction

Unlike most solid or semi-solid pharmaceutical dosage forms, the particles that form the drug delivery units of inhaled aerosol medicines have not historically been investigated for drug release, i.e. dissolution. However, evidence is emerging that dissolution may be a determining factor in the pharmacokinetics of some inhaled drugs and should be considered as a critical product attribute of inhaled medicines (Hastedt *et al*., 2016). An impediment to determining how and to what extent dissolution influences pulmonary and systemic exposure to inhaled drugs is a lack of validated, robust dissolution methods for quantitative investigation. This shortcoming raises the research questions that provide the basis for the research describer in this thesis:

- how do different dissolution methods compare?
- what factors influence *in vitro* dissolution data and do these interact?
- are *in vitro* methods fit for purpose or can they be improved?
- how can dissolution data be interpreted in terms of *in vivo* pharmacokinetics?
- is dissolution indicative of inhaled product quality or equivalence?

For a dissolution test for an inhaled product, it is important to consider both dose collection and dissolution techniques currently available when evaluating the challenges associated with developing such a test or system. An understanding on how to interpret the results obtained *in vitro,* and their implications is also very important which can be informed by the modelling approaches undertaken to estimate impacts on pharmacokinetics. To provide essential context to the topic and challenges described above, this introductory chapter discusses the anatomy of the lungs, dissolution mechanisms, considerations associated with developing a dissolution test for orally inhaled products, the techniques currently available and the methodologies and modelling approaches used to interpret data.

1.1 Anatomy of the lung and deposition of particles

1.1.1 Anatomy of the lung

The respiratory tract is a huge complex network of branches, predominantly divided into two main regions, the upper airway and the lower airway (Petersson and Glenny, 2014). The upper airway consists of the nose, mouth, pharynx and larynx and acts as an air transport system and the lower airway consists of the tracheobronchial, the gas-conducting airways and the gas exchanging acini. The lower airway is further subdivided into three zones: the respiratory, conducting and transitional zones. The respiratory zone mainly comprises of respiratory bronchioles and alveoli (Yu and Chien, 1997; Petersson and Glenny, 2014). The bronchial tree trunk that constitutes the lower airways, begins with the trachea that divides into the left and right primary bronchi then each bronchus divides into further smaller secondary bronchi. The secondary bronchi continue to branch into many tertiary bronchi that then continue to multiply divide, giving rise to many tiny bronchioles. It finally forms terminal bronchioles and respiratory bronchioles. The respiratory bronchioles sub-divides into alveolar ducts that end in clusters of small thin-walled air sacs known as alveoli (Thompson, 2004). A schematic on the structure of the lung and processes the inhaled drug is exposed to, is shown in Figure 1.1.

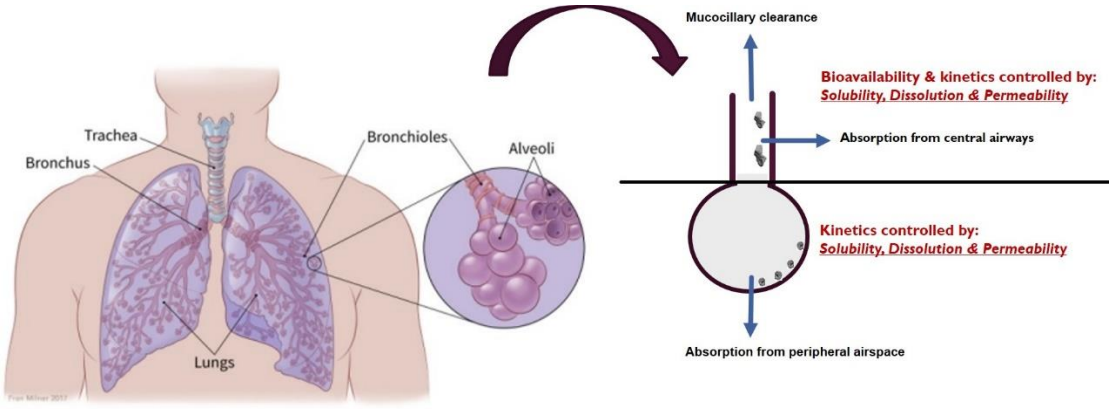

Figure 1. 1. A schematic diagram of the anatomy of the lung and the processes that occur to a drug particle once it lands in the lungs. Adapted from Hastedt et al (Hastedt *et al.*, 2016).

The alveolus provides the huge surface area exhibited by the lungs, giving a total human lung area of approximately 140 m^2. This causes it to become the principal site of gas exchange between the air and the blood, in the airways (Thompson, 2004). There are about 100 million alveoli found in each lung (Thompson, 2004) and the gases taken up by inhalation need to cross the alveolar epithelium, the capillary endothelium as well as their basement membranes to reach the blood, making the distance the air needs to travel up to around 500 nm in length (Thompson, 2004). As the air travels from the trachea to the alveolar sacs, two physical changes occur in the lungs, to allow for adequate penetration of air to the lower airways. These are, the airway diameter such as the tracheal diameter decreases with the respiratory branches and the high surface area of the airways increases.

The human lung also consists of five lobules and ten broncho-pulmonary segment (Crapo *et al.*, 1982). The luminal face of the airways in lined with ciliated cells, which are the most common cell types and these cells have mucus cells intermingles among them. The mucus cells secrete a layer of mucus, coating the walls of the conducting airways with an adhesive, viscoelastic layer with a thickness of 5-55 µm (Lai *et al.*, 2009). The mucus contains antibacterial proteins, peptides and lysozymes that inhibit microbial colonization of the airways and has several roles such as promoting the saturation of inhaled air and protecting the lungs from inhaled chemicals. The clearance of mucus from the lungs is driven by the motion of the ciliated cells, termed the 'mucociliary escalator', which generates a mucus flow rate of approximately 5 mm/min (Lai *et al.*, 2009). The main role of the mucociliary escalator is to serve as an important protective mechanism for removing small inhaled particles from the lungs.

The alveolar epithelium is predominantly composed of Type I and Type II alveolar cells. The Type I cells are thin pneumocyte cells that cover most of the surface of the alveoli, approximately 95% of the surface area. The Type II cells are cuboidal secretory pneumocyte cells, which are interspersed amount the Type I cells (Thompson, 1996). The alveolar space is coated with a complex surfactant lining that reduces the surface tension to minimise the work of breathing and to prevent the collapse of the alveoli during

expiration (D'Angelis, 2011). The surface activity of the surfactant is mainly provided by the phospholipids and surfactant proteins B and C.

1.1.2 Deposition and fate of an inhaled particle

Particles deposit in the respiratory tract via five mechanisms: impaction, sedimentation, Brownian motion, interception and electrostatic precipitation. The most crucial variable that dictates where the particles deposit, is the mass median aerodynamic diameter (MMAD) of the particle. It is important to note that the lung has a relative humidity of approximately 99.5% RH and the addition and removal of water can significantly affect the particle size of a hygroscopic aerosol and thus its deposition (Labiris and Dolovich, 2003). Small drug particles are known to be hygroscopic and a hygroscopic aerosol that is delivered at relatively low temperature and humidity into the high humidity exhibited by the lungs, would be expected to increase in size when inhaled into the lungs. This increase in size above its initial size further affects the deposition and distribution of particles within the lungs (Labiris and Dolovich, 2003).

Impaction is the inertial deposition of a particle onto an airway surface and the progressive branching and narrowing of the airways encourage impaction of the particles. It occurs at bifurcation of airway where flow velocities are at their highest and sudden change in direction of flow takes place, generating considerable inertial forces. The large particles with a MMAD of more than 5 µm experience the impaction forces in the oropharynx and the large conducting airways, due to their high momentum. The particle's momentum is also influenced by the speed and mass of the particle and hence, this impaction-based deposition is increased by higher velocity, high rate of breathing, and particle > 5 µm size and high density (Vaughan and Vaughan, 1969). The inspiratory and expiratory air flow rate in normal healthy lung range from 4.3 to 32.7 mL/s, depending on the pressure and region of the lung (Sul *et al.*, 2014). Sedimentation or gravitational sedimentation is an important mechanism for deposition of particles over 0.5 µm and below 5 µm in size in the small conducting airways, where the air velocity is low i.e. in the deeper airways and bronchioles. Deposition due to gravity is increased by large

particle size and by longer residence times and decreases with increasing breathing rate (Vaughan and Vaughan, 1969).

For particles with MMAD < 0.5 μm, the impact of the surrounding air causes a random motion in them, termed the 'Brownian motion'. This causes particles to deposit by diffusion in the small airways and alveoli, where air flow is low in contrast to the upper respiratory airways. However, most of these small particles remain suspended in air and are exhaled during normal breathing. The interception mechanism of deposition is usually significant for fibres and aggregates. In terms of electrostatic precipitation, some freshly generated particles can be electrically charged during the mechanical generation of aerosols and hence may exhibit enhanced deposition due to charge-induced deposition, though this is a low contribution in comparison to other mechanisms (Martonen and Katz, 1993).

The deposition of aerosol particles in the respiratory tract also depends on density, hygroscopicity, and the shape of the aerosolised particle. Deposition can also be affected by the patient's inhalation parameters such as flow rate, ventilation volume, end-inspiratory breath holding, and the aerosol delivery system. Therefore, the deposition pattern can be expressed as a function of these three key classes of variables: the respiratory tract morphologies, the aerosol characteristics such as particle size, shape and density as well as the ventilatory parameters. Hence, the efficiencies of the different deposition mechanisms of inertial impaction, sedimentation and diffusion can, in turn, be formulated in terms of these variables. Table 1.1 summarises the deposition of the inhaled particles in the lungs.

Table 1. 1. Deposition fate of inhaled particles in the lungs.

Aerodynamic diameter (μm)	Fate of the inhaled particle in the lungs
< 0.5	Particle remains suspended in lungs and are influenced by 'Brownian motion'.
1-5	Deposition of particle in the deep lungs by sedimentation and gravitational forces.
> 5	Particles deposit in upper respiratory tract by impaction.

1.1.3 Clearance mechanisms of the lungs

Several mechanisms are involved in the removal of particles from the respiratory tract, depending on where the particles have deposited in the airways. The most prominent defence mechanism of the respiratory region is the macrophage clearance. This occurs to the slow dissolving drug particles that have deposited deeper into the airways, in the alveolar region. A thin layer of alveolar fluid is secreted on the surface of the alveoli epithelium, composed of phospholipids and lung surfactants excreted by the Type II pneumocytes, as described in section 1.1.1. The phospholipid surfactant proteins B and C are responsible for lowering the surface tension of the lungs whereas the surfactant proteins A and D are responsible for opsonising foreign matter in the lungs (Goerke, 1998). The alveolar macrophages located in the alveoli rapidly engulf these foreign particles by phagocytosis. They then slowly migrate out of the lung and either follow the broncho-tracheal escalator or the lymphatic system (Geiser and Kreyling, 2010). The blood supply to the lung is provided by a pulmonary circulation and a systemic circulation, and the drug delivered in the lower airways can enter the systemic circulation by absorption into the alveolar capillaries.

Most of the insoluble particles that have deposited in the upper airways, approximately > 5 μm in size, are eliminated by mucociliary clearance (Geiser and Kreyling, 2010). The mucus cells intermingled amongst the ciliated cells at the luminal surface of the airways, secrete a layer of mucus. In the lungs of a healthy individual, the production of mucus reaches about 10-20 mL/day (West, 2013). It coats the walls of the conducting airways and the ciliated cells in the epithelium transport this mucus, together with any deposited particles in a proximal direction where eventually, the mucus is expectorated or swallowed (West, 2013). The smaller particles can penetrate the mucus and enter the bronchial epithelium. The smaller the particles, the faster they reach the epithelium and thus escape mucociliary clearance (West, 2013).

In healthy individuals, the mucus moves upwards at a rate of about 1 mm/min in the small peripheral airways but can be as quick as 20 mm/min in the trachea (West, 2013). The rate of mucociliary clearance decreases with age in healthy individuals but

can also be affected by airway diseases (Messina *et al.*, 1991; Munkholm and Mortensen, 2014). When mucociliary clearance is decreased, cough becomes an increasingly important mechanism for the removal of secretions from the airways (Puchelle *et al.*, 1980). It has been shown for example, a considerable large proportion of centrally deposited particles were eliminated by coughing, in patients with chronic obstructive pulmonary disease (COPD) compared with healthy individuals, 60% versus 8% of the particles (Puchelle *et al.*, 1980).

1.2 The dissolution process

1.2.1 Definition and theories of dissolution

Dissolution is a stepwise process, defined as the mass transfer of particles from a solid surface into the dissolution medium or surrounding solvent. It entails the separation of a solute molecule from adjacent solute molecules, followed by their transfer from the solid phase into a solution. The individual molecules insert into a vacancy in the solvent phase, large enough to accommodate for them, forming a homogenous mixture (Amiji and Sandmann, 2003).

Mathematically, dissolution is described in accordance to the Nernst-Brunner stagnant film theory, also termed the 'Diffusion Layer Model' (Larsson, 2009; Ashok, 2014). According to the theory the solute is initially transferred into a stagnant layer of solvent in direct contact with the solid surface, before being solvated by the solvent. The solvated molecule species subsequently diffuse through this stagnant diffusion layer to the interface of the bulk solvent region via convection. Therefore, the dissolution process is thought to be influenced by the effective diffusion boundary layer thickness, ∂, as approximated by Brunner and by the velocity of the stagnant layer in the immediate vicinity of the solid surface; where most efficient dissolution occurs with maximum contact between the dissolving solute and the dissolution medium i.e. maximum interfacial area. Since the dissolution operation predominantly involves mass transfer of solute particles, dissolution is also characterised by the *mass transfer coefficient, k,*

which accounts for the concentration difference between the interface and the bulk solution and is in turn determined by the degree of turbulence in the vicinity of the solid particles. Initially, Noyes and Whitey described the rate of dissolution in accordance to Fick's second law of diffusion (Ashok, 2014), as stated in equation (1):

$$dC/dt = k\,(Cs-Cb) \quad (1)$$

where dC/dt is the dissolution rate of the drug, k is the dissolution rate constant, Cs is the concentration of the drug in the stagnant layer and Cb is the concentration of the drug in the bulk of the solution at time t.

However, Nernst and Brunner used their theory to develop the equation further and incorporated Fick's first law of diffusion, modifying the Noyes-Whitney equation to equation (2):

$$dC/dt = [DAK_{w/o}\,(Cs–Cb)] / Vh \quad (2)$$

where D is the diffusion coefficient of the drug. A is the surface area of the dissolving solid, $K_{w/o}$ is the water/oil partition coefficient of the drug, V is the volume of dissolution medium, h is the thickness of stagnant layer and (Cs-Cb) is the concentration gradient for the diffusion of drug.

Taking these dissolution model parameters into consideration, the rate of dissolution can be further summarised into a simpler Noyes-Whitney equation (3):

$$dm/dt = DACs/h \quad (3)$$

Where m is the mass of the solute dissolved at time t, dm/dt is the mass rate of dissolution, Cs is the difference between equilibrium solubility of the drug and its solubility in the solvent and h is the thickness of the solvent diffusion boundary layer, which is influenced by the rate of stirring and temperature. The Noyes-Whitney equation assumed that the surface area of the dissolving solid remains constant during dissolution.

Since diffusion is often rate limiting, it is of special significance within the Noyes-Whitney equation. The D parameter in the equation is dependent on the Boltzmann constant, the absolute temperature, viscosity of the medium and the radius of the solute molecule and this is described by the Stokes-Einstein equation (4):

$$D = kT/6\pi\eta r \quad (4)$$

Where D is the diffusion coefficient of the drug in solution, k is the Boltzmann constant of 1.381 x 10^{-23} J/°K, T is the absolute temperature, η is the viscosity of the solvent and r is the radius of the drug molecule. The equation assumes a spherical particle, that is often influenced by Brownian motion, diffusing through a fluid of dynamic viscosity, with a low Reynolds number and at an absolute temperature (Kholodenko and Douglas, 1995). The Noyes-Whitney equation provides practical information relevant to the dissolution process and both the Noyes-Whitney and Stokes-Einstein equations reveal the parameters or factors that can affect the dissolution of a solute in a solvent.

Consequently, dissolution may also be described as diffusion-controlled dissolution, according to the particle dissolution model derived from Wang and Flanagen. The model suggests that under sink conditions, the smaller the ratio of particle size to diffusion layer thickness, the greater the nonlinearity of the concentration-time profile (Wang and Flanagan, 1999). It was found during the generation of the model, that the dissolution rate is dependent on the radius of curvature of the particle surface (Wang and Flanagan, 1999). Another study emphasised the influence of particle shape on dissolution and found that the effect of particle shape on dissolution is particularly significant for particles that deviate from sphericity (Mosharraf and Nyström, 1995)

Furthermore, dissolution may be described as a mixed-kinetic-controlled dissolution, in that the dissolution process is controlled by both the interfacial step and transport, according to Berthoud (Berthoud, 1912). Berthoud viewed the interfacial step as an equivalent permeation process through an interfacial barrier. However, it was realised that since all surface processes are lumped together into a single effective permeability coefficient, *p*, it does not provide a clear physical picture of the events occurring at the solid surface. This led to the development of another mixed-kinetic-controlled dissolution model, proposed by Rickard et al., who assumed that the interfacial reaction rate could be normalised with respect to the dissolving surface area (Rickard and Sjoberg, 1983). Dissolution could also be described as an interface-controlled process. This type of dissolution has little or no dependence on agitation type or

intensity, since fluid flow has no apparent effect on the interfacial step (Dokoumetzidis *et al*., 2008). Dokoumetzedis et al. developed an interface-controlled dissolution model, in which the interfacial step was regarded as a reversible reaction.

1.2.2 Factors that affect dissolution

The therapeutic effect of an inhaled drug, following its deposition, is realised after its dissolution in the respiratory tract lining fluid and subsequent absorption into the blood circulation. As explained in section 1.2.1, consideration of the Noyes-Whitney dissolution model and the Stokes-Einstein equation, and assuming diffusion-controlled dissolution, dissolution is driven by drug solubility (Cs), the surface area of the solid wetted by the dissolution fluids and the concentration of the drug in the surrounding liquid film, which in turn are governed by both the physical state of the inhaled compound and the thickness, composition, temperature and hydrodynamics of the lung dissolving media. Hence, dissolution is predominantly affected by interactions of all these variables.

In terms of the physicochemical properties of the drug, solubility of the drug in the respiratory lining fluid is determined by its physical form, size, lipophilicity and solubilisation by present surfactants and its pKa, in relation to the lung lining pH profile (Mangal *et al.*, 2018). With respect to the physical form for example, the solubility of a crystalline polymorph or an amorphous compound is greater than the solubility of a molecular high-order crystalline state. Different crystalline polymorphs tend to exhibit different solubilities to each other whereas, amorphous compounds generally have greater apparent solubility than the crystalline form. This is due to the amorphous state being less thermodynamically stable (Freiwald *et al.*, 2005). Hence, formulating poorly aqueous soluble drugs into the amorphous forms has become a well-recognised approach to improving solubility, dissolution and the overall efficacy (Khadka *et al.*, 2014).

In terms of particle size, it is well known that the smaller the size of the particles, the better the solubility and dissolution into fluids, since solubility is intrinsically related the particle size. A small sized particle corresponds to an increase in surface area and

hence an increase in the dissolution rate, dm/dt, when referring to the Noyes-Whitney equation. Based on this principle, particle size reduction has been one the oldest strategies to improving solubility of drugs, as it relies on safe methods and increases solubility without altering the chemical nature of the drug (Khadka *et al.*, 2014). However, for particles that exhibit large aerodynamic sizes, there have been attempts to reduce their mass density by making them porous, which can improve the deposition of the particles deeper within the lungs as well as its dissolution. For example, in a study conducted by Edwards et al, it was found that particles with mean diameters exceeding 5 μm and a mass density of less than 0.4 g/cm^3, were inspired deep into the lungs (Edwards *et al.*, 1997), and in a study by Khadka et al, the technique of producing porous particles, that exhibit low densities, has shown to improve the solubility of an inhaled solid and subsequently improve its dissolution, by means of providing large exposed surface area (Khadka *et al.*, 2014; Zhou *et al*., 2017).

The lipophilicity of a drug particle also affects its solubility and determines the extent of tissue affinity and whether an inhaled drug will have a more localised effect in the lungs or not (Tolman and Williams, 2010). For example, formoterol, which has an intermediary lipophilicity is likely to be retained in the membrane and interact with the lung receptors in a rapid and prolonged manner (Anderson, 1993; Lötvall and Ankerst, 2008). Consequently, a more lipophilic salmeterol molecule is likely to be retained in the tissue for long periods, meaning it becomes less available for a rapid onset of action (Anderson, 1993). This is because its lipophilicity results in very high partitioning of salmeterol in plasma membranes, very slow release from the membrane and very slow diffusion to the β2-receptors (Lötvall, 2001; Szczuka *et al*., 2009). Although this present some advantages in terms of achieving a prolonged effect in the lungs, since the composition of the epithelial lung lining fluid is known to be mainly water, contributing 96% to the fluid composition, it is important the inhaled drug exhibits relatively good aqueous solubility. A highly lipophilic drug would inevitably present poor solubility in the lining fluid. However, the lung lining fluid also consists of lipids and proteins which can increase the wetting, solubility and hence the dissolution of poorly soluble inhaled drugs

(Wiedmann *et al.*, 2000). The lung surfactants present can effectively enhance the solubility of small lipophilic drug molecules, and this has been demonstrated with a number of glucocorticoids and cationic compounds (Wiedmann *et al.*, 2000; Liao and Wiedmann, 2003).

With respect to pKa, it is defined as the pH at which the ionised and unionised form of a drug exists in equal concentrations (Peck *et al*, 2008). If a solute is ionizable and/or a weak electrolyte, altering the solvent pH can affect the surface or saturation concentration, Cs. Depending on the characteristics of the solute and solvent, this change can either increase or decrease Cs, causing either a decrease or increase in the concentration gradient and hence an increase or decrease in the dissolution rate, respectively. For the ionizable solute, the pKa will determine its degree of ionisation which then influences the solubility of the drug in a fluid. For a weak base for example, that exhibits a pKa value close to the physiological pH of the lung, it will have more molecules in the unionised lipid-soluble form, and hence have poor solubility in the lung lining fluid. The more the drug is in its ionised form, it will have an improved solubility and hence improved dissolution in the lung media.

In terms of the composition and hydrodynamics of the lung lining fluid, the dissolving media, its viscosity, temperature and movement speed properties very likely influence both solubility and dissolution of drug particles. Apart from the proteins and lipids present in the lung lining fluid that affect dissolution as mentioned previously, with regards to the dissolution media viscosity in general, it is well known that solutes will tend to dissolve more slowly in more viscous solvents. According to equation (4), the diffusion coefficient, D, is in part related to the solvent viscosity. The relationship is inversely proportional and hence, the diffusion coefficient decreases with increasing solvent viscosity with then decreases the dissolution rate as a result, considering equation (3).

With regards to temperature and in relation to equations (3) and (4), as the solution temperature increases, the diffusion coefficient increases and hence so does the dissolution rate. Practically, for many solids dissolved in media, the solubility increases because the increase in kinetic energy that comes with higher temperatures allows the

solvent molecules to break apart the solute molecules, that are held together by intermolecular forces, more effectively. This exposes more solute molecules to the solvent, increasing the rate at which the solute dissolves. Any added agitation and speed to the fluid would further introduce disturbances to the solute-solvent system. Stirring distributes the solvent molecules around the solute more quickly and increases the chances of the solute encountering the solvent, influencing the dissolution. The stirring rate has shown to affect the dissolution rate by virtue of the thickness of the diffusion layer of the particle (Ahuja and Scypinski, 2001); it decreases the thickness of the unstirred/stagnant layer, decreases the diffusion gradient, d, and hence increases the dissolution rate, dm/dt, inevitably.

1.3 The need for a dissolution test for OIPs

1.3.1 Current regulatory requirement for OIPs

The European Medicines Agency (EMA) issued guidelines describing the steps that need to be taken to approve a generic inhalation drug product and demonstrate therapeutic equivalence between two inhaled products (EMA, 2006). With regards to the formulation, the test and reference product must have the same active substance and identical dosage form. The pharmaceutical performance and safety profile of the inhaled product should be maintained and not influenced by differences in crystalline structure and/or qualitative differences in excipients. With regards to the device, the handling and resistance to airflow of the test and reference product should be identical. To assess the *in vitro* equivalence between the test and reference product, the key quality attributes are the dose delivery uniformity and particle size distribution profile, with a similar delivered dose. If the test product or generic product satisfies the pharmaceutical criteria enlisted, the use of only *in vitro* data may be considered acceptable for product approval.

In vitro dissolution testing is well established for solid oral dosage forms, as both a quality control test model and a predictive model to establish *in vitro-in vivo* correlation

(IVIVC) between *in vitro* dissolution data and pharmacokinetic data (Fotaki *et al.*, 2009; Fotaki and Vertzoni, 2010). Evidently, in the case of orally inhaled products (OIPs), the only requirements by the regulatory guidance are to assess the dose content uniformity and the aerodynamic particle size distribution (APSD) (US FDA CDER, 1998; EMA, 2006). Otherwise, *in vivo* studies would need to be carried out to understand the pharmacokinetics or pharmacodynamics of the product and substantiate equivalence. However, these approaches come with their limitations. These *in vitro* tests have shown to not fully predict the *in vivo* performance of the product, and the methods available to evaluate APSD does not have a direct relationship to pulmonary deposition profile (Newman and Chan, 2008). This is because in vitro methods do not reflect the realistic oropharyngeal geometry or inhalation manoeuvres but assumes the *in vitro* data can predict *in vivo* performance. The currently recommended tests do not account for the potential impact of dissolution rate on the clinical performance of an inhaled drug (Forbes *et al.*, 2015).

Since the dose of OIPs delivered to the patients is variable and dependent on the patient's inhalation techniques, disease state as well as the characteristics of the device itself, it makes it difficult to develop a suite of tests to demonstrate the effectiveness of OIPs *in vitro*. Hence, requirements for demonstrating the quality or equivalence of these products is still an evolving area of research. OIPs present unique challenges for in vitro testing and characterisation of the aerosol cloud generated and delivered by these devices. The advisory panel of USP has concluded in the past that dissolution is not necessarily 'kinetically and/or clinically crucial' for the approval of OIPs (Gray *et al.*, 2008). However, data has emerged to question whether dissolution should be used as a key quality attribute for current inhaled products (Davies and Feddah, 2003; Son and McConville, 2009; Arora *et al.*, 2010; May *et al.*, 2012; Rohrschneider *et al.*, 2015). Dissolution has proven to be useful and is already used widely in the pharmaceutical industry, for the optimisation of formulations, and for the development of quality control specifications for product manufacturing processes.

1.3.2 Applications and principles of a dissolution test

An *in vitro* dissolution test may provide a means for establishing quality criteria and inform the development and regulation of both generic and innovator products. As a QC tool, dissolution has the potential to provide inhaled pharmaceutical product quality information, helping identify formulation factors that influence the bioavailability of an active pharmaceutical ingredient (API) from the inhaler. It could also be used to follow up any post-approval changes to products such as changes in manufacturing site or process, allowing for the identification of critical manufacturing variables. Dissolution testing as a QC tool could assess quality during scale-up and production of batches, demonstrating any consistency or inconsistency in product manufacturing (Anand *et al.*, 2011). It could be used to support bioequivalence of an equal inhaled product for example, by demonstrating similarity between different product formulations of an active substance or a new or essentially similar product, and the reference medicinal product (Anand *et al.*, 2011).

Examples where the QC dissolution test would be useful, is for the comparison of formulation types, e.g. aerOsols delivered via dry powder inhalers (DPIs) with those delivered via the pressurised metered dose inhalers (pMDIs). This would provide an indication on whether the inhaled drug is delivered in the same physical form or not and hence, whether manufacturing an inhaled product in the form of a DPI or a suspension pMDI or solution pMDI has any influence on dissolution performance *in vivo* (Forbes *et al*., 2015). This is because unlike for the DPI, where the actual solid particle structures within the inhaler deposit on the lung mucosal surface, the drug particles dissolved in the propellant in a solution pMDI, generate a new solid phase due to the precipitation of the non-volatile solvent upon activation of the device. A study has previously demonstrated a difference and found that presence of glycerol as a non-volatile solvent significantly decreases the dissolution rate of beclomethasone dipropionate *in vitro* (Grainger *et al.*, 2012). Dissolution testing can also potentially help determine whether presence of a second drug in a combination inhaler influences the dissolution of the first API (Buttini *et al.*, 2014). For example, new formulations are being developed for triple therapy for

inflammatory lung disease or for the administration of antibiotic combinations for synergistic antimicrobial effects and dissolution testing can potentially address issues such as whether interaction between individual particles of two or more drugs occurs during product storage (Buttini *et al*., 2014).

With regards to clinical tests, both pharmacokinetic and pharmacodynamic studies are often components of OIPs bioequivalence studies, to help ensure equivalence in the safety and efficacy between a test and the reference inhalation product. Such studies would ensure that the pulmonary and systemic exposure i.e. the rate and extent of drug availability at the site of action and in the systemic circulation, are confirmed in an *in vivo* situation. It seems many regulatory agencies have currently put strong emphasis on PK and PD data because IVIVC correlations are not yet fully developed for OIPs. Hence, developing a dissolution tool to help establish IVIVC becomes necessary, since it allows the use of *in vitro* assessments as substitutes for such expensive time-consuming *in vivo* studies. Although it may seem ambitious to attempt to reproduce the lung environment faithfully, the need for a physiological representative *in vitro* method to evaluate the bioavailability of inhaled drugs has become apparent (Forbes and Ehrhardt, 2005). In a study conducted on solid oral dosage forms, dissolution testing using the biorelevant media, Fasted- and Fed – state simulated intestinal fluid (FaSSIF and FeSSIF), demonstrated clear improvements in establishing the IVIVC versus the compendial media (Sunesen *et al.*, 2005; Okumu *et al.*, 2008). Consequently, in studies conducted by Vertzoni and Fotaki et al, where they tested various aspects of dissolution media simulating the intralumenal composition of the small intestine, although it was found that using non-physiologically relevant buffers may be inevitable in some cases, there were certain components that must be necessary in the media for biorelevant purposes and to reflect the physiology as well as to predict the *in vivo* performance successfully (Vertzoni *et al.*, 2004; Fotaki and Vertzoni, 2010). This emphasised that development of an IVIVC tool for OIPs would require the design and application of a more biorelevant dissolution test, if we wish to truly reflect and predict the behaviour of an inhaled drug *in vivo*.

Dissolution testing would also help in developing a Biopharmaceutics Classification System (BCS) for OIPs. There is currently one in place for oral immediate release drugs, utilised by Research and Development (R&D) scientists and regulators to streamline product development (Hastedt *et al.*, 2016). This approach considers a combination of drug physicochemical properties and physiological properties with respect to their oral administration, and is based on three *in vitro* parameters: dose, dissolution and absorption (Hastedt *et al.*, 2016). A classification system, if fully developed, would certainly be useful for formulators and discovery scientists. Hence, there is huge interest in applying a similar principle or system to OIPs, with the current focus being on the dissolution of drugs in the lung. The dissolution of inhaled powders is a very crucial component of the BCS system, and so a standardised test methodology should be carefully considered.

According to the pharmacopeia and US FDA CDER (US FDA CDER, 1997), which defines the standards in which dissolution testing must be assessed, to conduct a reliable test, the dissolution apparatus reproduces the key *in vivo* environmental features. Since the aim is to evaluate how a product will dissolve in a physiological setting, the test should ideally be carried out at body temperature (37°C) and the aqueous based medium should exhibit a pH of 5 to 7. For a poorly soluble drug, it is a requirement to modify the medium in such a manner that it solubilises the drug but remains physiologically relevant. A fixed practical volume of medium is important, sufficient to dissolve the amount of drug released from the product and hence maintain 'sink conditions' for the quantitation of the drug. Another principle method development consideration is how to reproducibly present the particles to the dissolution test apparatus. This is because inhalation powders may deposit aggregated clumps of particles due to the electrostatic interactions in one instance, and free separate particles in another (Finlay, 2001). Consequently, the test should overall be robust, simple and easy to conduct as well as capable of discriminating between different drugs and inhaled formulations. A summary of the general considerations for the design of dissolution tests for OIPs is shown in Table 1.2.

Table 1. 2. Considerations for design of dissolution test for orally inhaled products.

Factors to consider	
Aerosol particles	Dissolution should be performed on the respirable fraction rather than the bulk emitted aerosol.
Particle loading	Comparison between products should be based on the same amount of drug loaded, since mass loading has an impact on the dissolution rate.
Stirring	Stirring rate has shown to affect the dissolution rate. It may provide more experimental control.
Membrane limitation	Diffusion through the membrane should not be the limiting step for the transfer of the drugs from donor to the receptor chamber in diffusion-controlled cell systems.
Discriminatory power	Dissolution rate should not be too fast so that it is discriminatory. The system should be able to adapt to different APIs solubilities for example.
Sink conditions	Sink conditions should be maintained, particularly for poorly-soluble drugs.

1.4 Challenges with developing a dissolution test for OIPs

1.4.1 Challenges associated with the geometry of the human respiratory tract

The challenge with assessing dissolution in the lungs stems predominantly from the complexity of the human respiratory tract geometry, making it difficult to replicate such an environment on an *in vitro* system. It has been recognised that the very small lung fluid (V_{LF}) available for particle dissolution, 10-30 mL, is a significant limitation since it is likely to be stagnant, and this can inhibit dissolution (Patton *et al.*, 2010). Considering that a clinically relevant dose of an inhaled drug, such as poorly soluble fluticasone propionate, would require excessive volumes for a complete dissolution in stationary liquid, assessment of its dissolution *in vitro* would not be accurately represented.

The surface-lining layer in the alveoli consists of numerous endogenous surfactants such as phosphatidylcholine (DPPC). Surfactants influence dissolution by increasing the wetting of poorly soluble drugs and as a result, increasing their dissolution rate. However, it has been recognised that the exact composition of the lung aqueous fluids and surfactants is not accurately established (Marques *et al.*, 2011) and the preparation of DPPC solutions is perceived to be difficult, since it may be lengthy and variable. Furthermore, the clearance mechanisms in the upper and lower lung, as discussed in section 1.1.3, provide physical and chemical barriers to particle diffusion

and dissolution, making it difficult to reliably reflect their dissolution *in vitro*. In addition to this, unlike the gastrointestinal tract in which dissolution is described as a 'continuous process' over a sequence of tanks (Yu *et al.*, 1996), the lung constitutes several different dissolution processes occurring in parallel, which is very difficult to consider when developing an in vitro dissolution test.

1.4.2 Challenges associated with the patient

In addition to the challenges listed in section 1.4.1, the specific relationship between dissolution and pharmacokinetic or pharmacodynamic data for OIPs is difficult to evaluate due to these being product or patient-specific. It is dependent on factors like the inhalation manoeuvre, inspiratory flow profile and the physiology and anatomy of the lung. The lung physiology tends to vary amongst a target population for example, their pulmonary disease state, whether severe or moderate, or treated condition, whether it is asthma or COPD. A study indicated clear lung physiological changes occur with aging; the alveoli dilate, the airspaces in the lungs enlarges and there is a general decrease in the exchange surface area and loss of supporting tissue for peripheral airways, which results in a decreased static elastic recoil of the lung and increased residual volume and functional residual capacity (Janssens *et al*., 1999). With regards to disease state, an asthmatic lung tends to have an increased amount of mucus, because as the airways become irritated and inflamed, the cells produce more mucus. The principle defect in asthma is the occlusion of the airway lumen by liquid, fibrin and the built-up mucus. The airways also become smaller as there is a general loss of lung volume, as a direct response to muscle tightening (Irvin and Bates, 2009). With regards to COPD, chronic expiratory flow limitation, hyperinflation and inspiratory muscle weakness are its mechanical hallmarks, with hyperinflation varying between chronic and acute airway obstruction (Scano *et al.*, 1999). Inspiratory muscle weakness leads to significantly lower aerosol penetration into the lungs, in comparison to a healthy lung, decreasing the depth of inhaled particle deposition and hence influencing the rate of dissolution of the inhaled drug; drugs deposited in the central airways dissolve in the fluid at a much slower rate

due to the presence of mucins and the increase in lung fluid viscosity in comparison to the peripheral airways (Labiris and Dolovich, 2003). Bronchial obstruction further modifies the deposition and distribution patterns of aerosols, affecting the rate and extent of dissolution of the inhaled drug. Again, the aerosolized drug becomes deposited more centrally in the lungs by inertial impaction compared with the uniform distribution achieved in the normal lung, influencing the therapeutic effectiveness of an inhaled drug (Labiris and Dolovich, 2003). Attempting to develop a standardised dissolution test to account for all these factors would be particularly challenging.

1.4.3 Challenges associated with experimentation

An important aspect to consider when developing a standardised method applicable to the lungs, is the challenges involved with sample preparation. To maximise the probability of generating data reflective of *in vivo* pulmonary dissolution, the test method requires the collection of the relevant respirable fraction of the aerosol dose emitted from the inhaler device i.e. collection of the particles with an aerodynamic size of 1-5 µm. The use of aerosol fractionation to prepare samples for dissolution testing compared to sampling the entire respirable fraction, may affect outcomes and influence the discriminatory power of the dissolution method (Forbes *et al.*, 2015). Consequently, for DPIs for example, the micronized API is blended with larger carrier lactose particles which requires detachment before conducting the dissolution test. The presence of very fine particles and the characteristics of the electrostatic powder within the inhaler may cause experimental difficulties (Telko and Hickey, 2005). For pMDIs, the drug is often suspended within propellant and therefore to collect the desired particles, the product would need to be fired into an apparatus where the particles can dry prior to their deposition on the collecting system (Labiris and Dolovich, 2003).

Consequently, the apparatus used to develop the dissolution test can present challenges since they do not entirely mimic the in vivo lung environment. For example, the Transwell® dissolution technique relies on a polyester, or other semi-permeable membranes attached to the transwell insert, to collect the respirable fraction of the

aerosol and provide a diffusion restriction (Arora *et al.*, 2010). This will be described in more detail in section 1.6. Another example, is the Rotating Paddle methodology which relies on the Next Generation Impactor (NGI) to collect the respirable fraction. Using this technique, the dissolution rate has shown dependence on drug loading, since the particles tend to accumulate under the air jets, and this causes poorly reproducible results (Son and McConville, 2009; Son *et al.*, 2010). Consequently, although the rotating paddle method uses substantial amount of media, ensuring sink conditions could be maintained, it does not reflect the limited amount of volume provided by the lungs, to allow for particle dissolution. This will also be discussed in more detail in section 1.6.

Furthermore, there is no standard dissolution medium that can be applied to the proposed dissolution methods for OIPs, presenting a further challenge. There are a huge variety of fluids that have been utilised to mimic or simulate the lung lining fluid, causing a general confusion as to what medium should be used. This will be discussed in section 1.7.

1.5 Dose collection methods available for OIPs

Despite the challenges and obstacles described above, several *in vitro* approaches of aerosolisation and inhaled dose collection have been proposed and evaluated for use in dissolution testing of OIPs.

1.5.1 NGI and ACI

Approaches used to collect the aerosolised particle fractions include using multistage impactors such as the Next Generator Impactor (NGI) and the Anderson Cascade Impactor (ACI). Both apparatus are incorporated into the US and European Pharmacopoeia for measurement of the aerodynamic size of pharmaceutical inhalation aerosols (Mitchell and Roberts, 2012). Generally, the particles impact on a dry surface and by modifying the geometry of the nozzle, they divide the emitted dose from the inhaler product into several fractions according to the particle aerodynamic size. The

primary advantage offered by these techniques is that they allow determination of an assay for the fine particle fraction and other size fractions and provide differentiation between the API and any other components in the formulation (Mitchell and Roberts, 2012). Hence, such techniques would ensure that the FPF is targeted for dissolution.

However, there are several limitations associated with these methods as dose collection methods for dissolution, which includes the difficulty in attempting to insert a collecting membrane into an impactor without affecting the air flow condition inside the instrument. Also, repeated actuations of the inhaler device are necessary to ensure the same amount of drug is captured from the different formulations. This is widely recommended, especially when the purpose of the study is to compare the kinetics of release from the different formulation types, since the amount of drug loading on the collecting surface may significantly influence the drug release and dissolution rate, especially for hydrophobic APIs (Forbes *et al*., 2015). However, when repeated doses are actuated, a powder bed is formed, and the thickness of the bed can influence the release rate of the molecules. In the case of impactors, rather than particles depositing evenly over the collection surface, powders may collect in clusters below the nozzle. To correct this, some modifications to the system have been attempted such as designing a membrane holder to be incorporated into the NGI for the collection of the API dose, positioning particulate filters in certain stages of the NGI to avoid capturing the coarse carrier particles when analysing DPIs (Mees *et al*., 2011) or mounting a glass microfiber filter on the end of the induction port of an ACI to form a greater surface area for the collection of the aerosolised particles (Davies and Feddah, 2003). When such modifications have been applied improvements in dissolution profiles were evident (Son and McConville, 2009; Son *et al.*, 2010).

1.5.2 TSI and FSI

Another approach is collecting particles deposited onto a liquid surface via a Fasted Screening Impactor (FSI) or Twin Stage Impinger (TSI), where they separate aerosols into two fractions according to the aerodynamic size. Essentially for both

methods, the collection stages are kept moist with a solvent to prevent impacted particles from re-entraining in airstream. Based on proven NGI preseparator technology, the FSI represents a purpose-made approach that segregates the dose into coarse particle mass (CPM) and fine particle mass (FPM) and uses the same induction port as the NGI. The TSI however, operates on the principle of liquid impingement to divide the dose emitted from the inhaler into respirable and non-respirable fractions, where the non-respirable dose that impacts on the oropharynx and is subsequently swallowed, is reflected by the back of the glass throat and the upper impingement chamber, and the respirable dose that penetrates the lungs, is collected in the lower glass impingement chamber. These techniques are considered relatively easy to use and assemble.

A limitation to these methods however relative to dissolution of OIPs, is that since they do not collect dry particles for introduction into the dissolution experiment, they are not useful for collecting aerosol particles for this purpose without modifications to the collection modality (Buttini *et al.*, 2013). Nevertheless, the advantages of the impinger system include its usefulness in capturing aerosol particle sizes reflective of the entire respirable dose and if the collection stages are moist, they simulate realistic impaction processes of particles on the liquid lining of the lungs. The TSI for example, has been adapted for the collection of drug particles from solution metered dose inhalers in a number of studies, and its performance in particle collection has been well documented (Grainger *et al.*, 2012).

1.5.3 PreciseInhale®

The PreciseInhale is a bespoke aerosol generator and particle collection method, developed by Inhalation Sciences in Sweden (Gerde *et al.*, 2017). It provides an exposure platform to collect the aerosolised powder on glass coverslips and has the advantage of simulating human breath using an automated system. A jet of high pressure air is shot through the powder chamber, aerosolising the powder upwards into the holding chamber, in a plume, then settles downwards in the holding chamber where

a controlled air flow 'pulls' the API past a real-time aerosol monitor. The real-time aerosol concentration and dose is logged, and the exposure is automatically calculated.

Despite the advantages of the PreciseInhale system, it does not separate the non-respirable fraction from the respirable fraction i.e. it does not entirely ensure that only 1-5 µm sized particles are collected on the platform. This often leads to collection of the coarse particles which are then taken further into the dissolution experiments, using the complimentary Dissolv*It*® system. This has led to modifications by the team at Hovione, where they studied the influence of a newly designed pre-separator on the particle collection (Noriega *et al*., 2017). A schematic diagram of this system is shown in chapter 4, figure 4.1.

1.6 Dissolution techniques available for OIPs

Using convenient dose collection techniques as a starting point, multiple dissolution techniques have been used in an attempt to create a suitable dissolution testing system for OIPs. For example, a study by McConville et al., (McConville *et al.*, 2000), was one of the first to employ a modified twin stage liquid impinger to disperse the inhaled powder onto an air-liquid interface and evaluate the dissolution of the inhaled drug in a specially designed dissolution reservoir. The dissolution system was not configured to specifically mimic the environment of the lungs. The powder particles that were <4.7 µm impinged on an air-water interface, presenting the fine particle mass for dissolution. In another study by Salama et al., a modified Franz diffusion apparatus was used that incorporated a heated membrane holder at its surface and a heated dissolution reservoir containing phosphate buffered saline (Salama *et al.*, 2009). Prior to this, Davies and Feddah reported using an NGI apparatus with a filter positioned to collect the aerosol powder at the base of the USP throat (Davies and Feddah, 2003), which was then sealed into a flow-through holder and a HPLC pump was used to pump the dissolution media through the filter. The technique used the oversized powder fraction, dispersed with the fine powder fraction. In a study by Jaspart et al., the aerosol powder

was sealed within a filter membrane and immersed within the basket of a USP type 1 dissolution method (Jaspart *et al.*, 2007), which demonstrated limitations in contact area between the particles and the media.

Predominately, the dissolution apparatuses that have been reported to date are the compendial (USP 2) paddle apparatus, the flow-through apparatus, diffusion-controlled cell systems, namely the Franz cell or Transwell® system, and the Dissolv*It*® system which is a module designed to interface with the PreciseInhale® aerosol delivery system. These techniques are discussed below.

1.6.1 USP 2 paddle apparatus

The paddle apparatus involves a cylindrical glass vessel with a paddle rotating at a speed of typically 50 or 75 rpm. The dosage form should remain at the bottom of the vessel and therefore, a 'sinker' such as a membrane cassette containing the membrane in which the inhaled dose is collected via an impactor, is used. In the case of paddle over disk, a stainless support disk is placed under the paddle and the membrane filter used to collect the respirable fraction can be directly positioned on top of the support (Son *et al.*, 2010).

The main advantage of this technique is that it is a standard USP 2 apparatus, which can be used in conjunction with different types of aerosol particle collection filters in different filter holders placed into the vessel (May *et al.*, 2012). However, the main limitation is the large volume of dissolution medium required, at least 300 mL, making it difficult to develop such a method if more complex dissolution media are used that are not available in such quantities. For reproducibility, unless the particle collector can be orientated consistently in the bath, its orientation could influence the contact area of the powder with the media and hence the dissolution rate (Son *et al.*, 2010; Mees *et al*, 2011).

1.6.2 Flow-through cell apparatus

The flow-through cell systems used for OIPs are referred to as a modified USP 4 apparatus (European Pharmacopoeia, 2012). The system consists of a cylindrical cell with a filter placed at the top, to prevent the escape of any undissolved products, as the dissolution medium is pumped through the cell from a reservoir. The bottom of the cell is filled with small glass beads in which the membrane used to collect the particles form the inhaler, is placed on or within the beads. The drug concentration is measured either directly in the flowing system or via the collection of samples from the cell exit. A schematic diagram of the modified flow through cell is shown in Figure 1.2.

Advantages of this method include the reduced influence of diffusion during dissolution testing and its suitability for poorly-soluble drugs since 'sink' conditions can be maintained due to the high volume of dissolution media pumped through. However, due to the geometry of the system, any air entrapment can potentially interfere with wetting and dissolution (Colombani-Dauvergne *et al*., 2006).

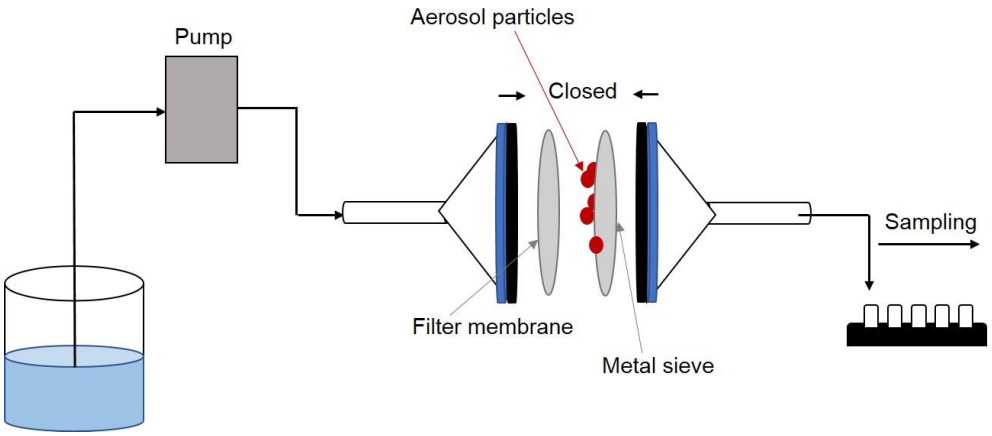

Figure 1. 2. A schematic diagram of the Flow Through Cell dissolution system. Adapted from May et al., (May *et al.*, 2012)

1.6.3 Diffusion-controlled systems

In the diffusion-controlled systems, the drug transfers between two compartments separated by a semi-permeable barrier. For dissolution of inhaled products using the Franz cell, a semi-permeable membrane with the test formulation has been added to the donor chamber and the receptor medium is stirred and heated to 37°C with samples

collected through a sampling arm in the receptor side of the cell. In the Transwell® apparatus, a membrane filter with the deposited drug collected from the NGI for example, can be placed on top of the insert membrane or alternatively the respirable fraction can be directly deposited onto the insert membrane, using the TSI for example.

A limitation to these methods is the inability to distinguish between the diffusion effects through the membrane and the dissolution rate (Arora *et al.*, 2010). However, a principle advantage of such systems is the very low volume of dissolution medium on the donor chamber in comparison to the receptor chamber, which offers the opportunity to mimic the limited lung lining fluid volume, providing an environment more reflective of the lung lumen. Some investigators have developed this system further to use the Transwell membrane to support culture respiratory cell monolayers, providing more mucosal-like conditions for the deposited particles to dissolve in, thus mimicking the lung permeability barrier that drugs must permeate, prior to their dissolution (Fiegel *et al.*, 2003; Forbes *et al.*, 2003; Grainger *et al.*, 2009). These advantages open a greater opportunity to develop a biorelevant methods for IVIVC purposes.

1.6.4 Dissolv*it*®

The DissolvIt system is an *in vitro* model designed to incorporate features reflective of the absorption and dissolution processes of respirable particles in the lungs. Aerosol particles are deposited on a glass surface via the PreciseInhale, then brought into contact with a simulated lung/airway mucus, represented by a polyethylene oxide gel. Dissolution (solid particle disappearance) is studied from the 'lumenal' side by optical microscopy and 'permeated drug' is quantified from the 'vascular' side by chemical analysis of the flow-past perfusion medium. The system is thermostatted at 37°C. It consists of a dissolution chamber, a precision-controlled peristaltic pump and an inverted microscope with a camera. The dissolution chamber is perfused in single-pass mode, after which the perfusate is collected in an automated fraction collector into a deep-well plate for analysis.

A key advantage of the system is that it simulates the physiological conditions in the lung more closely in comparison to the other methods and allows for monitoring of both permeation and dissolution processes. The optical microscopy shows real-time dissolution of particles and the programmable Fraction Collector allows for flexible sampling. The system provides *in vitro*-predictive PK data for the inhaled drug analysed, providing parameters such as the Cmax and Tmax, giving a greater insight into the critical coupling between dissolution and absorption for sparingly soluble drugs in the lungs for example (Gerde *et al.*, 2017). However, a limitation to the system is the DissolvIt represents a 60 µm air-blood barrier, simulating the absorption kinetics in the trachea and larger bronchi rather than the thinner barriers in the rest of the bronchi and alveoli. Therefore, when used as a general tool for lung dissolution, the DissolvIt likely overestimates the half-life of retention for the test formulations (Gerde *et al.*, 2017). A schematic diagram of the system is shown in chapter 4, figure 4.1.

1.7 Dissolution media

A critical factor in dissolution testing, is the dissolution medium, the selection of which strongly depends on the purpose of the study and the compound investigated. For routine QC purposes, using simple dissolution media such as methanol and water, are preferred over complex media due to their higher reproducibility, lower costs and ease of preparation (Marques *et al.*, 2011). However, for prediction and modelling purposes using medium as close to the biological fluid is preferred.

The epithelial lining fluid is the first physical interface with which aerosolised drugs come into contact in the airways. It is the biological fluid in which the aerosolised drug dissolves, before absorption into the lung tissue. The composition and properties attributed to the lining fluid vary greatly along the respiratory tract and can also vary markedly in different airway pathologies (Bicer *et al.*, 2012). For example, the large airways possess periciliary layer and gel mucus layer, consisting of water with antibacterial factors, ions, mucins and heparin sulphate (Rubin, 2014). The lung lining

fluid of the alveolar region however, is composed of a watery layer, known as the hypophase, and surfactants (Fehrenbach, 2001). The hypophase contains a range of surfactant proteins, complement proteins and antioxidants (Kobzik, 2007).

Although the composition of the lining fluid has been documented, the exact concentrations are generally subject to speculation (Cheng *et al.*, 1997; Son and McConville, 2009; Marques *et al.,* 2011). A wide range of dissolution media have been proposed for use for the dissolution testing of OIPs. They have ranged from simple aqueous fluids, buffered in the pH range of 6.8-7.4, such as water or phosphate buffered saline (PBS), representative of physiological electrolyte levels, through to fluids consisting of certain proteins or lipids. The medium used is also often supplemented with surfactants such as DPPC or co-solvents, particularly when analysing poorly soluble API, since they tend to significantly influence the dissolution rate (Davies and Feddah, 2003; Son *et al.*, 2010). It was hypothesised that data obtained from using such surfactant-containing media most likely replicate the effect lung surfactants would have on inhaled particle *in vivo*. However, with regards to biorelevance, the highly abundant proteins, composing the aqueous component of the fluid are often not included. Other media that have been tested include the commercially available surfactant preparations or diluted surfactant replacement products, used for the treatment of respiratory distress syndrome in neonates, such as Alveofact®, Exosurf®, Curosurf® and Survanta®. These are used clinically as well as applied for *in vitro* investigations (Pham and Wiedmann, 2001; El-Gendy *et al.*, 2013). The main limitations of these fluids is that they are expensive, and hence are often used in their diluted forms, and they only represent the surfactant component of distal respiratory tract lung lining fluids.

Another medium used to represent lung fluids in dissolution tests is Gamble's solution. This solution has been designed to model interactions of the particles with interstitial lung fluids and evaluate the bio-accessibility of aerosol inhaler products (Davies and Feddah, 2003). However, limitations to the preparation of such solution include the likelihood of salt precipitation if components were not added in the correct manner, and the solution often uses citrate instead of proteins to avoid foaming and use

acetate instead of organic acids, deviating from the original components of the lung lining fluid. Some researchers have attempted to modify Gamble's solution by including proteins and other organic components. However, it was found that addition of proteins can affect reproducibility of results due to putrefaction in the lab (Takaya *et al.*, 2006).

Although some of the media currently available and being used in dissolution testing have some physiological relevance, they do not fully simulate the epithelial lung fluid. In some cases, the fluid presents a low buffering effect, making them unsuitable for formulations that show pH dependency or sustained release dissolution profiles. For example, it was observed for one of the proposed DPPC-containing fluid, that the pH increased in 24 h from 7.4 to 8.8 (Son *et al.*, 2010). Consequently, in the study by Son et al., (Son *et al.*, 2010), the dissolution profiles of budesonide in phosphate buffer pH 7.4 were similar to the ones obtained in their version of simulated lung fluid, indicating that the version of simulated lung fluid used in the study much closely resembles a simple PBS solution rather than truly simulating the RTLF. Furthermore, for fluticasone propionate and beclomethasone dipropionate, the solubility values in water were unaltered from those in PBS (Arora *et al.*, 2010).

These limitations suggest there may be a need to develop a 'fit for purpose' simulant that possesses physiological relevance to simulate the *in vivo* epithelial lung fluid. For such a fluid to find sufficient application to evaluate its advantages and usefulness it would have to fulfil criteria of being able to be manufactured in a simple, standardised and cost-effective manner.

1.8 Comparison of dissolution profiles

The comparison of dissolution profiles is a critical test for assessing the performance of many drug products (Solid and Dosage, 1997). It can help establish the similarity of the pharmaceutical dosage forms, for which composition, manufacture site, scale of manufacture and the manufacture process or equipment may have changed within defined limits.

Graphical method is the first step in comparing dissolution profiles and is easy to implement (Leblond *et al.*, 2016). It is the method of plotting a graph of time versus concentration of drug in the dissolution medium and comparing the dissolution pattern and concentration of drug at each point. If two or more curves are overlapping then the dissolution profile is comparable however, if the difference is small, then it is acceptable but higher differences indicate that the dissolution profile is not comparable. It is very difficult to make definitive conclusions from the graphical method. Therefore, dissolution profiles of two pharmaceutical products can be compared by other methods such as statistical t-Test or ANOVA-based methods, via multivariate ANOVA, multiple univariate ANOVA and the level and shape approach or by various model independent methods such as comparing the mean dissolution time, the similarity and difference factor and sampling time or by model-dependent approaches. Table 1.3 lists the methods that can be applied to compare dissolution profiles.

Table 1. 3. Categories of methods to compare dissolution profiles.

Methods to compare dissolution profile	
Graphical method	-
Statistical method	T-test ANOVA
Model independent method	Difference factor, f1 Similarity factor, f2
Model dependent methods	Zero order First order Hixson-Crowell Higuchi Korsmeyer-Poppas Weibull Gompertz Baker-Lonsdale Hopfenberg

1.8.1 Statistical approaches

One of the statistical approaches that can be applied is the student's t-test (Leblond *et al.*, 2016). The two tests commonly used are the paired t-test and unpaired t-test. It is calculated using equation 5:

$$t = \overline{D}/SE \quad (5)$$

where D is the mean difference and SE is standard error. The calculated t value is compared with tabulated value of t and if the magnitude of difference between the two gives a $p<0.05$, then the null hypothesis should be rejected and vice versa.

In terms of the ANOVA method, the test is generally applied to different groups of data where the variance of different groups of data is compared and a prediction is made on whether the data is comparable or not. A minimum of three sets of data are required and first the variance within each individual group is found then compared with each other. These approaches are relatively easy to apply and provide detailed, discriminative information between dissolution profiles and data.

1.8.2 Model-independent approaches

Flanner and Moore proposed the model-independent mathematical approach to compare dissolution profiles (Flanner and Moore, 1996). The model-independent approaches can be classified into two groups: Ratio test procedures and Pairwise procedures (Costa and Sousa Lobo, 2001). Example of ratio test procedures are ratio of percent dissolved, ratio of area under the dissolution curves and ratio of mean dissolution time. Pairwise procedures include the Difference factor (*f1*) or the Similarity factor (*f2*). Both procedures compare the dissolution profiles of a pair of products and employ a 90% confidence interval approach. The difference factor calculates the percent difference between the two dissolution curves at each time point and is a measurement of the relative error between the two curves. It is determined using equation 6:

$$f1 = (\sum_{t=1}^{n} |\boldsymbol{Rt} - \boldsymbol{Tt}| / \sum_{t=1}^{n} \boldsymbol{Rt}) \times 100 \quad (6)$$

Where n is the number of dissolution sample time points, t is the time sample index, and Rt and Tt are the individual or mean percent dissolved at each time point for the reference

and test dissolution profiles respectively. A calculated value of zero for *f1* indicates that the profiles of the test and reference are identical. As the value increases from zero, dissimilarity between the two profiles increases, and usually a value of 15 or below suggests similarity (Costa and Sousa Lobo, 2001).

The similarity factor is a measurement of the similarity in the percent dissolution between the two dissolution curves and is determined using equation 7:

$$f2 = 50 \times \log \{[1 + (1/n)\sum_{t=1}^{n} \boldsymbol{Rt} - Tt)^2]^{-0.5} \times 100\} \quad (7)$$

The f2 values are between 0 and 100, and if the calculated value is greater than 50, the test and reference profiles are considered similar.

The similarity factor is gaining popularity due to its recommendation by a number of regulatory authorities, such as the FDA, as a criterion for the assessment of similarity between dissolution profiles (Costa and Sousa Lobo, 2001). Advantages of this method is that they are easy to compute and interpret, it is the most widely used method to compare dissolution profiles and they provide a single number to describe the comparison of dissolution profile data. Consequently, they directly compare the dissolution data without having to rely on model functions that may prove to be artificial. However, the values of *f1* and *f2* are sensitive to the number of dissolution time points used i.e. it is a more appropriate method when more than three or four dissolution time points are available.

1.8.3 Model-dependent approaches

There are many different types of model-dependent approaches that can be applied to compare dissolution profiles. Examples of these models are Zero-order, First-order, Hixson-Crowell, Higuchi, Korsmeyer-Poppas, Weibull, Gompertz, Baker-Lonsdale and Hopfenberg model.

For the zero-order kinetics, a plot of cumulative amount of drug dissolved versus time is made. The model can be expressed by equation 8:

$$Q_t = Q_0 + K_0 t \quad (8)$$

Where Q_t is the amount of drug dissolved in time t, Q_0 is the initial amount of drug in the solution and K_0 is the zero-order release constant expressed in units of concentration/time. The release mechanism associated here is a constant release rate. The model often represents drug dissolution from pharmaceutical dosage forms that do not disaggregate and releases the drug slowly and is often applied to transdermal systems and modified release dosage forms such as matrix tablets with low solubility drugs.

For the first-order kinetics, a plot of log concentration of drug remaining versus time is made, yielding a straight line with a slope of -K/2.303. It follows equation 9:

$$\text{Log } C = \text{Log } C_0 - Kt / 2.303 \quad (9)$$

Where C_0 is the initial concentration of drug, K is the first order rate constant, and t is the time. This relationship originated by the Noyes-Whitney equation as stated in equation 1 and follows Fick's first law of diffusion mechanism. It can be used to describe the drug dissolution in pharmaceutical dosage forms such as those containing water soluble drugs in porous matrices (Costa and Sousa Lobo, 2001).

For the Hixson-Crowell model, Hixson and Crowell recognised that the particle regular area is proportional to the cubic root of its volume and described dissolution via equation 10:

$$W_0^{1/3} - W_t^{1/3} = Kt \quad (10)$$

Where W_0 is the initial amount of drug, W_t is the remaining amount of drug at time t and K is a constant incorporating surface-volume relation. The data is plotted as cube root of drug percentage remaining in matrix versus time and gives a linear relationship. It presumes an erosion release mechanism and the expression can be applied to pharmaceutical dosage forms such as tablets, where dissolution occurs in planes that are parallel to the drug surface if the tablet dimensions diminish proportionally in such a manner that the initial geometrical form keeps constant all the time (Costa and Sousa Lobo, 2001).

For the Higuchi model, a plot of cumulative percentage drug release versus square root of time is made and follows a simple expression, equation 11:

$$Q = K\sqrt{T} \quad (11)$$

Where Q is the amount of drug released in time t per unit area, K is the Higuchi constant and T is time in hours. Higuchi describes drug dissolution as a diffusion process based in the Fick's law, square root time dependent. It is often applied to modified release pharmaceutical dosage forms, transdermal systems and matrix tablets with water soluble drugs (Costa and Sousa Lobo, 2001).

For the Korsemeyer Peppas kinetics, a plot of percent drug dissolved versus square root time is made which gives rise to a linear graph. The model assumes dissolution is diffusion-controlled and describes dissolution via equation 12:

$$M_t/M_\infty = Kt^n \quad (12)$$

Where M_t/M_∞ is fraction of the drug dissolved, t is time, K is a constant which includes structural and geometrical characteristics of the dosage form and n is the release component which is indicative of drug dissolution mechanism. If n=1, the dissolution is zero order, n=0.5, the dissolution is best described by the Fickian diffusion and if n is between 0.5 and 1, then dissolution is through anomalous diffusion or case two diffusion (Ramteke *et al.*, 2014). To use this equation, it is necessary that release occurs in a one-dimensional way and that the system width thickness or length thickness relation is at least 10 (Ramteke *et al.*, 2014). It is therefore a semi-empirical model and is generally applied to pharmaceutical polymeric dosage forms, when the dissolution mechanism is not well known or when it is likely that there is more than one type of dissolution phenomena involved.

The Weibull model is a general empirical equation that is adapted to dissolution, giving a linear relationship when a plot of log amount of drug dissolved versus log time is made (Langenbucher, 1972). The equation described by Weibull can be applied to almost all kinds of dissolution curves. The Weibull equation is expressed as equation 13:

$$\text{Log}\,[-\ln(1-m)] = b \log (t-T_i) - \log a \quad (13)$$

Where m is the accumulated fraction of the drug dissolved and b is a shape parameter that characterises the curve as either exponential if b=1, sigmoidal S-shape with an upward curvature followed by a turning point if b>1 or parabolic, with a higher initial slope

followed by consistency with the exponential if b<1. The parameter, t, is time, Ti is the location parameter, which represents the lag time before the onset of the dissolution and in most cases, T_i is equal to zero, and a is the scale parameter. The parameter, a, can be replaced by a more informative dissolution time parameter, T_d, which represents the time taken to dissolve 63.2% of the drug present in the pharmaceutical dosage form (Langenbucher, 1972). This is because $a=(T_d)^b$ and is read from the graph at the time value corresponding to the ordinate -ln(1-m)=1 which is equivalent to m=0.632. It is considered to have a lifetime distribution function. Since Weibull is an empirical model and has no kinetic fundament, it comes with some limitations. For example, it can only describe dissolution and does not adequately characterise the dissolution kinetic properties of the drug, there is not any single parameter related to the intrinsic dissolution rate of the drug and it is of limited use for establishing IVIVCs.

The Gompertz model describes dissolution profiles of pharmaceutical dosage forms via equation 14:

$$X(t) = X_{max} \exp[-a e^{\beta \log t}] \quad (14)$$

Where X(t) is the amount dissolved at time t divided by 100, X_{max} is the maximum dissolution, α describes the location or scale parameter and determines the undissolved proportion at time t=1 and β corresponds to the dissolution rate per unit of time and describes the shape parameter. This model tends to have a steep increase in the beginning and converges slowly to the asymptotic maximal dissolution (Maharjan, 2014) and is more useful for comparing the dissolution of drugs that have good solubility and intermediate release rate (Dash *et al.*, 2010).

The Baker-Lonsdale model was developed from the Higuchi model and is expressed via equation 15:

$$3/2 [1-(1-M_t/M_\infty)^{2/3}] – M_t/M_\infty = kt \quad (15)$$

Where M_t is the amount of drug dissolved at time t and M_∞ is the amount of drug dissolved at an infinite time. The parameter k corresponds to the slope of a linear graphical presentation relating the left side of the equation and the time. This model can be applied to microcapsule formulations or microspheres (Dash *et al.*, 2010).

In terms of the Hopfenberg model, Hopfenberg developed a general mathematical equation, equation 16, that correlates the drug dissolution from surface-eroding polymers so long as the surface area remains constant during the degradation process:

$$M_t/M_\infty = 1-[1-K_1t(t-l)]^n \quad (16)$$

Where M_t is the amount of drug dissolved at time t, M_∞ is the amount of drug dissolved at an infinite time and K_1 is equal to K_0/C_0a_0 (k_0 is the erosion rate constant, C_0 is the initial concentration of drug in the matrix and a_0 is the initial radius for a sphere or cylinder). The model comes with the assumption that the rate-limiting step of drug dissolution is the erosion of the matrix itself and that the time-dependent diffusional resistance internal or external to the eroding matrix, does not influence it. It was developed to describe dissolution from surface-eroding devices such as slabs, spheres and infinite cylinders displaying heterogenous erosion (Ramteke *et al*., 2014).

1.8.4 Application and selection of models

The models can be applied to the dissolution data manually by plotting the graphs associated with each model, as described in section 1.8.3. Linearity is used to identify the model that is most appropriate for the data set. Otherwise, a newly developed program by Zhang et al., (Zhang *et al.*, 2010) can be used. The DDSolver program was developed to facilitate the modelling and comparison of drug dissolution data, where it fits the data with non-linear optimization techniques using Excel spreadsheet. The program automatically calculates all the parameters associated with each model, especially the R^2, and facilitates the complicated calculations associated with dissolution data analysis. This provides the advantage of minimising calculation errors and time and hence provides a quicker method to screen for the most appropriate model to apply.

There are various criteria for the selection of the mathematical model to be applied to dissolution or release profiles. The selected model should be able to predict future data, without being too highly sensitive to small changes in data. The most widely used method employs the coefficient of determination, R^2, to assess the fit of the model equation. This method is often used when the parameters of the model equations are

similar. However, since this value inevitably increases with more model parameters, when the number parameters of the comparing equations are different, a modification is incorporated in this technique. Instead, an adjusted coefficient of determination is used to assess the fit of the model and this is given by equation 17:

$$R^2 \text{ adjusted} = 1 - \{[(n-1)/(n-p)][1-R^2]\} \quad (17)$$

Where n is the number of dissolution data points and p is the number of parameters in the model. The best model is the one with the highest R^2 or adjusted R^2 value.

Other criteria used include the correlation coefficient (R), the sum of squares od residues (SSR), the mean square error (MSE), the Akaike Information Criterion (AIC) and the F-ratio. The AIC is a measure of goodness of fit based on maximum likelihood and the model that provides the lowest AIC value is regarded as the best fit model (Bozdogan, 1987). This method is only appropriate when comparing models using the same weighting scheme and requires calculation of the weighed sum of the SSR.

1.9 Models for characterising the pharmacokinetics of OIPs

Following aerosol drug deposition and dissolution in the lung, the particles are absorbed through the pulmonary membrane barriers primarily via diffusion (Hastedt *et al.*, 2016). It has been reported that for low molecular weight drugs, the intrinsic lung absorption rates are generally fast with absorption half-lives ≤ 1 h, irrespective of lipophilicity (Hastedt *et al.*, 2016). The permeability of a compound across the epithelial membrane is dependent on a combination of its lipophilicity, molecular size and charge (Fan and de Lannoy, 2014). Small molecules that are highly water-soluble permeate readily via paracellular transport through tight junctions between epithelial cells, whereas small lipophilic compounds cross the cell membrane via passive diffusion down a concentration gradient. Exceptions may occur if small compounds are also substrates for efflux transporters that can limit their net permeation across the membrane and there may be exceptions to the above general rule, if there is sustained binding or slow dissociation from the lung membrane components such as the target proteins or if there

are any intracellular trapping (Patton *et al.*, 2010). These intrinsic properties of lung absorption or permeability can be studied via *in vitro* lung epithelial cell monolayer systems, such as using Calu-3 cells (Forbes and Ehrhardt, 2005). Since permeability values are well-correlated with the *in vivo* rate constants (Ka) for lung absorption in animals, this makes them useful in rank ordering and screening drugs with respect to their intrinsic lung absorption rates. However, in the lung, the absorptive elimination is in kinetic competition with non-absorptive elimination such as mucociliary clearance from the upper regions of the lungs, making it more complicated to predict inhaled drug absorption. Consequently, the overall performance of an inhaled drug i.e. its local therapeutic lung effect and systemic adverse effects not only depends on its intrinsic absorption and permeability properties, but also on the aerosol formulation, device, delivery and drug dissolution properties which contribute to determination of their PK/PD profiles. For example, it has been reported that a poorly soluble and highly permeable selective glucocorticoid receptor modulator caused a 2-fold change in PK profiles, the Cmax and AUC, in humans following inhaled delivery from different dry powder inhalers and nebulizers, and this was attributed to the differences in dissolution rate (Leach, Davidson and Boudreau, 1998). Hence, dissolution data has a potential to provide relevant PK/PD outcomes or predictions for aerosol drugs, via application of compartmental modelling or computational simulations. Generally, modelling dissolution profiles in this manner is a useful technique to help develop IVIVC, which can ultimately help reduce costs, speed up product development and reduce the need to perform costly bioavailability human volunteer studies.

1.9.1 Compartmental PBPK modelling

To predict the pharmacokinetic behaviour of OIPs in humans using preclinical data, physiologically-based pharmacokinetic (PBPK) modelling and computer simulations can be carried out. PBPK modelling is gaining popularity in drug discovery and development and is utilised to have a better understanding on the absorption, distribution, metabolism and excretion (ADME) of a drug candidate as well as explore the effects of age, ethnicity

or disease state on human pharmacokinetic and hence help guide dose and dose regiments (Zhuang and Lu, 2016).

PBPK models are made of compartments corresponding to the different physiological organs of the body of the species of interest, linked by the circulating blood system. Each compartment is described by a tissue volume and each tissue is defined as either perfusion-rate limited or permeability-rate limited. Perfusion-rate limited kinetics often applied to small lipophilic molecules when the blood flow to the tissue is the limiting process of absorption (Jones *et al.*, 2015). Permeability-rate limited kinetics occurs for larger hydrophilic drugs where the permeability across the cell membrane is the limiting process of absorption (Jones *et al.*, 2015).

It has been suggested through previous studies, that factors that increase the lung residence time such as slow dissolution, low permeability and hence slow absorption and intracellular trapping, tend to increase pulmonary targeting of drugs following inhalation (Tayab and Hochhaus, 2005; Olsson *et al.*, 2011; Weber and Hochhaus, 2013). Consequently, since mucociliary clearance only occurs in the upper regions of the lungs, an optimal dissolution rate would further maximise pulmonary targeting. Based on these theories, many realistic compartmental lung deposition kinetic models have been developed for poorly soluble corticosteroids, incorporating regional lung i.e. central and peripheral deposition, dissolution rate-controlled absorption and mucociliary clearance (Tayab and Hochhaus, 2005; Gray *et al.*, 2008; Weber and Hochhaus, 2013; Sakagami, 2014; Fröhlich *et al.*, 2016; Salar-Behzadi *et al.*, 2017). There has been reported success in these models simulating and describing the different PK profiles of poorly soluble fluticasone propionate (FP) formulated in various inhaler products, while yielding its lung region-independent, dissolution-controlled slow absorption rate with a half-life of approximately 3.5 h (Tayab and Hochhaus, 2005; Weber and Hochhaus, 2013). Another study implied that *in vitro*-based mean dissolution times may be an indicator for the *in vivo* lung absorption rates of slowly-dissolving, lipophilic corticosteroids such as FP and budesonide (Möllmann *et al.*, 1998).

1.9.2 *In-Silico* (computational) PBPK modelling

More current studies tend to utilise mechanistic computer-based modelling to provide a better understanding on how deposition, dissolution, clearance and absorption influence the clinical performance of an inhaled product. An example of a computational model is the GastroPlus™ (Simulations Pluc Inc). The concept behind these models includes the use of computational fluid dynamics (CFD) simulations that can capture aerosol formation, inhaler-patient interface, airway deposition and PK. Generally, the CFD process subdivides the geometry into small discrete volumes which then make up the grid or mesh.

One-dimensional (1D) algebraic approaches, such as ICRP-96, treat the airways as a series of filters in which gravitational settling, diffusion and impaction are competing deposition processes and this helps with the interpretation of drug exposure data (Forbes *et al.*, 2015). However, more recently with CFD modelling, transport equations are solved in realistic 3D geometries, which are constructed from medical scans and literature data, providing improved predictions of aerosol deposition on airway surfaces (Forbes *et al.*, 2015).

Benefits of *in silico* modelling have been demonstrated extensively. In a study conducted by Olsson and Backman in 2014 for example, where they developed a mouth-throat model to mimic the *in vivo* situation and predict initial total lung deposition, evaluation of the results demonstrated that the shape of the plasma PK profile was well predicted by the mechanistic model (Olsson and Bäckman, 2014). It was demonstrated in the study that computational methods based on the ex-throat particle size distribution and knowledge of the biopharmaceutical properties may allow modelling regional distribution, dissolution, clearance and absorption and therefore help predict the pulmonary bioavailability of drugs. Consequently, in a study conducted by Wu et al, it was found that the data such as lung bioavailability and drug plasma levels were simulated well by the GastroPlus™, since they corresponded to the *in vivo* data in healthy individuals (Wu *et al.*, 2014). The findings suggested that since the GastroPlus™ *in silico* modelling software correctly identified changes in lung deposition upon changes in the

tidal volume and airflow, it could be suitable for identification of most promising candidate formulations in the context of development of inhaled compounds at reduced costs.

1.10 Fluticasone Propionate as the model drug

Dissolution is likely to be a key rate-limiting step for the systemic absorption of OIPs containing drugs or formulations with low aqueous solubility (Forbes *et al.*, 2015; Hastedt *et al.*, 2016). Poor solubility has shown to be a major problem encountered with formulation development of new chemical entities and for generic drug/formulation development (Gowthamarajan and Singh, 2010). Hence, meaningful dissolution tests for such products are particularly useful to both the pharmaceutical industry and the agencies that regulate them.

The challenges associated with this include developing and validating the dissolution test method, ensuring the method is appropriately discriminatory and addressing the potential for IVIVC (Rohrs, 2001). Satisfying these challenges have proven to be a large task, because the extent of release is too low i.e. it is difficult to get 100% of the dosage form to dissolve and the rate of release is too slow i.e. it is difficult to get dissolution fast enough for a convenient test. Thus, drugs with limited water solubility provide an excellent starting point to developing dissolution tests for OIPs since tests that provide discriminatory outcomes using these drugs, have the potential to be developed as appropriate and universal dissolution system for all types and classes of inhaled drugs.

Examples of inhaled drugs that possess the property of poor aqueous solubility include fluticasone propionate (FP), beclomethasone dipropionate, budesonide and ciclesonide. FP, in particular, has been subject of many dissolution studies, used as a comparator for the remainder of inhaled compounds (Davies and Feddah, 2003; Arora *et al.*, 2010; May *et al.*, 2014). FP is a neutral glucocorticoid administered by inhalation, either as a DPI, pMDI or nebulisation formulation, as a first line treatment of chronic obstructive pulmonary disease (COPD) and asthma allergic rhinitis. It is often delivered

alone under the brand names Flovent® or Flixotide®, and available in varied strengths such as an Accuhaler of 50, 100 and 250 µg strengths or Evohaler of 50, 125 and 250 µg strengths. However, FP is also available in combination with other drugs such as salmeterol, a long-acting β2-andrenergic agonist, under the brand names of Advair® or Seretide®. FP predominantly works on the air passages in the lungs to help inhibit the inflammatory processes responsible for causing airway obstruction associated with both diseases. It is often required as a long-term preventer inhaler, not to help control asthma immediately.

With regards to its physicochemical properties, it is highly hydrophobic with a low aqueous solubility of approximately 0.1 µg/mL (Hastedt *et al.*, 2016). It exhibits a log P value of 4.5 and a high molecular weight of 500.6 g/mol. Due to its properties, FP exhibits slow dissolution rates and since both DPI and pMDI formulations deliver solid FP particles to the lung, these formulations often tend to rely on API particle size reduction techniques in order to modify dissolution rates (Patel *et al*., 2008). Consequently, FP has been shown to present a challenge in attempting to maintain sink conditions or ensure reproducible data are obtained when developing dissolution systems for OIPs (Rohrschneider, 2012; May, 2013). For these reasons, FP was selected as the model inhaled drug throughout this study.

Aim & Objectives

Despite increasing interest in dissolution as a critical product attribute determining the performance of inhaled pharmaceuticals, there is yet no standard dissolution technique for OIPs. To date, ad hoc comparisons have been made to dose collection and dissolution methods to discern the most promising dissolution techniques for development; however, there is still a need to understand and evidence the factors that make a dissolution system reliable, representative of the lung environment and suitable for QC purposes or for the establishment of IVIVC. Using FP as a model drug, the major aim of this thesis was to develop dissolution methods for OIPs and determine their advantages and limitations.

To address this aim, the specific objectives were:

(1) To explore the critical parameters of dissolution tests and identify where improvements are required.

(2) To design a biologically-based simulated lung fluid (SLF) that can be applied to dissolution systems for OIPs, based on the recognition on the lack of biorelevant medium currently available

(3) To assess the impact of using SLF in dissolution testing

(4) To discern the interaction and impact of variables relevant to a biorelevant dissolution system for OIPs

(5) To measure the dissolution of different inhaled formulations, using dissolution system developed through in accomplishing the aforementioned objectives

Chapter 2

Development and evaluation of the dissolution methods

2.1 Introduction

It has been established that dissolution testing is widely and routinely employed within the pharmaceutical sector, for various pharmaceutical formulation types, underpinning both their development and quality control. Characterising and controlling the dissolution rate of inhaled active ingredients, particularly those designed for systemic therapy, would enable tailoring of formulation properties, dosing levels and dosing frequencies. It would allow the study of drug-release mechanisms, enable batch-to-batch consistency, monitoring of formulation stability and demonstration of bioequivalence between formulations (Burmeister Getz *et al.*, 2016). Consequently, for the assessment and implementation of a Quality by Design of any pharmaceutical product, the dissolution rate of the product is typically a Critical Quality Attribute. This is because the PK of a drug is very sensitive to differences in dissolution and its regional deposition, which affects the absorption and permeation rates of the drug (Hochhaus *et al.*, 2015). Hence, a clear understanding of dissolution is important to obtaining an IVIVC insight (Cardot *et al.*, 2007) and an important requirement for the proposed development of a BCS for inhaled medicines. The IPAC-RS Dissolution Working Group concluded that dissolution testing would certainly be a valuable technique in the development of inhaled dosage forms; it can be used as a selection tool for drug substances and formulations and as a quality test. Yet, as mentioned in Chapter 1, it is not currently recognised as a key *in vitro* investigation, during drug R&D processes for OIPs.

However, over the years there have been several reports assessing the implications of dissolution testing for inhaled products or proposing different methodologies for assessing the dissolution behaviour of OIPs (Davies and Feddah, 2003; Son and McConville, 2009; Arora *et al.*, 2010; Son *et al.*, 2010; Riley *et al.*, 2012; Rohrschneider *et al.*, 2015). Of these methods, two are emerging as the predominant choices for measuring dissolution, (i) the Rotating Paddle dissolution apparatus and (ii)

the Transwell® system. It was identified and concluded by the research conducted by Sabine May, where comparisons were made between various proposed dissolution methods, that these two techniques are the most suitable for inhaled formulations, capturing a suitably representative sample for OIP dissolution testing (May *et al.*, 2012, 2014). The Transwell system provides a platform that can represent the lung environment because it allows drug particles to dissolve in a limited volume of medium and can be configured to provide sink conditions for the dissolution of drugs. It has been adapted to allow the application of aerosols to cell layers, for transport and permeability studies or for the investigation of the effects of biorelevant medium or physiological surfactants on the dissolution of OIPs, moving towards potentially establishing IVIVC (Davies and Feddah, 2003; Meindl *et al.*, 2015). However, a theoretical limitation to the system is the presence of the membrane which creates a diffusion barrier and limits the rate of drug transfer to the receptor compartment. This has led to modification of the system and assessment of alternative membranes on the dissolution of drug particles (May *et al.*, 2014; Rohrschneider *et al.*, 2015). In terms of the rotating paddle method, the principle advantage is the use of USP 2 standard apparatus, which can be used in conjunction with different types of aerosol particle collection methods (Riley *et al.*, 2012). It uses a large volume of dissolution medium which readily provides sink conditions. This system has also been under development, to optimise its ability to evaluate the dissolution of inhaled formulations. In a study by Son et al, particles were collected on a filter paper placed on a cup in the NGI then transferred this to the dissolution vessel (Son *et al.*, 2010). An alternative method has been proposed, where the aerosol particles are collected directly onto a stainless-steel filter and placed directly into the dissolution bath (Mees *et al*., 2011). However, a limitation to these methods is the inability to collect evenly-distributed drug particles on the surface of the filter, since the particles tend to clump on the central region (Price, 2015).

These limitations suggest that the current *in vitro* aerosol collection and dissolution testing methods are not as reliable and predictable of the *in vivo* performance of the drug as anticipated. Hence, it provides motive to further develop and evaluate these systems

to overcome the pitfalls associated with them. During the development of a dissolution system, before any type of IVIVC can be considered, it must be realised that the dissolution test can be used to make a comparison between formulations under standardised conditions. Consequently, the test, just like any other *in vitro* test, must be sufficiently reproducible so as to provide confident results and also be very easy to set up and easy to use.

Aim:

In this chapter, using FP as the model drug, the aim was to develop and compare the dissolution methods based on a pharmacopoeial standard dissolution apparatus (rotating paddle) and a diffusion labware apparatus (Transwell system) as suitable dissolution systems for the evaluation of OIPs. The comparisons would allow the exploration of the critical parameters required for a dissolution test and would help identify the most robust, simple, easy to conduct, repeatable and reliable methodology, that is sensitive to differences and able to discriminate between profiles of different inhaled formulations.

Objectives:

To reach the aim, the objectives were to, (i) validate a RP-HPLC-UV for analysis and quantification of FP in the dissolution media, (ii) develop the TSI/Transwell® system and the NGI/Rotating Paddle system (iii) compare and evaluate the performance of both systems and their suitability for orally inhaled products.

2.2 Materials

For FP assay validation, micronized FP (USP grade, purity 98%) was supplied by LGM pharma Inc (Boca Raton, USA). Flixotide® 50 µg Evohalers were provided by GSK. For mobile phase preparation, HPLC-grade methanol (MeOH) and HPLC-grade water were supplied by Fischer Chemicals (Loughborough, UK). Ammonium acetate was supplied by VWR International Ltd (Lutterworth, UK). Sodium Dodecyl Sulphate Lauryl (SDS) was obtained from Thermo Fisher Scientific (Paisley, UK) and Phosphate Buffer Saline tablets (PBS) were purchased from Sigma-Aldrich Ltd (Dorset, UK). Whatman Grade GF/A glass microfiber filter sheets were purchased from Scientific Laboratory Supplies Ltd (Nottingham, UK). The equipment/glassware necessary for the setup of the Twin Stage Impinger (TSI) were purchased from Copley Scientific Limited (Nottingham, UK). The equipment necessary for the setup of the rotating paddle dissolution system were provided by Copley Scientific Limited (Nottingham, UK).

2.3 Methods

2.3.1 Validation of RP-HPLC-UV for assay of FP

Validation was carried out using a calibration series prepared over a concentration range of 0.05-10 µg mL^{-1}. A 100 µg mL^{-1} FP standard solution was prepared in 50% v/v MeOH in water, by accurately weighing out 10 mg of FP powder and making it up to 100 mL; dissolving by sonication, before being made up to final volume. The calibration series was prepared by serial dilution of the standard solution to achieve the desired concentration range.

Linearity of peak area response was determined by replicate injections (n=6) of each of the eight concentration standards. The relative standard deviation (%CV) of the peak area of the six injections was used to estimate instrument precision. For intra-day variability, the calibration standard series prepared on day 1 were re-analysed three times and the %CV at each of the concentration levels was calculated. For inter-day variability, two further calibration curves were analysed by the preparation of a fresh

series of calibration standards on days 2 and 3. The concentration was the same from day-to-day since same weight of FP was ensured during the preparation of the standard solution. The %CV at each of the concentration levels was calculated. Additionally, linearity of the combined data from the three calibration curves was determined. The limits of detection (LOD) and limits of quantification (LOQ) were calculated based on equations (18) and (19) respectively (ICH, 1996):

$$LOD = 3.3 \times [SD/slope] \quad (18)$$

$$LOQ = 10 \times [SD/slope] \quad (19)$$

Where SD is the standard deviation of the y estimate and slope is the gradient of the line, obtained from linear regression analysis, using Microsoft Excel.

2.3.2 Quantification of FP by RP-HPLC-UV

Quantification of FP in the samples was achieved using a novel, specially developed and validated RP-HPLC-UV method (Waters 2795 Separations Module). Integration was carried out using an Empower Pro data analysis software. Separation was achieved using a Luna® 3U column (100A, 150 mm x 4.6 mm), packed with C-18 (Phenomenex, Hurdsfield, UK) and maintained at 40°C using a column heater. The mobile phase was a mixture of methanol- 0.6% w/v aqueous ammonium acetate solution (75:25% v/v), filtered through a 0.2 µm nylon membrane (Whatman International Ltd, Maidstone, UK) and with a flow rate of 0.5 mL min^{-1}. The injection volume was 60 µL and samples were analysed in duplicate with a run time of 7 min. Detection was at 240 nm, where the detection wavelength was determined using Waters 2296 Photodiode Array Detector and following injection of a standard solution of FP.

2.3.3 Preliminary evaluation of the novel NGI particle collection method

A Flixotide® 50 µg Evohaler was actuated 10 times to produce a loading dose of 500 µg in the NGI. The filter paper was removed from the filter holder and small sections of the filter were pierced out in the centre and outer skirts of the paper, as well as in the middle of the sections. These sections were dissolved into 1 mL methanol and then injected into the RP-HPLC-UV for quantification of FP.

2.3.4 Deposition and dissolution of FP by NGI and USP2 Rotating Paddle system

The NGI was used to collect particles for evaluation of the rotating paddle dissolution system, using apparatus provided by Copley Scientific Ltd (Nottingham, UK). It was adapted for collection of particle using a filter-holding device, which is primarily designed for the archival calibration of the NGI (Marple *et al.*, 2003). The method is presented in Figure 2.1. The fine particle fraction of the inhaler was collected using the next generation impactor (NGI). The NGI lid was replaced with a 'Flow Access' lid provided by Copley Scientific Ltd. After stage 2, the cover on the access port was removed and a filter holder, retaining a 47-mm diameter of GF/A glass microfibre filter paper, was attached via the O-ring. The Flixotide 50 µg Evohaler was connected to the NGI via a mouthpiece adaptor and actuated into the NGI 10 times to produce a mass loading of 500 µg. Deposition was carried out at a constant air flow of 48 L/min, produced by a vacuum pump (Copley Scientific Limited, Nottingham, UK). Following deposition, the filter paper was removed carefully, sealed onto a circular glass tile and immediately transferred into a vessel containing 900 mL of the dissolution medium (50% v/v MeOH: H_2O). The paddle was set to rotate at 50 rpm, and 1 mL sample at each time point (2, 5, 10, 15, 30, 45, 60 min) was removed using a syringe and placed into a HPLC vial for analysis. At 60 min, the filter paper was removed and placed into a glass beaker containing 50 mL of pure methanol to recover the deposited amount of FP. The beaker was sonicated for 20 min and then left aside until at 180 min, when 1 mL of sample was removed for analysis by HPLC. The tests were performed at ambient temperature and data was collected in triplicate.

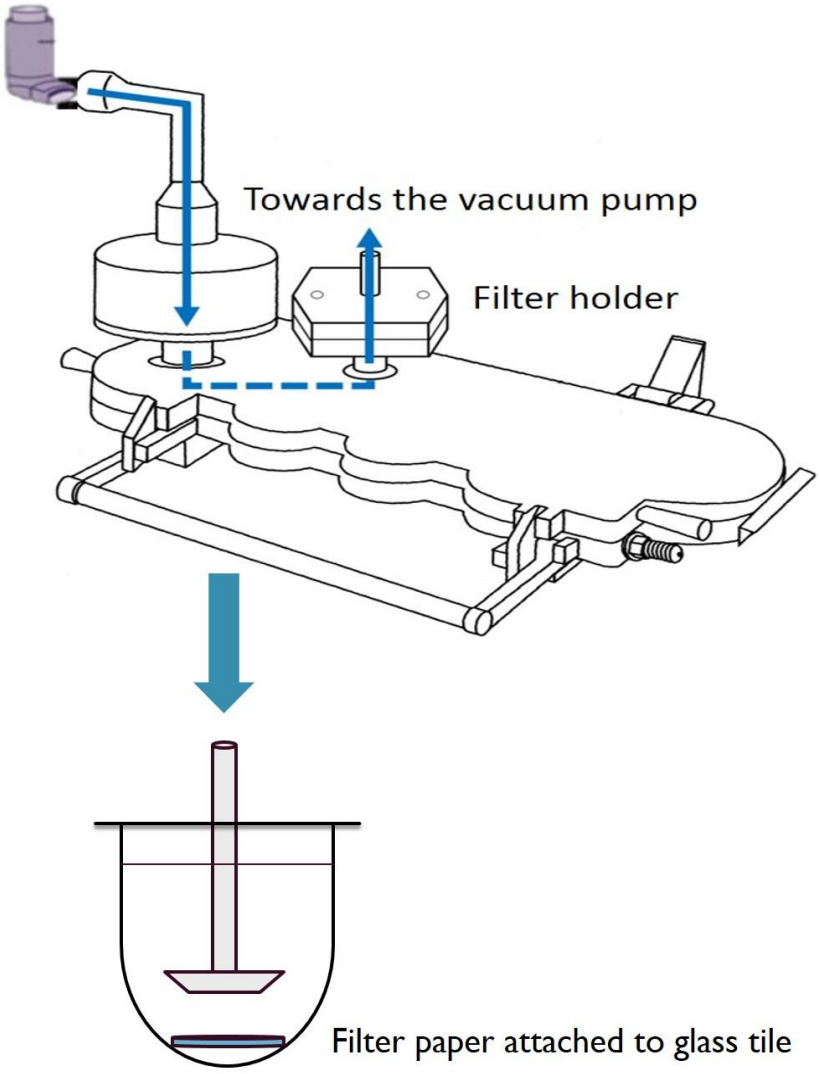

Figure 2. 1. A schematic diagram of the NGI/rotating paddle dissolution system.

2.3.5 Deposition and dissolution of FP by TSI and Transwell® dissolution system

The twin stage impinger was used to deposit respirable particles onto the surface of the Transwell insert, which was adapted as described by Arora et al (Arora *et al.*, 2010) and is presented in Figure 2.2. A Transwell® insert (Corning, UK) with a 0.45 μm pore polyester membrane was placed into the lower impingement chamber of a TSI to collect the fine particle fraction of the inhaler (particles < 6.4 μm). The upper bulb of the TSI was filled with 7 mL of the dissolution medium. The Flixotide® inhaler was connected to the TSI inlet via a silicone rubber mouthpiece adaptor and actuated into the TSI, to emit a total mass of 500 μg. Deposition was carried out at a constant air flow of 60 ± 1 L/min, produced by a vacuum pump (Copley Scientific Ltd). Following deposition, the Transwell donor chamber was filled with 100 μL solvent system (50% v/v MeOH:H_2O) and transferred immediately into a well of a 24-well plate containing 600 μL of the dissolution medium. At each sample time point (2, 5, 10, 15, 30, 45 and 60 min), the Transwell insert was moved to a new well containing 600 μL of fresh medium, to ensure sink conditions were maintained and 175 μL of each sample was collected into a HPLC vial for analysis. At 60 min, the total amount of FP particles deposited on the membrane was recovered by removing the 100 μL on the membrane and adding it to the 600 μL medium in the 180 min well, placing the Transwell insert into the well and adding 100 μL of pure methanol on top of the membrane before leaving it until 180 min was reached. At 180 min, the 100 μL on the membrane was removed and mixed into the well and 175 μL of sample was removed for analysis.

Various types, strengths and batch of Flixotide® inhalers were assessed. The dissolution media utilised in this study were 25%, 50%, 75% and 90% v/v MeOH in water as well as 0.5% w/v SDS in PBS. To quantify FP in 0.5% w/v SDS in PBS, 100 μL sample was removed and diluted with 100 μL MeOH prior to injection into HPLC. The tests were performed at ambient temperature and data was collected in triplicate.

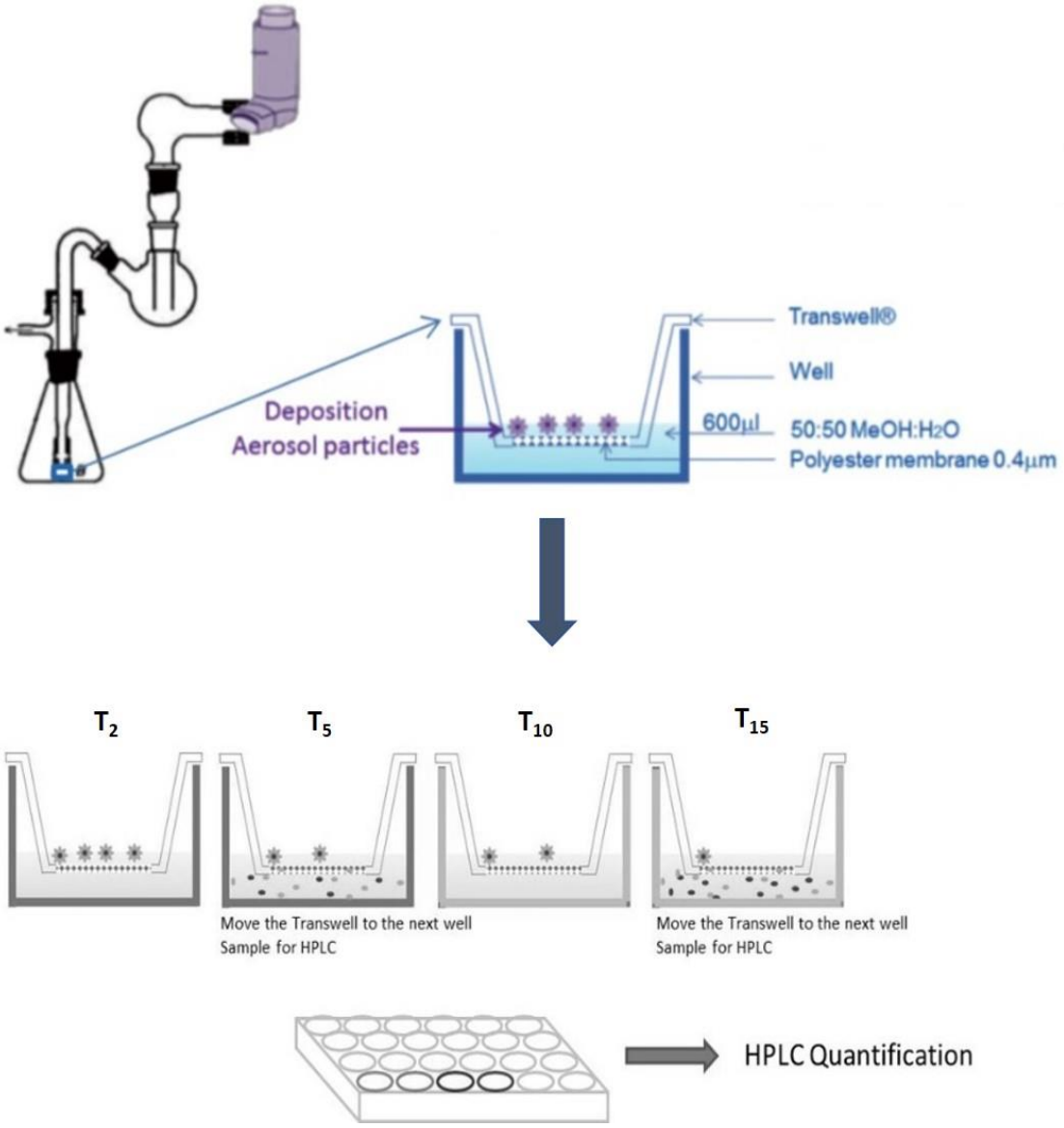

Figure 2. 2. A schematic of the TSI/Transwell® dissolution system

2.3.6 Deposition and dissolution of FP by TSI and fluid-capacity limited Transwell® dissolution system

The dissolution method followed section 2.3.4. However, instead of filling the Transwell donor chamber with 100 µL of the solvent system following FP deposition on the polyester membrane, the insert membrane was pre-wetted with 100 µL solvent prior to its addition to the TSI.

2.3.7 Deposition and dissolution of FP by modified TSI and fluid-capacity limited Transwell® dissolution system

The dissolution method followed section 2.3.5, except that the Transwell membrane was modified, using an adapted method in Rohrschneider et al., study (Rohrschneider *et al.*, 2015). The polyester membrane was removed from the Transwell insert and replaced with a GF/A glass microfiber filter paper, attached via cyanoacrylate.

2.4 Results

2.4.1 Validation of RP-HPLC-UV for assay of FP

The RP-HPLC-UV chromatogram of FP is shown in Figure 2.3. There was no interference of the matrix and good separation peaks were observed. A distinctive FP peak appeared at a retention time of approximately 9.5 min. Validation of the assay and instrument performance, in terms of graph linearity and data precision are shown in Figure 2.4 and Table 2.1, respectively. The curves of the three calibration sets prepared on the same day overlapped perfectly (Figure 2.4a) but the inter-day curves did not. However, each calibration curve displayed very good linearity ($R^2 > 0.999$). Excellent linearity was also highlighted in the combined inter-day data of the three calibration curve sets. The SD value for six replicate injections were very low for all FP concentrations, highlighted by the absence of error bars (Figure 2.4). Accuracy of data generated fell within the accepted range of 85-115% (ICH, 1996), except for FP concentration below 0.25 µg mL^{-1}.

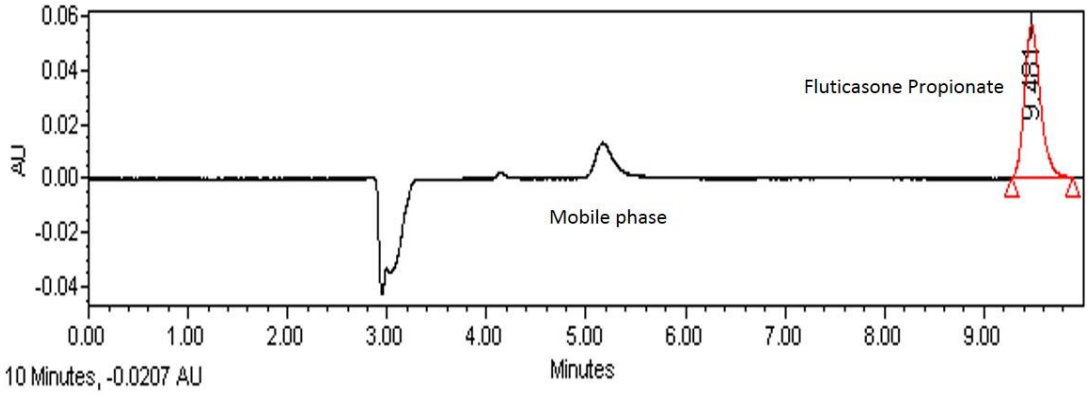

Figure 2. 3. RP-HPLC-UV chromatogram of 10 µg mL-1 fluticasone propionate (FP) solution, where the FP peak corresponds to the retention time of approximately 9.5 min, detected at 240 nm.

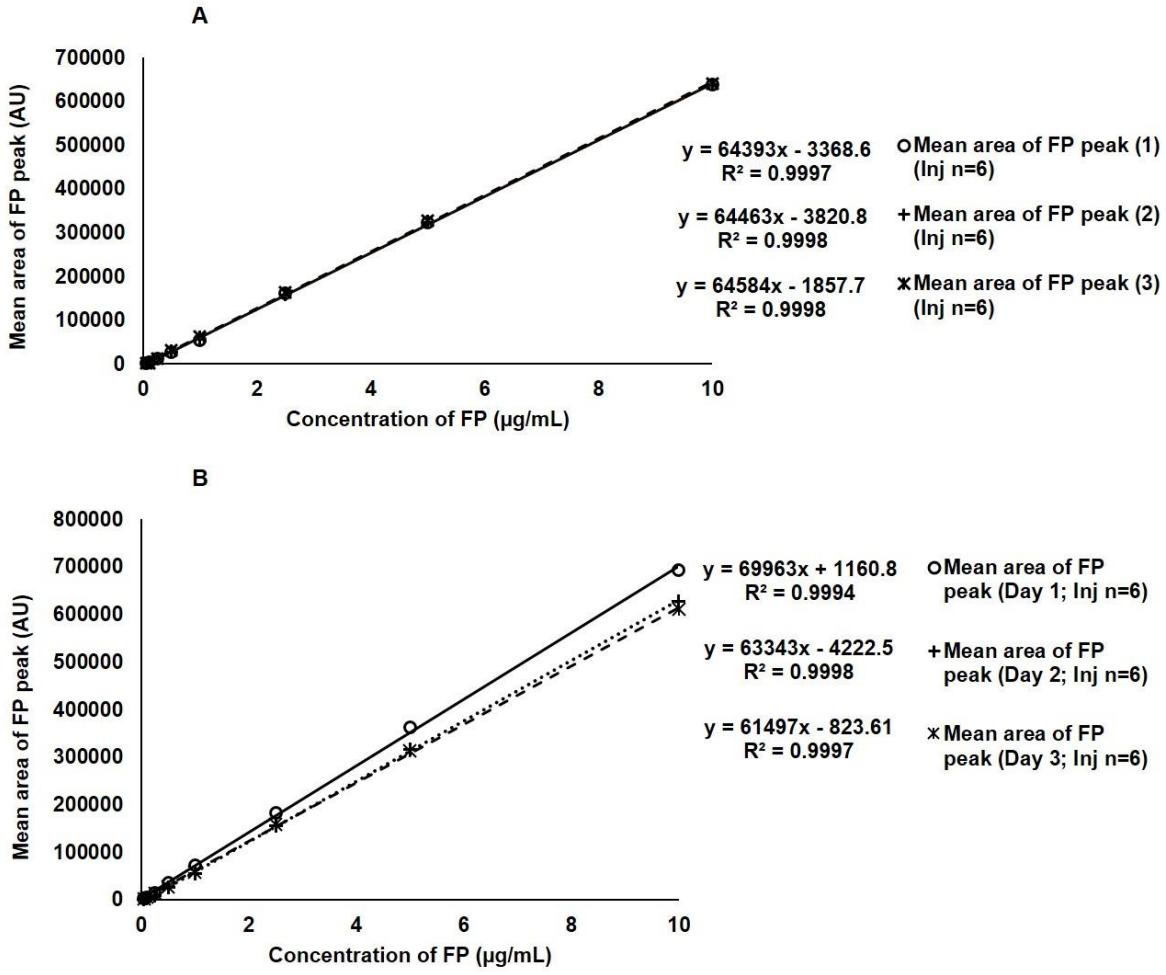

Figure 2. 4. Validation of RP-HPLC-UV for analysis of fluticasone propionate (FP) based on linearity of a) intra-day FP calibration curve sets (3 batches) and b) inter-day FP calibration curve sets. Data obtained expressed as the mean area of FP peak (n=6) ± SD.

Intra- and inter-day variation (Table 2.1) were determined at eight concentration levels (n=6). The %CV for the intra-day and inter-day calibration sets ranged from 0.29 to 2.54 % and 1.94 to 31.65 % respectively, with the %CV exceeding 2% once the FP concentration became below 2.5 µg mL^{-1}.

Table 2. 1. Validation of RP-HPLC-UV for analysis of fluticasone propionate (FP) based on intra-day and inter-day precision evaluation (relative standard deviation, %CV).

Analytical method	Concentration of FP (µg/mL)	Intra-day variation (%CV)	Inter-day variation (%CV)
RP-HPLC-UV	0.05	1.46	31.65
	0.1	2.54	21.05
	0.25	2.39	23.78
	0.5	0.45	5.17
	1	0.78	3.18
	2.5	0.52	2.46
	5	0.45	2.53
	10	0.29	1.94

The limit of detection and limit of quantification calculated using equations (18) and (19) were in the ranges of 0.04 to 0.07 µg mL^{-1} and 0.13 to 0.20 µg mL^{-1} respectively (Table 2.2).

Table 2. 2. Limits of detection (LOD) and quantification (LOQ) for the RP-HPLC-UV analysis of fluticasone propionate.

Analytical method	Day	LOD (µg mL^{-1})	LOQ (µg mL^{-1})
RP-HPLC-UV	1	0.04	0.13
	2	0.05	0.18
	3	0.07	0.20

2.4.2 Preliminary evaluation of the novel NGI particle collection method

The outer regions of the filter paper contained less FP particles in comparison to the middle region, with values being 6.49 ± 0.57 µg and 7.17 ± 0.47 respectively. However, differences in the result was statistically insignificant ($p>0.05$).

2.4.3 Novel NGI/Rotating paddle system as a suitable dissolution method for OIPs

The novel NGI/Rotating Paddle technique was evaluated as a suitable method to assess dissolution of inhaled products. The dissolution of FP from Flixotide® 50, 125 and 250 µg pMDIs, using this method, is shown in Figure 2.5. Regardless of the strength of inhaler, it appeared the dissolution profile of FP was the same, with insignificant differences seen between them. A high percentage of FP dissolved over time, reaching close to 100% by the end of the 60 min experiments. The dissolution of FP from the same batch and different batch of Flixotide® Evohalers/pMDIs is shown in Figure 2.6. Again, it was evident that regardless of the batch the inhaler was selected from, the dissolution of FP was the same. The experiments appeared to be well repeatable, as indicated by the overlap in profiles and the very small error bars associated with each result.

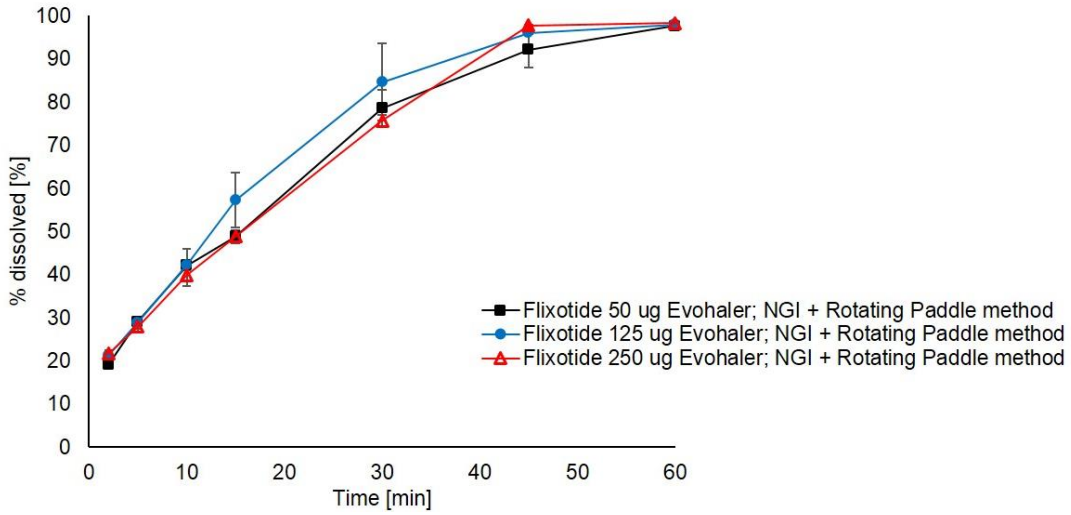

Figure 2. 5. Dissolution profiles of fluticasone propionate from Flixotide® 50, 125 and 250 µg Evohalers (pMDIs) in 50% v/v methanol: water. Profiles obtained from the NGI/Rotating Paddle dissolution method. Data expressed as mean ± SD (n=3).

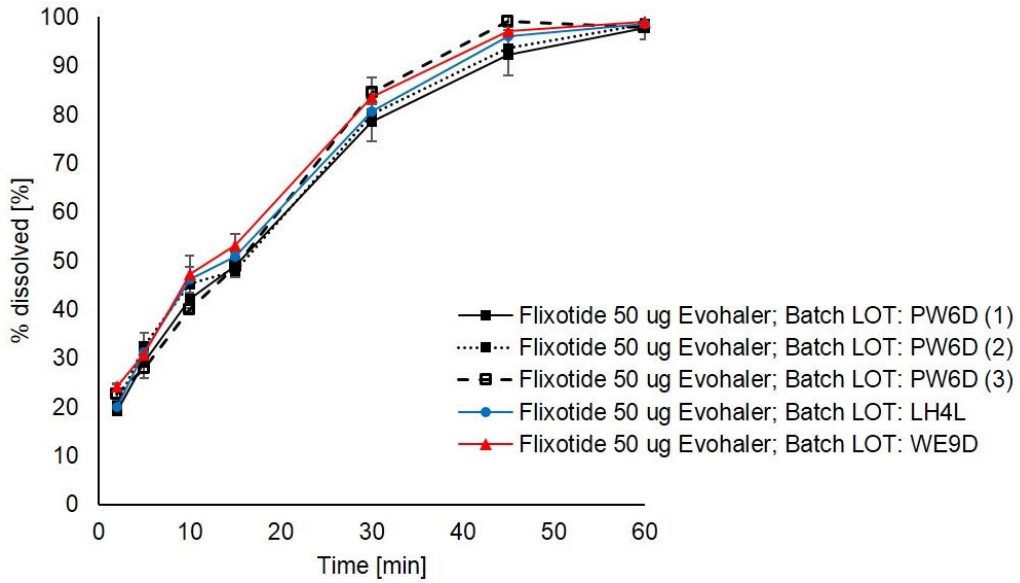

Figure 2. 6. Dissolution profiles of fluticasone propionate from the same and different batch of Flixotide® 50 µg Evohalers (pMDIs), in 50% v/v methanol: water. Profiles obtained from the NGI/Rotating Paddle dissolution method. Data expressed as mean ± SD (n=3).

2.4.4 Preliminary evaluation of the TSI/Transwell® dissolution method for OIPs

To evaluate the performance of the TSI/Transwell dissolution method, experiments were conducted on the unmodified system, to assess its ease of handling and the reproducibility of results, when assessing the dissolution profiles of FP from varied strengths and types of Flixotide® inhalers. The dissolution of FP from Flixotide® 50, 125 and 250 µg pMDIs and Flixotide® 50, 100 and 250 µg DPIs are shown in Figure 2.7. It appeared that the dissolution of FP from Flixotide same strength pMDI and DPI was very close, with some dissolution points overlapping. Dissolution of FP from different strengths of Evohalers and from different strengths of Accuhalers, was also very similar. Insignificant differences were seen between all the FP dissolution profiles, as indicated by the overlap of the error bars associated with each time point.

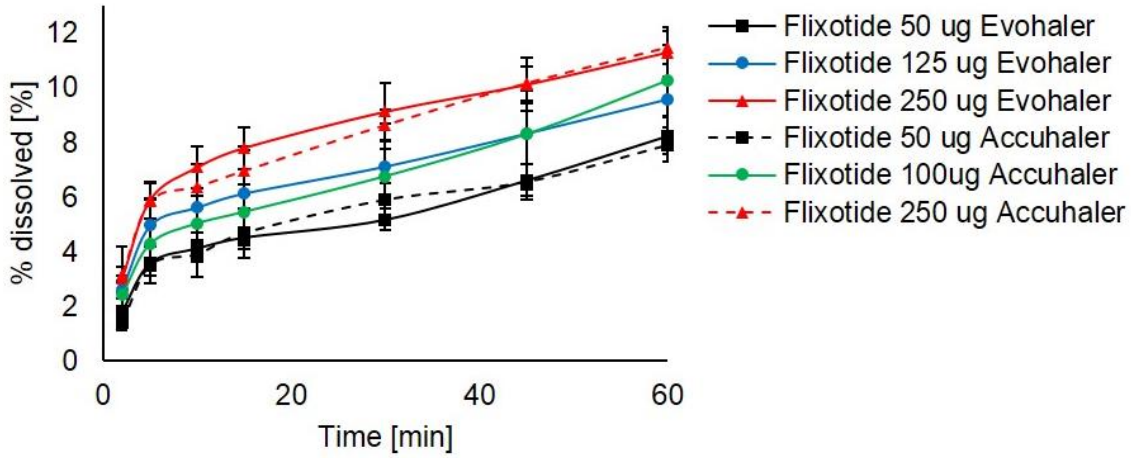

Figure 2. 7. Dissolution profiles of fluticasone propionate from Flixotide® 50, 125 and 250 µg Evohalers (pMDIs) and 50, 100 and 250 µg Accuhalers (Powder/DPIs), in 50% v/v methanol: water. Profiles obtained from the TSI/Transwell® dissolution method. Data expressed as mean ± SD (n=3).

Consequently, the system was evaluated in terms of its ability to identify for any batch-batch differences in inhalers. The dissolution of FP from same batch and different batch of Flixotide pMDIs is shown in Figure 2.8. There was evidently no difference in the dissolution profiles of FP regardless of the batch LOT the inhaler was selected from.

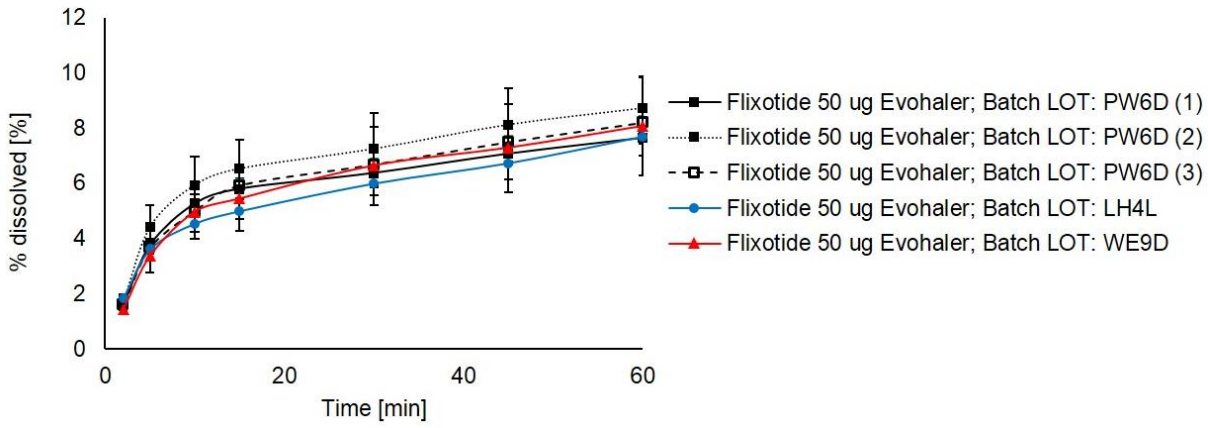

Figure 2. 8. Dissolution profiles of fluticasone propionate from same and different batch of Flixotide® 50 µg Evohalers (pMDIs), in 50% v/v methanol: water. Profiles obtained from the TSI/Transwell® dissolution method. Data expressed as mean ± SD (n=3).

2.4.5 Optimisation of the TSI/Transwell® dissolution method

2.4.5.1 Limiting the fluid capacity on the Transwell® insert

To develop or optimise the TSI/Transwell dissolution method, the fluid in the donor chamber of the Transwell, initially added to mediate FP dissolution, was first limited, in attempt to more closely mimic the *in vivo* environment. Comparisons of dissolution profiles obtained from the unmodified Transwell® dissolution method with the fluid-capacity limited method, is shown in Figure 2.9. The dissolution profiles generated from the Flixotide® inhaler were very low, with a mean % FP dissolved reaching approximately 8% for both the Evohaler® and Accuhaler®, in the original Transwell dissolution method. However, in the fluid-capacity limited method, the % FP dissolved by 60 min reached ≈ 11%. The small-sized and similarity in error bars at each time point, for both methods, indicated that both methods provided relatively reproducible dissolution profiles. However, at all time points, the mean % FP dissolved was significantly higher with the fluid-capacity limited method. Dissolution of FP seemed to follow the same kinetics regardless of the method. The general pattern was, within the first 15 min, the rate of FP dissolution is high, highlighted by the steepness of the curve, after which the rate of dissolution slows down.

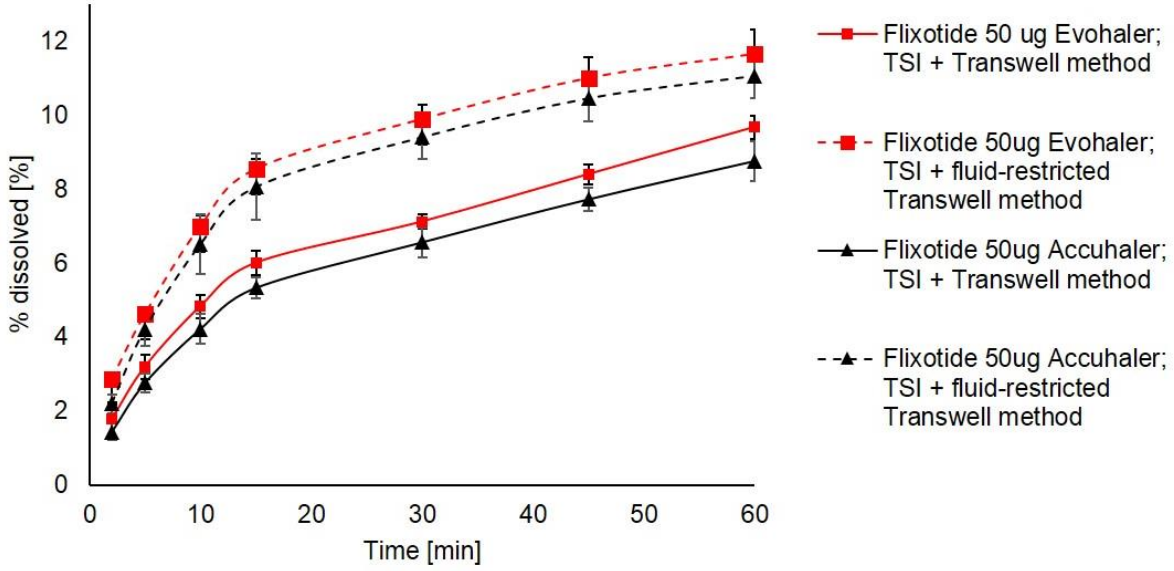

Figure 2. 9. Dissolution of fluticasone propionate from Flixotide® 50 µg Evohaler (pMDI) and 50 µg Accuhaler (powder/DPI), in 50% v/v methanol: water, obtained from the unmodified TSI/Transwell® method and the TSI/Fluid-capacity limited Transwell® method. Data expressed as mean ± SD (n=3).

2.4.5.2 Modification of the Transwell® insert membrane

To develop the TSI/Fluid-capacity limited Transwell system further, the aerosol particle collection surface was modified, such that the Transwell insert collection surface was a GF/A microfibre filter as oppose to the original polyester membrane. The dissolution of FP from Flixotide® Evohalers and Flixotide® Accuhalers, using the TSI/ fluid-capacity limited Transwell method versus the modified TSI/ fluid-capacity limited Transwell method is shown in Figures 2.10a and 2.10b. It was evident that regardless of the inhaler type or the inhaler strength, there was a significantly higher % FP dissolved after 15 min, when using the modified TSI system in comparison to when using the original system.

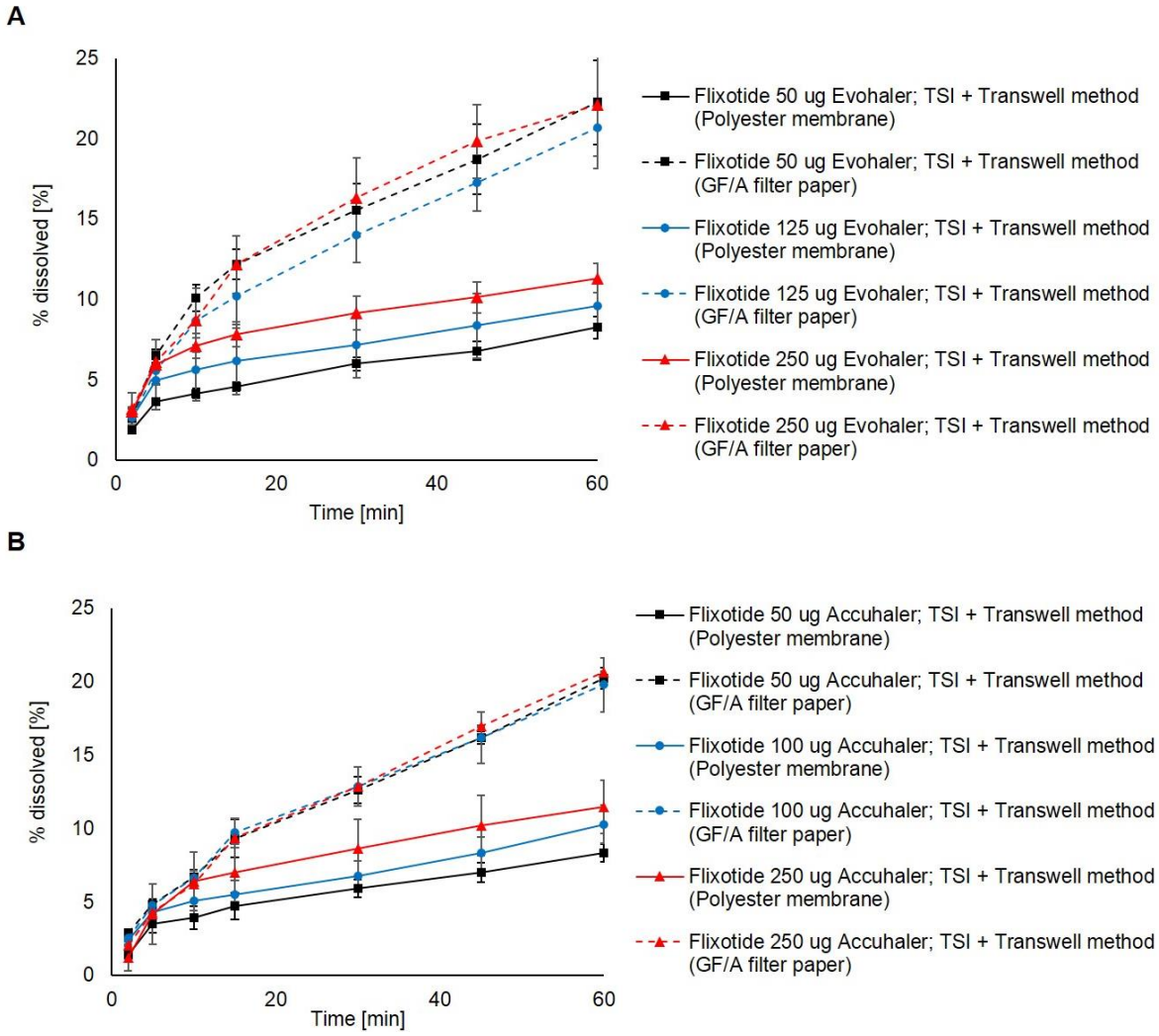

Figure 2. 10. Dissolution of fluticasone propionate from Flixotide® a) 50, 125 and 250 µg Evohalers (pMDIs) and b) 50, 100 and 250 µg Accuhalers (DPIs), obtained from the TSI/Fluid-capacity limited Transwell® method (utilising the polyester membrane) versus the Modified TSI/Fluid-capacity limited Transwell® method (utilising the GF/A microfiber filter). Dissolution media was 50% v/v methanol: water. Data expressed as mean ± SD (n=3).

2.4.6 Comparison of NGI/Rotating paddle and TSI/Transwell dissolution methods

The dissolution of FP from the various strength of Flixotide Evohalers and via the TSI/fluid-capacity limited Transwell method, the modified TSI/ Transwell method and the NGI/Rotating Paddle method is shown in Figure 2.11. It was evident that the % FP dissolved at each time point was highest when dissolution testing was carried out using the NGI/Rotating Paddle apparatus and lowest when using the TSI/fluid-capacity limited Transwell method. Both Transwell systems exhibited a slow and incomplete dissolution of FP in the medium over the investigated time, whereas the rotating paddle enabled a

more complete dissolution, reaching up to 98-99% of the deposited amount. The profiles seemed to be relatively repeatable and reproducible for all methods used.

Comparison of the deposited amount of FP from various Flixotide inhalers, on the filter, when using the TSI and the NGI aerosol collection techniques, was also made. This is shown in Table 2.3. A significantly higher amount of FP was deposited on the GF/A filter paper from the NGI than from the TSI. Consequently, the amount of FP deposited when using the NGI appeared to be a lot more repeatable than from the TSI.

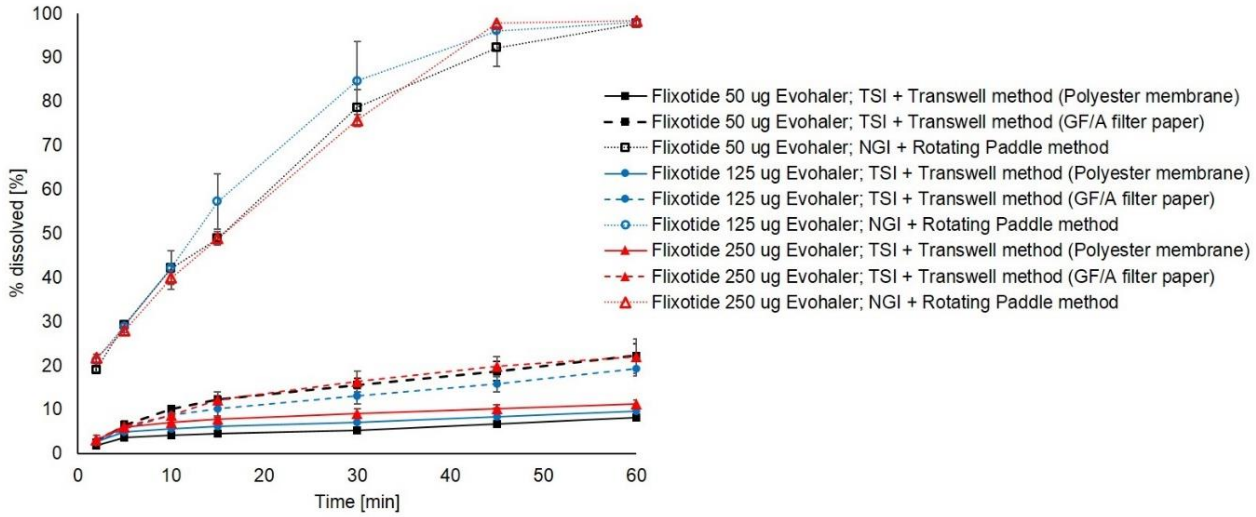

Figure 2. 11. Dissolution of fluticasone propionate from Flixotide® 50, 125 and 250 µg Evohalers (pMDIs), obtained from the TSI/Fluid-capacity limited Transwell® method versus the Modified TSI/Fluid-capacity limited Transwell® method versus the NGI/Rotating paddle method. Dissolution media was 50% v/v methanol: water. Data expressed as mean ± SD.

Table 2. 3. Amount of fluticasone propionate (FP) particles deposited from different strength Flixotide® Evohalers, when collected via the twin stage impinger (TSI) and via the next generation impactor (NGI). Data expressed as mean ± SD.

Inhaler	FP deposited on GF/A filter from TSI [µg]	FP deposited on GF/A filter from NGI [µg]
Flixotide 50µg Evohaler	12.70 ± 1.26	196.50 ± 3.64
Flixotide 125µg Evohaler	8.26 ± 1.85	197.25 ± 1.80
Flixotide 250µg Evohaler	10.59 ± 0.53	197.56 ± 3.64

The dissolution methods were also compared in terms of their sensitivity to differences in the dissolution media applied and their discriminatory ability. FP dissolution profiles in the TSI/fluid-capacity limited, modified TSI/fluid-capacity limited and the NGI/Rotating Paddle systems is shown in Figure 2.12. Difference in dissolution profiles of FP were evident when the dissolution medium composition was changed. Regardless of the dissolution method, an increase in the percentage of methanol in the medium, from 25 to 90% v/v. resulted in an increase in the dissolution rate of FP. 0.5% w/v SDS in PBS was also applied as the dissolution media. In the Transwell system. The dissolution profile of FP in 0.5% w/v SDS in PBS laid between the dissolution profile of FP in 75% and 90% v/v methanol in water. However, in the rotating paddle system, the dissolution profile of FP laid between the profiles obtained using 50% and 75% v/v methanol in water. There was no overlap in the dissolution profiles. There was a clearer discrimination of the dissolution kinetics of FP over time, in the media of different solubilising capacity, when the rotating paddle system was used than in the Transwell system (Figure 2.12 C).

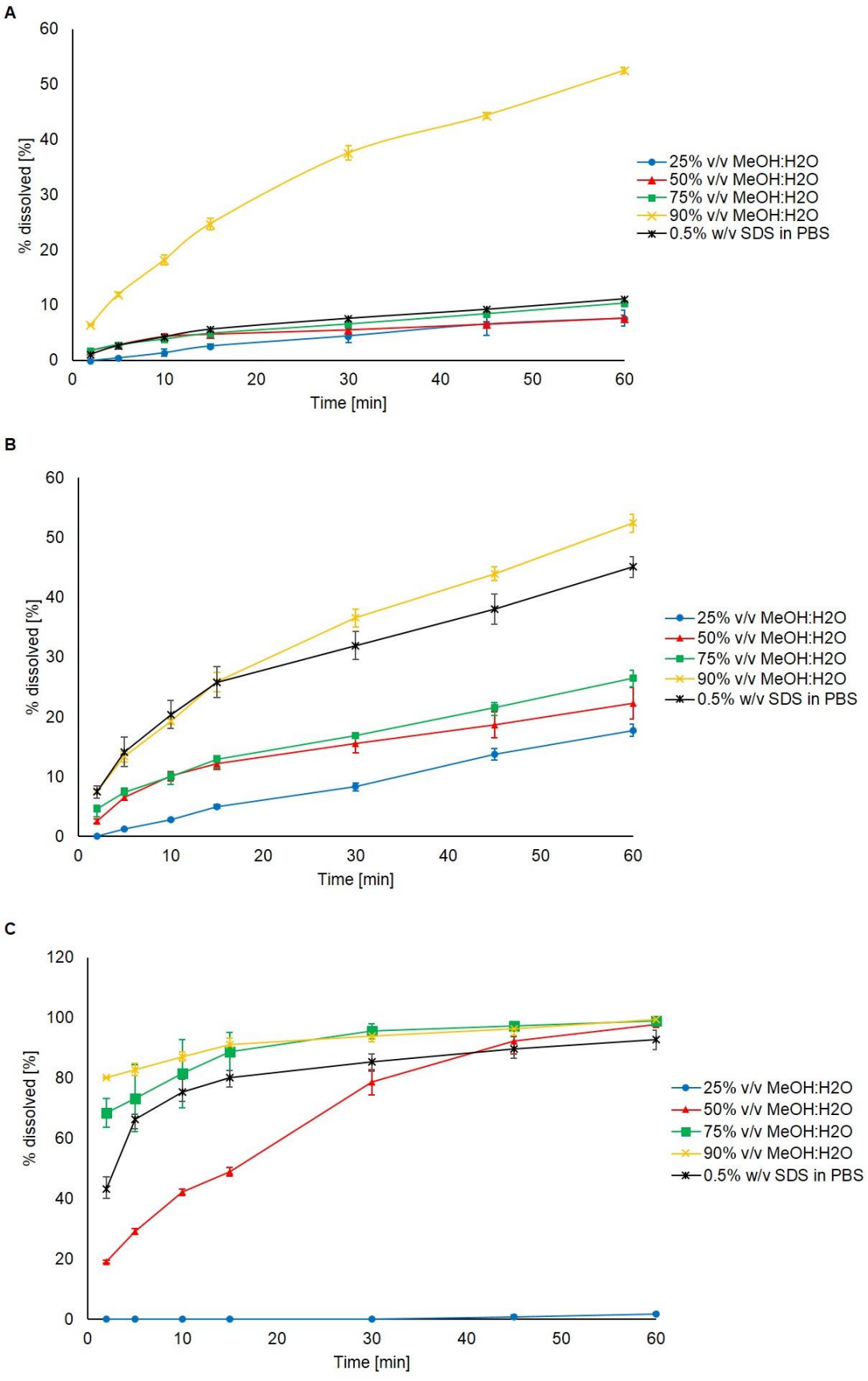

Figure 2. 12. Dissolution of fluticasone propionate from Flixotide® 50 µg Evohaler, in 25%, 50%, 75%, 90% v/v methanol: water and 0.5% w/v SDS: PBS from a) TSI/Fluid-capacity limited Transwell® dissolution system, b) Modified TSI/Fluid-capacity limited Transwell® dissolution system and c) NGI/Rotating paddle dissolution system. Data expressed as mean ± SD (n=3).

2.5 Discussion

The varied propositions of dissolution methodologies for OIPs have continuously been developed and refined, both in terms of the practicalities of use and applicability. The uses and advantages of developing a potential dissolution test, as mentioned previously, underlines the need to obtain sensitive and reliable data from the *in vitro* test utilised. Taking this into consideration, my PhD prioritised evaluating the performance of two dissolution methods, considered to be the most appropriate for OIPs, the TSI/Transwell system and the NGI/Rotating Paddle system, as suitable dissolution methods for OIPs. However, this initially required validation of a HPLC assay to be able to quantify the FP in the dissolution medium applied to these systems.

2.5.1 Validation of RP-HPLC-UV for assay of FP

The suitability of an analytical method to quantify the drug released in a dissolution assay is based on the chemical properties of the drug to be analysed and on its compatibility with the dissolution media, ensuring minimal analytical interference. However, the sensitivity of the method tends to be the predominant limiting factor to the design of dissolution assays. The RP-HPLC-UV detection analysis used in this study is most suitable for microgram quantities of the fine drug particles deposited. For the validation of an analytical method, factors that needed to be explored include accuracy, precision, reproducibility, linearity and robustness. In this study, the RP-HPLC-UV instrument was validated based on methods adapted from to Murnane et al (Murnane *et al.*, 2006) and was generally shown to be suitable for the assay of FP.

The calibration standard series prepared were within the limits of detection. The excellent linearity shown in all calibration curves produced, highlighted the good correlation between FP peak area at 240 nm and the concentration of FP in the sample. The intra-day validation data showed good repeatability and instrument precision, with %CV being < 2.54% at all concentration levels. It indicated that only one set of calibration curve was needed to be prepared on the day of analysing the dissolution samples, since

all three calibration curve sets overlapped perfectly. The reproducibility of the assay, indicated by the data derived for all three calibration curves produced on different days was not as good, producing higher %CV values. This reflected the influence of instrument conditions, which changes from day to day, on quantifying FP and hence, confirmed the need of a new calibration set to be prepared on the day of sample analysis. In comparison to the validation evaluation carried out by Murnane et al, their inter-day data for FP indicated excellent assay reproducibility since the %CV was <2% for all standard concentrations. However, they validated within a concentration range of 2 to 50 µg mL^{-1} and according to the data generated in this study, between 3.5 and 10 µg mL^{-1}, the %CV proved to be equally good (< 2.54%). Therefore, the assay was considered fit for the purpose of this study.

2.5.2 NGI/Rotating paddle system as a suitable dissolution method for OIPs

The novelty of the NGI/Rotating Paddle dissolution method lied with the respirable fraction collection method, whereby the NGI was adapted for collection of particles using a filter-holding device, which is primarily designed for the archival calibration of the NGI. The system presented the advantage of utilising a well-recognised and well-accepted Regulatory standard USP 2 apparatus for dissolution, a rotating paddle. This advantage draws some initial reliability to the potential data obtained. The attempts that have been made to modify the NGI to date have not proven to overcome the key limitation, in which the deposited aerosol particles is very likely to clump within the central region of the filter paper, affecting the reliability of the dissolution results. This novel system was designed to overcome this recognised limitation and potentially allow for an evenly distributed layer of particles to deposit, ensuring adequate repeatable dissolution data for OIPs.

During experimentation, it was recognised that the shape of the filter holder in which the aerosol particles travel through to deposit onto the filter, may not be sufficient to eliminate the associated risk of particle clumping. This is because the filter holder cone is designed at an angle of 30°, which can predispose the particles to travel in a linear direction and not smoothly along the inner walls of the cone. Therefore, this can

cause risk of particle channelling, in which the particles focus their deposition in the central region of the filter. However, in the preliminary experiments carried out to validate the particle collection technique and assess particle deposition, it was evident that the FP particles were evenly distributed on the filter paper. According to the cut-off calculations, attachment of the filter holder to Stage 2 of the NGI and conducting the experiment at a constant air flow of 48 L/min, ensured that only the fine particle fraction (FPF) i.e. particles <5 µm in diameter, deposited on the filter for dissolution. Taking these into consideration, it can be concluded that the novel particle collection technique used here was efficient for the evaluation of the dissolution of OIPs.

To evaluate the performance of the NGI/Rotating Paddle dissolution system overall, various strengths of Evohalers were applied. The results obtained showed excellent repeatability and demonstrated batch-to-batch consistency. This was as anticipated because the variations in the strength and type of inhaler was made for patient suitability or for the improved treatment of lung diseases and should not affect the PK of an inhaled *drug in vivo*. Overall, the system was simple to follow and easy to conduct.

2.5.3 TSI/Transwell® as a suitable dissolution method for OIPs

A challenge towards developing a suitable system to assess the dissolution of OIPs, is the ability of the *in vitro* system to replicate the *in vivo* conditions. For example, to accurately collect the respirable fraction of the drug particles that deposit into the lung, to utilise a limited volume of dissolution media to simulate the limited volume of lung fluid available *in vivo* and replicate the systemic circulation which act as a sink for poor water-soluble drugs, even though the entire respired dose is not soluble in the limited volume. The TSI captures a suitably representative sample of inhaled drugs, allowing only the aerosol particles that are < 6.4 µm in size to deposit on the surface of the filter paper. The Transwell dissolution assay consequently uses a limited volume of dissolution media, the filter paper for deposition was prewetted and 600 µL was used in the receptor chamber. Movement of the transwell insert across the well, containing fresh solvent

system, simplifies the sampling and suggests that sink conditions can be maintained in the receptor chamber. The fact that the dissolution profiles of Flixotide® MDIs and DPIs overlapped and appeared to be identical, with similar kinetics visualised, may be indicative that sink conditions was not reached, with this system, as suggested by the works of Rohrshneider (Rohrschneider, 2012). However, in his studies, only approximately 2% of the deposited amount of drug had dissolved after 5 hours, whereas, in this study, considering a slightly different TSI/Transwell system was used, dissolution reached up to 8% within 1 h of testing, suggesting that my system slightly improved the non-sink condition exhibited by the Transwell. Consequently, the overlap in profiles between the pMDI and DPI, supported the overlap seen in Arora et al., study (Arora *et al*., 2010) and was suggested to be in fact consistent with the *in vivo* pharmacokinetic evidence of no real difference between the pMDI and DPI inhalation in humans (Brindley *et al*., 2000). These replicating characteristics suggested that the TSI/Transwell method has the potential to be developed as both a QC tool and an IVIVC tool, potentially reaching the overarching aim to the study. Hence, it was selected to be evaluated as a suitable system for OIPs.

From the perspective of QC, the dissolution system demonstrated its ability to show batch-to-batch consistency between inhalers and showed that dissolution of FP is independent of the strength and type of inhaler used, similar to the NGI/rotating paddle method. The profile kinetics for FP also very closely matched the FP dissolution profiles obtained from previously reported Transwell dissolution studies (May *et al.*, 2012; Rohrschneider *et al.*, 2015).

2.5.4 Optimisation of the TSI/Transwell® dissolution system

With regards to development of the system, the original TSI/Transwell method required the addition of 100 µL of the solvent system onto the Transwell polyester membrane prior to its introduction to the Transwell dissolution plate. This is because it was originally hypothesised that the addition of a dissolution layer on the membrane would generate better dissolution profiles, with respect to profile reproducibility and

acceleration of the dissolution process (Arora *et al.*, 2010). This is because in the Transwell dissolution system, a diffusion barrier is separating the donor compartment, in which dissolution occurs, from the receptor compartment, in which sampling of the dissolved drug occurs. The fine particles dissolve in the donor chamber fluid before crossing the polyester membrane via gradient diffusion, according to Fick's law (May *et al.*, 2014) so with more fluid available for dissolution in the donor chamber, means the drug particles are exposed to more medium and so the condition presented by the Transwell are less non-sink, in comparison to the more limited volume available for dissolution. Therefore, there would be a faster dissolution rate However, this expected benefit was not given here and a greater dissolution rate was identified in the fluid-capacity limited Transwell system, in which the 100 µl of fluid on the transwell surface was absent. This opposing effect may be attributed to the fact that an extremely limited volume of fluid available for the FP drug particles to dissolve into, results in an even higher concentration of FP in the donor chamber in comparison to the receptor chamber. There is an amplified difference in FP concentration between the donor and receptor chambers, providing a stronger driving force for the diffusion of FP particles in one direction, into the receptor chamber for quantification. The result obtained here was similar to those observed by May et al (May *et al.*, 2014), who recognised that impact of the diffusion barrier is substance dependent.

The TSI/fluid-capacity limited Transwell method was therefore selected to be taken forward for further developments. However, omitting the small volume of dissolution medium in the donor compartment and since there is no stirring of the medium in the receptor compartment, this increases the likelihood of a concentration gradient-based diffusion effect, as described above. Hence, the Transwell membrane was modified in attempt to reduce this effect. The results indicated that the modified Transwell insert caused a significantly higher percent of FP to dissolve in the dissolution medium compared to the unmodified insert membrane. This is because in the Transwell dissolution system, where the insert retained its polyester membrane, both dissolution and diffusion processes were the limiting steps to the transfer of the FP particles from

the donor compartment to the receptor compartment. However, in the modified Transwell system, the filter paper reduced the extent of the rate-limiting diffusion step. The glass microfibre filter was more permeable than the polyester membrane and allowed for faster diffusion of the dissolved drug through to the receptor compartment. Although this diffusion barrier is not always the principle limiting factor (Arora *et al.*, 2010), similar faster rates of dissolution in the modified system have been observed for other poorly soluble corticosteroids (Rohrschneider *et al.*, 2015). In terms of the dissolution kinetics, the modified Transwell system seemed to be well optimised in that the dissolution kinetics of FP from inhalers was a lot clearer, with the profile steeping upwards as oppose to closely reaching a plateau. Regardless of the system used, the dissolution kinetics appeared to approximate to zero-order, whereby a constant amount of drug was eliminated per unit time. However, to understand the kinetics or dissolution mechanism better, the in vitro dissolution data need to be fitted to kinetic models, which was performed and is described in Chapter 5.

Overall, modifying the Transwell in this manner proved to not cause any extra difficulty in operation or make it any less user-friendly. It remained an economic procedure since the Whatmann GF/A filter was not considered expensive. Regardless of the TSI/Transwell dissolution system used, the system was simple to use, experiments were easy to conduct, and the results produced were reproducible.

2.5.5 Comparison of the dissolution methods

Comparisons of the two dissolution systems was made in terms of their simplicity, ease of handling, robustness and discriminatory power. These characteristics were evaluated in experiments which obtained QC-like data on commercially available Flixotide® inhalers, and experiments which measured the influence of the dissolution medium on the dissolution of FP. The comparisons are simplified in Table 2.4.

In terms of using the systems investigated, even those prior to optimisation, all systems proved to be simple to use and relatively easy to handle and operate. However, the NGI/Rotating Paddle apparatus appeared to be more time-consuming to set-up

prepare the particles for dissolution. Preliminary investigations showed that the TSI set-up can be used three times for the same strength inhaler without the need to wash in between, and two 24-well plates would be sufficient to investigate the dissolution of an inhaler in triplicates, in a simultaneous manner. Whereas, in the case of the NGI, preliminary investigations showed poor reproducibility when three vessels and three paddles were used to conduct experiments in triplicate. Therefore, a single vessel was used and required thorough washing in between experiments. Consequently, attaching the filter to the filter holder and securely introducing the filter holder to the NGI apparatus at stage 2 was quite time-consuming and made the method slightly less user-friendly. From an economic point of view, the NGI/Rotating Paddle system was less economic in comparison to the TSI/Transwell system since it required huge amount of solvent system or dissolution media, up to at least 600 mL is required per experiment.

With regards to the deposition and collection of the aerosol particles for dissolution, the NGI allowed for significantly higher and repeatable deposition compared to the TSI. This was because the 47-mm diameter filter paper used in the NGI provided a larger surface area than the Transwell insert, facilitating the capture of up to 40-45% of the loading dose and ensuring the particles were evenly distributed, and hence, a consistent amount deposited. The NGI system was also optimised such that it ensures the FPF is collected, increasing the reliability of the results obtained from the system. In contrast, it is presumed the Transwell insert captures the sub-deposited amount of particles (particles <6.4 μm) and not specifically the FPF, and the amount of particles deposited was significantly lower, ranging between 7 and 14 μg. The inconsistency in the amount deposited is likely attributed to the very small confined surface offered by the Transwell insert filter, increasing the likelihood for particle aggregation. However, it is important to acknowledge that yet, the dissolution profiles obtained from the TSI/Transwell system did not seem to be significantly influenced by this. The large amount of FP deposited via NGI meant that once the filter was placed into a vessel containing a large volume of medium, the particles would dissolve a lot more readily than in the small volume provided by the Transwell hence why the dissolution profiles from the NGI appeared to be clearer

and allowed better understanding of the FP dissolution kinetics. On the contrary, the dissolution profiles from the Transwell method appeared to almost plateau at an early stage, leading to a poor understanding of the dissolution kinetics. Consequently, although modifications to the TSI/Transwell system provided less non-sink conditions and reduced the diffusion effects that occurred simultaneously with the dissolution process, the large volumes of media provided by the Rotating Paddle apparatus and the constant stirring of the medium over the deposited particles, meant that the NGI/Rotating Paddle dissolution system provided efficient sink conditions for the dissolution of OIPs, and provided more reliable *in vitro* dissolution data, since the deposited particles were immediately exposed to the medium and were not influenced by the process of diffusion.

With regards to system sensitivity, regardless of the dissolution method, changes in the medium composition led to changes in the dissolution profile. An increase in the percentage of methanol in the medium from 25 to 90% v/v, resulted in an increase in the dissolution rate of FP and this was due to the greater solubilising capacity of methanol for FP, which has poor aqueous solubility, approximately 0.1 µg/mL in water (Hastedt *et al.*, 2016). However, the rotating paddle arrangement was more sensitive to changes to the dissolution media since the dissolution profiles for FP were more distinct, also suggesting that the system has stronger discriminatory power. The profiles obtained from this system was slightly more reproducible.

Dissolution was initially carried out in different proportions of methanol to water, because it is a simple aqueous solvent that can be used to evaluate the dissolution of both aqueous soluble and poorly-aqueous soluble inhaled drug compounds. Consequently, for QC purposes, using a simple dissolution media is preferred over complex medium due to their general high reproducibility, lower costs and ease of preparation (Fotaki and Vertzoni, 2010). However, the experiments also evaluated the effect of 0.5% w/v SDS in PBS on the dissolution of FP, since many studies have utilised a surfactant to obtain rank order of dissolution rates for poorly soluble hydrophobic drugs, and 0.5% w/v SDS in PBS has been shown to differentiate between different dosage forms of OIPs (Amidon *et al.*, 1995; Thorsson *et al.*, 2001). It was hypothesised that

since surfactants significantly increases the wetting of deposited particles and improve drug solubility, they have a major impact on the dissolution rate of FP in comparison to a simple aqueous system (Coowanitwong *et al.*, 2008). However, the results suggested that it did not impact the dissolution rate enough to overcome the high dissolution profile/rate exhibited for FP in 90% v/v methanol in water. The fact that the profile in 0.5% w/v SDS in PBS did not overlap the profiles in simple aqueous solutions, provided some indication that physiological surfactants and an overall more biorelevant medium consisting of a range of surfactants found in lung lining fluid may be useful to study the dissolution of OIPs, under conditions that mimic those found in the lung in health and disease.

From an IVIVC perspective, the TSI/Transwell system exhibited better potential. This is because it is fluid-capacity limited, mimicking the limited volume of fluid in the lungs *in vivo*. Due to this, it allows for application of physiologically-relevant fluids such as Survanta® or proposed simulated lung fluids. However, the NGI/Rotating Paddle system requires a large volume of fluid, meaning it is less representative of the *in vivo* environment and it would be too expensive and inappropriate to study dissolution in such biorelevant fluids.

Table 2. 4. Comparison of the TSI/Transwell and the NGI/Rotating Paddle dissolution systems.

Quality Characteristic	TSI/Transwell system	NGI/Rotating Paddle system
Simplicity in handling	✓	✓
Ease of conducting	✓	✓
Reproducible	✓	✓
Discriminatory	?	✓
Economic	✓	X
Potential for IVIVC	✓	X

Summary and conclusions

The study explored, evaluated and compared prototype dissolution systems for inhaled products, by investigation the dissolution of FP delivered by various Flixotide inhalers and by varying the dissolution medium. The dissolution systems compared were the TSI/Transwell and the NGI/Rotating Paddle. The study showed that overall, it was difficult to have a single standardised dissolution test that can be utilised for both QC and IVIVC purposes. The modified Transwell system with a higher permeability membrane provided a superior system to the unmodified Transwell for studying dissolution of inhaled products. However, the rotating paddle dissolution method not only had the advantage of using standard USP 2 dissolution apparatus but collected the emitted fine particle fraction with greater efficiency using an adaptation of standard aerosol characterisation apparatus. It also provided greater discrimination between dissolution profiles when experimental variables were modified.

Therefore, the NGI particle collection, together with the rotating paddle dissolution system represents a good starting point for QC purposes and to evaluate batch-batch consistency during drug formulation R&D. However, the modified TSI/Fluid-capacity limited Transwell dissolution method is advantageous in that it provides the best representation of lung geology; allows for application of physiologically-relevant fluids and hence, can be developed further and utilised as a potential tool to establish IVIVC or develop/model PK data of inhaled drugs. Hence, this TSI/Transwell dissolution system was selected for future dissolution experimentations.

Chapter 3

Development of a biorelevant simulant

3.1 Introduction

It was recognised in Chapter 1 that the dissolution media currently available and that have been applied to dissolution tests for OIPs, do not fully simulate the epithelial lung fluid *in vivo*, suggesting a need for a more biorelevant simulant to be developed and applied to such systems. Consequently, it is widely recognised that drug solubility is key in the development of inhaled medicines, including drug design/discovery (Edwards *et al.*, 2016), formulation (Hastedt *et al.*, 2016) and toxicokinetics (Jones and Neef, 2012). The importance of both solubility and dissolution in predicting the pharmacokinetics of OIPs has been demonstrated convincingly (Bhagwat *et al.*, 2017) and from the perspective of the FDA and EMA, application of *in vitro* test methods to assess these behaviour of OIPs *in vivo* is important. Consequently, identifications of ways to modify the *in vitro* tests beyond a standard test developed primarily for QC, towards giving more improved IVIVC that are useful for bioequivalent studies, is a key focus to the industry. This requires more biorelevant fluids, in which to make meaningful *in vitro* experimental measurements.

Since the first biological destination of inhaled medicinal aerosols in the RTLF in which they deposit, it was surprising how little is published about models of RTLF in which to study interactions with particles, e.g. requirements for fluid composition or critical attributes. In contrast to intestinal fluid in which drug solubility and dissolution has been investigated extensively (Lennernäs *et al.*, 2014), the development of lung fluid simulants appeared to be in its infancy. Human intestinal fluids have been characterised thoroughly in terms of their composition and structure (Wuyts *et al.*, 2015; Riethorst *et al.*, 2016). Simulants have been designed to represent fed and fasted conditions (Marques *et al.*, 2011; Wuyts *et al.*, 2015), studied for their biocompatibilities with human *in vitro* cell lines (Patel *et al.*, 2006) and made available as commercial products (Klein, 2010). A variety of approaches have been adopted practically, to simulate the RTLF,

ranging from simple solutions to surfactant-containing solutions, and the tendency to refer to such solutions as 'simulated lung fluid' reflects a confusion regarding how best to simulate RTLF *in vitro*. Based on this, in a PhD study conducted by Bicer (Bicer, 2015), the key lipids and proteins that constitutes the RTLF was identified accurately, and a protocol for the preparation of SLF was established. It provides a 'base' SLF that reflects human lung fluid composition and can be incorporated into *in vitro* experimental models and be supplemented for specific applications, e.g. if particular surfactant proteins, specific metabolic activities or model inflammatory disease states are of interest. However, there remains a need to standardise the SLF and develop a quality specification for the simulant. Also, for maximum utility, such a simulant should be biocompatible with respiratory cells so that it can be used in models to study lung-particle interactions *in vitro*.

Consequently, if a simulant is to prove useful, it must be readily available, convenient, economic and well-defined conditions for storage and use. For a complex aqueous fluid with components susceptible to chemical degradation, physical instability or microbial spoilage, freeze-drying provides an excellent means of preservation. Desiccation will protect the SLF since it minimises chemical reactions, e.g. the rate of lipid hydrolysis during storage (Nounou and El-Khordagui, 2005), and deters microbial growth. Accordingly, freeze-drying the SLF would allow batch manufacture in a form that has extended use-by date and is easily handled and transported for reconstitution at its place and time of use (Tang and Pikal, 2004; Lee *et al.*, 2007).

Aim:

Therefore, in this chapter, the aim was to develop the biorelevant SLF that can be made readily available for *in vitro* experimentations such as dissolution testing of OIPs or to contribute to inhalation biopharmaceutics studies, where it can be used as the medium to assess and rank the solubility of inhaled drug compounds. The application of SLF in this manner will contribute to the development of a biorelevant dissolution system that can potentially be utilised beyond just QC purposes, moving towards

IVIVC. Consequently, it is a contributing step towards establishing a potential BCS for OIPs.

Objectives:

To reach this aim, the objectives were to, (i) optimise the manufacture of SLF, (ii) characterise the physiochemical properties of SLF (iii) carry out stability assessment of SLF under different conditions for different lengths of time, to determine or define its storage conditions, (iv) freeze-dry SLF and assess its stability, (v) asses the biocompatibility of SLF with A549 lung epithelial cells and (vi) investigate a range of inhalable compounds in SLF and compare with other simulated versions of lung fluid.

3.2 Materials

The 25 mg/mL stock solutions of 1,2-dipalmitoyl-*sn*-glycero-3-phosphocholine (DPPC) and 1,2-dipalmitoyl-s*n*-glycero-3-phospho-(1'-*rac*-glycerol) sodium salt (DPPG), both >99% purity, were obtained from Avanti Polar Lipids, Inc. (Alabama, USA). Reagent-grade purified human immunoglobulin (IgG), lyophilized human serum albumin, Bioreagent-grade transferrin, cholesterol, ascorbate, urate, certified reference material-grade glutathione was supplied by Sigma-Aldrich Company Limited (Dorset, UK). Hanks' Balanced Salt Solution (HBSS), phenol red-free, was also supplied by Sigma-Aldrich and consisted of: 0.19 g/L calcium chloride dihydrate, 0.09 g/L magnesium sulphate anhydrous, 0.40 g/L potassium chloride, 0.06 g/L potassium phosphate, 0.35 g/L sodium bicarbonate, 8.00 g/L sodium chloride, 0.05 g/L sodium phosphate dibasic, and 1.00 g/L D-Glucose. HPLC-grade chloroform and methanol were supplied by Fischer Chemicals (Loughborough, UK). 25% ammonium hydroxide, sodium chloride and 2 M hydrochloric acid solutions were obtained from Sigma-Aldrich Company Limited (Dorset, UK). For biocompatibility experiments, all ingredients were also purchased from Sigma-Aldrich Company Limited (Dorset, UK). The ingredients used for the manufacture of Gamble's solution (Appendix A Table A.2) were all analytical grade and purchased from Sigma-Aldrich Company Limited (Dorset, UK). Sodium Dodecyl Sulphate Lauryl (SDS) was obtained from Thermo Fisher Scientific (Paisley, UK) and phosphate buffered saline (PBS) was purchased from Sigma-Aldrich Ltd (Dorset, UK). Survanta® was purchased from AbbVie Ltd (Maidenhead, UK). Fluticasone propionate (FP), mometasone furoate (MF) and budesonide were purchased from Adooq Bioscience (Irwin, CA). Beclometasone dipropionate was purchased from Medchem Express (US).

3.3 Methods

3.3.1 Preparation of SLF

Preparation of SLF is shown in Figure 3.1. SLF consisted of the key components found in healthy human RTLF, the major soluble proteins, the abundant lipids and the antioxidants that were identified in the study by Bicer (Bicer, 2015). The proteins were albumin, IgG and transferrin, and the lipids were DPPC, DPPG and cholesterol. The preparation method was optimised into two stages, with the manufacture of a liposomal dispersion followed by addition of the proteins (Table 3.1). To prepare the liposomal component, 1.92 mL DPPC and 0.1 mL DPPG, from 25 mg/mL stock solutions in chloroform were combined in a bijou bottle, with 5 µL of cholesterol from a 200 mg/mL stock solution in chloroform also added. The mixture was stirred gently, and the chloroform evaporated under a stream of nitrogen gas for 30 min (sufficient to ensure that the lipid film was solvent free) to produce a thin film of lipids. The proteins were added to the lipid film in aliquots of aqueous stock solutions: 4 mL of albumin (88 mg/mL), 4 mL of IgG (26 mg/mL) and 1 mL of transferrin (15 mg/mL). To represent lung antioxidant levels, 88.5 µL of the following antioxidant stock solutions were added: 10 mM ascorbate, 10 mM glutathione, and 5 mM urate in HPLC-grade water. The mixture was vortexed for 5 min. Using an ultrasonicator/ probe for 10 min at a pulse of 10 amplitude, the lipids were dispersed into the solution, in the form of polydisperse multi-sized liposomes. Finally, 10 µL of 50 mg/mL gentamicin was added to minimise microbial growth followed by 775 µL of HBSS, under gently agitation, to make up to 10 mL volume.

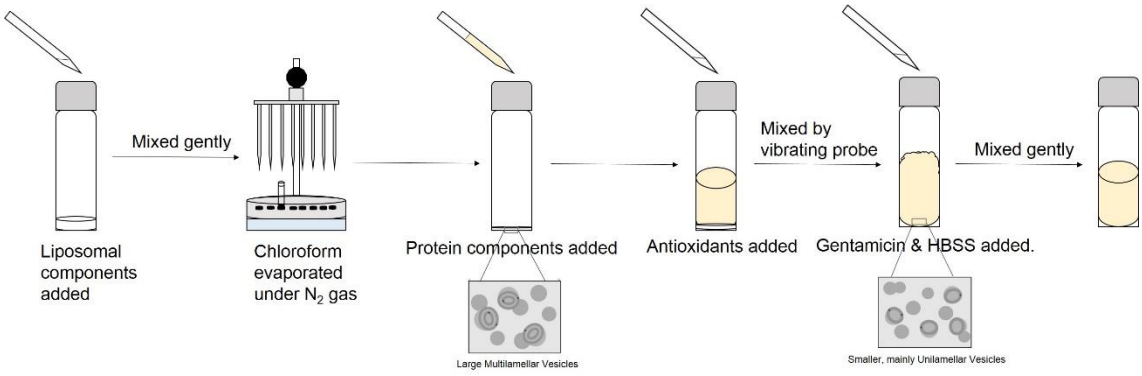

Figure 3. 1. A schematic diagram on the manufacture of simulated lung fluid (SLF).

Table 3. 1. The components of simulated lung fluid (SLF) and their relative concentrations.

Components		Concentration
Lipids	DPPC (1,2-Dipalmitoyl-sn-glycero-3-phosphocholine)	4.8 mg/mL
	DPPG (1,2-Dipalmitoyl-sn-glycerol-3-phosphor-rac(1-glycerol) ammonium salt)	0.5 mg/mL
	Cholesterol	0.1 mg/mL
Proteins	Albumin	8.8 mg/mL
	IgG	2.6 mg/mL
	Transferrin	1.5 mg/mL
Antioxidants	Ascorbate	140 µM
	Urate	95 µM
	Glutathione	170 µM
Ions (HBSS)	Calcium chloride anhydrous	0.1 mg/mL
	Magnesium chloride	0..1 mg/mL
	Magnesium sulphate	0.1 mg/mL
	Potassium chloride	0.4 mg/mL
	Potassium phosphate monobasic	0.1 mg/mL
	Sodium bicarbonate	0.4 mg/mL
	Sodium chloride	8.0 mg/mL
	Sodium phosphate dibasic anhydrous	0.05 mg/mL

3.3.2 Characterisation of fresh aqueous SLF

The SLF was characterised in this study in terms of its appearance, pH, particle morphology, particle size distribution, conductivity, viscosity, density, surface tension and monolayer behaviour. The appearance and colour were analysed visually and via measurements of the mean grey value, using the Image J software (Java 1.8.0-25, version 1.51p). Using the software, the images captured were first converted to '8-bit' prior to obtaining the mean grey value. The pH was measured using a pH probe (Ph level 2 InoLab, WTW, Germany). Particle structure and morphology was characterised via Cryo-transmission electron microscopy (cryo-TEM), using a Zeiss Libra 120 Transmission Electron Microscope (Carl Zeiss NTS, Oberkochen, Germany). The microscope was operated at 80 kV in zero loss bright-field mode under cryo conditions and the digital images were recorded under low dose conditions, with a slow-scan CCD camera (TRS GmbH, Moorenweis, Germany) and iTEM software (Olympus Soft Imaging System GmbH, Munster, Germany). An under focus of 1-2 µm was used to enhance the image contrast. Samples were spread thinly and prepared in a 100% humidity chamber to avoid dehydration, then quickly vitrified in liquid ethane held at a temperature just above its freezing point (-182°C). The sample were then transferred to the microscope, using a Gatan CT3500 cryo-transfer (Gatan, Oxon, UK) to maintain samples below -165°C. To measure the hydrodynamic diameter of structures in SLF, photon correlation spectroscopy (Nanosizer, Malvern Instruments, UK) at a scattered angle of 173° was used. Suspensions of SLF, 1 mL, was analysed using instrument parameter: reflective index 1.330, temperature 25°C, dynamic viscosity 0.8882 x 10^{-3} Pa s. Zetasizer software 6.20 was used to analyse data.

The conductivity of SLF was measured using a conductivity probe and meter (Jenway A520, Cole-Parmer, UK), calibrated using 0.01 M potassium chloride solution, providing a value of 1413 ± 1 µS/cm. The density of SLF was measured using a density meter (DMA 35, Anton Paar, UK) whereby the inverted capillary cell was filled with approximately 5 mL of SLF. Distilled water was used as the reference. The viscosity was measured using the Automated Micro Viscometer (AMVn 320, Anton Paar, UK). A

1.6 mm capillary, containing a 1.5 mm ball was filled with 400 µL SLF, sealed with a luer cap and measurements made with the capillary tilted at 50°, 60° and 70°. The surface tension of SLF was measured using a torsion balance (Model OS, TBS, UK), using distilled water as the reference sample which gave a surface tension value of 72.5 ± 0.5 mN/m. A 4 cm circumference platinum ring was immersed approximately 0.5 cm into SLF ring and the force required for withdrawal of the platinum ring from the surface of the fluid was recorded as the surface tension. All measurements were conducted in triplicate at ambient temperature.

A Langmuir trough (Model 602A; Nima Technologies Ltd., Coventry, UK) was used to evaluate the monolayer behaviour or make surface pressure-area measurements at 23°C, using a PS4 surface pressure microbalance (0-240 mN/m range, 0.1 mN/m resolution) fitted with a Wilhelmy plate (1 cm width Whatman Grade 1 chromatographic paper, GE Healthcare life sciences, Little Chalfont, UK) and controlled by Nima IU4 computer interface unit software. Suspensions of freeze-dried SLF, 1 mg/mL, were prepared in chloroform, vortexed for 10 min, then bath sonicated at 37 kHz, 25°C, for 10 min. For each isotherm, the test fluid was deposited dropwise onto a 0.9% w/v NaCl sub-phase surface using a Hamilton syringe and spreads rapidly to cover the available area of the trough until the surface pressure reached 20 mN/m, with the barriers open at their maximum. The solvent was allowed to evaporate for 10 min before the barriers were compressed at 35 cm^2/min. The mean molecular weights of the surface-active components of SLF (38,760.9 g/mol) were calculated from their defined compositions and together with the known masses of the deposited monolayers, were used to determine the molecular area of SLF. The isotonic saline subphase was used to simulate the influence of normal lung fluid counter-ions on the behaviours of the monolayer components (Scarpelli *et al.*, 1965). Individual compressions were used to determine the collapse pressure of SLF, which was 50 mN/m. Subsequently, each film was compressed to a surface pressure 5 mN/m below its collapse pressure and then expanded to reach the initial surface pressure, 20 mN/m. Triplicate experiments of ten isotherm cycles was performed, without an equilibration period between the expansion

and re-compression. Each individual compression-expression cycle took 10-25 min to complete. The degree of hysteresis was determined from differences between the compression and expansion isotherms for each cycle. The surface compressional modulus (K) (Vollhardt and Fainerman, 2006), was calculated using equation (20):

$$K = I / C = -A \times (d\pi/dA)_T \quad (20)$$

Where *C* is compressibility, *A* is the mean area per molecule and $(d\pi/dA)_T$ is the slope of the isotherm at a defined surface pressure. Compressibility is characterised by high surface elasticity and low interfacial stiffness (Choi *et al.*, 2014). K ranges between 12.5 and 50 mN/m for the liquid expanded phase, 50 – 100 mN/m liquid intermediate phase and 100-250 mN/m for the liquid condensed phase (Dynarowicz-ŁĄtka and Hąc-Wydro, 2004), whilst the condensed state has $\underline{K}$ values > 250 mN/m.

3.3.3 Standardisation of SLF

SLF was prepared three times on day 1 and prepared once on day 2 and day 3. The SLF was also manufactured once in the absence of the protein components and in the absence of the lipid components. The solutions were then characterised in terms of their appearance and their physicochemical properties: appearance, pH, conductivity, viscosity and surface tension, using the methods described in section 3.3.2.

3.3.4 Freeze-drying of SLF

SLF, 10 mL solution, was prepared in SCHOTT tubular glass freeze drying vials. The samples were frozen overnight at 20°C and then placed into a vacuum freeze-drying system (Lyotrap, LTE Scientific Ltd, UK) with condenser temperature -45°C and a vacuum of 0.060 millibars for 48 h. The samples were covered in a thin layer of parafilm with a couple of piercings to allow for vapor to escape during sublimation. Thermogravimetric analysis (Discovery TGA, TA Instruments, UK) was used to analyse the residual moisture content in the freeze-dried SLF powder, heating the sample at a

heating rate of 10°C/min to a maximum of 200°C. The powder was reconstituted with 10 mL de-ionised water and compared to fresh SLF using the physicochemical parameters described in section 3.3.3.

3.3.5 Stability assessment of fresh aqueous SLF and freeze-dried SLF

Fresh and freeze-dried SLF study was determined for samples stored in the fridge (4°C) and at room temperature (20°C) and at human physiological temperature (37°C). The stability was assessed by analysis pH, viscosity, conductivity and surface tension after their storage for 1, 2, 3, 4, 7, 14 and 28 days for the aqueous SLF and for 7 days, 28 days, 3, 6 and 9 months for freeze-dried SLF, using the methods described in section 3.3.3.

Lipid degradation was evaluated using one-dimension thin layer chromatography (TLC). The lipid components were extracted from the SLF fluid, using an adapted version of the method detailed by Bligh and Dyer (Bligh and Dyer., 1959). Briefly, 1 mL SLF sample was ultracentrifuged at 13, 000 rpm for 10 min to sediment out the lipids and proteins. To the pellet obtained, 1 mL of a mix consisting of chloroform: methanol [2:1] and 0.26 mL, was added and mixed to form a single phase. The sample was left to incubate with gentle agitation for 90 min at 37°C. Acidified saline (150 mM sodium chloride adjusted to pH 2 with hydrochloric acid), 0.5 mL was added, and vortex mixed for 5 min followed by centrifugation at 2000 rpm for 15 min (Biofuge, Pico, Jencons-PLS Scientific, UK). The aqueous phase was removed, and 0.25 mL methanol and 0.25 mL acidified saline was added to the remaining organic phase. This was vortex mixed and centrifuged again at 2000 rpm for 15 min, then the aqueous layer was removed, and the organic solvent evaporated to concentrate the lipids.

To analyse the isolated lipids by TLC, the sample was spotted approximately 1 cm from the bottom of a plain silica gel 60 TLC plate. The plate was transferred to a glass TLC tank containing 1 cm of the mobile phase, consisting of chloroform, methanol and 25% ammonium hydroxide solution at a ratio of 65:25:10. When the mobile phase reached three-quarters way up the plate the lipids were visualised as yellow spots using

potassium permanganate stain. The retardation factor (RF) was calculated as the distance travelled by centre of the spot divided by the distance travelled by the solvent front. A calibration between spot intensity (using the mean grey value) and concentration of DPPC and DPPG was established and used to estimate the content of lipid in the SLF.

3.3.6 Biocompatibility of SLF with Human A549 cell line

The biocompatibility of both fresh SLF (SLF stored at 4°C for one week) and degraded SLF (SLF stored at 37°C for one week), with human alveolar epithelial A549 cells was carried out. The 3-(4,5-dimethylthiazol-2-yl)-2,5-diphenyltetrazolium bromide (MTT) assay was used to assess the effects of exogenously applied compounds on the cell layer metabolism. The cells were cultured in a humidified atmosphere at 37°C, 5% CO_2 using a cell culture medium (CCM) composed of RPMI-1640 medium supplemented with 10% v/v fetal bovine serum (FBS), 1% v/v L-glutamine and 0.1% v/v gentamicin. For the MTT assay, A549 cells were seeded in 96-well plates at 20,000 cells/cm^2 using reduced serum (2% FBS) CCM before exposure to SLF for 24 h. After 24 h, cells were washed with PBS and 100 µL of fresh CCM containing 25 µL of MTT solution (5 mg/mL in PBS) was added to each well and the plate was incubated for 4 h in a humidified incubator. After 4 h this medium was removed by gentle inversion and tapping onto paper. The cells were lysed, and any formazan crystals formed within the adherent cell layers were solubilised with 100 µL of a surfactant solution, 10% v/v SDS in dimethylformamide: water [1:1]. Cells were incubated with lysis solution overnight at 37°C before the absorbance of solubilised formazan was measured at 570 nm using a SpectraMax microplate reader (Molecular Devices, UK). The relative cell proliferation (% cell viability) was calculated using equation (21):

$$\text{Cell viability (\%)} = [T\text{-}N/P\text{-}N] \times 100 \quad (21)$$

Where T is the absorbance obtained for each concentration of the test substance, N is the absorbance obtained for the negative control (SDS solution/ no viability) and P is the

positive control (the medium/ absolute viability). The measurements were corrected for background absorbance, using a wavelength of 650 nm. Experiment was carried out in triplicate.

3.3.7 Solubility of inhaled drug compounds in SLF

The solubility of fluticasone propionate, beclomethasone dipropionate, mometasone furoate and budesonide were measured in SLF and compared with Gamble's solution, Survanta and 0.5% w/v SDS in PBS. It was done by mixing excess drug powder (approximately 0.5 mg) with 0.5 mL of the solvent in a microcentrifuge tube. The sealed tubes were vortex mixed for 5 min before sonication at 37°C for 30 min before transfer to a shaking water-bath at 37°C. After 48 h, the drug suspensions were centrifuged at 13000 rpm for 10 min, then the supernatant (0.2 mL) was centrifuged for a second time before 0.1 ml of supernatant was diluted 10 times with methanol. This sample was analysed for drug concentration by RP-HPLC-UV, using similar method described in Chapter 2, section 2.3.2, with mobile phases specific to the compound (Table 3.2). Solubility of FP was also carried out in degraded SLF/ SLF stored in poor conditions and compared with its solubility in SLF stored under appropriate conditions. All measurements were carried out in triplicates.

Table 3. 2. List of inhaled drug compounds and the mobile phases used in the RP-HPLC-UV system for quantification in simulated lung fluid (SLF).

Inhaled drug	Mobile Phase
Fluticasone propionate	Methanol: 0.6% w/v aqueous ammonium acetate solution (75:25 %v/v)
Beclomethasone dipropionate	Acetonitrile: water (65:35 % v/v)
Mometasone furoate	Methanol: water (80:20 %v/v)
Budesonide	Ethanol: acetonitrile: phosphate buffer (pH 3.4, 25.6 mM) (2:30:68 %v/v/v)

3.3.8 Dissolution of inhaled compounds in SLF

The dissolution of a couple of inhaled compounds, FP and BDP was carried in SLF and compared with Gamble's solution, Survanta® and 0.5% w/v SDS in PBS. For these experiments, Flixotide® 50 µg Evohaler or QVAR® 50 µg pMDI was used and the dissolution method was as described in Chapter 2, section 2.3.5. Dissolution of FP was

also carried out in degraded SLF and compared to its dissolution in SLF stored under appropriate conditions. To quantify FP in samples dissolved in Gamble's solution, 175 µL of sample was removed from the well plate at each time point and placed into a HPLC vial for analysis. To quantify FP in samples dissolved in 0.5% SDS in PBS, 100 µL sample was removed and diluted with 100 µL MeOH prior to injection into HPLC. For samples dissolved in Survanta® or SLF, 200 µL sample was removed and placed into a microcentrifuge tube and centrifuged at 13,000 rpm for 10 min. The supernatant, 100 µL was removed and diluted with 100 µL MeOH prior to injection into HPLC. The tests were carried out at ambient temperature and in triplicates.

3.3.9 Statistical analysis

The physicochemical properties were derived from three independent batches of SLF; the data for the stability study was for 3 vials from a single batch of SLF. Data comparing the freeze-dried SLF with the non-freeze-dried material were normally distributed (Histogram; Skewness and Kurtosis). Therefore, the non-parametric paired sample T-test was applied. However, for biocompatibility assessment, comparing the SLF stored at 37°C with the SLF stored at 4°C and at variable SLF concentrations, Two-Way ANOVA was applied. Stability data were also normally-distributed (Histogram; Skewness and Kurtosis) and One-way ANOVA was applied. All statistical analyses were performed using the IBM SPSS software, version 24, (SPSS, Armonk, NY, USA). Data was regarded statistically significant when $p \leq 0.05$.

3.4 Results

3.4.1 Composition and characterisation of SLF

The physicochemical characteristics of SLF is listed in Table 3.3. The freshly prepared SLF was peach in colour due to the presence of transferrin and very frothy as a result of the albumin. In terms of mean grey value, it gave a value 165.5 ± 0.3. The pH of SLF was neutral, pH 7.2, due to the buffering provided by the HBSS as a base medium, maintaining the physiological pH range of 7.2-7.6, according to the product specification. Uni-, bi- and oligolamellar liposomes were visualised in the SLF, using the Cryo-TEM. Irregular electron-dense structures could also be seen, which may have been indicative of protein aggregates. Dynamic light scattering also detected structures in SLF, with a strong signal for structures with a size of 57 nm and a weaker signal for 946 nm. However, there were a lot of background scattering. The density of SLF was closer to that of water, which approximates to 1 g/cm^3. The surface tension of SLF was lower than that of water, which is typically 72.0 ± 0.5 mN/m. Langmuir isotherms (pressure-area relationships) was explored to determine the physicochemical behaviour of monolayers formed on water. The mean molecular area of SLF was 668-800 Å^2, over the 10 cycles. SLF seemed to form a stable monolayer after the first compression-expansion cycle. During compression, it underwent transitions from a liquid expanded to intermediate phase, followed by a liquid condensed phase. A large hysteresis loop and shift towards lower molecular area was observed between the first and second compression cycle. The remaining cycles were identical, indicating the formation of a stable monolayer. The same physicochemical properties were maintained for all SLF samples, prepared on the same or alternative days. There were no significant differences in the properties between 3 separate batches of SLF (Table 3.4).

Table 3. 3. Physicochemical characteristics of simulated lung fluid (SLF). All measurements made at 25°C and data represent mean ± SD (n=3).

Physicochemical property	SLF
Mean grey value	168.5 ± 0.5
pH	7.20 ± 0.02
Particle morphology	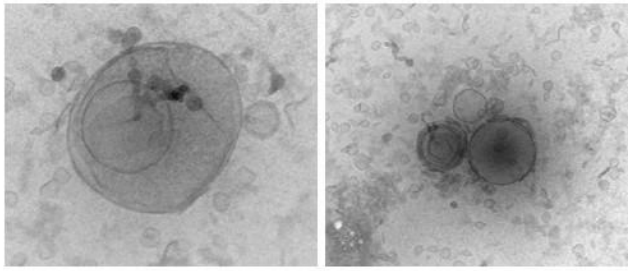
Particle size distribution	Strong signal for ~ 57 nm; weaker signal for ~ 946 nm.
Conductivity [mS/m]	14.45 ± 0.08
Viscosity [Pa.s, $x10^{-3}$]	1.138 ± 0.008
Density [g/cm^3]	0.999 ± 0.002
Surface Tension [mN/m]	54.95 ± 0.45
Monolayer behaviour	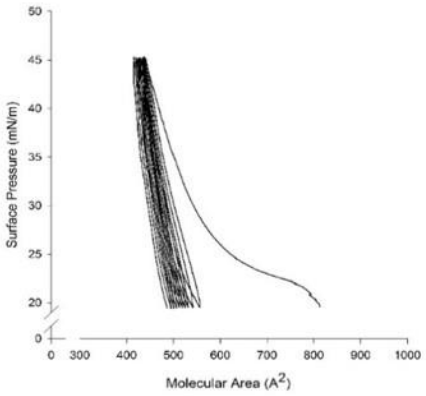 (Langmuir isotherm)
	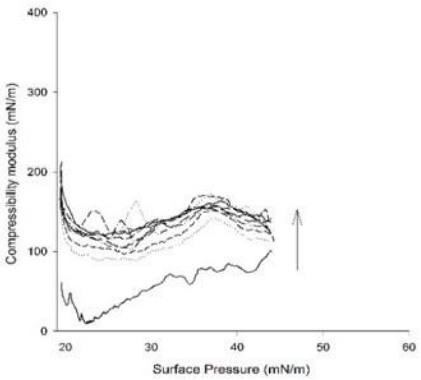 (Compressibility)

Table 3. 4. Physicochemical properties of three batches of simulated lung fluid (SLF) prepared on day 1, 2 and 3. All measurements made at 25°C and data represent mean ± SD (n=3).

Physicochemical property	SLF		
	Batch 1	Batch 2	Batch 3
Appearance [mean grey value]	168.2 ± 0.2	169.0 ± 0.3	168.1 ± 0.6
pH	7.2 ± 0.2	7.1 ± 0.2	7.1 ± 0.1
Conductivity [mS/m]	14.2 ± 0.4	14.7 ± 0.3	14.5 ± 0.2
Viscosity [Pa.s x 10^{-3}]	1.130 ± 0.005	1.138 ± 0.010	1.135 ± 0.009
Surface Tension	54.5 ± 0.5	54.0 ± 0.7	55.0 ± 0.5

3.4.2 Stability of fresh SLF

Preliminary studies showed that appearance and four physiochemical properties were stability-indicating; these were used to evaluate SLF over 28 days at three temperatures, 4, 20 and 37°C (Figure 3.2). In terms of appearance, SLF was peach coloured when freshly made. This was quantified using Image J as a mean grey value on a scale where 0 corresponds to black and a value of 225 corresponds to white (Figure 3.2.a). SLF lightened in colour visibly, becoming white by day 2, with the mean grey value rising from 168.5 ± 0.4 to 174.5 ± 0.1 at 20°C and 169.7 ± 0.3 to 175.3 ± 0.3 at 37°C. At 4°C, the mean grey value was unchanged at day 14 and only increased from 168.9 ± 0.3 to 175.9 ± 0.3 at day 28. The pH and viscosity of the SLF samples stored at 20 and 37°C also began to decrease after day 2 of storage (Figure 3.2.b and 3.2.c). Conductivity and surface tension were affected similarly (Figure 3.2.d and 3.2.e), at 37°C there was a reduction of surface tension from 54.6 ± 0.5 mN/m to 53.0 ± 0.2 mN/m at day 2, which continued to decrease until 28 days (One-way ANOVA, $p \leq 0.05$).

TLC analysis was used to probe lipid stability further. Potassium permanganate was used to detect phospholipids by oxidising the phosphorus groups, giving a distinctive colour change from pink to yellow. At day 0, TLC of SLF revealed two spots with RF values of 0.66 ± 0.01 and 0.85 ± 0.01, which were identified as DPPC and DPPG, respectively, by comparison to reference standards (Appendix A Figure A.2). From day 3 and day 2, SLF stored at 20°C and 37°C exhibited an additional spot with RF value of 0.48 ± 0.01, indicating presence of a lipid hydrolysis product. The TLC was also used for

quantitative determination, where spot intensity can be correlated to the concentration of DPPC or DPPG (see Appendix A Figure A.3). For SLF stored at 20°C, DPPC concentration fell by approximately 15% and DPPG concentration fell by 25% by day 3. For SLF stored at 37°C, both DPPC and DPPG concentrations decreased by approximately 20% by day 2. In contrast, less than 10% loss of DPPC and DPPG was measured in SLF stored at 4°C.

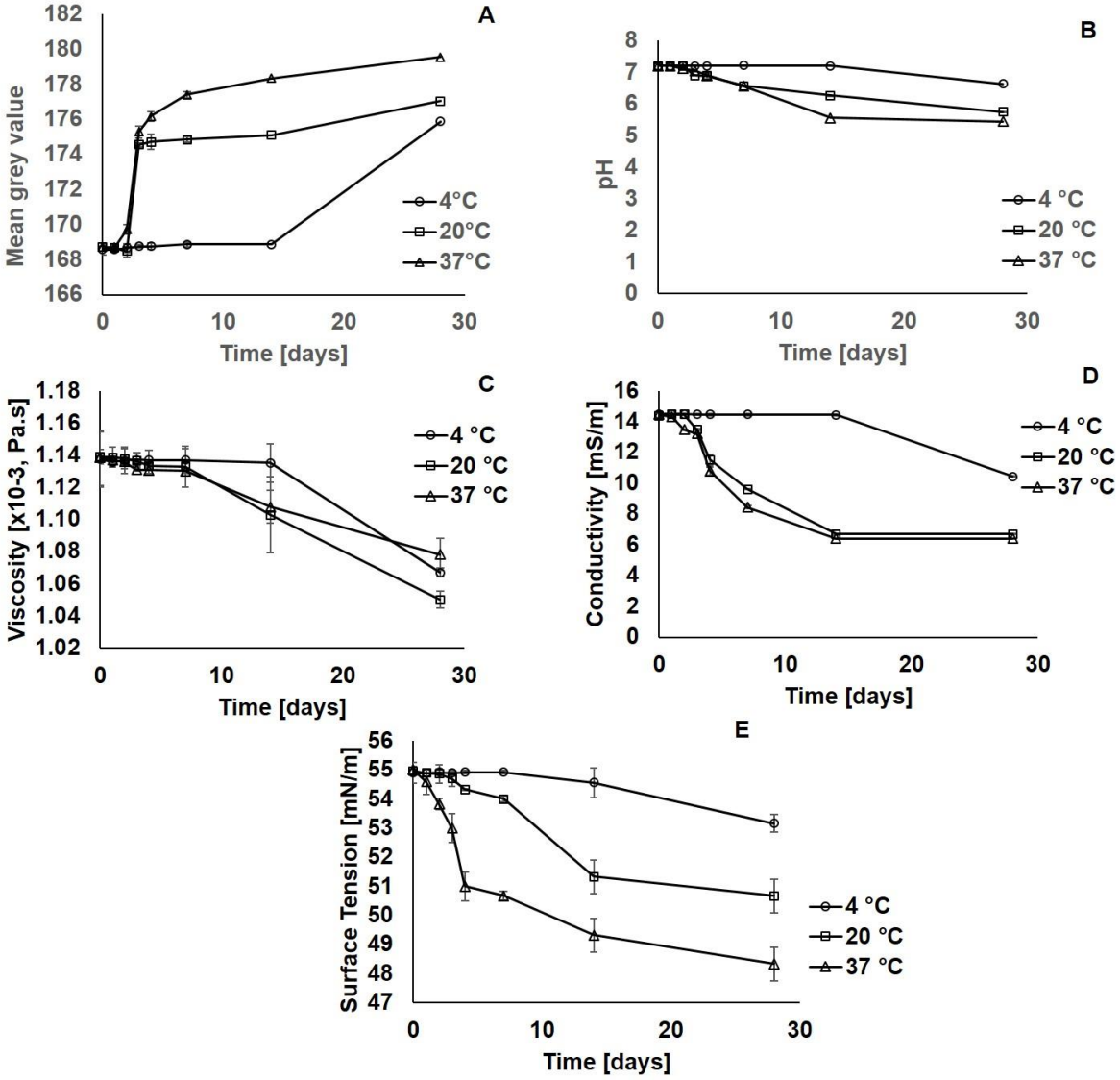

Figure 3. 2. Stability assessment of simulated lung fluid (SLF) after its storage at 4, 20 and 37°C for 0, 1, 2, 3, 4, 7, 14 and 28 days based on changes in a) colour, b) pH, c) viscosity, d) conductivity and e) surface tension. All measurements made at 25°C and data represent mean ± SD (n=3).

It was evident that the appearance, pH, viscosity, conductivity and surface tension remained constant for 14 days at 4°C, and significant changes in SLF characteristic do not become evident until day 28 (One-Way ANOVA, $p \leq 0.05$) (Table 3.5). This indicated that SLF can be stored in a refrigerator for 2 weeks. At 20°C, changes in the SLF characteristics only became significant after 3-4 days of storage, indicating that SLF is stable for 48 h. At 37°C, changes in SLF characteristics became significant at day 2, indicating that its use is only restricted to 24 h.

Table 3. 5. The day at which the simulated lung fluid (SLF) changes with regards to its appearance and physicochemical properties (tested at days 1, 2, 3, 4, 7, 14, 28) under storage at 4, 20 and 37°C.

Physicochemical property	**Day at which there is a significant difference* from day 0 [day]**		
	4°C	**20°C**	**37°C**
Appearance [mean grey value]	28	3	2
pH	28	3	3
Conductivity [mS/m]	28	3	2
Viscosity [Pa.s x 10^{-3}]	28	4	3
Surface Tension [mN/m]	28	4	2
Stability	**14 days**	**2 days**	**1 day**

*Significance determined by One-way ANOVA, $p \leq 0.05$)

3.4.3 Freeze-dried SLF

Images of the freshly prepared SLF, freeze-dried powder and reconstituted SLF is shown in Figure 3.3. The powder appeared to be very lyophilised and of small quantity at the base of the vial. The reconstituted SLF exhibited a similar peach colour and frothy solution, to the original SLF. The same physicochemical chemicals used to assess stability, were also used to compare the freeze-dried material with the original SLF. The appearance and physicochemical properties of SLF was restored successfully after rehydration with de-ionised water, except for a higher pH (Table 3.6). TGA indicated that 4.42 ± 0.15% moisture was retained in the powder (Appendix A Figure A.2).

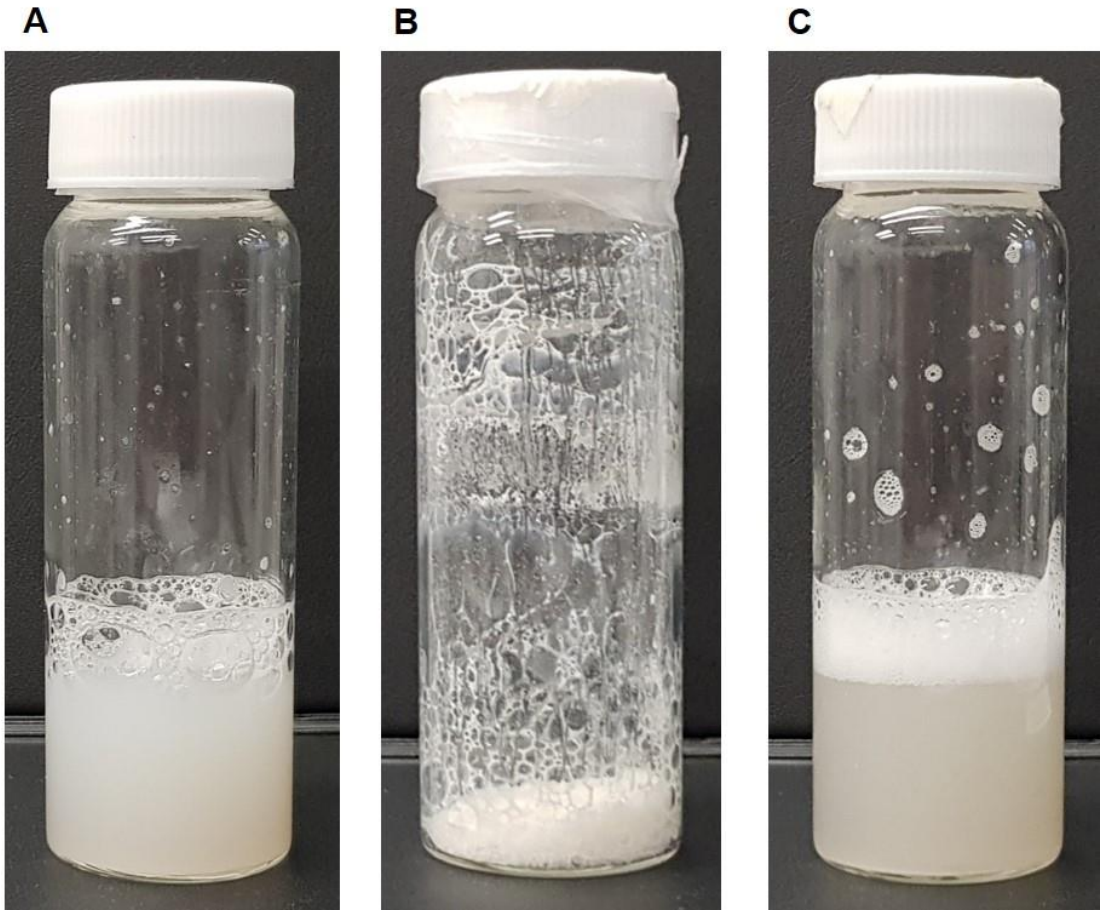

Figure 3. 3. Images captured of a) Freshly prepared simulated lung fluid (SLF), b) Freeze-dried SLF powder and c) Reconstituted SLF powder with deionised water.

Table 3. 6. Physicochemical properties of simulated lung fluid (SLF) when freshly manufactured and when reconstituted after freeze-drying. All measurements made at 25°C and data represent mean ± SD (n=3).

Physicochemical property	SLF before freeze-dried	SLF after freeze-dried
Appearance [mean grey value]	168.6 ± 0.4	168.6 ± 0.1
pH	7.2 ± 0.0 *	7.7 ± 0.1 *
Conductivity [mS/m]	14.5 ± 0.1	14.6 ± 0.2
Viscosity [Pa.s x 10^{-3}]	1.138 ± 0.008	1.111 ± 0.015
Surface Tension [mN/m]	54.9 ± 0.3	55.6 ± 0.7

*Difference is significant (T-Test, $p \leq 0.05$)

3.4.4 Stability of freeze-dried SLF

The appearance, pH, viscosity, conductivity and surface tension were also used as indicators to assess the stability of the freeze-dried SLF (Figure 3.4). For the freeze-dried powder, the stability was assessed for a longer period, up to 168 days, as oppose to 28 days for the aqueous SLF. It appeared that the appearance and all physicochemical properties of the re-constituted powder remained consistent over the course of 168 days. TLC analysis showed no extra spots, apart from the two spots indicative of the presence of DPPC and DPPG.

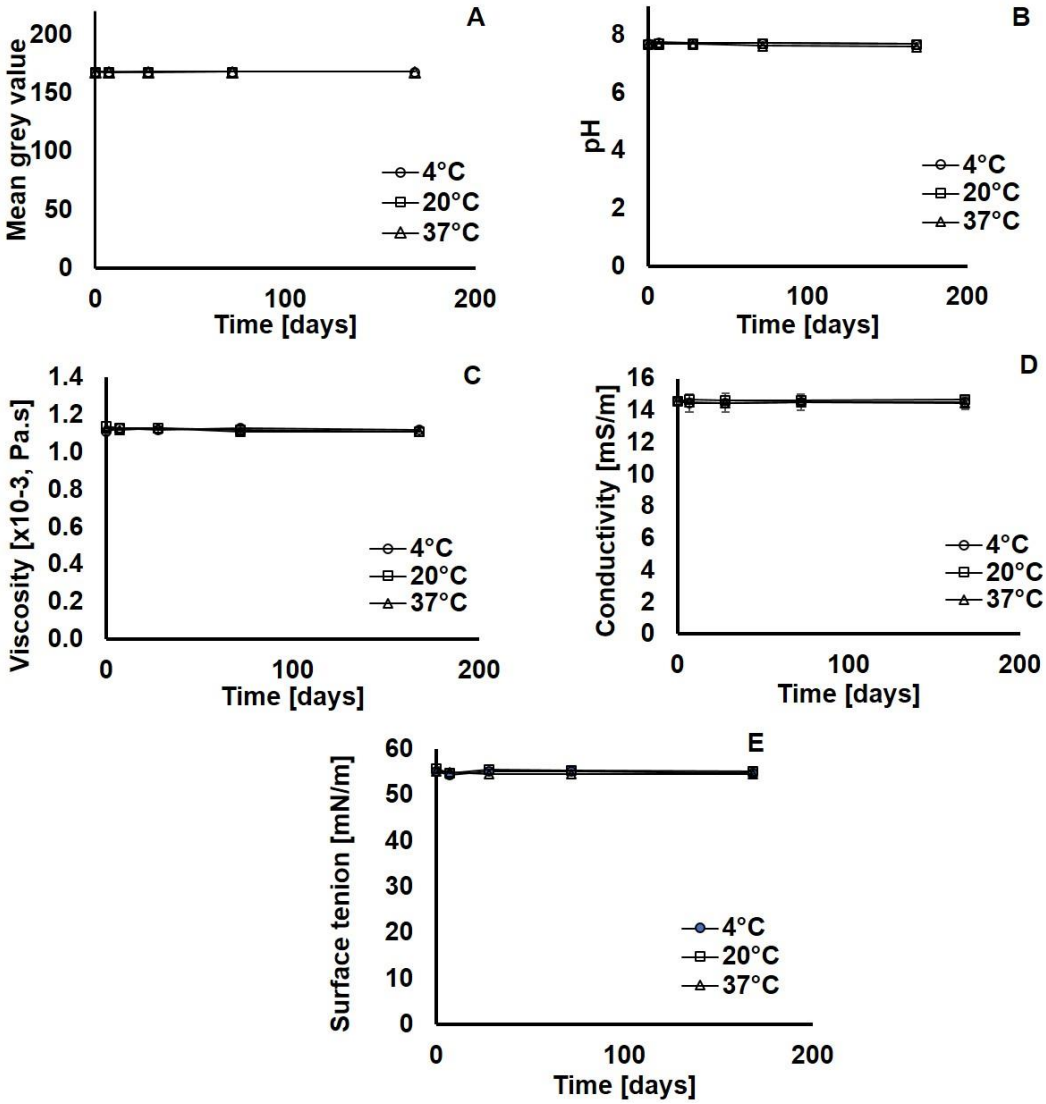

Figure 3. 4. Stability assessment of freeze-dried simulated lung fluid (SLF) after its storage at 4, 20 and 37°C for 0, 7, 28 days and at 3 and 6 months, based on changes in a) colour, b) pH, c) viscosity, d) conductivity and e) surface tension. All measurements made at 25°C and data represent mean ± SD (n=3).

3.4.5 Biocompatibility of fresh and degraded SLF with A549 cells

The MTT assay, a colorimetric assay, is used to measure the metabolic activity of the cells, whereby the mitochondrial reductase enzyme reduces the yellow MTT salt to formazan dye which has a purple colour. This allows the investigator to assess the viability and proliferation of the cells, where the darker the intensity of the purple colour means there were more living cells and hence represents a higher % cell viability. The % cell viability and thus the biocompatibility of SLF stored under the correct condition versus SLF stored under poor condition, at different concentrations, with human alveolar epithelial A549 cells is shown in Figure 3.5. Exposure of the cells to SLF after 24 h, immediately dropped the % cell viability from 100% to approximately 60%. There were evidently yet some mitochondrial activity and cellular metabolism occurring in the cells. The % cell viability remained consistent regardless of the concentration of SLF applied, with insignificant differences seen at all concentrations (Two-Way ANOVA, $p \leq 0.05$). Insignificant differences were observed between the effects of SLF stored at 37°C and SLF stored at 4°C on % cell viability, at all concentrations (Two-Way ANOVA, $p \leq 0.05$).

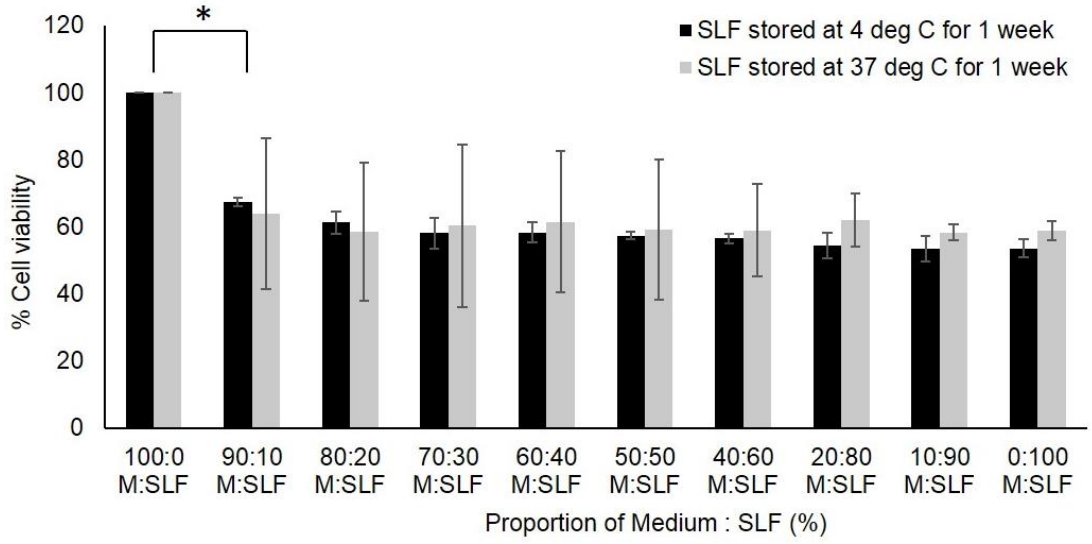

Figure 3. 5. MTT assay to assess the biocompatibility of different concentrations of good quality and degraded simulated lung fluid (SLF) with human alveolar epithelial A549 cells. Good SLF was described as SLF stored at 4°C for 1 week and degraded SLF was described as SLF stored at 37°C for 1 week. Data represent mean ± SD (n=3). * Represents significant difference (p ≤ 0.05).

3.4.6 Solubility and dissolution of FP in fresh and degraded SLF

SLF stored under poor conditions had a significant impact on the solubility of FP, as seen in Table 3.7. Solubility of FP in the degraded solution was approximately three times higher than in the good SLF. The dissolution rate of FP in degraded SLF appeared to also be significantly higher than in SLF stored under appropriate conditions, since the % dissolved at each time was much higher and the SD associated with them did not overlap (Figure 3.6).

Table 3. 7. Solubility of fluticasone propionate in fresh/good simulated lung fluid (SLF) and in degraded SLF. Data represent mean ± SD (n=3).

Inhaled drug compound	Solubility (µg/mL)	
	Good SLF (stored at 4°C for 1 week)	Degraded SLF (stored at 37°C for 1 week)
Fluticasone Propionate	2.20 ± 0.29*	6.80 ± 0.55*

*Difference is significant (Paired sample T-test, $p \leq 0.05$)

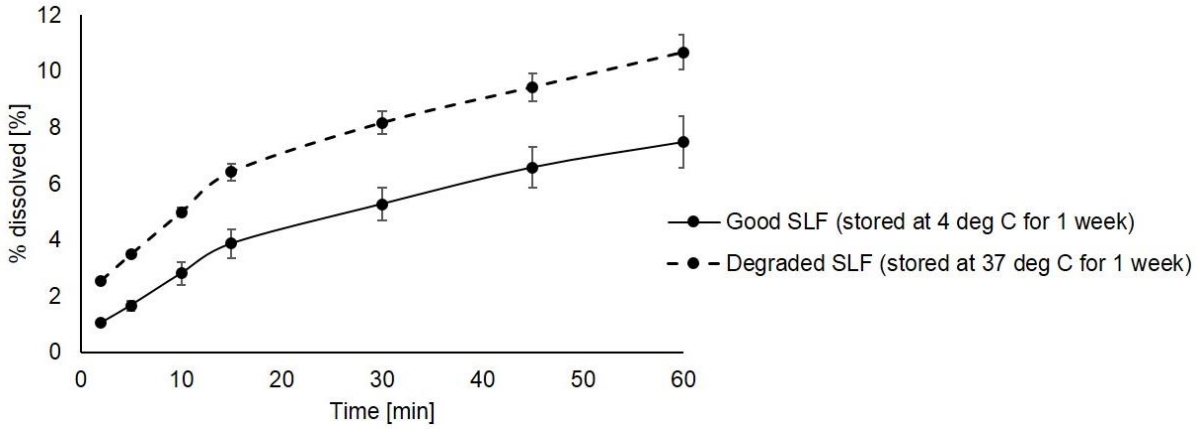

Figure 3. 6. Dissolution of fluticasone propionate in fresh/good simulated lung fluid (SLF) and in degraded SLF, carried out using the TSI/Transwell® dissolution system. Data represent mean ± SD (n=3).

3.4.7 Solubility and dissolution of inhaled compounds in simulated fluids

The solubility of a few inhaled drug compounds: Beclometasone dipropionate (BDP), Budesonide, Fluticasone propionate (FP) and Mometasone furoate (MF) in SLF was identified and compared to other reported versions of simulated fluids (Table 3.7). For all drugs, the solubility in Gamble's solution was the lowest. Solubility of the drugs in 0.5% w/v SDS in PBS was the highest, except for solubility of FP, which seemed to be influenced greatly by the components in Survanta®. For BDP and Budesonide, their solubility in SLF was closest to their solubility in Survanta, in comparison to the other fluids. However, unexpectedly FP and MF solubility in SLF were much closer to Gamble's solution than Survanta. The dissolution of FP and BDP from licensed inhaler products correlated with drug solubility in the dissolution medium (Figure 3.8). BDP appeared to dissolve more readily than FP and for both drugs, the dissolution rate in SLF was greater than in Gamble's solution, but lower than the rate in 0.5% w/v SDS in PBS.

Table 3. 8. Solubility of inhaled compounds in Gamble's solution, Simulated Lung Fluid (SLF), 0.5% w/v SDS in PBS and Survanta®. Data represent mean ± SD (n=3).

Inhaled drug compound	Solubility (µg/mL)			
	Gamble's solution	SLF	0.5% w/v SDS in PBS	Survanta®
Beclometasone Dipropionate	1.03 ± 0.12	16.79 ± 0.17	64.36 ± 1.38	37.16 ± 0.89
Budesonide	12.84 ± 0.21	26.24 ± 0.56	379.36 ± 3.09	18.79 ± 0.44
Fluticasone Propionate	0.74 ± 0.03	2.04 ± 0.09	13.08 ± 0.26	20.28 ± 1.51
Mometasone Furoate	0.59 ± 0.03	0.80 ± 0.15	87.89 ± 1.70	2.30 ± 0.03

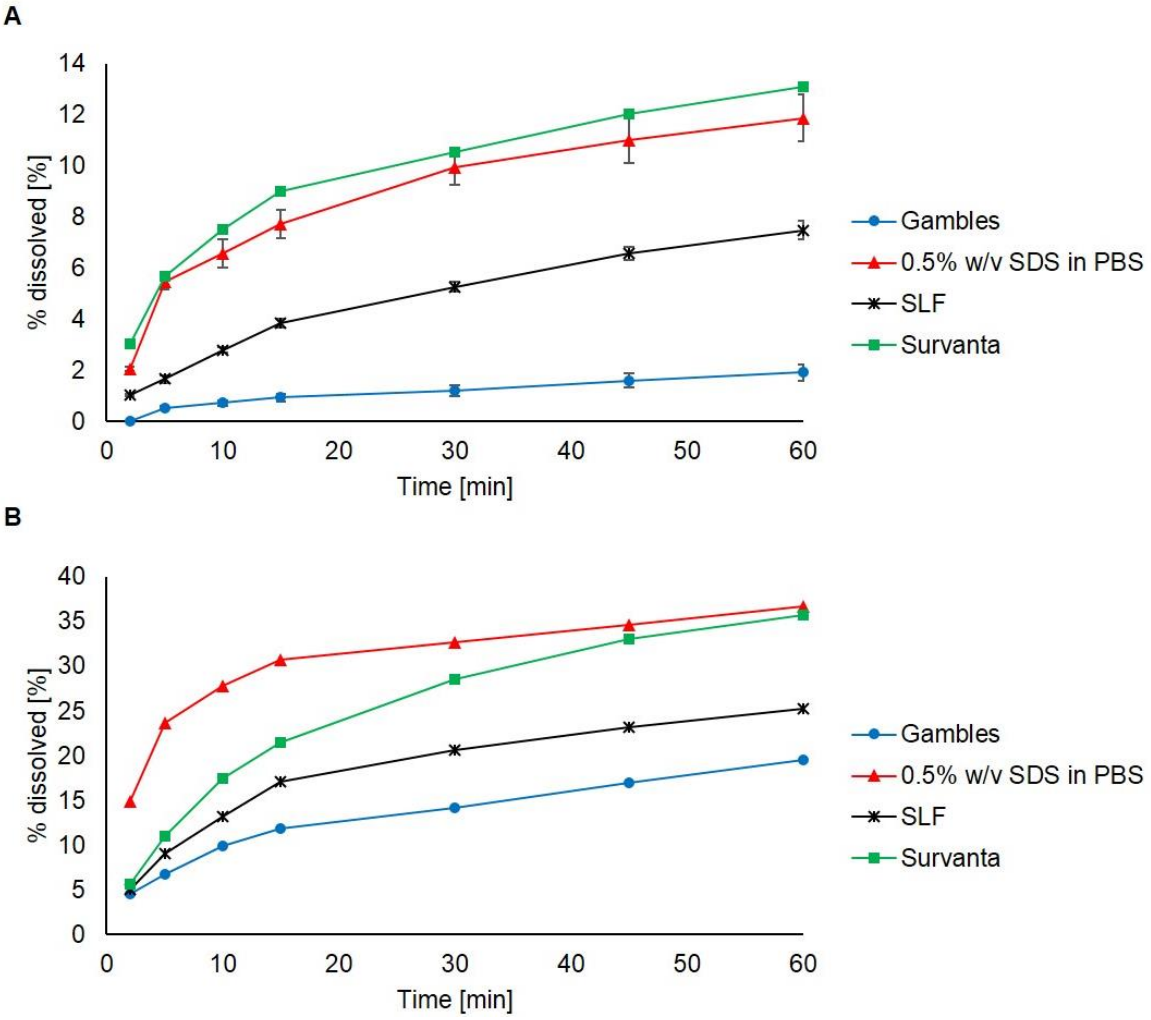

Figure 3. 7. Dissolution of A) fluticasone propionate and B) Beclometasone dipropionate in Gamble's solution, simulated lung fluid (SLF), 0.5% w/v SDS in PBS and Survanta®. Data represent mean ± SD (n=3).

3.5 Discussion

3.5.1 Manufacture and characterisation of SLF

The SLF was designed to provide a simulant that trades off the biorelevance of featuring the full complexity of lung lining fluid with the pragmatic need for a simulant that can be manufactured economically, reproducibly and is fit for the majority of applications in inhaled medicines biopharmaceutics. It consisted of key components found in healthy human RTLF, the major soluble proteins, the abundant lipids and the antioxidants that were identified in a study by Bicer (Bicer, 2015). The lipid components were DPPC and DPPG to represent the surfactant phospholipids in the lungs and cholesterol, a neutral steroid lipid. Although DPPC, which contributed approximately 80% w/v of the surfactant phospholipids, is often used as a sole representative phospholipid component in model lung fluids, for physiological relevance other lipid components were included. DPPG was included since it represents approximately 10% of total phospholipids and cholesterol, which accounts for 5-10% surfactant, was included since it has been shown to have a stabilising role in the bilayer structures. Urea corrected total protein concentration measured in human lavage samples is in the range 17.9 ± 8.6 mg/mL (Bicer, 2015), but due to the limited commercial availability and consistency of some human protein components, e.g. the surfactant proteins: SP-A, SP-B, SP-C and IgA and A1TA, the total proteins used in the preparation of SLF was 12.9 mg/mL Biorelevant concentrations of antioxidants were included to promote biocompatibility of SLF with respiratory epithelial cells.

The preparation method in this study was optimised to counteract few theoretical limitations associated with the method reported in Bicer's study. For example, the main two steps are the preparation of the liposomal components and the preparation of the protein components. This means SLF could be prepared more simply with fewer steps, taking only 20 min to prepare. Also, stock solutions of the ingredients were prepared prior to this, whereby the lipid components were prepared in chloroform, protein components were prepared in HBSS and antioxidants in deionised water. Taking

samples immediately from the stock solutions, minimised the complexity and transfer errors associated with weighing out powders. Consequently, the method for the re-submersion of the surfactant bilayers within the fluid was chosen to ensure minimal damage to the structures created in SLF. The manufacturing process was a robust method since the SLF appeared to be the same and present the same properties regardless of the time and day prepared.

In terms of the characterisation of SLF, the physicochemical properties and the characterisation techniques to identify them, were selected based on previous studies that focused on characterisation of physiological fluids such as saliva or simulated intestinal fluids (Boni *et al.*, 2009; Gittings *et al.*, 2015). SLF appeared peach in colour and when converted to a mean grey value, it gave a value closer to white than black on the 0 to 225 scale on Image J (0 corresponds to back and 225 corresponds to white). SLF exhibited a neutral pH, buffered by the HBSS and closely matched the pH of *in vivo* lung, although subject to some variability. For example, the pH in the nasal cavity is approximately 6.3 (range 5.2-8.1) (Washington *et al.*, 2000), pH is 6.9-9.0 in the trachea (Karnad *et al.*, 1990) and suggested to be more acidic in inflammation and infection (Karnad *et al.*, 1990). The buffering effect provided by HBSS was evidently not influenced by the addition of multiple protein and lipid components. The HBSS not only provides a buffering effect, but the essential inorganic ions present provide a physiological salt composition, tonicity (280 mOsM) and are responsible for the high conductivity of SLF in comparison to de-ionised water, matching the properties of lung lining fluid in healthy subjects (Effros *et al.*, 2005). Consequently. the ions present in HBSS are a mix of polydisperse ions, large and small. The larger ions tend to act as chaotropes and cause the HBSS solution to have a higher density than pure water, and the smaller ions or macromolecules compensates for the chaotrope content and presents a counter-acting effect (Hribar *et al.*, 2002). As a result, the SLF exhibited a similar density to water.

The particle structure and size were analysed via Cryo-TEM and DLS respectively. Initially optical microscopy was used to study the particle structures involved in SLF. The

technique confirmed the presence of particles, that appeared predominantly agglomerated. Agglomeration was an expected observation since SLF consisted of high protein content, which can cluster together forming bimolecular protein agglomerates (Filipe *et al*., 2010). However, the exact identification of the agglomerate composition could not be fully established via this method. Cryo-TEM imaging better confirmed presence of lipids, that were too small to be identified by optical microscopy. The use of cryo-TEM technique originated from a study by Almgren et al and the method was adapted to their study (Almgren *et al*., 2000). Although it has been reported that HBSS, due to its high salt content, may interfere with TEM imaging (Bicer, 2015), the images captured in this study proved the technique to be powerful in characterising the liposome morphology and allowed for visualisation of the fine detail of surfactant structure in SLF. There were varied sizes of undamaged liposomes present and this emphasised the benefit of the optimised preparation technique for SLF. The polydispersity in bilayer structures was like the polydispersity exhibited by the human RTLF (Appendix A Table A.1). It has been suggested that cholesterol, present in both, is responsible for increasing bilayer stiffness and cohesive strength, producing defined circular structures (Almgren *et al.*, 2000). However, the slightly more cohesive lamellar array observed in RTLF, is likely due to the additional presence of SP-A, which promoted the formation of surfactant films (Bernardino de la Serna *et al.*, 2013). The presence of the smaller irregular structures is likely reflective of protein aggregates, and DLS supported the detection of these structures, since the stronger signal for structures with a size of 57 nm corresponded to the size of the liposomes, and the weaker signal for 946 nm likely corresponded to the proteins and protein aggregates. However, further interpretation of the DLS result was not possible, due to background scattering by the multi-molecular protein agglomerates. This is a recognised limitation of dynamic light scattering size analysis in media with high protein content (Filipe *et al*., 2010).

The lower surface tension exhibited by SLF, in comparison to the reference water, was due to the surfactants in SLF. DPPC is the most surface-active molecule in the pulmonary surfactant mix and hence, was responsible for the significantly reduced

surface tension (Pérez-Gil and Keough, 1998). Proper pulmonary function requires low surface tensions during expiration to minimise the work of breathing (Schürch *et al.*, 1976). The pulmonary surfactants in human RTLF form a lipid-rich film with a significantly reduced surface tension from 70 mN/m at the upper airways, to near 0 mN/m at the alveoli (Siebert and Rugonyi, 2008; Ikegami *et al.*, 2009). It has been reported that DPPC forms a semi-crystalline monolayer capable of surface tensions reaching near zero when fully compressed (Ding *et al.*, 2001). However, in this study, although SLF consisted of a relatively high concentration of DPPC, it appeared to exhibit a higher surface tension than would otherwise be anticipated. This is likely due to the absence surfactant proteins, particularly of SP-B, a small hydrophobic protein. In a study conducted by Ikegami et al (Ikegami *et al.*, 2009), they found that removal or reduction of SP-B, increases the surfactant surface tension, demonstrating its important role in regulating the surface tension-lowering properties of surfactants. Surfactant proteins also play a role in fluid viscosity, whereby SP-C interacts with lipids to produce high surface viscosity (Alonso *et al*., 2005). However, despite the absence of SP-C in SLF, the viscosity of SLF was higher than that of simple aqueous solutions and this was attributed to the presence of protein macromolecules and complex lipids in their physiological concentrations.

The Langmuir trough experiment characterises both the structural and mechanical properties of SLF. The phase behaviour of surfactants in two dimensions is determined by the pressure-area isotherms. It appeared that SLF formed a stable lipid monolayer on water surface, after the first compression-expansion cycle. For the lungs to function effectively, it would require the lung surfactants to form a rigid monolayer of low surface tension upon compression, but also be fluid enough to spread rapidly during the expansion of the interface that accompanies inspiration (Bastacky *et al.*, 1995). DPPC is reported to be responsible for the semi-crystalline monolayer rigidity and stability, whereas proteins are responsible for fluidising the monolayer (Ding *et al.*, 2001). This contradictory requirement of the lung surfactant monolayer has led to the ‘squeeze-out’ theory of lung surfactant function, whereby it is

thought that any unsaturated lipids and proteins present in lung surfactants *in vivo* are selectively removed or 'squeezed-out' from the monolayer during compression, leading to a DPPC-enriched stable monolayer (Schürch *et al*., 1976; Ding *et al.*, 2001). The surfactant proteins in SLF, especially SP-B and SP-C, are thought to interact with the lipids to create a localised monolayer-to-multilayer transitions that provide low surface pressures on compression and rapid and repeatable re-spreading on expansion (Schürch *et al*., 1976; Ding *et al.*, 2001). However, although surfactant proteins are absent in SLF, this theory seemed to yet be supported by the *in vitro* results reported from the Langmuir. Results indicated that SLF is a simple stable colloidal system, that required a composition-refining process during the first isotherm cycle, in which excess material such as the incorporated albumin or transferring proteins, is removed from the interface before the stability of the DPPC-enriched monolayer is maintained with the remaining compression-expansion cycles. The absence of specialist surfactant proteins in general, limits the application of the SLF for some specialist immunological applications, e.g. where SP A and D are important in host-defence or biological studies.

3.5.2 Stability of SLF and its significance

SLF is predominantly a liposomal formulation and liposomes in aqueous dispersions tend to be relatively unstable, where hydrolysis and oxidation degradation often occur over time and are accelerated when exposed to heat (Nawar, 1969; Reis and Spickett, 2012; Mahdy and Yang, 2014). More specifically, the ester functionality connecting the fatty acid and glycerol backbone is susceptible to hydrolysis resulting in free fatty acids, lysophospholipids and/or glycerophospho compounds (Aveldaño and Horrocks, 1983; GRIT *et al.*, 1993). It has been shown that hydrolytic degradation influences liposome size and bilayer rigidity (Zhang *et al.*, 2004). Peroxidation, which involves the removal of a hydrogen atom from the fatty acid constituents to produce the free radical, is a serious concern with liposomal formulations. The lipid radical may react with oxygen in the air to produce a peroxyl radical (Reis and Spickett, 2012) and additional reactions can occur such as cyclization, fragmentation and rearrangement

(Payton *et al.*, 2014). These reactivity processes have shown to alter the physical properties of the liposome bilayers such as the fluidity and hence, the physicochemical properties of the whole liposomal formulation (Payton *et al.*, 2014). This provided motive to study the stability of SLF.

In this study, the stability of SLF was carried out according to the recommended ICH guidelines (ICH EMEA, 1993). The assays chosen to assess stability were simple approaches, the apparatus used are relatively cheap to purchase and easily accessible and can be carried out in all labs. Consequently, these methods are sensitive in identifying the physical changes that occur in solutions and in this study, they were congruous in detecting conditions and time at which SLF began to degrade and in profiling temporal stability at each storage temperature. The background scattering seen in the DLS results complicated interpretation of the results and thus was not suitable as a stability test. The results were consistent with changes that occur to lipids at elevated temperature or over periods of time, as mentioned above. Although antioxidants are present in SLF in small quantities, they are not fully protective, and it has been reported that ascorbate may even catalyse the oxidation of phospholipids in solvent systems (Deutsch *et al*., 1941). Degradation of the phospholipids can reduce pH as lipid dissociate into their constituent fatty acids (Abramson *et al.*, 1968). Metal cations, such as the sodium ion present in DPPG and the quaternary ammonium ion in DPPC, can participate in reactions that produce a sharp decrease in viscosity (Abramson *et al.*, 1968). Hydrolysis of phospholipids produces two main lysoforms, with the 1-acyl lysoform being predominant (Jeschek *et al.*, 2016). The higher levels of lipids tend to reduce the surface tension of protein-containing solutions (Xu *et al.*, 2013) and the electrical conductivity of aqueous solutions (McClements, 2005).

TLC analysis identified more spots of different RF values on the plate after it was stained with potassium permanganate, further supporting the concept of lipid hydrolysis at higher temperatures to its constituent fatty acids. It can also be used for quantitative determination (Askal *et al.*, 2008), thus in this study, image analysis was used to provide a semi-quantitative measure of spot intensity for DPPC and DPPG, whereby the mean

grey value of the spot was plotted as a function of lipid concentration (Appendix A Figure A.3). There was a strong positive correlation between the two factors, which meant the percent degradation of the lipids could be estimated. The results suggested that DPPG was more vulnerable to degradation, since its concentration fell more than DPPC in the SLF stored at room temperature.

Identifying the conditions in which SLF must be stored under is important, as results in this study indicated that SLF stored in poor conditions affects the solubility of FP significantly, by a factor of three. This was likely attributed to the increase in the hydrophobic fatty acid content in SLF, a result of phospholipid hydrolysis, when SLF was stored at 37°C for 1 week. With more hydrophobic tails present in SLF, although not tightly packed, they provide more regions or reservoirs for FP to adhere to, and thus increases its solubility and its dissolution rate as a response. However, poor storage of SLF did not seem to have a significant impact on its biocompatibility with lung A549 cells. The MTT assay was applied in this study to determine the cytotoxicity of poorly-stored SLF, since it was thought that its degradation products would interfere with cell viability and growth. However, the results suggested that although the physicochemical properties of SLF changes with poor storage conditions, the fatty acids do not present any further toxicity to the cells. The antioxidants seemed to maintain this good biocompatibility. Regardless of the SLF concentration the cells were exposed to, the % cell viability remained relatively constant, indicating that the fluids may have a synergistic effect on the cells. However, the SLF did not provide any nutrients to the cells to allow for sufficient metabolism in comparison to the medium, since the % cell viability immediately dropped from 100% viability in the presence of only medium to approximately 60%, in the presence of pure SLF. This means that the medium is the dominant provider of nutrients to the cells to allow for cell growth and proliferation, whereas the components of SLF provides some form of protection to the cells. Although it has been shown that presence of antioxidants can stimulate the proliferation of cultured endothelial cells (Kuzuya *et al.*, 1991), the antioxidant components in the fluid did not seem to do so to a large extent, but provided limited protection to the available cells from

oxidant-induced apoptosis for example and thus allowed for up 50% cell growth. Consequently, it has been shown previously that A549 cells benefit from cholesterol and DPPC, which exhibits anti-inflammatory effects to the cells (Morris *et al.*, 2008). Therefore, it may be that incubation of the cells with SLF has an immunomodulatory protective role, as oppose to detrimental effects. Consequently, although the degradation products of SLF caused the pH to decrease, it was not substantially far from physiological pH (6.5-7.6) and the HBSS present provided the physiologically relevant electrolytes and glucose concentrations which further protected the cells. Overall, the data suggested that there was no adverse impact of the physiologically relevant protein, liposome and their fatty acid constituent concentrations within the simulant, on the proliferation of A549 cell monolayers and hence, the simulants were biocompatible with this human epithelial cell line.

3.5.3 Freeze-dried SLF and assessment of its stability

Freeze-drying is a unique drying process used particularly for heat-sensitive materials or to improve the stability of lipids that are susceptible to chemical degradation (Hua *et al*., 2010). Water in the dilute aqueous solution is usually removed, leaving behind a dried product that can be packaged and stored under various conditions, without its stability being affected (Hua *et al*., 2010). The stability of freeze-dried SLF powder was studied here and compared to the aqueous form of SLF. Stability was carried out in a similar manner to the aqueous solution, and in accordance to the ICH guidelines; however, for a longer time. Although freeze-dried material could be prepared as a single large batch of powder, with each opening and closing of the batch to carry out the stability tests, it is likely air and humidity would be introduced to the powder, affecting the stability measurements. To prevent this, separate disposable samples of SLF was freeze-dried and stored for analysis. Part of the freeze-drying technique, involved the sample bottles being huddled in the centre of the stand and surrounded by empty bottles on the outside. This is because preliminary studies showed that samples placed at the periphery of the stand is likely to be exposed to a different temperature

profile to the samples in the centre. Hence, this technique ensured the samples were freeze-dried in a more uniform and consistent manner. All samples were placed on the same cooling shelf level. Where possible, SCHOTT freeze-drying vials were used with a tight-sealing lid to eliminate the influence of relative humidity of the storage conditions, on the stability of the powder. In some cases, this was eliminated by sealing the glass bijou bottles tightly with parafilm. Consequently, the sample were removed from the freeze-drier under the presence of nitrogen gas, again to ensure no oxygen, air humidity or water was introduced upon removal of the samples, which would otherwise compromise SLF sample stability. Moisture has been reported to significantly influence the stability of lyophilised powder (Wang *et al.*, 2012).

For freeze-drying to be determined as successful, a dry fluffy lyophilised powder should be produced which can be easily reconstituted to possess physicochemical properties that match the original sample (Hua *et al*., 2010). This is because the direct transition of water from solid to vapour via sublimation, without a liquid phase, helps to preserve the initial raw material's properties. Studies have shown that lyophilised powder of liposomes without addition of cryoprotectants is likely to be compact, clumpy and difficult to reconstitute and thus cryoprotectants have been considered as a critical processing parameter to consider when undergoing freeze-drying (Nounou and El-Khordagui, 2005; El-Nesr *et al*., 2010; Soares *et al.*, 2013). However, in this study, the SLF was successfully freeze-dried without the need for additional formulation components to act as cryoprotectants; the powder produced was very fluffy and easy to reconstitute with water to restore the appearance and physicochemical properties of the SLF. The results indicated that freeze-drying did not compromise the stability of the liposomal structures present in the fluid. The reconstituted freeze-dried formulation was identical to the freshly made solution, except for a small statistically significant increase in pH, which can be readily corrected. Although water is predominantly neutral in pH, the use of different grades for reconstitution e.g. distilled water, de-ionised water, HPLC-grade water or ultrapure water, may result in variations in pH (Kulthanan *et al.*, 2013).

Freeze-drying is effectively a drying operation, in which the water is removed by sublimation and a vacuum chamber is used to increase the speed of this process (Mujumdar and Devahastin, 2008). While freeze-drying can improve the storage of liposomal formulations, it has been recognised that the process can also cause damage to the liposome structures which are exposed to stress conditions, such as excessive dryness, upon long periods of sublimation, which can pierce the liposomes or predispose them to aggregation (Nounou and El-Khordagui, 2005; Ingvarsson *et al.*, 2011). However, the TGA results indicated that sufficient moisture was retained in the powder, so the liposomes were not subjected to excessive dryness and the process did not seem to induce destabilising stress factors to SLF solution. Hence, the freeze-drying process parameters such as the freezing rate, freezing temperature and processing time can be considered optimal for this study. The process evidently prolonged the stability of SLF, regardless of its storage conditions to up to 6 months so far, yielding a product with an extended shelf-life. This is because due to the absence of water in the solid material, the degradation pathways or reactivity processes such as hydrolysis and oxidation, which becomes profound at higher temperatures, is far less pronounced than in the aqueous state.

3.5.4 Recommendations for use of SLF

The results from the stability study indicated that SLF can be stored in the refrigerator for 2 weeks and remain stable, with its physicochemical properties preserved well. SLF is only stable for 2 days on the shelf, where it can be utilised for laboratory experiments such as, for solubility or dissolution testing which are often carried out at room temperature. If SLF was required for *in vitro* experiments which involve cell culture or the use of physiological temperature, based on the results when SLF was stored at 37°C, these experimentations should be restricted to 24 h.

The appearance and physiochemical properties of the reconstituted lyophilised SLF powder remained unchanged after 6 months of storage, regardless of the storage temperature and there was no degradation of or chemical changes to the lipids detected

by TLC, indicating an improved stability of the lyophilised liposomal formulations in contrast to the aqueous formulation, and hence allowing for longer-term storage of material. Lyophilisation clearly increases the shelf-life of liposomes, preserving it in a dry form that can easily be reconstituted with water immediately prior to use.

3.5.5 Solubility and dissolution of inhaled compounds in SLF

Drug solubility in lung fluid is an important determinant of the fate of inhaled aerosol medicines hence, studies have focused attention on the need to measure drug solubility in mediums that is representative of human RTLF (Riley *et al.*, 2012). The components and physicochemical properties of SLF very likely influences the solubility of inhaled compounds. For example, results from the Langmuir suggested very stable colloidal structures in SLF, which may make them less likely to sequester poorly soluble drugs in its micelles. In this context, the FP, BDP provide excellent references since they are considered as very poorly water-soluble drugs, reported to have concentrations of approximately 0.1-2 µg/mL in water (Appendix Table A.4,Murnane *et al*., 2008; Sahib *et al.*, 2012; Hastedt *et al.*, 2016). In simple aqueous media, such as gambles, which is only composed of a variety of salts (Appendix A Table A.2), it was expected for the inhaled drugs to exhibit low solubility. However, in the remaining surfactant-containing media, the solubility of the drugs increased hugely particularly in the 0.5% w/v SDS in PBS, which was expected and reflective of *in vivo* conditions. *In vivo*, lung surfactants tend to enhance the solubility of small, lipophilic drug molecules, such as corticosteroids and cationic compounds, because they form structures with lipid domains (Wiedmann *et al.*, 2000; Liao and Wiedmann, 2003). However, some results were unexpected. For example, Budesonide exhibits much better aqueous solubility, reported to be approximately 45 µg/mL yet its solubility increased significantly in surfactant-containing media but MF and FP, with low aqueous solubility, presented a solubility in SLF that was much closer to Gamble's solution than the remaining surfactant-containing solutions. This suggested that solubilisation may be determined not only by lipid content but also the interaction of the components, including the drug, which affect liposomal structures.

For example, cholesterol may form tight nanodomain complexes with DPPC stabilising the lamellar structures formed (Kim *et al.*, 2013) and forcing the retention of drugs within, whereas albumin may solubilise the cholesterol (Kim, 2007) and reduce the stability of the lamellar phase and the extent to which drug is solubilised in these structures. Consequently, the difference in solubilities across the range of compounds is influenced by the difference in the compounds' intrinsic lipophilicity and pKa, influencing the compound partitioning into the lipid compositions of the fluid versus the aqueous composition (Fan and de Lannoy, 2014),

However, an estimate for the solubility of FP in the lungs using mechanistic modelling (Boger *et al.*, 2016) appears to support the value obtained with SLF. Since the aqueous solubility of poorly soluble compounds tends to underpredict the *in vivo* dissolution rate, the parameter *Cs*, which defines the solubility of a drug according to Nernst-Brunner equation, should be estimated from observations of total drug concentrations in the lung made in an inhalation study The estimated *Cs* of FP, obtained following incorporation of parameters into a developed mechanistic physiologically based pharmacokinetic model, was 4530 nM and when converting the solubilities of FP in the fluids used in this study to nM, the value of FP in SLF was 4400 nM, which most closely correlated to the predicted *Cs*. This finding supported the hypothesis that the salt solution is likely to underestimate the dissolution of hydrophobic drugs, while 0.5% SDS may overestimate solubility and hence dissolution in the lungs. For the dissolution experiment, FP and BDP were selected to represent inhaled drugs that have poor aqueous solubility and likely to be dissolution limited, accounting for their relatively low dissolution profiles. The solubility of BDP in all fluids, was significantly higher than the solubility values of FP, indicating that the impact of the lipid or surfactants present to solubilise FP was much greater than expected for BDP. These results emphasised that the use of biorelevant medium provides a more realistic estimate for both solubility and dissolution.

Summary and conclusions

A SLF of biorelevant composition was characterised and shown to possess physicochemical properties comparable to those of RTLF. The simulant was determined to be stable for 24 and 48 h at 37 and 20°C, respectively (in-use stability) and for 14 days when stored in a refrigerator (storage stability). Colour, surface tension and conductivity were the most sensitive indicators of product deterioration. The SLF can be freeze-dried which provides a means of prolonged storage, for up to 6 months, with studies ongoing. This means it can be manufactured in large batches, in a form that has an extended use-by date and is easily handled and transported for reconstitution at its place and time of use. Overall, the study presented and provides a readily available, biorelevant and biocompatible SLF that can be used for *in vitro* investigations in the field of inhalation biopharmaceutics, e.g. the solubility of inhaled compounds, the dissolution of inhaled medicines and the interaction of aerosol drugs or particles with lung cells. Relative to this thesis, it can now be applied to dissolution tests, in attempt to develop a biorelevant dissolution system for OIPs.

Chapter 4

Biorelevant *in vitro/in silico* modelling of inhaled drug dissolution in the lungs

4.1 Introduction

The next key step to the study was to evaluate the applicability and assess the necessity of SLF in the development of an *in vitro* biorelevant dissolution system, for discerning the quality attributes of inhaled medicines or for predicting the *in vivo* performance of inhaled products. To do this, a recently-developed integrated apparatus, comprising the PreciseInhale® and Dissolv*It*® systems, will be used since it simulates the physiological conditions in the lung and mimics the pharmacokinetic data of inhaled particles. Although this means the Dissolv*It*® dissolution system addresses various limitation exhibited by the other proposed dissolution tests for OIPs, the dissolution vessel requires 5.7 µl of a polyethylene oxide (PEO) gel as the dissolution matrix rather than a biorelevant medium. This provides motive to apply the SLF, developed in Chapter 3, to enhance the bio-relevance of the dissolution system and investigate the impact it has on the dissolution of FP, by comparing it to the other version of simulated fluids. Since the system is very novel, there is already very little reported data on the performance of the system in predicting dissolution, and hence, using this system in this study proves to be particularly useful.

Consequently, delivery of FP to the Dissolv*It*® with different biorelevant media in the chamber, permits comparison to FP dissolution-absorption profiles in other systems, such as Isolated Perfused Lung (IPL). This allows for IVIVC. To perform such experiments however, requires accurate quantification of sub-micromolar concentrations of FP using a sensitive assay and an efficient extraction method (Krishnaswami *et al.*, 2000; US FDA CDER, 2011; Lombardi, 2015). It has been reported that the liquid-chromatography with tandem mass spectrometric detection (LC-MS/MS) technique provides selective and sensitive analysis of glucocorticoids in biological fluids (Li *et al*., 1997; Krishnaswami *et al.*, 2000; Matuszewski *et al.*, 2003). However, conducting many

of the reported liquid-liquid phase or solid phase extraction methods during my preliminary experiments, proved to be difficult to replicate and showed very poor repeatability. This required the development of a solid phase extraction (SPE) method, which was easy to conduct, well validated, repeatable and reliable, requiring minimal sample preparations.

The main value of *in vitro* systems is in providing decision-making data e.g. dissolution measurements for predicting and modelling impacts on drug PK in the early stages of the drug development process. This can expedite drug development and prevent unexpected toxicokinetics and ultimately avoid the costly end-stage failures (Di *et al.*, 2013). The current PK and PD studies not only add in time and cost but may also introduce additional risk, with poor IVIVC data complicating the demonstration of bioequivalence (BE) between OIPs. Therefore, improving the *in vitro* dissolution test to access better IVIVC and enable the greater reliance on *in vitro* methods for BE testing for example, has become an important goal in industry (Copley and Sipitanou, 2018). The ideal model should be able to reflect *in vivo* predictability. Good predictive models for pharmacokinetics depends strongly on selecting appropriate mathematical approaches, and more current studies tend to utilise *in silico* techniques (Chen *et al.*, 2012; Gaohua *et al.*, 2015; Fröhlich *et al.*, 2016). For modelling dissolution, Backman et al have described how recent advances in mechanistic models may aid in getting a better understanding of dissolution which can be used to predict systemic exposure (AUC) and hence its influence on drug therapeutic effect (Bäckman *et al.*, 2014). Therefore, for this study, it required a mechanistic model to be developed and utilised to evaluate the dissolution data derived from the biorelevant approach adapted onto the Dissolv*It*® system.

Aim:

In this chapter, the predominant aim was to take the first steps into developing dissolution as a biorelevant system, that can potentially be used as an *in vitro in vivo* correlation tool for OIPs, by applying the developed SLF to Dissolv*It*® system and

comparing the dissolution performance of FP with other proposed dissolution medium. In doing this, it provides an indication into the significance and necessity for SLF, if we wish to develop a dissolution system that provides profiles that truly mimic the dissolution of aerosol particles *in vivo*.

Objectives:

To reach this aim, the objectives were to, (i) validate a novel LC-MS/MS method for the measurement of low FP drug concentrations in lung fluid samples, (ii) apply different examples of dissolution/ bio-relevant medium to the DissolvIt system: a) 1.5% w/v PEO + 0.4% w/v L-alphaphosphatidyl choline, b) Survanta® and c) SLF and investigate the effect of the dissolution medium on FP aerosol particle dissolution, evaluating for significance of SLF application and (iii) compare the dissolution profiles obtained from the Dissolv*It*® system with the profiles obtained from rat IPL and (iv) apply a developed *in-silico* model to the data, to explore the impact of the dissolution rates derived on *in vivo* PK.

4.2 Materials

Flixotide® 50µg Evohaler was provided by GSK. Polyethylene oxide (PEO) and L-alphaphosphatidyl choline were supplied by Sigma Aldrich Limited (Dorset, UK) whereas Survanta® was obtained from AbbVie Ltd (Maidenhead, UK). The materials required for the aerosolisation, deposition and dissolution of FP were provided by Inhalation Sciences, Sweden. For FP dissolution in rat IPL, female CD IGS (Sprague Dawley) rat were obtained from Charles River (Sulzfeld, Germany) and the necessary equipment were provided by Inhalation Sciences, Sweden. The Chemicals required for the manufacture of SLF were as listed in Chapter 3. For solid phase extraction validation, the chemicals included were micronized FP (USP grade, purity 98%) supplied by LGM Pharma Inc (Boca Raton, USA), FP-d5 (USP grade, purity 97%) by Insight Biotechnology Limited (Wembley, UK) and rabbit serum, purchased from Sigma-Aldrich Company Limited (Dorset, UK). Chemicals required for the extraction procedure were zinc sulphate powder, supplied by VWR International Limited (Lutterworth, UK), HPLC-gradient grade acetonitrile, 35% v/v ammonium hydroxide solution and Analytical-Reagent grade dichloromethane, which were all purchased from Fischer Chemical (Loughborough, UK).

4.3 Methods

4.3.1 Validation of the SPE and LC-MS/MS assay for quantification of FP

Validation of the assay required preparation of calibration curves. Primary stock solutions of FP and FP-d5 (I.S.) were prepared by adding 1mg of FP or FP-d5 into a 10-mL volumetric flask and filled to the volume with pure acetonitrile, producing 100 µg/mL solutions, and stored at -20°C. A 1 µg/mL FP working solution was prepared by the appropriate dilution of the stock with pure acetonitrile. The calibration standards (156, 313, 625, 1250, 2500, 5000 and 10,000 pg/mL) were prepared from serial dilution of the working solution with pure acetonitrile. The QC samples (470, 1880 and 7500 pg/mL) were prepared by mixing the appropriate FP standard solutions to achieve the desired

concentrations. Working I.S. plasma solution (0.1 µg/mL) was prepared by adding 50 µL of an intermediates FP-d5 solution (10 µg/ml in pure acetonitrile) to 5 mL rabbit plasma.

Solid phase extraction was used for sample extraction of the calibration and quality control samples. 1225 µL of rabbit plasma was placed into 10 Eppendorf micro-centrifuge tubes, labelled C1 to C7 and LQC, MQC, HQC, respectively. 25 µL of each FP standard and QC samples were placed into the tubes and vortexed for 5 min. The remaining steps were as described in section 4.3.4.

Partial method validation was conducted in terms of linearity, precision (intra-day and inter-day), accuracy, limit of detection and limit of quantification, following the specific recommendations stated by the US FDA industrial Bioanalytical Method Validation Guidance (US FDA CDER, 2001). Linearity was evaluated by plotting a calibration curve of mean peak area ratio of FP/FP-d5 (n=9) against the concentrations of 7 standards, using a weighted (1/x) linear regression model. The relative standard deviation (%CV) provided information on assay and instrument precision. For intra-day precision, the %CV values across 3 calibration sets prepared on the same day were looked at however, for inter-day precision, another 3 fresh series of calibration standards prepared on days 2 and 3 were analysed. Accuracy of the data was evaluated across 9 determinants of each standard, ensuring it was within ±15% of the theoretical standard concentration. The limit of detection (LOD) and limit of quantification (LOQ) were calculated based on equations (18) and (19), in Chapter 2.3.1.

Evaluation of the extraction recovery was done in accordance to a paper by Matuszewski et al (Matuszewski *et al*., 2003) on the LQC, MQC and HQC, whereby a set of those QC samples were prepared in plasma extract and spiked before extraction, and a fresh set of samples prepared in plasma extract and spiked after extraction. The % recovery was determined using equation (22):

Extraction recovery % = [Mean peak area ratio from extracted LQC, MQC or HQC / Mean peak area ratio from post extraction blank plasma-spiked with neat standard] X 100 (19)

4.3.2 Deposition and dissolution of FP in the Dissolv*it*® system

The aerosolisation of Flixotide® was carried out using the PreciseInhale® aerosol system (Inhalation Sciences, Stockholm), whereby the Flixotide pMDI canister was connected to the US Pharmacopeia Induction Port No 1 (standardised simulation of the throat) of the aerosol system, (Figure 4.1). The aerosol particles were deposited on 9 circular microscope glass cover slips, 13 mm in diameter and the dissolution of the deposited particles was investigated on the Dissolv*it*® system (Inhalation Sciences, Stockholm), thermostatted to 37°C. The prepared perfusate consisted of 0.1 M phosphate buffer plus 4% albumin solution, mixed thoroughly using a magnetic stirrer. Helium was bubbled through the perfusate to remove excess bubbles. The SLF was prepared via the method described in Chapter 3, section 3.3.1. The Survanta was diluted with PBS to provide a lipid concentration of 4.0 mg/mL. The composition of the three mucus simulants investigated, PEO, SLF and Survanta®, are listed in Table 4.1. Pre-warmed mucus simulant, 5.7 µL, was applied on one side of the polycarbonate membrane of a single-use cell, with the perfusate buffer streaming on the other side. The dissolved particles were absorbed at a perfusate flow rate of 0.4 mL/min over a period of 4 h and the perfusate samples were collected by an automated controlled fraction collector at 0, 3, 6, 9, 12, 15, 20, 25, 30, 40, 50, 60, 120 and 240 min time-points.

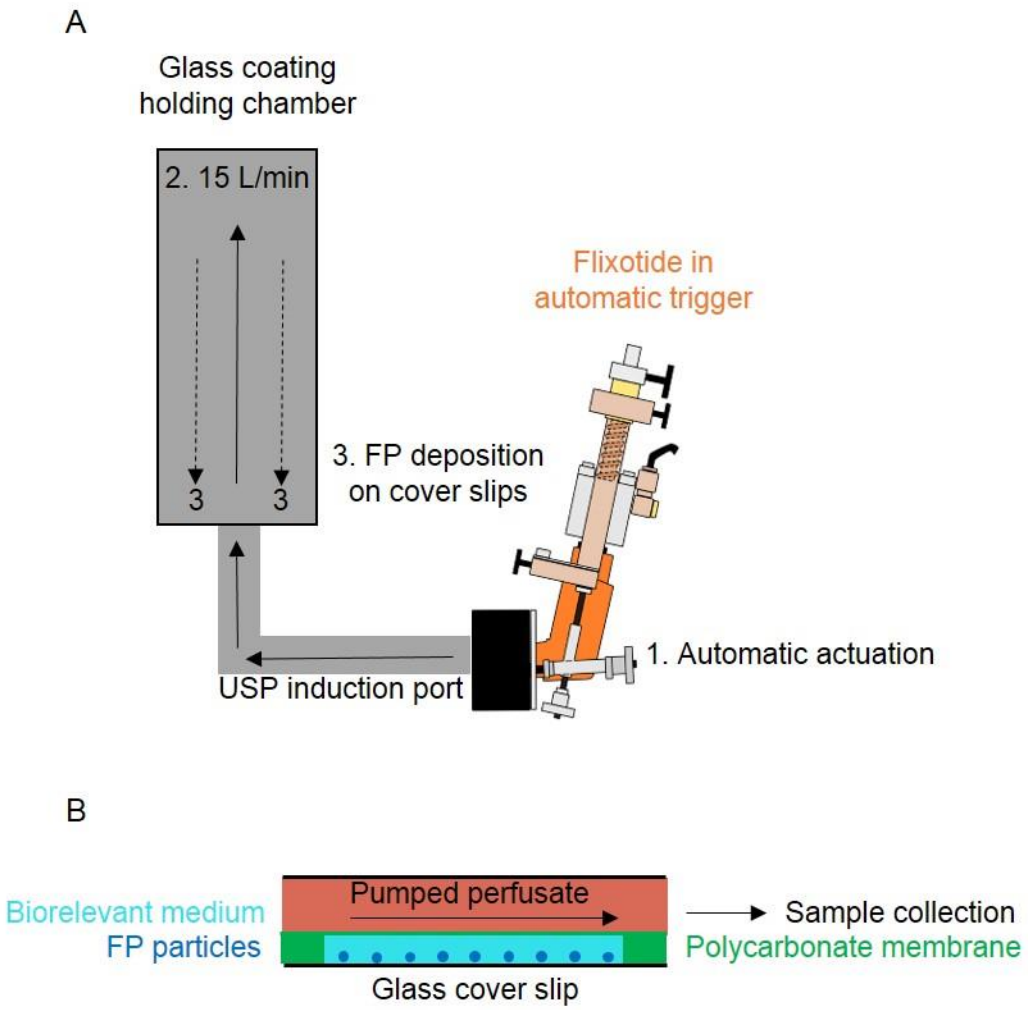

Figure 4. 1. A schematic of a) fluticasone propionate aerosolisation and particle deposition and b) the dissolution system.

Table 4. 1. The protein and lipid compositions of the three mucus simulants/ bio-relevant dissolution media: 1.5% w/v Polyethylene oxide + 0.4% w/v L-alphaphosphatidyl choline (PEO), simulated lung lining fluid (SLF) and diluted Survanta®.

Simulant	Protein concentration (mg/mL)	Lipid concentration (mg/mL)
PEO	-	4.0
SLF	12.9	5.4
Survanta® (diluted)	0.01-0.16	4.0

4.3.3 Dissolution of FP in rat isolated perfused lung

This work was carried out by scientists in Inhalation Sciences. Female CD IGS, with body weight of 279 ± 20 g, were euthanised with phenobarbital sodium (100 mg/kg, i.p.) and their whole lung prepared as described in other reports (Kroll *et al*., 1986; Sundstrom *et al.*, 2003). The lungs were placed in the artificial thoracic chamber. They were ventilated with room air at 75 breaths/min by creating an alternating negative pressure (-0.2 to -0.8 kPa)[3] inside the chamber, using an Ugo Basile model 7025 animal respirator (Varese, Italy), with a stroke volume of 6 mL, superimposed on a constant vacuum source connected to the chamber. The tracheal air flow velocity and pressure inside the chamber were measured with a heated 8430 series pneumotachograph (Kansas City, MO, USA) at 0-3 L/min and a differential pressure transducer (EMKA Technologies, Paris, France) respectively. The physiological lung-function variables: tidal volume (V_t), dynamic lung compliance (C_{dyn})[3] and lung conductance (G_{aw}), which is inversely proportional to lung resistance (RL)[3] were calculated from each breath in real time and logged by a data acquisition system using the software IOX v. 6.1a (EMKA Technologies). The lungs were perfused via the pulmonary artery in a single-pass mode, at a constant hydrostatic pressure of approx. 12 cm H_2O and the perfusate reservoir was continually overflowing into a recirculation drain pipe, to keep a constant liquid pressure head. Throughout the experiments, the perfusate flow rate after the passage through the lung (Q_{perf}) was measured gravimetrically using a custom-made fraction collector with a scale. The perfusion medium consisted of Krebs-Henseleit buffer, 5.5 mM glucose, 12.6 mM HEPES and 4% bovine serum albumin. The temperature of the perfusate and the artificial thoracic chamber was maintained at 37°C. The lungs were left to stabilize for 30 min prior to aerosol exposures and only the lung preparations with stable baseline values for V_t, C_{dyn}, G_{aw} and Q_{perf} during at least a 15-min period were used. The measured values were: V_t: 1.8 ± 0.2 mL, C_{dyn}: 6.6 ± 1.0 mL/kPa; G_{aw}: 279 ± 20 ml/s/kPa, and Q_{perf}: 32 ± 2 mL/min (n=6). For the exposure of the IPL to the Flixotide® aerosol, this was carried out using the PreciseInhale® as described above, where the aerosol was delivered to the lung by the active dosing system and the system automatically

terminated the exposure when the inhaled target dose was reached. The perfusate was repeatedly sampled in an automatic fraction collector during a 2-h period from the start of the aerosol exposure and the sampling intervals were 4.5, 6, 7.5, 9, 12, 15, 30, 60 and 120 min. After the end of the perfusion period, the lungs and trachea were harvested for analysis of the amount of FP retained in the tissues after the perfusion period. The experiments were approved by a local ethical review board in Stockholm.

4.3.4 Sample extraction by SPE

Samples were prepared for analysis following the new, validated solid phase extraction method. 325 µL of each sample was loaded into a deep-well sample plate (Thermo-Scientific, Surrey, UK) followed by 50 µL of working I.S. solution (0.1ug/mL FP-D5). 300 µL of 0.1 M zinc sulphate followed by 75 µL of 10% ammonium hydroxide were added and mixed using a multichannel pipette. The SPE plate was placed on an orbital shaker (Stuart-Scientific, UK) for 30 min followed by centrifugation at 3700 rpm for 5 min. The samples were then transferred to a pre-conditioned Evolute® Express ABN 10mg SPE 96-well plate (Biotage, Sweden). With little vacuum applied (< 5 mm Hg pressure), they were washed with 200 µL HPLC-grade water followed by 200 µL of 25% v/v methanol in water. The analytes were eluted twice with 200 µL of pure acetonitrile followed by once with 100µL dichloromethane and vacuum centrifuged (Genevec EZ-2, UK) to dryness. Samples were reconstituted with 30 µL of 55% v/v acetonitrile in water and sonicated rapidly for 10 min. The MS plate was then covered with a transparent seal film (Thermo-Scientific, Surrey, UK), ready for analysis. An aliquot of the final sample solution (20 µL) was injected into the LC-MS/MS system.

4.3.5 FP quantification by LC-MS/MS

Quantification of FP was carried out by Waters® Xevo TQ tandem quadrupole mass spectrometer (Waters, Elstree, UK) equipped with an ESI interface, corporate with an Ultra Performance LC system (Waters, Eltree, UK), equipped with a binary solvent delivery system and an Acquity auto-sampler. Chromatographic separations were

carried out on a 100A Acquity BEH (2.1 x 50 mm) analytical HPLC column, packed with 1.7 µm C-18 (Waters, Eltree, UK). The mobile phase was a mix of mobile phase A and mobile phase B, which were 0.1% ammonium hydroxide in water and 1:1 v/v acetonitrile in water respectively. The chromatograms of FP and FP-d5 from the plasma extract were obtained from a mobile phase flow rate of 0.2 mL/min with a 2-min gradient flow from 50% to 95% B. Argon was used as the collision gas and the collision energy was set at 12 V. The LC-MS/MS operations were controlled by the computer software, MassLynx 4.1 and analyte quantification was done with the following parameters: m/z 501.4 > 313.1 for FP and m/z 506.5 > 313.1 for FP-d5.

4.3.6 Data analysis

For the validation process, peak integrations and data analysis were performed using the MassLynx 4.1 computer software. The relationship between peak area ratio (y) and analyte concentration (x, pg/mL), was performed and calculated using the LINEST function in Microsoft Excel. Data was expressed as the mean ± SD of replicate determinations, whereby $n \geq 3$. The acceptance criteria for the calibration standards and the QCs were identified from the US FDA industrial Bioanalytical Method Validation Guidance (US FDA CDER, 2001). For the FP dissolution graph, the %FP in the perfusate was expressed as a percent of the deposited amount on the glass slide.

4.3.7 Statistical analysis

Data were normally distributed (Histogram, Skewness and Kurtosis). Therefore, One-Way ANOVA was applied to the data followed by Tukey POST-HOC analysis. Statistical analysis was performed using the IBM SPS software, version 24, (SPSS, Armonk, NY, USA). Data was regarded statistically significant when $p \leq 0.05$.

4.3.8 Dissolution PBPK modelling

A mechanistic physiologically based pharmacokinetic (PBPK) model for predicting the fate of inhaled FP (Figure 4.2) was developed by Sumit Arora and collaborators at

University of Graz, in Austria. The model was carried out using Java (Version 1.8.0_111, Oracle, Redwood City, US). The integration of the system of ordinary differential equations was performed via the 8(5,3) Dormand-Prince integrator (Hairer and Wanner, 1991) as realized in the Apache Commons Math library (Version 3.6.1, Apache Software Foundation, Forest Hill, U.S.). The model was adapted from recently published paper by Boger et al (Boger *et al.*, 2016). Briefly, the model was based on the respiratory physiology divided into three compartments; extra-thoracic, tracheobronchial (central lung) and alveolar (peripheral lung) region (Figure 4.2). The particles deposited in the extra thoracic region were swallowed and transferred to gut, where they were subjected to systemic absorption, based on their bioavailable fraction (F). Particles deposited in central and peripheral lung were modelled for their dissolution, using input from the *in vitro* dissolution experiments in DissolvIt® system, in epithelial lung lining fluid followed by their permeation in lung tissues and considering that the particles deposited in the central lung were also subjected to mucociliary clearance, as described by Boger et al. The central and peripheral lung areas were perfused by the bronchial blood flow (Q_central lung) and entire cardiac output (Q_cardiac output) respectively. Perfusion-rate limited distribution was assumed to apply for all tissues. System-specific input parameters for central lung, peripheral lung, blood flows and volume of the tissue compartments included are presented under supporting information (Appendix B Tables B.1 and B.2).

For regional lung deposition modelling, the particle size distribution of the tested formulations was determined using next generation impactor (NGI), resulting in a discrete distribution of seven particle sizes with corresponding mass fraction deposited (f0,….f6). Multiple-Path Particle Dosimetry model (MPPD V2.11, Applied Research Associates Inc., Albuquerque, N.M, US, 2009) was used to calculate the regional deposition of particles from the tested formulations. A breathing pattern with 2 s inspiration, 1 s expiration, 10 s breath hold, and a tidal volume of 625 mL was used. The Yeh-Shum 5-lobe lung model was chosen for the calculations of regional deposition

fraction (Yeh and Schum, 1980). The drug and formulation specific parameters for FP inhaled in the model is presented under supporting information (Appendix B Table B.3).

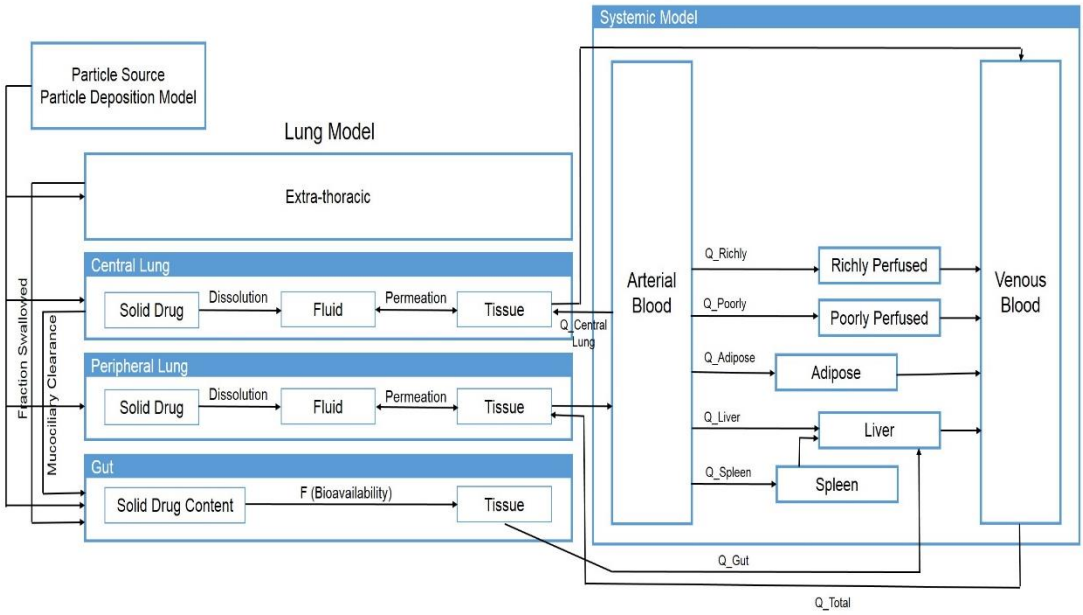

Figure 4. 2. A schematic representing the whole body physiologically based pharmacokinetic (PBPK) model.

4.3.9 Sensitvity analysis of disoslution kinetics

A sensitivity analysis of the pharmacokinetic parameters to the *in vitro* dissolution kinetics of FP was performed using the mechanistic PBPK model (described in section 4.3.8). Hypothetical *in vitro* dissolution profiles of FP were created by means of numerical approximation with maximum cumulative percent dissolved fixed to mimic the cumulative percent of FP in SLF. The numerical approximations were selected in order to probe three different possible *in vitro* dissolution scenarios: a profile where release greatly exceeded that observed experimentally in SLF (case 1) and two profiles that are similar to SLF but initially more rapid (case 2) or slower (case 3).

4.4 Results

4.4.1 Validation of the SPE and LC-MS/MS assay for quantification of FP

The SPE and LC-MS/MS methodologies required for the quantification of FP in bio-relevant media were very easy to conduct and with good sensitivity to low concentrations of FP. LC-MS/MS provided sharp distinctive peaks in the mass spectra representative of FP and FP-d5, with minimal background noise, as shown in Figure 4.3. Good data repeatability and excellent linearity between the mean peak area ratio of FP/FP-d5 and the concentration of FP in the samples was observed (most R^2 values = 0.999) (Figure 4.4).

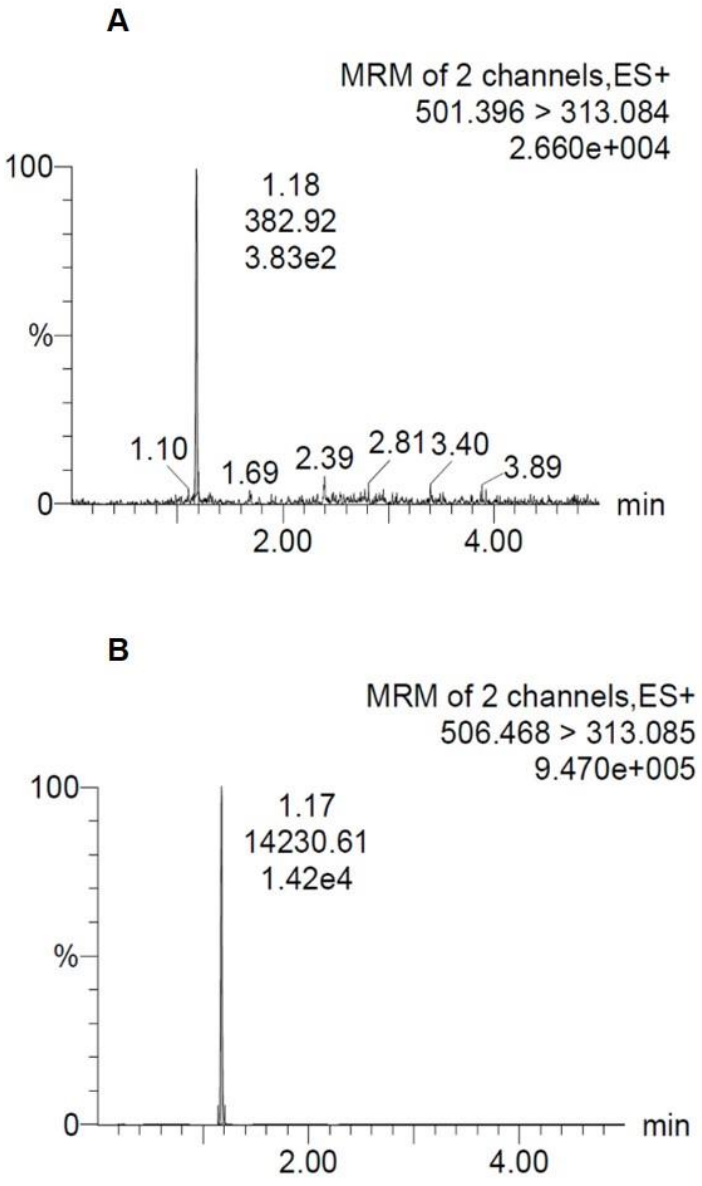

Figure 4. 3. Daughter scan mass spectra of a) FP and b) FP-d5, obtained from LC-MS/MS, with base peaks at 382.92 m/z and 14230.61 m/z respectively.

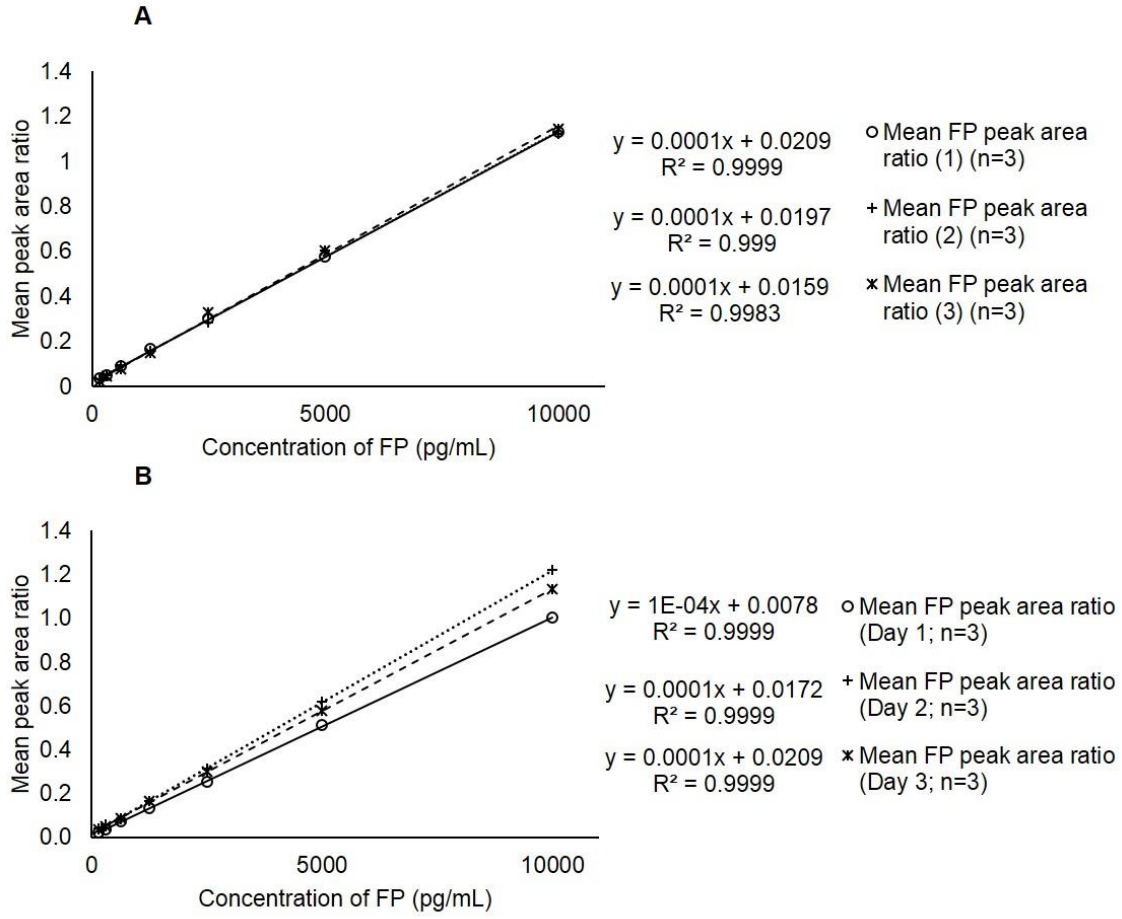

Figure 4. 4. Validation of solid phase extraction and LC-MS/MS for analysis of fluticasone propionate (FP) based on linearity of a) intra-day FP calibration curve sets (3 batches) and b) inter-day FP calibration curve sets. Data represent mean ± SD (n=3).

The inter-day and intra-day precision data complied with the validation guidance, with all CV being < 20%, except for 156 pg/mL which had a CV of 35.5% (Table 4.2). The accuracy data for all FP standard concentrations passed the accepted criteria of 85-115% (Table 4.3). Furthermore, both the precision and the accuracy of the QC standards successfully met the validation criteria (Table 4.4). The LOD and LOQ were 106 pg/mL and 312 pg/mL respectively.

Table 4. 2. Inter- and intra-day precision (CV, %) of the data obtained for each fluticasone propionate (FP) standard concentrations, using the LC-MS/MS. Data represent mean ± SD (n=3).

FP (pg mL^{-1})							
Theoretical concentration	156	313	625	1250	2500	5000	10000
Batch 1 (n=3)							
Mean measured concentration	122.6	209.0	548.0	1240.3	2407.9	4940.2	9423.6
± SD	± 43.3	± 25.9	± 26.5	± 103.2	± 78.2	± 46.7	± 395.3
CV (%)	35.3	12.4	4.8	8.3	3.2	0.9	4.2
Batch 2 (n=3)							
Mean measured concentration	193.3	346.7	703.3	1566.7	2920	5973.3	11860
± SD	± 75.1	± 65.1	± 56.9	± 120.6	± 98.5	± 240.1	± 251.2
CV (%)	38.8	18.8	8.1	7.7	3.4	4.0	2.1
Batch 3 (n=3)							
Mean measured concentration	112.0	308.7	685.3	1405.3	2868.7	5758.7	11142.0
± SD	± 65.6	± 25.2	± 96.1	± 80.2	± 230.3	± 153.7	± 95.4
CV (%)	58.5	8.2	14.0	5.7	8.0	2.7	0.9

Table 4. 3. Accuracy of the data obtained for each fluticasone propionate (FP) standard concentration, using the LC-MS/MS. Data represent mean ± SD (n=9).

FP (pg mL^{-1})							
Theoretical concentration	156	313	625	1250	2500	5000	10000
Mean concentration[a]	142.6	288.1	645.6	1404.1	2732.2	5557.4	10808.5
± SD	± 66.5	± 71.9	± 93.3	± 166.9	± 277.3	± 493.7	± 1110.2
Accuracy[b] (%)	91.4	92.0	103.3	112.3	109.3	111.1	108.1

[a] n = 9

[b] accepted range = 85-115%

Table 4. 4. Precision (CV, %) and accuracy of the fluticasone propionate (FP) quality control standard concentrations. Data represent mean ± SD (n=2).

Theoretical concentration (pg mL^{-1})	469	1875	7500
Mean measured concentration[a]	415.0	1973.5	6590
± SD	± 42.4	±238.3	±21.2
CV (%)	10.2	12.1	0.32
Accuracy[b] (%)	88.5	105.3	87.9

[a] n = 2

[b] accepted range = 85-115%

The % extraction recovery was low, between 20-30% for all FP QC standards (Table 4.4) however, the values were consistent overall when evaluating the intra-day and inter-day % recovery.

Table 4. 5. Extraction recovery (%) of fluticasone propionate (FP) quality control standard concentrations. Data represent mean ± SD (n=9).

Theoretical concentration (pg mL^{-1})	469	1875	7500
Mean extraction recovery (%) [a,b] ± SD	26.4 ± 3.5	24.4 ± 1.2	23.7 ± 2.1

[a] n = 9

[b] Extraction recovery = [peak area response of extracted sample/ peak area response of post-extracted sample] x 100

4.4.2 Application of bio-relevant media in the Dissolv*it*® system

The PEO medium used as the standard solvent in the Dissolv*it*® system possessed a lipid content of 4 mg/mL, which was lower than the lipid content of SLF, 5.4 mg/mL (Table 4.1). The FP concentration in the perfusate was highest at all time points when FP dissolved in PEO and lowest in SLF (Figure 4.5). However, the overall difference in the FP concentration values in all three lung fluids at most time points, were not statistically significant (One-Way ANOVA, $p \geq 0.05$). This is except the difference in FP concentration in PEO and SLF at 20 min. The FP concentration profile in perfusate was very similar between PEO and Survanta®, both reaching a Cmax at approximately 20 min.

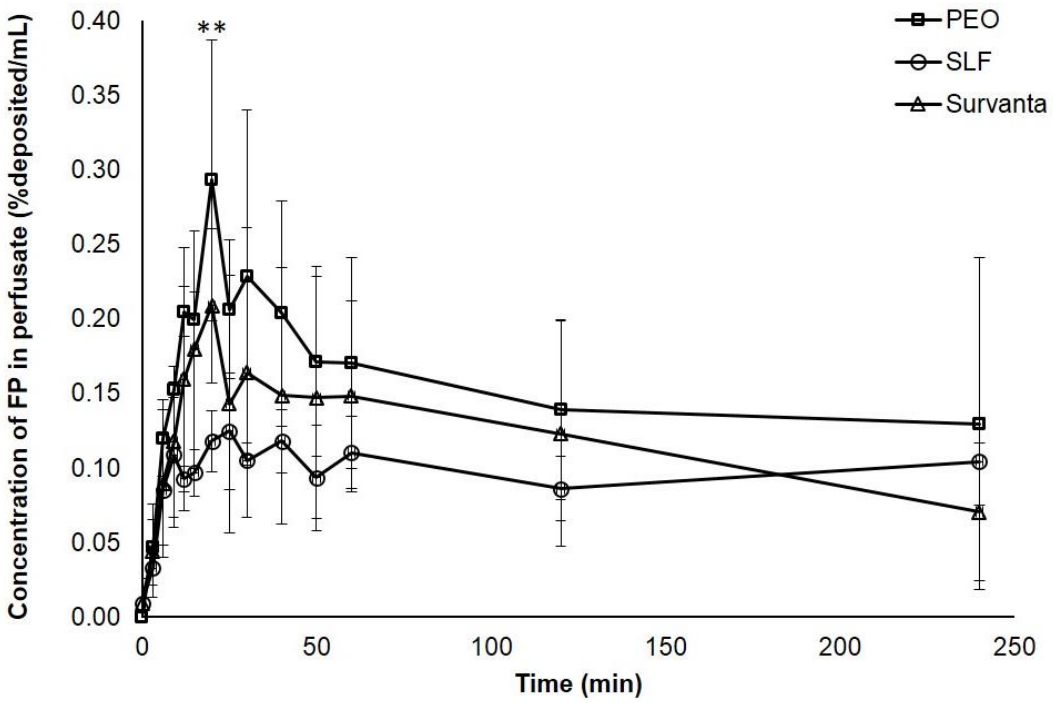

Figure 4. 5. Concentration of fluticasone propionate (FP) in the perfusate over time, following dissolution in 1.5% w/v Polyethylene oxide + 0.4% w/v L-alphaphosphatidyl choline (PEO), simulated lung lining fluid (SLF) and diluted Survanta®. Concentration normalised to mass deposited on the glass cover slips. **Difference in FP concentration in PEO and SLF is statistically significant (One-Way ANOVA, p ≤ 0.05). Data represent mean ± SD (n=3).

4.4.3 Evaluation of the dissolution of FP in Dissolv*it*® versus in IPL

The concentration of FP and the cumulative percent of FP transferred into the perfusate over time is shown in Figure 4.6. There were similar profiles in each medium reflecting the ranking observed in the perfusate in Figure 4.5. The concentration of FP and cumulative % FP in the perfusate was significantly highest, at nearly all time points, following its dissolution in rat IPL in comparison to all the bio-relevant medium applied to the Dissolv*it*® system (One-Way ANOVA, $p \leq 0.05$). However, with regards to the FP concentration profile shape over 120 min, the shape for IPL most closely matched that of SLF, whereby the graph seemed to plateau after approximately 10 min and there was no obvious concentration peak.

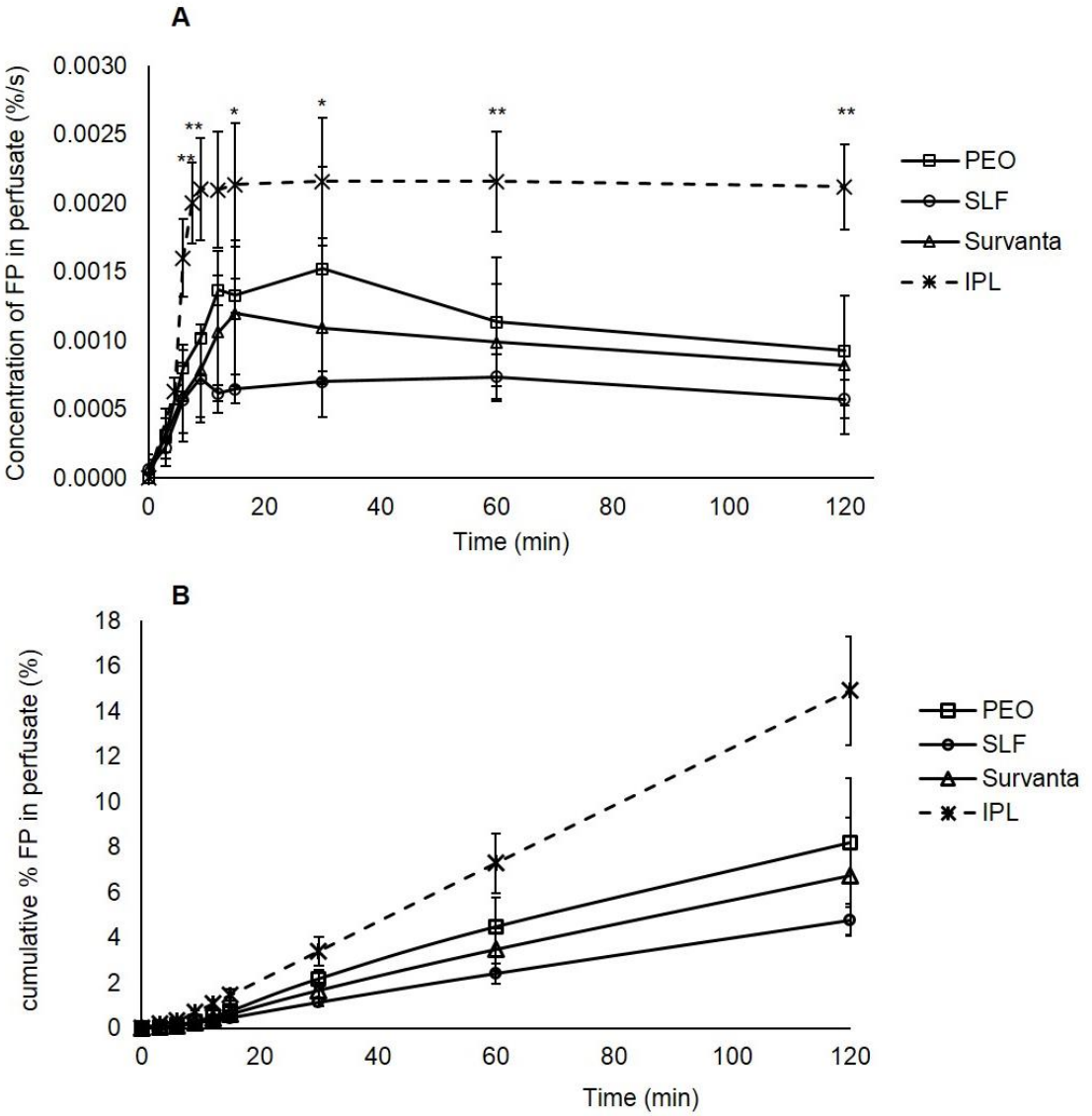

Figure 4. 6. a) Concentration of fluticasone propionate (FP) in the perfusate over time following dissolution in 1.5% w/v Polyethylene oxide + 0.4% w/v L-alphaphosphatidyl choline (PEO), simulated lung lining fluid (SLF), diluted Survanta® and rat isolated perfused lung (IPL). *Difference in FP concentration in IPL and SLF is statistically significant (One-Way ANOVA, p ≤ 0.05). **Difference in FP concentration in IPL and the remaining three lung fluid is statistically significant (One-Way ANOVA, p ≤ 0.05), and b) Cumulative % of FP transferred into the perfusate over time, following its dissolution in PEO, SLF, Survanta and IPL. Data represent mean ± SD (n=3).

4.4.4 *In silico* modelling of FP dissolution

Development of the *in-silico* model and data collection was done by Sumit and collaborators at University of Graz, in Austria. The *in vitro* data collected were fitted to a Weibull function to extract the shape and time scale parameters, that were then used to model the dissolution of particles in the developed model (Figure 4.7). Pharmacokinetic parameters (Cmax, Tmax and $AUC_{0-\infty}$) calculated from the simulated profiles for the different lung fluid simulants, all seemed to reasonably well predict (within two folds) the pharmacokinetic parameters of inhaled FP (1000 µg dose) administered via Flixotide Evohaler® 250 µg strength inhaler, obtained from a study by Mackie et al (Mackie *et al.*, 2000) (Table 4.6). No significant difference was found between the clinically observed and simulated pharmacokinetic parameters when *in vitro* dissolution input from PEO and Survanta was used in the developed PBPK model (One-Way ANOVA, $p \geq 0.05$). On the contrary, statistically significant differences in Cmax and $AUC_{0-\infty}$ were found when the slower *in vitro* dissolution of FP in SLF was modelled compared to dissolution in PEO. The $AUC_{0-\infty}$ predicted by the model in all three bio-relevant mediums were slightly underestimated, in comparison to the *in vivo* profile. However, it appeared that the pharmacokinetic parameters from the *in vivo* profile most closely matched the values obtained from PEO than from the other bio-relevant medium.

To gain a better understanding of the sensitivity of the predicted PK parameters towards the dissolution profiles of FP, different hypothetical dissolution profiles were created (Figure 4.8) and the data was fitted to the Weibull function to extract the shape and time parameters of these profiles (Table 4.7). The parameters were obtained using a rearranged version of the Weibull equation (equation 13, stated in Chapter 1); it was applied to describe various hypothetical dissolution curves and used as an input to the PBPK model. The exact equation used in this context was equation (23):

$$M = 1 - \exp\left[-(t-T_i)^b / \alpha\right] \quad (23)$$

The location parameter (T_i) in all the investigated cases was zero. In the cases where the dissolution-time curves differed from the SLF profile only in terms of faster or slower

initial rate (cases 2 and 3), a similar shape parameter described the exponential curves (b~1). Fitting of an immediate release type hypothetical dissolution profile (case 1) resulted in a value describing a sigmoidal curve (b>>1). Calculated values of AUC for the cases were similar to the values generated for SLF, reflecting the fixing of the cumulative percentage of dissolved FP to 9.34% in 4 h. However, major differences were observed in terms of Cmax and Tmax with profiles when drug dissolution was faster/slower than *in vitro* dissolution profile of FP in SLF. Dissolution profiles mimicking the faster dissolution rates (case 1 and case 2) predicted higher values of Cmax (6- and 2- folds), and lower values of Tmax (6- and 4- folds) compared to the values observed in SLF. In case 3, where the initial rate of *in vitro* dissolution was lower than that in SLF, a lower Cmax and higher Tmax value were predicted.

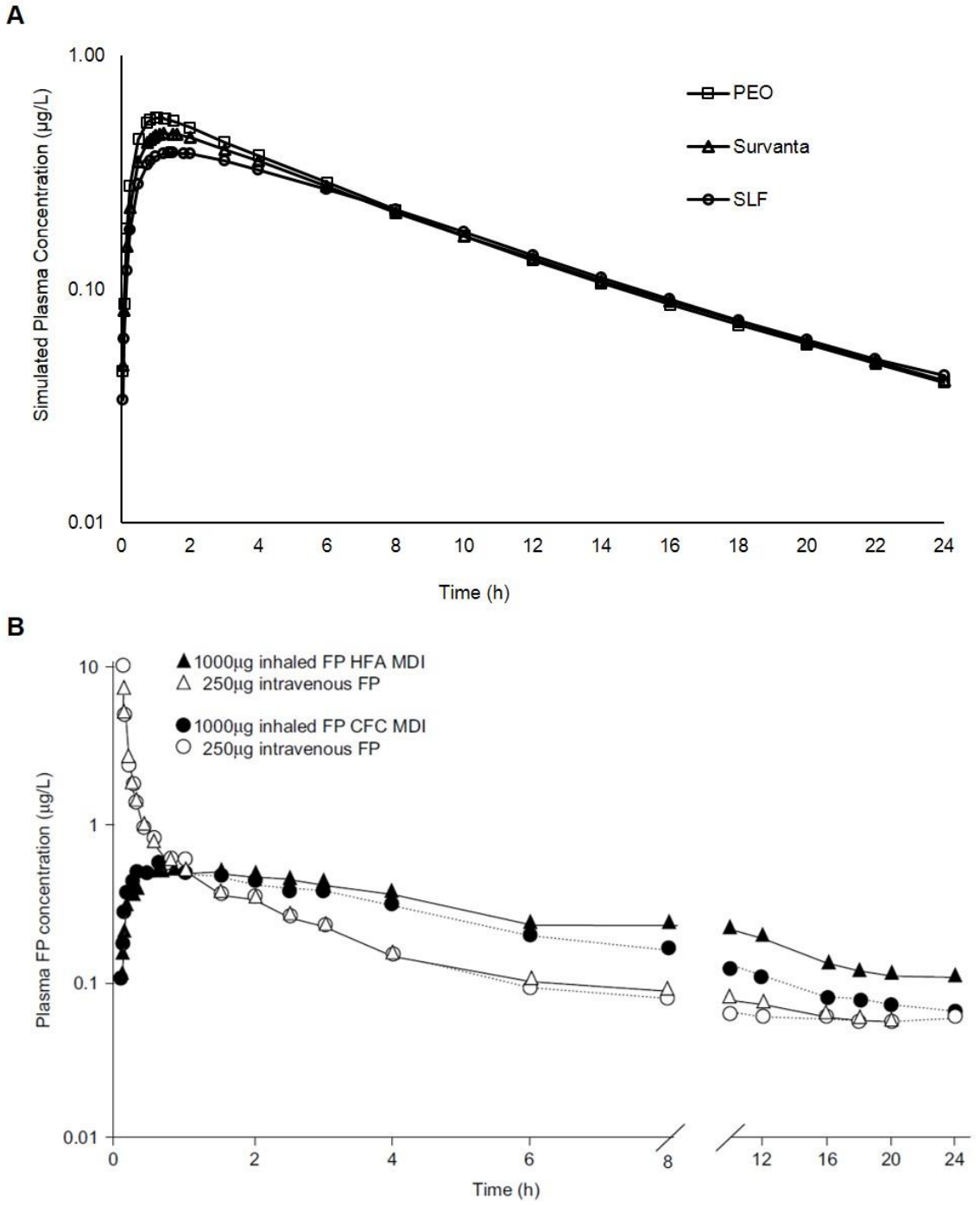

Figure 4. 7. In-silico modelling. A) Simulated plasma concentration of fluticasone propionate (FP) over time, following its dissolution in 1.5% w/v Polyethylene oxide + 0.4% w/v L-alphaphosphatidyl choline (PEO), simulated lung lining fluid (SLF), diluted Survanta®. B) The median plasma FP concentrations in healthy volunteers after administration of FP 1000 µg via a chlorofluorocarbon (CFC) and a hydrofluoroalkane (HFA) metered-dose inhaler (MDI) and administration of FP 250 µg by short intravenous infusion. Data obtained by Mackie et al (Mackie et al., 2000).

Table 4. 6. Pharmacokinetic data of fluticasone propionate (FP) absorbed in plasma from healthy volunteers, after inhalation of FP pMDI (In-vivo) and of FP absorbed in perfusate, following its dissolution in 1.5% w/v Polyethylene oxide + 0.4% w/v L-alphaphosphatidyl choline (PEO), simulated lung lining fluid (SLF), diluted Survanta®. Data represent mean ± SD (n=3 or n=9).

Pharmacokinetic parameter	In-vivo profile*	PEO**	SLF**	Survanta®**
Cmax (µg/L)	0.54	0.54 ± 0.08	0.39 ± 0.03	0.47 ± 0.10
Tmax (h)	0.80	1.11 ± 0.15	1.55 ± 0.26	1.22 ± 0.36
AUC0-∞ (µg/L.h)	6.54	4.97 ± 0.10	4.61 ± 0.09	4.74 ± 0.40

*n=9; reported by Makie et al, 2000.
**n=3

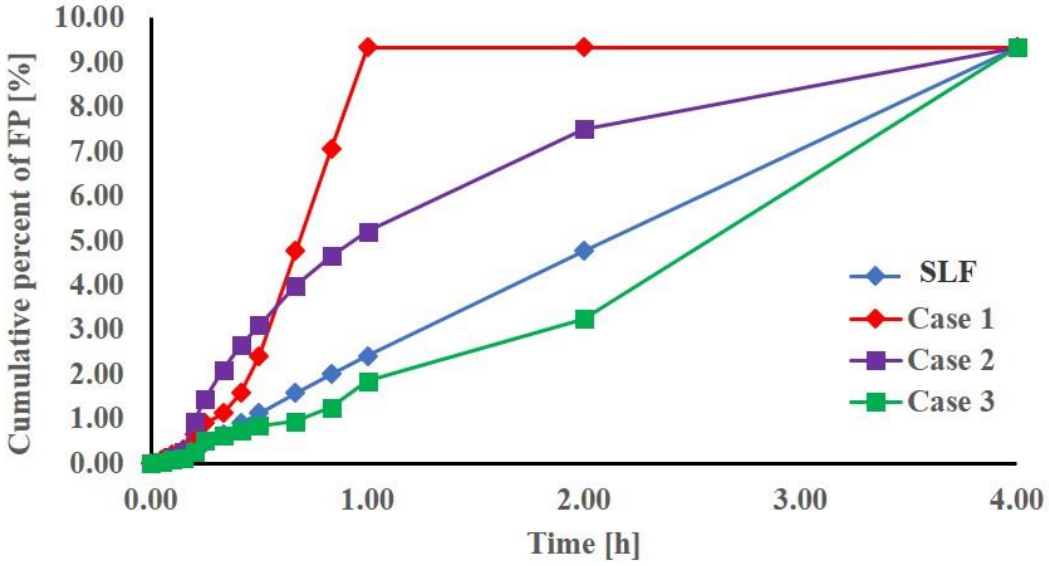

Figure 4. 8. Sensitivity testing using numerical approximation to derive three dissolution profiles that vary from the experimental observations for dissolution of fluticasone in simulated lung fluid (SLF) (observed): a profile where release greatly exceeded that observed experimentally in SLF (case 1) and two profiles that are similar to dissolution SLF but initially more rapid (case 2) or slower (case 3).

*Table 4. 7. Fitted Weibull shape factor (b) together with pharmacokinetic data of FP following its dissolution in simulated lung fluid (SLF) and artificial dissolution profiles (Cases 1-3); *n=3, **n=1*

Parameter	SLF*	Case 1**	Case 2**	Case 3**
Weibull shape parameter	1.5285 ± 0.08	3.0204	1.1508	1.8716
C_{max} (ug/L)	0.74 ± 0.05	4.61	1.44	0.53
T_{max} (h)	3.01 ± 0.58	0.50	0.75	6.00
$AUC_{0-\infty}$ (ug/L h)	6.46 ± 0.08	6.92	6.87	6.04

4.5 Discussion

4.5.1 Solid phase extraction and LC-MS/MS validation for assay of FP

It is well known that SPE offers an improved extraction method over liquid phase extraction. Although liquid-liquid extraction is more cost-effective, SPE is less time-consuming and requires minimal sample preparation and solvent use (Zwir-Ferene and Biziuk, 2006). Initially, a couple of liquid-liquid extraction methods were attempted to extract the FP from the biological fluids (Guan *et al*., 2003; Byrro *et al*., 2012). However, the methods proved to be non-repeatable since when attempting to validate the liquid-liquid extraction and LC-MS.MS assay, the calibration curves were not always linear and the %CV were very inconsistent. Therefore, for this study, SPE was chosen as the preferred extraction method. However, it was found that there are currently little reports of SPE methods or simplified easy to follow methodologies. Consequently, the methods that are published for FP analysis (Krishnaswami *et al.*, 2000; Matuszewski *et al.*, 2003) proved to be difficult to replicate with adequate reproducibility and sensitivity. Hence, this study first prioritised developing and validating a newly-modified SPE, LC-MS/MS method for quantification of low concentrations of FP in biological fluids.

The SPE conditions for sample preparation initially required optimisation. SPE preconditioning, washing with water, low percentage organic solution and elution solvent were optimised with different volumes and different percent of organic solution. For example, for preconditioning the SPE columns, water was added followed by 50% v/v methanol in water, to ensure adequate wash and preparation of the column. However, at this step, a small peak corresponding to the FP analyte was detected. Therefore, conditioning with 25% v/v methanol in water was a better option since no peaks were detected, indicating no FP was lost in the wash step. For the extraction procedure, zinc sulphate was added first to the samples to allow for FP drug to detach from the albumin in the rat plasma and this was mixed well, before addition of ammonium hydroxide to resuspend the detached FP into the solution. However, this produced very poor extraction with smaller peak areas for FP and FP-d5, in comparison to when zinc

sulphate and ammonium hydroxide were added simultaneously prior to the adequate mixing. For elution of FP, eluting with acetonitrile alone also produced very little peak areas in comparison to eluting with acetonitrile and dichloromethane. However, when using high volumes of each chemical, this produced an extra peak in the chromatograms indicating that too much organic solvent was added. Therefore, both chemicals were used, whereby FP was eluted twice with 200 µL of pure acetonitrile followed by once with 100µL dichloromethane, enhancing material recovery and quantification.

It can be concluded that the final assay for quantification of FP in rat plasma was developed well and validated successfully. The sensitivity of an assay is dependent upon the efficiency of the extraction method and the sharpness of the chromatographic peak (US FDA CDER, 2011). This method appeared to be highly selective and sensitive, and effectively eliminated the interference by endogenous impurities, as clear distinctive peaks corresponding to the analyte of interest were seen in all chromatograms generated, at all standard concentrations. Most of the validation data fell within the accepted criteria or ranges, except for the lowest standard concentration, at 156 pg/mL. This is most likely attributed to the concentration of the drug being so close to the reported LOD, causing more noise signal interference and affecting the precision and repeatability of the result. However, since the FP concentrations in all dissolution experiments predominantly fell within the upper concentration range of the calibration curve, the method was deemed as fit for purpose. The method was suitable for this study and can be applied to biological fluids such as the lung lining mucus, to allow for accurate pharmacokinetic analysis of compounds following their inhaled administration.

With respect to the percent analyte recovered, a very low percent was recovered from the SPE extraction method. This is likely due to the inevitable high binding-affinity FP tends to have to plastic, binding to the extraction plates (Otero *et al*., 2001). To minimise this and further optimise SPE, low-binding deep-well plates were used for the study and low-binding pipette tips. However, this only increased recovery by a small percentage.

It is important to note that to complete the validation process, an assessment of the matrix effect is often required, particularly if one wishes to validate an entirely novel SPE, LC-MS/MS quantitative method, since the full validation recommendations must ideally be followed. This matrix effect allows for the assessment of any ion suppression or ion enhancement caused by the plasma media used and if this interferes with the results. However, assessment of the matrix effect has been reported to be only critical when homologues, rather than stable, isotope-labelled analytes are utilized as internal standards (Matuszewski *et al.*, 2003). The internal standard used in this study was FP-d5, which is a stable isotope labelled deuterated FP and hence, assessment of the matrix effect was not a necessity for the study. Again, this indicated that the novel SPE/LC-MS/MS technique developed here was fit for purpose.

4.5.2 Application of bio-relevant media in the Dissolv*it*® system

Applying different versions of proposed lung fluid to the Dissolv*it*® system was a first step towards developing dissolution as a biorelevant system, as it allows for the assessment on the necessity for the application of SLF, if we truly wish to mimic the dissolution of aerosol particles that occur in the lungs.

The Survanta used in this study was diluted with PBS in attempt to normalise the data generated to lipid concentration, however, the SLF yet exhibited slightly higher lipid concentration to the others. It was hypothesised, based on this, that dissolution in SLF would be enhanced as the greater lipid content may facilitate the lipophilic FP drug solubilisation via encapsulation into the lipid lamellar structures. However, the results showed differently; FP concentration in the perfusate was lowest when FP dissolved in SLF compared to when FP dissolved in the other media. This is likely attributed to the characteristics of SLF as identified and described in Chapter 3. It was made evident in Chapter 3 that the FP exhibited solubility in SLF that was very close to its solubility in Gambles, even though SLF is predominantly a liposomal formulation and Gambles in a simple aqueous solution. This may be attributed to SLF liposomes forming stable colloidal structures, making them less likely to sequester such poorly soluble drugs.

However, solubilisation and hence dissolution may not only be influenced by the lipid content but also by the interaction of the extra components present in SLF. For example, the albumin present in the media may solubilise the cholesterol that contributes to the formation of tight lamellar structures (Kim *et al*., 2013) and thus reduce their stability and the extent to which drug is solubilised within them. However, such influence in FP dissolution may not be regarded as substantial since the overall difference in the FP concentration values in all three lung fluids at most time points, were not statistically significant. The FP concentration profile in perfusate was very similar between PEO and Survanta as expected, since both have the same lipid concentration of 4 mg/mL, influencing the dissolution of FP in the same manner.

4.5.3 Evaluation of the dissolution of FP in Dissolv*It*® versus in IPL

The next clear step to this study was to undergo some pre-clinical investigations using rat IPL. The concentration of FP in the perfusate profiles, obtained following FP dissolution in the different proposed media, can be compared directly with the profile obtained following FP dissolution in rat lung. This allows for a better understanding on how close the dissolution profiles and dissolution kinetics of FP obtained from a developing *in vitro* system, is, to the true dissolution of FP that occurs *in vivo* in mammals.

It was evident that the concentration of FP and cumulative % of FP in the perfusate was significantly highest at nearly all time points following its dissolution in rat IPL, and this is likely attributed to the IPL possessing a comparatively rapid peripheral (alveolar) dissolution and permeation as well as a slower central (airway) dissolution and permeation, compared to what the Dissolv*It*® system models. In the central regions of the lungs, non-sink conditions may be expected as the dose is distributed over a small area compared to the alveolar region and dissolved FP particles are required to diffuse across the 5-20 µm pseudostratified epithelium compared to 1-2 µm in the alveoli of the lungs, to reach the perfusate. However, the Dissolv*It*® system possess an area of 1.3 cm^2 and the penetration distance is approximately 60 µm (Gerde *et al*., 2017). However, visually, the overall perfusate concentration profile of FP following its dissolution in rat

IPL most closely mimicked the profile from SLF, in comparison to the remaining applied fluids. This suggested that there is a potential similarity in the FP pharmacokinetics following its dissolution in SLF and its dissolution *in vivo*, providing an indication that SLF may be necessary if we truly wish to mimic the dissolution that occurs *in vivo*.

4.5.4 *In silico* modelling of FP dissolution

Since FP has been reported in literature to exhibit dissolution rate-limited absorption (Edsbäcker and Johansson, 2006; Boger *et al.*, 2016) it is important to mechanistically understand the dissolution process of this molecule, to then accurately predict its deposition and absorption in the lungs. Hence, modelling was carried out to rationalise the *in vitro* dissolution data generated from the Dissolv*It*® and identify the effect of using different lung fluid simulants on the simulated plasma concentration time profiles of inhaled FP.

Although comparison with rat IPL data suggested that SLF may be a necessary dissolution media, if we wish to predict what occurs *in vivo* obtain reliable IVIVC data, *in silico* modelling suggested differently. The data indicated that pharmacokinetics of inhaled FP can be much closely predicted following its dissolution in PEO, then in the other fluids, since the Cmax, Tmax and $AUC_{0-\infty}$ most closely resembled the FP pharmacokinetics in the *in vivo* plasma. However, the $AUC_{0-\infty}$ predicted by the model in all three cases appeared to be significantly low in comparison to the *in vivo* data. It is likely the values are underestimated due to the underestimation of terminal time points of plasma concentration time profile of inhaled FP, as reported in the literature. This leads to the speculation that FP is retained for longer in the airways, which if incorporated into the model would improve further the quality of the simulation. Consequently, it was recognised that the model developed exhibited some intrinsic limitations. This is because the *in vitro* dissolution data incorporated into the model, to obtain PK data, was in fact a combination of both dissolution and diffusion of the FP, both processes that inevitably and simultaneously occurred when analysing the dissolution of FP using the Transwell® dissolution method. Eliminating the diffusion process entirely from the

Transwell® dissolution system, would further improve the quality and reliability of the model.

However, the model proved to be sensitive to differences in *in vitro* dissolution profiles and translate the differences effectively to the respective PK parameters. When evaluating the sensitivity of the predicted PK parameters towards the different hypothetical dissolution profiles of FP, the similarity in AUC in all three cases and SLF was expected. This is because AUC differences would only be likely if there were different extent of *in vivo* dissolution of the drug over the period of 4 h. The differences in Cmax and Tmax observed for the dissolution profiles mimicking faster dissolution rates (cases 1 and 2) was as expected, considering that these dissolution profiles provided higher drug concentration in solution during the early stages of dissolution process. The results illustrated how dissolution profiles can have significant impact on the PK parameters of a poorly soluble inhaled drug, and the application of biorelevant *in vitro* assays together with PBPK modelling to study the impact of dissolution.

Summary and conclusions

A novel and sensitive solid phase extraction and LC-MS/MS technique for the assay of FP was established and validated successfully, where it can quantify FP at low concentration levels, in biological lung fluids. With respect to application of various dissolution media to the Dissolv*It*® system, the overall insignificant differences in the concentration of FP in perfusate/time and the FP dissolution profiles seen between the SLF, PEO and Survanta®, suggested that SLF is not a necessary medium if we truly wish to mimic the dissolution behaviour of inhaled pharmaceuticals *in vivo*.

The developed *in silico* model was successful in translating the differences observed in the *in vitro* dissolution of FP to physiologically relevant simulated *in vivo* plasma concentration time profiles, leading to an enhanced understanding on how dissolution of FP may influence absorption in the lung. It appeared that using PEO as the dissolution media in the Dissolv*It*® system provided the best approximation for dissolution *in vivo* so far, and thus provides better correlation and bioequivalence.

The study suggested overall that although SLF consists of the key components that constitutes the *in vivo* lung lining fluid and hence contributes to making a dissolution system to most closely mimic the *in vivo* lung environment, in comparison to other proposed fluids, it does not provide any added significance in terms of obtaining more predictive or reliable IVIVC data or profiles. Therefore, in taking this further, a simpler surfactant-based solution, seems to be reasonable for application in dissolution systems as the proposed 'biorelevant' media.

Chapter 5

Development of a biorelevant dissolution test using Experimental Design methodology

5.1 Introduction

In addition to the Dissolv*It*® system, the Transwell® system developed in Chapter 2, was found to be another convenient starting point towards the development of a biorelevant dissolution system. It was concluded that the Transwell dissolution method provides the best representation of lung geology, with the transwell insert allowing for applications of physiologically-relevant fluids, at little volumes. Hence, this system can be developed further to potentially become a tool to establish IVIVC and model PK data. In this context, for the *in vitro* test to be biorelevant, i.e. reflective of the *in vivo* lung environment, and to be used for the purpose of describing the *in vivo* situation, it requires conditions that reflect those encountered in vivo to be utilised. Hence, it was necessary to consider factors that potentially influence dissolution *in vivo* and apply these to the *in vitro* system, evaluating their significance and effects. This would help identify the ideal physiologically-relevant factors that must necessarily be controlled, if we wish to obtain dissolution data that is predictive of what occurs *in vivo*. Key influential factors include dissolution medium concentration, the temperature at which dissolution occurs at and the stirring rate at which dissolution is exposed to.

With regards to the dissolution medium concentration, there has been a general lack of understanding of the true composition of the lung lining fluid at which dissolution of particles occur and as a result, the application of previously proposed fluids has led to the overestimation and underestimation of the dissolution rate of inhaled drugs. To improve this, part of this PhD considered developing a SLF, which consists of the components of healthy human alveolar RTLF (described in Chapter 2). However, when SLF was applied to the Dissolv*It*® system as an initial step towards identifying its necessity in developing a biorelevant system (described in Chapter 4), it was concluded that the PK data of FP obtained from the *in-silico* model did not correlate significantly

with the *in vivo* profile, in comparison to the other proposed media. Therefore, for this part of the study, the dissolution medium used was a simple surfactant solution, SDS in PBS, as utilised by many studies previously (Arora *et al.*, 2010; Son *et al.*, 2010; Rohrschneider *et al.*, 2015). With regards to the temperature, dissolution experiments may be conducted at room temperature, 21°C, for practical reasons of convenience or performed at 37°C to mimic normal human body temperature (Martins *et al.*, 2010; Huang *et al.*, 2016). The impact of conducting the experiment under different temperatures has not been evaluated, to date, nor has the necessity to conduct the experiment under physiological temperatures to obtain accurate dissolution profiles been addressed. Consequently, with respect to the stirring rate, although implications of this has not been studied extensively, a study conducted by Rohrschneider et al, found that a stirred Ciclesonide solution versus an unstirred solution, produces a higher dissolution rate (Rohrschneider *et al.*, 2015). In the lungs, the lining fluid is not stirred and is often described as 'stagnant'. However, the fluid is exposed to dynamic changes during breathing and the implications of this on dissolution and the biorelevant level of agitation required *in vitro,* are unclear. Hence, for this study, there was clear rationale to assess the impact of these three factors on dissolution.

An aspect of system development and improvement, and to obtain valuable information on the influences of factors on a system, statistical Design of Experiment approach (DOE) can be employed (Dean, 2000). DOE allows variables to be changed together, permitting the assessment of the effects of the individual variable on the system as well as the evaluation for any variable-variable interactions. Consequently, it ensures efficiency, whereby meaningful and multiple conclusions can be drawn from small number of experiments (Lakeram *et al.*, 2008). This approach has been applied to many previous studies, evaluating and optimising physiologically-relevant experimental conditions on an *in vitro* assay (Lakeram *et al.*, 2008; Jivani *et al.*, 2012; Mogal and Derle, 2017). However, it has not yet be applied to dissolution systems for OIPs and hence presents a novel opportunity that can be exploited in this study.

The development of dissolution tests to be utilised in drug research and development, must allow for adequate comparison between the dissolution profiles obtained. To compare dissolution profiles between different pharmaceutical products or dissolution profiles from the same product but under different conditions, mathematical models can be applied (Dash *et al.*, 2010; Lokhandwala *et al.*, 2013; Caccavo *et al.*, 2017). Many studies have modelled drug dissolution or drug-release profiles quantitatively, using the model-dependent approach (Patel *et al.*, 2008; Gonjari *et al.*, 2009; Simionato *et al.*, 2018). However, this has been widely applied to solid and semi-solid dosage forms, with very little reports on the modelling of dissolution profiles obtained from OIPs specifically. In a single previous study, Weibull modelling has however been applied on the dissolution profiles of FP obtained from the Transwell® method (Kippax *et al.*, 2016). Application of the model provided a description of the dissolution process in more detail in comparison to other models and provided time parameters that allows for quantitative comparisons between the dissolution profiles, such as T25 or Td, which represent the time taken for 25% and 63.2% of the drug to dissolve, respectively (Langenbucher, 1972). To use a suitable 'Response' parameter for the DOE analysis, identification of the most convenient time parameter to use, is required. Generally, modelling such profiles is a relatively novel approach and using such parameters to constitute the 'Response' of the DOE, can help provide an indication of the factors that need to be controlled and the optimal, physiological dissolution conditions required, to produce the desired dissolution rate for an inhaled product.

Aim:

In this chapter, the aim was to take an alternative route into developing dissolution as a biorelevant system, that can potentially be used as an IVIVC tool for OIPs. This will be done by evaluating the influence of and the need for physiologically-relevant factors on the Transwell® dissolution system and optimising the system to exhibit conditions that most closely relate to the conditions that exist *in vivo*.

Objectives:

To reach this aim, the objectives were to, (i) identify convenient factor levels of each factor studied via preliminary experimentations, (ii) use experimental design to conduct a suite of dissolution experiments under various physiological conditions, (iii) employ a model-dependent approach to quantitatively compare dissolution profiles (iv) use experimental design methodology to evaluate the influence of these physiological factors on dissolution and assess for factor-factor interactions and (v) identify the optimal levels of these selected factors at which dissolution is to be conducted.

5.2 Materials

Dissolution was carried out via the TSI/Transwell dissolution system, using the materials listed in Chapter 2, section 2.2. The equipment/glassware necessary for the setup of the Twin Stage Impinger (TSI) were purchased from Copley Scientific Limited (Nottingham, UK).

5.3 Methods

5.3.1 Solubility of FP

The solubility of FP in different concentrations of SDS in PBS: 0.02, 0.05, 0.10, 0.15, 0.20, 0.25 and 0.50% w/v were carried out according to the method described in Chapter 3, section 3.3.7.

5.3.2 Deposition and dissolution of FP

The dissolution method used was as described in Chapter 2, section 2.3.6. However, the dissolution medium was either 0.02%, 0.1% or 0.5% w/v SDS in PBS. Following deposition and transfer of the Transwell insert into a well of 24-well plate containing 600 µL of the dissolution medium, the plate was placed on an orbital rotator, set to stir at either 15, 50 or 85 rev p min. The tests were performed at either 21, 29 or 37°C. For the validation of the selected mathematical dissolution model, dissolution of FP was carried out over an 8 h period, were the time points were 2, 5, 10, 15, 30, 45, 60, 120, 240, 360, 480 and 540 min. To obtain the deposited amount of FP, the recovery of the filter at 540 min was carried out exactly as the recovery of sample 180 min, as described in section 2.3.6.

5.3.3 Quantification of FP by RP-HPLC-UV

Quantification of FP in the samples was carried out using the method described in Chapter 2, section 2.3.2.

5.3.4 Experimental Design

A three-level three factorial Box-Behnken experimental design (constructed using Design-Expert 11) was used to evaluate the effects of selected independent variables on the response. The selected response in this study was a dissolution rate parameter, T25, which represents the time taken for 25% of deposited drug to dissolve. For the Box-Behnken experimental design, a total of 45 experimental runs were used (Table 5.1). The design required three factors to be chosen with three levels of each factor evenly spaced. The factors were coded for low, medium and high settings, as -1, 0 and +1 respectively, as similarly set out in previous studies (Singh *et al.*, 1996; Lakeram *et al.*, 2008). The factors studied that constitutes the experimental design were the dissolution media concentration, stirring rate of the dissolution process and temperature at which dissolution was carried out (Table 5.2). Each factor was set at limits determined via preliminary investigations (Figure 5.1) and included practically-relevant and physiologically-relevant conditions.

Experiment	Factor and Factor Level		
	a	b	c
1	-1	-1	+1
2	0	-1	+1
3	+1	-1	+1
4	0	+1	+1
5	+1	+1	+1
6	-1	+1	+1
7	0	0	0
8	+1	0	0
9	-1	0	0
10	-1	+1	0
11	-1	+1	0
12	-1	+1	0
13	-1	-1	-1
14	0	-1	-1
15	+1	-1	-1
16	-1	0	+1
17	+1	0	+1
18	+1	0	+1
19	-1	+1	-1
20	0	+1	-1
21	+1	+1	-1
22	+1	-1	+1
23	-1	-1	+1
24	0	-1	+1
25	0	0	0
26	-1	0	0
27	+1	0	0
28	-1	+1	-1
29	0	+1	-1
30	+1	+1	-1
31	+1	0	0
32	0	0	0
33	-1	0	0
34	-1	+1	+1
35	+1	+1	+1
36	0	+1	+1
37	0	+1	0
38	+1	+1	0
39	-1	+1	0
40	+1	-1	-1
41	0	-1	-1
42	-1	-1	-1
43	-1	0	+1
44	+1	0	+1
45	0	0	+1

Table 5. 1. List of the 45 dissolution experiments, with factor levels presented as coded values for the Box-Behnken Experimental Design, where 'a' represents concentration of the dissolution media/concentration of SDS in PBS, 'b' represents temperature and 'c' represents the stirring rate. -1, 0 and +1 represent low, medium and high factor levels respectively.

Table 5. 2. The factors and their factor levels investigated in the Box-Behnken Experimental Design. -1, 0 and +1 represent low, medium and high factor levels respectively.

	Factor	Level		
		-1	0	+1
a	Concentration of SDS in PBS/ Dissolution media (% w/v)	0.02	0.1	0.5
b	Temperature (°C)	21	29	37
c	Stirring rate (rev p min)	15	50	85

5.3.5 Dissolution profile modelling

To decide the response parameter for the Experimental Design, mathematical models were applied to the drug dissolution graphs obtained from the 45 experiments. The models applied describe the dissolution kinetics and provide a dissolution parameter, such as dissolution rate constant or time taken for an amount of drug to dissolve. An excel add-in, DDSolver software, was used to facilitate the application and comparisons of the mathematical models (Zhang *et al.*, 2010). All models were applied to a random selection of a few dissolution experiments from the 45 runs, ranging from experiments that were carried out under low, medium and high factor conditions. The best fit model was selected based on the R^2 values obtained, an approach taken by many other studies (Costa and Sousa Lobo, 2001; Patel *et al.*, 2008; Cascone, 2017). After comparison of the R^2 values and via logical rational, Weibull was selected. All dissolution data gathered were then fitted to the Weibull probability distribution model and Weibull parameters were calculated and compared. The parameters were obtained using equation 13, as stated in Chapter 1:

$$\text{Log}\,[-\ln(1-m)] = \beta \log(t - T_i) - \log \alpha \qquad (10)$$

Where m is the accumulated fraction of the drug, β is a shape parameter, α is a scale parameter and T_i is a location parameter. Td can be calculated from the α and β parameters and represents the time taken for 63.2% of the drug to dissolve. Other parameters included the T25, T50, T75 and T80 which corresponds to the time taken for

25%, 50%, 75% and 80% of the drug to dissolve. The T25 was used as the 'response' values and inputted into the Experimental Design for data analysis.

5.3.6 Data analysis

Statistical data analyses were performed using analysis of variance (ANOVA), with the Design-Expert 11 software. Data comparing the dissolution of FP in SLF and in 0.1% w/v SDS in PBS, the f2 similarity factor, equation (7), and the non-parametric paired sample T-test was applied.

5.4 Results

5.4.1 Preliminary investigations

The preliminary solubility study carried out to identify the solution with the appropriate SDS concentration, in which the solubility of FP in it matches the solubility of FP in SLF, is shown in Table 5.3. It was evident that the solubility of FP in 0.10% w/v SDS in PBS most closely matched the solubility of FP in SLF and thus was considered the biorelevant dissolution medium to be applied to the Transwell® dissolution system.

Preliminary investigations to identify or confirm the three factors to select for DOE is shown in Figure 5.1. The factors that have the potential to increase dissolution of FP were selected for this study, since significant differences were seen when the respective factor levels were altered (Figure 5.1). The stirring rate was selected to be 15, 50 and 85 rev p min. They were considered appropriate and reflective of physiological stirring since they match the human breathing rate at rest, human breathing rate during exercise and the breathing rate of mice, respectively (European Lung Foundation, 2016; Johns Hopkins University, 2019). The temperature ranged from 21 to 37°C since they reflect room to human body temperature. To establish the influence of these factors, dissolution of FP was studied under the factor levels that created highest, medium, lowest, biorelevant and practical conditions for dissolution. The highest conditions at which dissolution was carried out appeared to present a steeper dissolution profile, with greater % of FP dissolved at all time points in comparison to the other conditions and dissolution reached a maximum of 22% by 60 min. The biorelevant conditions exhibited an FP dissolution profile that was in between the lowest and the medium conditions. The conditions considered to be more ‘practical’ showed no significant difference in FP dissolution to the ‘biorelevant’ profile for the first 15 min of dissolution.

Table 5. 3. The solubility of fluticasone propionate in simulated lung fluid (SLF) and in different concentrations of sodium dodecyl sulphate (SDS) in phosphate buffered saline (PBS). Data obtained at 37°C and expressed as mean ± SD (n=3).

Fluid	FP solubility
	Mean Concentration [µg/mL]
SLF	2.04 ± 0.09
0.02% w/v SDS in PBS	0.75 ± 0.34
0.05% w/v SDS in PBS	1.53 ± 0.01
0.10% w/v SDS in PBS	2.14 ± 0.00
0.15% w/v SDS in PBS	4.11 ± 0.01
0.20% w/v SDS in PBS	6.10 ± 0.02
0.25% w/v SDS in PBS	7.86 ± 0.01
0.50% w/v SDS in PBS	13.08 ± 0.06

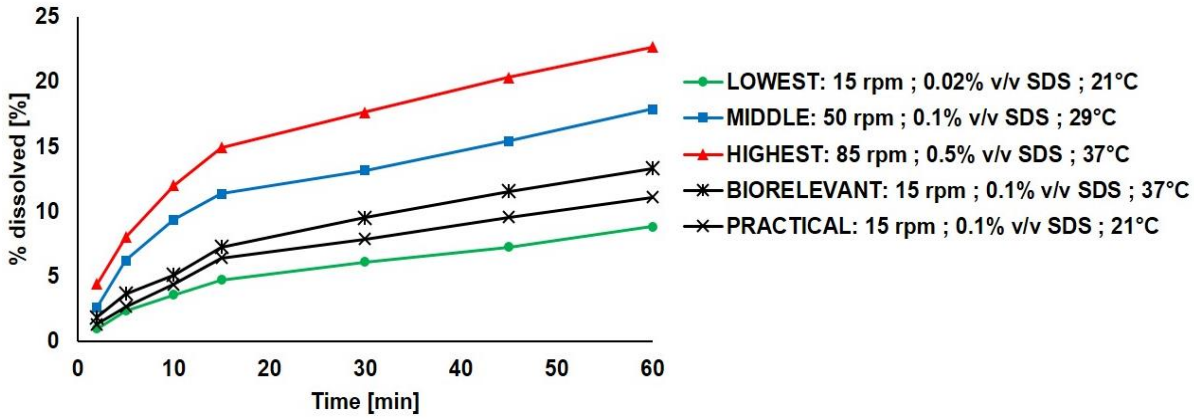

Figure 5. 1. Dissolution of fluticasone propionate via the Transwell® method, under the influence of the lowest, middle, highest, biorelevant and practical factor levels.

5.4.2 Dissolution profile modelling

The dissolution profiles and tables of percent and amount of FP dissolved in each of the 45 experiments, are shown in (Appendix C, Tables C.1 and C.2). Parameters from the Weibull probability distribution model, that was applied to the 45 dissolution profiles, are listed in Table 5.4. The co-efficient, R^2, provides an indication on the correlation between the Weibull model profiles and the dissolution profiles. For all dissolution profiles, the R^2 was approximately 0.99. The β value provides an indication of the dissolution kinetics and it appeared that for all profiles, the value was < 1. A lower T25 value indicated a higher dissolution rate, since it means that under set conditions, it takes less time for 25% of the FP drug to dissolve. Experiment number 5, which represents the conditions: dissolution media of 0.5% w/v SDS in PBS, 37°C and 85 rev p min seem to exhibit the lowest T25 value of 73.29 min. Experiment number 13, which represents the conditions: dissolution media of 0.02% w/v SDS in PBS, 21°C and 15 rev p min seem to exhibit the highest T25 value of 757.84 min.

Experiment	R^2	β	α	T25 (min)
1	0.9928	0.44	60.28	645.29
2	0.9936	0.51	38.56	115.25
3	0.9957	0.39	22.47	122.53
4	0.9966	0.38	20.54	113.10
5	0.9944	0.37	17.09	73.29
6	0.9964	0.51	46.95	170.74
7	0.9958	0.40	22.56	113.25
8	0.9964	0.39	20.56	101.77
9	0.9950	0.44	45.56	341.07
10	0.9935	0.46	44.18	245.88
11	0.9942	0.44	39.27	266.47
12	0.9968	0.37	19.84	106.49
13	0.9954	0.45	70.01	757.84
14	0.9971	0.48	65.20	471.73
15	0.9928	0.56	67.54	195.08
16	0.9968	0.46	45.82	266.49
17	0.9948	0.34	18.42	145.02
18	0.9966	0.31	16.34	140.31
19	0.9936	0.45	49.72	358.18
20	0.9958	0.52	42.50	127.43
21	0.9949	0.45	27.16	101.60
22	0.9950	0.37	21.39	134.37
23	0.9919	0.44	61.35	698.13
24	0.9959	0.48	36.06	133.49
25	0.9974	0.44	27.47	107.29
26	0.9947	0.44	45.27	330.13
27	0.9930	0.39	20.29	93.12
28	0.9974	0.50	59.11	294.25
29	0.9954	0.49	39.56	146.37
30	0.9918	0.49	32.93	95.62
31	0.9937	0.40	20.93	92.80
32	0.9930	0.44	20.28	113.79
33	0.9956	0.49	52.37	268.83
34	0.9971	0.44	36.92	224.26
35	0.9983	0.37	17.36	79.48
36	0.9978	0.41	23.94	106.35
37	0.9954	0.43	30.14	147.09
38	0.9944	0.40	22.55	104.52
39	0.9959	0.51	55.36	222.80
40	0.9943	0.70	114.80	147.95
41	0.9936	0.51	75.67	425.78
42	0.9985	0.41	63.40	1158.54
43	0.9961	0.44	43.00	320.17
44	0.9950	0.41	22.74	100.63
45	0.9971	0.43	29.05	147.43

Table 5. 4. The parameters and determination co-efficient for the 45 dissolution experiments, obtained from the Weibull probability distribution model. β is a shape parameter, α is a scale parameter and T25 represents the time interval necessary to dissolve 25% of the deposited drug.

5.4.3 Validity of the Weibull model

To validate the Weibull model that was selected to obtain a dissolution rate parameter for each experiment, a selection of the lowest, medium and highest factor conditions experiment was repeated. This time, the dissolution process was prolonged for 8 h rather than for 1 h (Appendix C, Figure C.1). This was to evaluate whether the T25 obtained from these experiments match the predicted T25 derived from the applied Weibull model. The T25 values are shown that the in Table 5.5. It was evident T25 values obtained directly from the dissolution curves fell within the predicted ranges from the Weibull model.

Table 5. 5. Comparison of the T25 value obtained from the dissolution curve with the predicted T25 value derived from application of Weibull model. Experiment numbers 13, 25 and 35 corresponds to the dissolution experiments conducted under the lowest, medium and highest factor conditions respectively. Where relevant, data expressed as mean ± SD (n=3).

Experiment number	T25 obtained from dissolution curve (min)	T25 predicted from Weibull model (min)
13	-	-
25	≈ 115	104.45 ± 10.52
35	≈ 75	76.39 ± 4.38

5.4.4 Influence of the factors on dissolution

To evaluate the influence the tested factors had on dissolution, Design-Expert 11 software was used, whereby the T25 values were inputted and graphical presentations and table of results were obtained. The data appeared to be normally distributed and according to the 'Residuals vs. Predicted graph', the variations in data seem to be well distributed overall, with no outstanding results. It was evident that the concentration of the dissolution media and the temperature had very significant effects on the response, T25 ($p<0.0001$) (Table 5.6). However, stirring rate did not have significant effects. With respect to the quadratic terms for each factor, a^2 and b^2, which represent the concentration of the dissolution media and temperature respectively, were significant, although a^2 was a lot more significant, with p value < 0.0001. In terms of factor-factor interactions, it appeared that the interaction between concentration of dissolution media and the temperature was very significant ($p<0.0001$), and the interaction between the concentration of the dissolution media with the stirring rate was somewhat significant ($p<0.05$). Interactions between the temperature and stirring rate factors were evidently insignificant.

Table 5. 6. Significance of the effects of each factor on the response, T25, at their respective P value. Data obtained from Design Expert 11 analysis.

Factor / Factor interactions	P-value	Significance
a: Concentration of SDS in PBS/ Dissolution media (% w/v)	< 0.0001	Significant
b: Temperature (°C)	0.0001	Significant
c: Stirring rate (rev p min)	0.0604	Not significant
a^2	< 0.0001	Significant
b^2	0.0171	Significant
c^2	0.2682	Not significant
ab	< 0.0001	Significant
ac	0.0252	Significant
bc	0.0719	Not significant

The co-efficient for each factor was a negative value, as highlighted in Table 5.7. This indicated that increases in the dissolution media concentration, temperature and stirring rate factors each caused a decrease in the T25 response. Increase in the concentration of dissolution media caused the greatest drop in T25, where for every increase in 1% w/v SDS in PBS, there was a drop in T25 by 157.17 min. Changes in stirring rate had the least influence on T25; for every increase in 1 rev p min, there was a decrease in T25 by 48.18 min.

Table 5. 7. The co-efficient of each factor effect on the response, T25. Data obtained from Design Expert 11 analysis.

Factor	Co-efficient
a: Concentration of SDS in PBS/Dissolution media (% w/v)	-157.17
b: Temperature (°C)	-108.65
c: Stirring rate (rev p min)	-48.18

To assess the change of the response surface, 3 dimensional (3D) plots for the measured responses were constructed based on the model polynomial functions (Figure 5.2). Since there was no interaction between the temperature and stirring rate, and their effects on T25 were independent of each other, a 3D plot incorporating the two factors was not required for interpretation. Figures 5.2a and 5.2b represented a Type I plot, an inverted dome shaped plot, in which they looked like parabolas opening upwards. The plots featured a linear decrease in the T25 value along one axis (temperature in Figure 5.2a or stirring rate in Figure 5.2b) while along the other axis (concentration of the dissolution media), there was a decrease in T25 value up to a minimum then an increase in the value thereafter. The linearity of the temperature actor appeared to be a lot more profound and steep than the stirring rate, causing slight difference in plot shape between Figure 5.2a and Figure 5.2b.

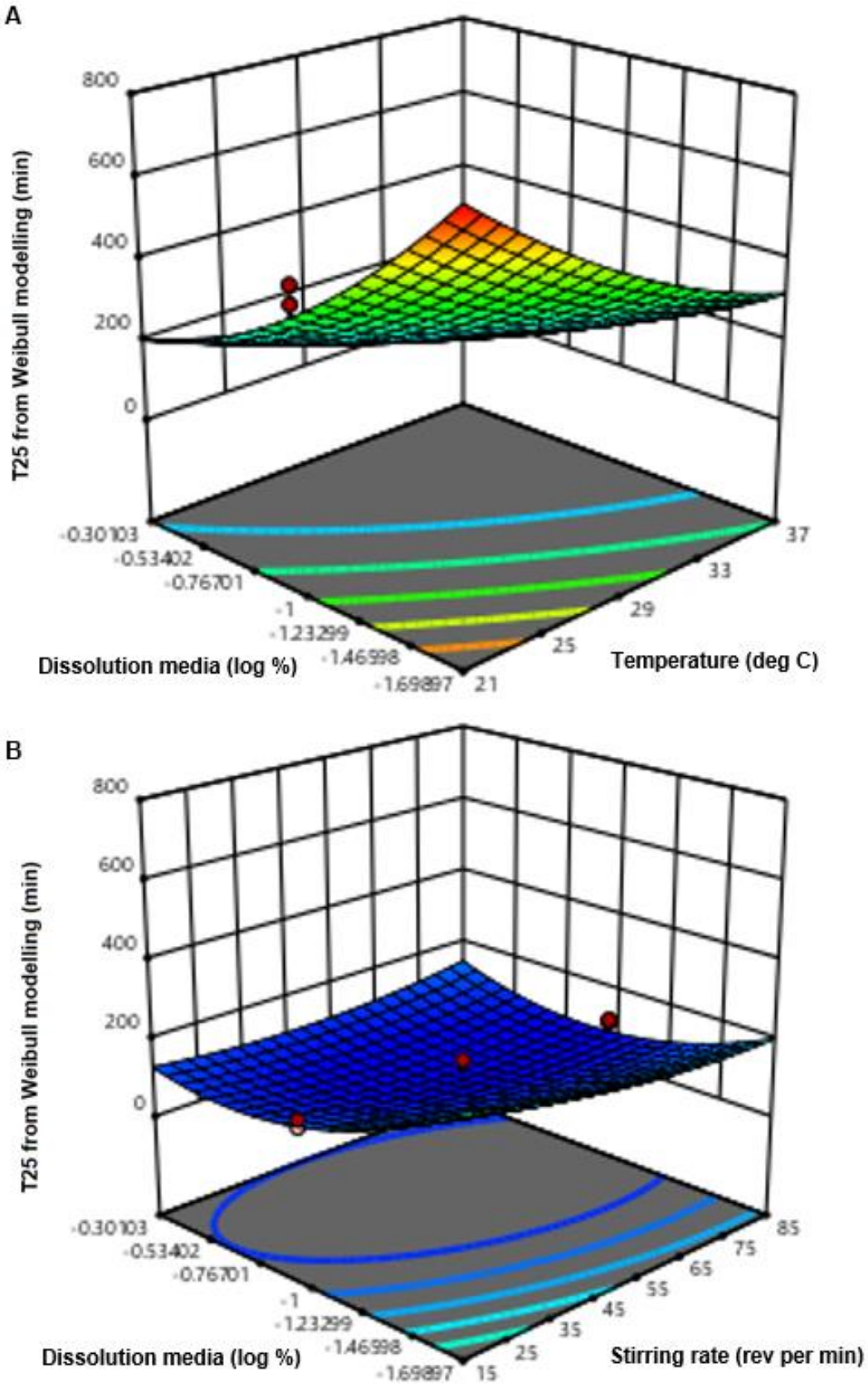

Figure 5. 2. Response surface plots (3D) showing the effects of the factors: dissolution media, temperature and stirring rate, on the response: T25. A) Fixed stirring rate of 15 rev p min, B) Fixed temperature of 37°C.

Figure 5.3 provides an insight into the individual effects of each factor on T25. The dissolution media concentration curve was evidently parabolic, correlating to the huge significance of the a^2 value in Table 5.5 (Figure 5.3a). However, the temperature was somewhat parabolic closer to the end and stirring rate appeared to be relatively linear (Figure 5.3b and 5.3c). This indicated that as the dissolution media concentration increases from 0.02% w/v to 0.1% w/v SDS in PBS, the T25 decreases to a minimal value, after which from 0.1% w/v to 0.5% w/v SDS in PBS, the T25 value increases. However, the effects of temperature and stirring rate on T25 were more proportional, whereby as they increase, the T25 decreases linearly. The minimal T25 value for the temperature appears to be at 37°C, where after that value, the graph provides a visual indication that the T25 value will increase (Figure 5.3b). Changes in stirring rate did not cause major changes in the T25, again correlating to Tables 5.5 and 5.6.

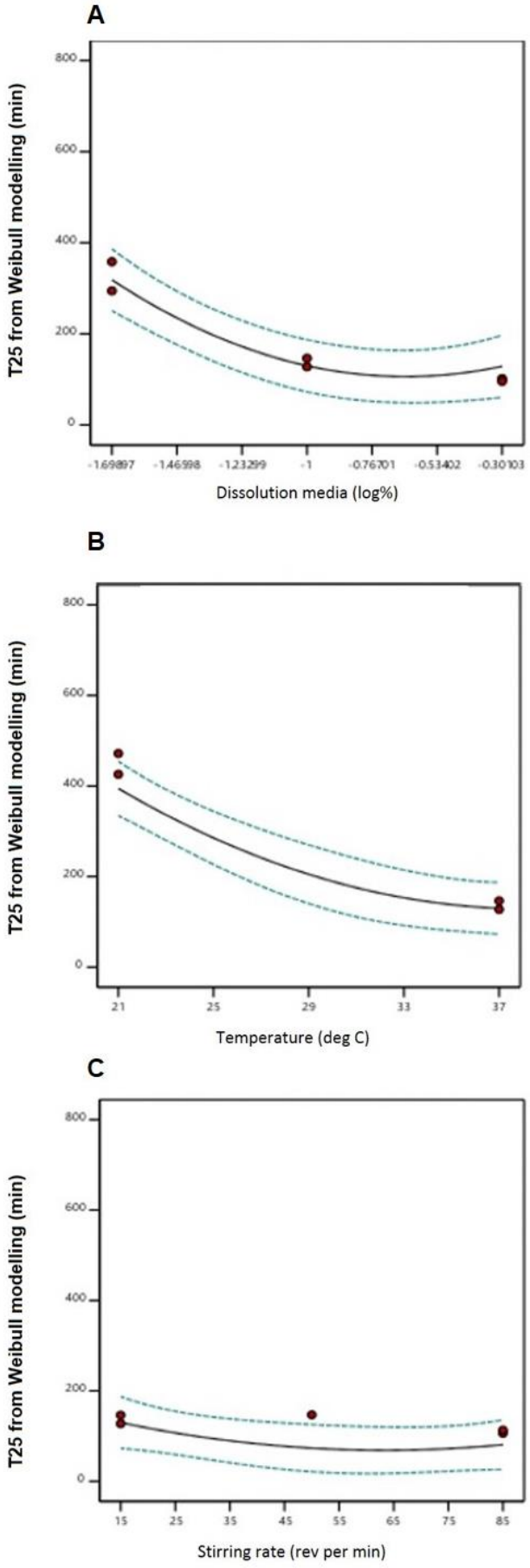

Figure 5. 3. 1D graphs showing the effects of A) Dissolution media, B) Temperature and C) Stirring rate on the response, T25.

5.5 Discussion

To develop the Transwell® dissolution system as a biorelevant system for OIPs to potentially obtain data that is predictive of what occurs *in vivo*, this study considered the interactions and impact of three variable, the dissolution media, temperature and stirring rate, on the dissolution rate of FP from a pMDI. This helped identify the optimal conditions and condition levels at which dissolution testing should be carried out, if we wish to achieve the desired dissolution rate and obtain reliable QC and' IVIVC-type data.

5.5.1 Selection of factors and factors levels

Whilst many studies select conditions to carry out their *in vitro* dissolution analysis for either practicality reasons, physiological relevance or to achieve the highest dissolution rate, the results from the preliminary investigations confirmed that changes in the composition of the dissolution media, the temperature and the stirring rate causes major differences in the dissolution profiles of inhaled FP. Hence, they emerged to be key obvious factors to evaluate in this study.

To truly predict the dissolution rate of an inhaled drug *in vivo*, this requires the determination of the solubility of the drug in the RTLF and this value is currently unknown. However, from my work on estimating the solubility of inhaled compounds in the SLF developed in Chapter 3, which is proposed to consist of the ingredients found in human respiratory tract lavage samples, it became evident that the solubility of those inhaled drugs in SLF were significantly different to their solubilities in other more simpler versions or simulations of RTLF, and more precisely, the estimated solubility of FP in the lungs using mechanistic models, strongly supported the value obtained in SLF in comparison to the other fluids (Boger *et al.*, 2016). Hence, it only seemed appropriate to apply the SLF to the Transwell® dissolution system. However, since the DOE design required a set of 45 experiments and due to the expense of SLF, this could not be done. Therefore, as part of the preliminary investigations, the study considered reversing back to simpler surfactant solutions and the match between the FP solubility in 0.1% w/v SDS in PBS

and in SLF meant that the medium (0.1% w/v SDS in PBS) factor level for dissolution media could represent biorelevance. A dissolution medium concentration of 0.5% w/v SDS in PBS was selected as the highest factor level, since previous studies have utilised this concentration to obtain a rank order of dissolution rates for poorly soluble hydrophobic drugs such as FP, and 0.5% w/v SDS in PBS has shown to differentiate between different dosage forms of OIPs (Rohrschneider *et al.*, 2015). It was hypothesised that as the concentration of SDS in the dissolution media increases, the dissolution rate will significantly increase. This is because surfactants increase the wetting of the deposited FP particles and improves its solubility in the receptor chamber of the Transwell®, causing a steeper concentration gradient and hence a faster dissolution rate (Coowanitwong *et al.*, 2008; Rohrschneider *et al.*, 2015).

With regards to temperature, the temperature of the dissolution medium has shown to be an influential parameter, specifically in FP dissolution studies, whereby faster dissolution rates were seen at higher temperatures (Noriega, 2017). Most studies carry out dissolution testing at 37°C, body temperature, to obtain reliable data predictive of *in vivo* situations. However, the significance or necessity of condition has not been evaluated extensively and hence, it was considered an important factor to study.

In terms of the stirring rate, implications of changes in stirring rate on dissolution of OIPs has not yet been evaluated although it was understood that dynamic movements caused by breathing could influence the dissolution of inhaled particles. All three levels of stirring rate were selected based on physiological relevance, where the levels corresponded to the rested breathing rate of a human, the exercised breathing rate of a human and the breathing rate of mice which may. It was hypothesised, that the stirring rate would have minimal effects on dissolution, because the drug particles that have deposited deeper into the lung have likely embedded into the surface of the lung fluid *in vivo*, and thus are not exposed to too much movement with each breath. With such limited volume of fluid at the alveoli surface, it was likely that it remained relatively stagnant with each breath.

5.5.2 Dissolution profile modelling

Rather than apply *in-silico* modelling to obtain some predictive PK data of FP, a model-dependent mathematical approach was applied in this study to obtain a quantitative value to allow for direct comparisons between the dissolution profiles and obtain a quantitative understanding of the dissolution rate i.e. a dissolution rate parameter. Once a suitable model or function is selected, the dissolution profiles can be evaluated based on the chosen derived model parameter.

To select the most appropriate model for and model the dissolution data, few of the lowest, medium and highest dissolution condition data were selected randomly. Initially, an attempt was made to model the data manually, plotting various graphs, following the methodologies stated in many studies that have attempted to model the dissolution or release kinetics of solid oral dosage forms (Maharjan, 2014). The model graph that gave the highest R^2 value was determined to be the best mathematical model to fit the data (Costa and Sousa Lobo, 2001; Cascone, 2017). However, it appeared that either Higuchi or Weibull modelling was ranking as number 1 for the data that were selected to be evaluated. Mechanistically, the Higuchi model did not seem entirely appropriate for the purpose of this study, since it is often applied to matrix-systems such as studying dissolution from a planar heterogenous matrix system, where the drug concentration in the matrix is lower than its solubility and the dissolution or release occurs through the pores in the matrix (Maharjan, 2014). However, it was not disregarded since it may be that wetting is a key mechanism for the dissolution of FP particles i.e. it may be that water must enter the pores of the FP particles before it can disintegrate and dissolve. Otherwise, it may be that since the FP particles actuated from a pMDI, may land on the Transwell® insert, surrounded with some propellant, the propellant may act as a matrix and impact the dissolution of FP. This provided some justifications to why this model ranked number 1.

Since the data seemed to fit multiple models, it was decided to apply the DDSolver software to evaluate the selected dissolution data with all the possible mathematical models available, and potentially screen out the single most appropriate model to apply.

The software is very easy to use and fits nonlinear equations to drug release or drug dissolution data, facilitating modelling and is based on a built-in library containing at least forty dissolution models (Zhang *et al.*, 2010; Zuo *et al.*, 2014). It presents a key advantage in speeding up calculations associated with the manual method, reducing user error and providing a convenient conclusive report of dissolution data.

After ranking the R^2 values, it was derived from the software and confirmed, that the two most appropriate models were Higuchi and Weibull as suggested via the manual application. Although the Higuchi model could be somewhat justified, the Weibull model was eventually selected. This was on the basis that this model holds more logical rationale for application to the data. It is one of the most commonly used in varied dissolution and drug release studies and can be applied widely and successfully to all pharmaceutical dosage forms, and to almost all kinds of dissolution curves. The Weibull model has also been applied in a previous study conducted on the dissolution of FP specifically via the Transwell® method (Kippax *et al.*, 2016). Consequently, Weibull presents the advantage of being an empirical mathematical equation, indicating it does not make any assumptions or characterisations on the kinetic property of the drug *in vivo*. To pharmaceutical dosage systems following this model, linearization of the dissolution rate curve is obtained from a plot of the logarithm of the dissolved amount of drug versus the logarithm of the time (Langenbucher, 1972). Application of the model provides a description of the dissolution process in more detail to the other models, via parameters such β, the shape parameter that describes the dissolution curve or via time parameters that allows for quantitative comparisons between the dissolution profiles, such as T25, T50, Td, T75 and T80 which represent the time taken for 25%, 50%, 63.2%, 75% and 80% of the drug to dissolve respectively (Langenbucher, 1972). Validation experiments further proved Weibull modelling to be appropriate for this study.

The β parameter characterises the curve as either exponential if β=1, s-shaped with upward curvature followed by a turning point if β>1 or as a parabolic curve with a steeper initial slope than is consistent with the exponential if β<1 (Langenbucher, 1972). The calculated β were all <1, which indicated the dissolution profiles' kinetics were

parabolic. In terms of the time parameter, Td can also be selected because few studies who have applied the Weibull model on their drug release or drug dissolution data, compared the Td values between them (Patel *et al*., 2008). Consequently, since the validation experiments indicated a very close match between the actual T25 and the predicted T25, this allowed the presumption that the Td would not be overestimated. However, regardless, T25 was selected as the key response parameter in the DOE to ensure reliability of the analysis. The preliminary studies indicated that by the end of 60 min and even under the influence of the highest condition factors, only a maximum of 22% of the deposited FP particles dissolved. The conditions that exhibited the highest T25 value i.e. the lowest dissolution rate, was expected since they were the lowest levels of each factor. An SDS concentration of 0.02% w/v was not enough to improve the wettability of the FP drug particles and increase its solubility and a temperature of 21°C and stirring rate of 15 rev p min did not provide sufficient heat or kinetic energy to the particles to enhance dissolution. The condition that gave rise to the lowest T25 value, also supported our hypothesis since all the factor levels were at their highest.

5.5.3 Design of Experiment

The choice of an experimental design depends on the objectives of an experiment and on the number of factors the study hopes to investigate (LP and XL, 2012). This study investigated the effects of three factors on a single response. It aimed to estimate the interaction between the factors with each other and between each factor and the response and evaluate for any quadratic effects/quadratic relationships between the response and the factors, thus the study had a 'Response Surface' objective. This study also aimed to identify the optimum factor levels or conditions required for a proposed response. The combination of these reasonings meant that the Box-Behnken design was adequate for this investigation.

When analysing the T25 values obtained for the 45 experiments at first glance and relative to the dissolution media concentrations, it was generally presumed that a higher concentration of surfactants would improve the solubility and hence the dissolution of

poorly soluble drugs like FP. The results from Design-Expert highlighted that this occurs to a certain extent, after which presence of too much surfactant would limit the dissolution of FP rather than improve it. Surfactants, such as SDS, tend to reduce the surface tension of an aqueous solution by accumulating at the air-liquid interface, whereby its hydrophobic tail is exposed to the air and its hydrophilic head remains incorporated into the solution, interfering with the water-water hydrogen bond (Hu *et al*., 2016). Exposure of the hydrophobic tail attracts poorly soluble compounds into the solution, such as FP, increasing FP wettability. The FP concentration in the medium increases and hence, its solubility and dissolution rate. The effect evidently becomes profound as SDS concentration increased from 0.02% to 0.1% w/v in PBS. The effect of SDS on increasing a hydrophobic drug's solubility in aqueous solutions even below the Critical Micelle Concentration (CMC) has been reported previously (Madelung *et al.*, 2014). However, once the SDS reaches above its CMC, it forms micelles. These micelles further enhance FP solubility by incorporating and accumulating it into the hydrophobic core of the micelles (Rangel-Yagui *et al*., 2005; Marcolongo and Mirenda, 2011). The CMC of SDS in PBS at ambient temperature,21°C is reported to be 1.1 mM (0.03 %w/v) (Sikorska *et al*., 2016). The CMC of SDS in PBS at higher temperatures has not been reported, however, it is expected to be of a higher value as the temperature increases since, the CMC of SDS in water for example, changed from 8 mM to 8,4 mM, when the temperature increased from 21 °C to 37 °C (Marcolongo and Mirenda, 2011). This indicated that at dissolution media concentrations of 0.02% w/v and 0.1% w/v, there were no micelles present but at 0.5% w/v, there was plenty since the concentration exceeds the CMC, regardless of the temperature at which the dissolution has occurred in. Although this was expected to cause a further linear decrease in T25, based on the theory above, this did not occur. This may be a result of the interplay of factors and conditions the dissolution system was exposed to andhence it was key to evaluate the results further using 3D plots and significant tables, obtained from Design Expert.

Results from Design-Expert highlighted that changes in dissolution media concentration and in temperature had the most statistically significant impact on the

dissolution rate, whereas changes in stirring rate did not. This seemed to be truly reflective of what occurs *in vivo* since once the inhaled drug particles land and are attached or embedded within the lung lining fluid at the alveoli surface, they tend to not be exposed to too much movement/stirring with each breath. Consequently, it has been reported that respiratory frequency has shown to be a contributing factor to the residence time of aerosol particles in the lungs and causes marked differences in the deposition pattern, affecting the probability of deposition by gravitational and diffusional forces, but does not affect the rate at which the particle dissolve (National Research Council, 1991). The influence of all factors assessed in general however, was negative to T25, in that for every increase in factor value, there was a decrease in T25. With less time taken for 25% of the deposited drug to dissolve, this meant that the dissolution process was faster and hence describes the dissolution rate well. It appeared that the effect of dissolution media concentration is very quadratic, proving that the concentration of SDS in PBS must be at an optimum and more specific value if we wish to obtain a desired low T25 value.

There were clear interactions between the dissolution media concentration and temperature or the dissolution media concentration and stirring rate. When evaluating the interaction between the dissolution media concentration and temperature, it was expected that as the temperature increases and at low SDS concentrations, the rate at which the SDS molecules settle at the air-liquid interface to attract and adsorb the FP drug particles increases, gradually increasing the solubility of FP and hence its dissolution rate, indicated by the smaller T25 value. However, for the maximum SDS concentration of 0.5% w/v SDS in PBS, increases in temperature is expected to have caused the contradicting effect, as visualised in the graphs. This is likely because the added kinetic energy increased the rate at which micelles were formed in the solution, yielding smaller micelles, which would inevitably reduce the extent of effectively entrapping and solubilising all the FP particles within (Hammouda, 2013). Similar conclusions can be used to explain the interactions between the dissolution media concentration and the stirring rate. Again, at high dissolution media concentration and

high stirring rate, the kinetic energy causes the water structure to become disrupted, so they cannot stabilise the hydrophobic head group of the surfactant well, and this disfavours micelle formation. Hence, this decreases solubility of FP and increases the T25 value, indicative of a higher dissolution rate. Based on these explanations, both 3D interaction graphs gave rise to an inverted dome-shape. Generally, it was clear that the factors analysed were co-dependent on each other, indicating that specific and controlled levels of each factor is necessary to provide a system in which one can obtain the desired T25 value or desired dissolution rate.

5.5.4 Optimal Experimental Parameters

The optimal experimental parameters suggested by this study were:

- **Dissolution media concentration of 0.1% w/v SDS in PBS**
- **Temperature of 37°C**
- **Stirring rate of 15 rev p min**

These were in fact representative of the *in vivo* physiological conditions, whereby the experiment is conducted at the correct body temperature, a dissolution media that exhibits the same solubilising capacity towards FP as the SLF and a stirring rate that is reflective of the average human breathing rate at rest. Since changes in the stirring rate did not have a significant impact on the T25 value and hence did not need to be specified, it was appropriate to carry out dissolution at the lowest rate. The conditions supported the hypothesis that if we wish to conduct an *in vitro* dissolution test for OIPs and obtain reliable dissolution data, reflective of the *in vivo* environment, we must do so under physiological relevant condition sets.

To validate this further, a dissolution graph comparison between FP dissolution under the above set of optimum conditions, was made, with FP dissolution under the same conditions but with SLF applied as oppose to the 0.1% w/v SDS in PBS (Figure 5.4a) and a comparison of the predicted T25 values was also made (Figure 5.4b). Insignificant differences in the FP dissolution profiles were seen overall in both dissolution medium, as expected, except for a slightly significant difference in the % FP

dissolved at 30 min ($p \leq 0.05$). The profiles were very similar, giving an f2 value of 90.52%. This was accounted by the similarity in the solubilising capacity both medium have towards FP. There were also insignificant differences in the predicted T25 values, obtained from the Weibull model ($p > 0.05$).

A

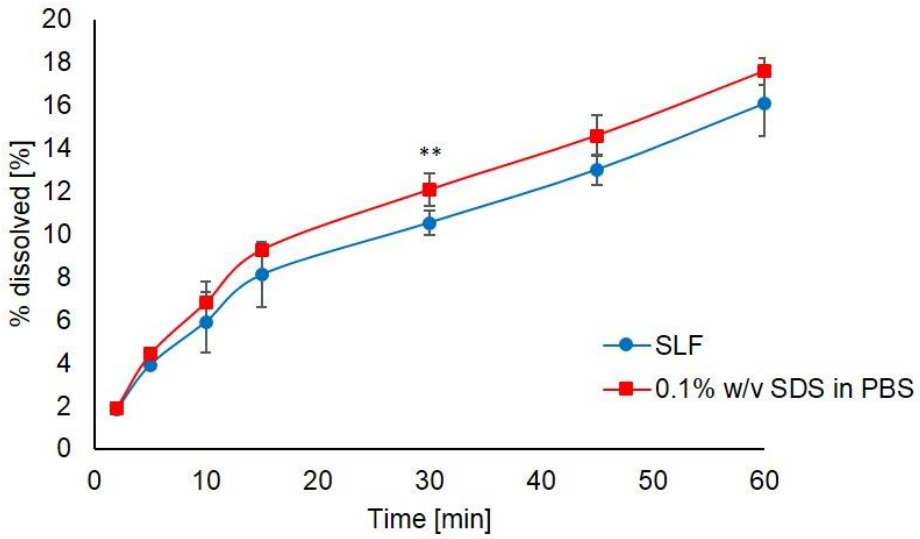

B

Dissolution medium	T25 predicted from Weibull model (min)
SLF	159.02 ± 11.41
0.1% w/v SDS in PBS	136.41 ± 11.82

Figure 5. 4. A) Dissolution profile of fluticasone propionate (FP) under the conditions: temperature of 37°C, stirring rate of 15 rev p min and dissolution media of 0.1% w/v SDS in PBS and dissolution profile of FP under the same conditions, except using SLF as the dissolution media. B) T25 values predicted from Weibull modelling of the dissolution profiles of FP in the two different dissolution media. Data obtained from the TSI/Transwell® system. Data expressed as mean ± SD (n=3).

Summary and conclusions

The utility of using an experimental design such as Box-Behnken for the optimisation of *in vitro* assays and systems has been generally illustrated in this study. It can be concluded the experimental design guided the development of an optimal set of experimental conditions required for the evaluation of the dissolution rate of orally inhaled products. The optimum conditions were to use a dissolution media composed of 0.1% w/v SDS in PBS and conduct the experiment under the temperature of 37°C and stirring rate of 15 rev p min. These were all considered as physiologically relevant conditions and can be employed in the future, when using the Transwell® dissolution system. The work also showed that a further step has been taken towards the establishment of a standardised, biorelevant dissolution system, that can be used for OIPs during drug research and development. A future work here would be to potentially compare the dissolution of FP under the ideal set of conditions with dissolution of FP in rate IPL, to provide a further indication into how close the correlation is or how predictive is the *in vitro* data to the *in vivo* performance.

Chapter 6

Dissolution of nebulised dosage forms

6.1 Introduction

The chapters in this thesis have looked at the dissolution of DPIs and pMDIs but have not considered applying or assessing the dissolution of nebulised formulations. In principle, the FPF of suspensions aerosolised by nebulisation can be analysed using the same dissolution techniques proposed for DPIs and pMDIs, however, to date there seemed to be no examples of this reported in literature. Hence, this chapter focuses on assessing the dissolution of nebulised fluticasone propionate, using the opportunity to develop a novel nebulised prototype and comparing its performance with the reference commercially-available product. The nebulised aerosol medicine developed in this study, is a fluticasone propionate microemulsion and the success of the formulation was envisaged via a variety of tests including application of the developed biorelevant dissolution system, to assess its dissolution, and compared with the commercially available Flixotide® suspension nebule.

To develop a novel inhaled formulation, the benefits of the delivery device must be considered for the selection of the most appropriate for patients. Although the pMDIs and DPIs have increasingly replaced the nebuliser over the years, the nebuliser has an advantage with respect to its universal ability to deliver treatment to all age groups of patients. They are particularly useful for the elderly, the very young or very sick who may find it difficult to maintain good co-ordination when operating the inhalation device or to ensure they receive the adequate dose of drug during an exacerbation (Pritchard *et al.*, 2018). Nebulisers also allow for the delivery of large doses or volumes of drugs and can produce small aerosol droplets, in the nanometre range, allowing the aerosolised drug to penetrate the lung more deeply (Rogueda and Traini, 2007; Amani *et al.*, 2011; Amini *et al.*, 2014). Of the available nebuliser technologies, jet nebulisers are generally more accommodating to a huge range of pulmonary drugs and more convenient to patients. They have numerous benefits such as they tend to be least expensive, the easiest to

clean, can be used for thermosensitive drugs and can deliver formulations with a huge range of surface tensions and viscosities (McCallion *et al.*, 1996; Lavorini, 2013).

When considering the nebulisation of poorly soluble drugs such as FP, there is currently only one type of formulation commercially available, which is the microsuspension. However, these have shown to be less than optimal in the delivery of drugs to the respiratory tract (Nikander *et al*.,1999; Amani *et al.*, 2011; O'Callaghan *et al*, 2014). For instance, there have been reports of large variations in dose, inconsistencies in droplet drug concentrations and due to the production of large droplet sizes, excessive impaction on the upper airways and subsequent ciliary clearance leading to loss of delivered dose (Cheng, 2014; O'Callaghan, White and Kantar, 2014). Consequently, there is a need for preservative when formulating nebuliser suspensions, which may be incompatible with the respiratory tract and for time-consuming aseptic preparation techniques to ensure minimum sterility assurance level for the API and/or excipients. This is because filtration sterilisation would lead to a significant loss of drug from the suspension formulation. Also, fluticasone suspensions specifically, have reportedly experienced the hygroscopic growth effect phenomenon, where the size of the aerosol droplet increases with increasing relative humidity from the oral cavity through to the lungs and this has negatively impacted on the therapeutic efficacy of the formulation in clinical use (Haddrell et al., 2014).

This provided a rationale to look for alternative nebulisable formulations. For example, colloidal systems, whereby the drug is entrapped in liposomes. This has improved the aerosol output performance and aerodynamic particle size profile however, it has shown to have poor shelf life stability and requires a tight control of the lipid concentration as high concentrations can significantly decrease the aerosol output rate (Wagner *et al.*, 2006). Other formulations include polymeric nanoparticles, which have shown high-nebulisation ability and sufficient stability (Lim *et al.*, 2016). However, a major limitation to this nebulised preparation is the control of the aerodynamic particle size, to ensure adequate efficacy of delivery (Tashkin, 2016). Studies have also focused on cyclodextrin solutions as alternative formulations for poorly aqueous soluble drugs

(Le *et al.*, 2006). Although they significantly enhance solubility and allow for large quantities of aerosol to be nebulised within acceptable nebulisation times, only a selection of pulmonary drugs can be complexed with the cyclodextrin thus not all categories of drugs are suitable substrates for the formulation (Tiwari *et al*., 2010). Other formulations include incorporation of steroids into micellar solutions and microemulsions (Malcolmson and Lawrence, 1993; Malcolmson *et al.*, 1998). However, micellar solutions have caused toxicity to cells. Studies have shown that toxicity of drugs was significantly reduced when formulated as a microemulsion in comparison to their corresponding micellar solution (Warisnoicharoen *et al.*, 2000).

Microemulsion formulations have currently attracted most attention as an alternative nebulisable formulation. They circumvent the limitations of other systems and potentially allow nebulisers to be utilised to their utmost advantage in clinical care (Lawrence and Rees, 2000; Smola *et al*., 2008; Amani *et al.*, 2010; Fanun, 2012). They present as thermodynamically-stable systems that enhance the solubility of hydrophobic drugs by incorporating the drug into the oil phase. Microemulsions have been hypothesised to be better formulations for drug delivery because they behave, for the most part, like solutions meaning they allow for sterilisation via filtration, more uniform distribution of aerosol droplet size and greater reproducibility in droplet drug content (Fialho and da Silva-Cunha, 2004). However, there are currently no commercially available microemulsion formulations for the inhaled delivery of glucocorticoids, due to the relatively small number of pharmaceutically acceptable excipients available for inhalation (Tiwari *et al.*, 2012). Formulation of microemulsions for pulmonary route is particularly limited by the sensitivity of the respiratory tract to some of the surfactants and co-surfactants used to stabilise the formulations. Taking this into account, the microemulsion prepared in this study used excipients which were reported to have good biocompatibility (Amani *et al.*, 2010).

When carrying out *in vitro* investigations, for a microemulsion formulation to present as the better alternative to the corresponding suspension for nebulised delivery, it should ideally provide a high solubilising capacity for the hydrophobic drug and exhibit excellent

aerosol output performance, with a high fine particle fraction (FPF), as this indicates the likelihood for deeper deposition of particles into the alveolar *in vivo*. Following deposition, the interactions of the aerosol particles or drug *in vivo*, with the epithelial lung lining fluid and subsequent dissolution determines the drug bioavailability and the rate and extant of absorption to the systemic circulation (Bäckman *et al.*, 2018). It was anticipated that the microemulsion exhibit a different dissolution profile to the suspension, hence why investigating the dissolution profiles of the formulations is of interest.

Aim:

The main aim of this chapter was to apply the biorelevant dissolution system established in the previous chapters, to a nebulised formulation and evaluate a novel formulation compared to a licensed suspension formulation. Since there are no studies on the manufacture of an inhaled microemulsion formulation of FP, it was interesting to investigate the *in vitro* dissolution performance of such formulations.

Objectives:

The objectives were to (i) prepare a prototype microemulsion that solubilises fluticasone propionate (ii) characterise the physicochemical properties and test the potential for the microemulsion to be nebulised via a jet nebuliser and (iii) compare the properties of the emitted aerosol including its *in-vitro* dissolution with the commercially available Flixotide® suspension.

6.2 Materials

The fluticasone propionate was purchased from Generon (Slough, UK). The Tween 80 BioChemica and sterile normal saline solution (0.9% NaCL) were purchased from VWR International Ltd (Lutterworth, UK). Medium chain trigyceride (Crodamol GTCC) was a sample provided by Croda International Plc (East Yorkshire, UK) and Flixotide® nebules 0.5 mg/2mL were purchased from GSK (Middlesex, UK). HPLC-grade ethanol, methanol and water were supplied by Sigma-Aldrich Company Limited (Dorset, UK). Dissolution was carried out using the Transwell dissolution method, using the materials as listed in Chapter 2, section 2.2. The equipment/glassware necessary for the setup of the Twin Stage Impinger (TSI) were purchased from Copley Scientific Limited (Nottingham, UK). The equipment/glassware necessary for the identification of any undissolved crystalline FP, aerosolisation and characterisation of the aerosol output of the FP microemulsion and suspension formulations were provided by Intertek-Melbourn Scientific (Melbourn, UK).

6.3 Methods

6.3.1 Manufacture of FP microemulsion

Fluticasone propionate microemulsion (20 mL) was prepared, using the ingredients listed in Table 6.1. The ingredients were adapted from a commercially available budesonide nebuliser formulation (Amani *et al.*, 2010 and Appendix D, Table D.1). FP, 4 mg, was dissolved in 156 µL of ethanol and vortexed for 5 min to form a drug mix [Dmix]. The surfactant mix [Smix] was prepared by vortex mixing 5 g tween 80 and 0.2 g crodamol together. The Dmix and Smix were combined and vortexed for a further 5 min prior to the addition of normal saline. The formulation was then sonicated for another 10 min, using a high shear ultrasonicator probe, to ensure efficient homogenisation of the oil and aqueous phases of the formulation. The concentration of FP in the microemulsion was 0.02% w/w.

Table 6. 1. List of the components of the fluticasone propionate microemulsion and their concentrations.

Ingredient	Microemulsion component	Concentration (% w/v)
Fluticasone propionate	API	0.02
Tween 80	Surfactant	25
Ethanol	Co-surfactant	1
Crodamol	Oil phase / inner phase	1
Normal saline (0.9% NaCL w/v)	Aqueous phase	To the required volume

6.3.2 Assessment of microemulsion solubilising capacity to FP

To determine the solubilising capacity of FP into the microemulsion, the formulation was diluted and prepared for assay using RP-HPLC-UV. A sample of the microemulsion (2-3 mL) was pushed through a 0.22 µm filter using a plastic syringe and the resulting filtrate was diluted 1:1 with methanol. The unfiltered microemulsion was also quantified and the solubilising calculated, using equation (24):

Solubilising capacity (%) = (filtered FP concentration / unfiltered FP concentration) x 100 (24)

The experiments were carried out in triplicate.

6.3.3 Identification of any undissolved crystalline FP

Raman Chemical Imaging Technology (Morphologi G3SE-ID, Malvern Instruments, UK) was used for the identification of undissolved FP particles within the FP microemulsion and Flixotide® nebule formulations. A single droplet of each formulation was placed carefully on a chrome-coated glass microscope slide and covered with a glass cover-slip, sealed tightly around the edges with silicone grease. Using the Morphologi software v. 8.23, particles were visualised and selected to obtain a full Raman spectrum, using a laser excitation of 532 nm and exposure time of 30 sec.

The spectra were compared with the FP standard, whereby a monolayer of FP powder particles was dispersed on the microscope slide and viewed under the instrument. Although full spectra were obtained, a duplet peak at Raman laser wavelength of 1663 cm^{-1} was prominent and particularly characteristic of FP and thus was deemed API-specific. The work was carried out at Intertek Melbourn.

6.3.4 Characterisation of the physicochemical properties of the FP microemulsion and Flixotide® suspension nebules

The formulations were characterised in terms of their pH, density, viscosity, conductivity, surface tension and hydrodynamic diameter of the lamellar structures, using the methodologies described in Chapter 3, section 3.3.2. All measurements were made at ambient temperature and recorded as a mean of six measurements ± SD.

6.3.5 Aerosolisation of the FP microemulsion and Flixotide® suspension formulations

The formulations were aerosolised using the Pari LC Sprint jet nebuliser, connected to a Pari TurboBoy SX compressor, provided by Intertek-Melbourn Scientific (Melbourn, UK). Approximately 2 mL of the 0.25% w/v Flixotide® suspension and 2.5 mL of the FP microemulsion were aerosolised at a flow rate of 15 L/min. A sputtering sound was taken as an indication that the entire drug concentration in the formulation had been aerosolised. The Flixotide® suspension and FP microemulsion formulations was thus nebulised for 2 min 40 sec and 9 min respectively, providing an equal emitted dose of 500 µg. The work was carried out at Intertek Melbourn.

6.3.6 Characterisation of the aerosol output performance of the FP microemulsion and Flixotide® suspension formulations

The delivery rate and delivered dose experiments were carried out using the apparatus set up according to the European Pharmacopoeia specification (Figure 6.1). The Pari LC Sprint nebuliser, containing the formulation, was connected to the breath simulator (Copley Scientific, Nottingham, UK), which was set to run at 15 breaths per minute. Three filters, held in filter pads (Pari GmBH, Germany) were used to collect the FP released from the nebuliser, two of which (filters 1 and 2) were the inhalation filters and one exhalation filter (filter 3). Filter 1 was replaced with filter 2 after 1 minute of nebulisation. After testing, the filters were washed with diluent, consisting of 65:35 % v/v methanol: water, into 50 mL volumetric flasks to provide three solutions for filters 1, 2 and 3 respectively. The nebuliser device was washed into a 250 mL volumetric flask for mass balance. The solutions were then analysed by RP-HPLC-UV (Section 6.3.8). The delivered dose was calculated using equation (25):

Delivered dose (%) = [(filter 1 + filter 2) / total emitted dose] x 100 (25)

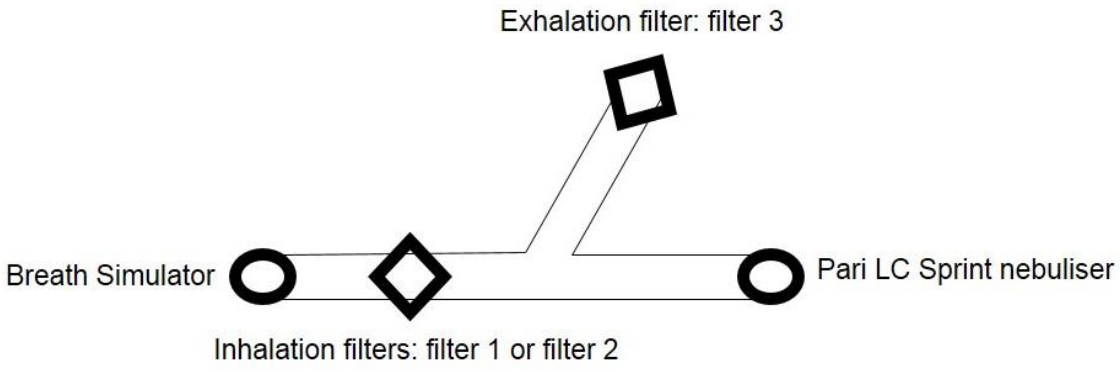

Figure 6. 1. A Schematic diagram of the delivery rate test

The aerosol droplet size distribution was obtained using Spraytec Laser diffraction technology (Malvern Instruments, UK), with an inhalation cell to support the nebuliser. Following aerosolisation of the formulations, the stable phase of the generated aerosol

was selected, and data was generated automatically on the accompanying Spraytec v. 3.20 software (Malvern Instruments, UK). The $Dv_{(90)}$, $Dv_{(50)}$, $Dv_{(10)}$, alveolar deposition and oropharyngeal deposition were obtained from the generated data. The span was calculated using equation (26):

$$\text{Span} = [Dv_{(90)} - Dv_{(10)}] / Dv_{(50)} \quad (26)$$

To obtain an aerodynamic particle size profile of the formulations, samples were nebulised into the Next Generation Impactor (NGI). The NGI experiments were carried out in a cooling cabinet, maintained at temperatures between 2-8 °C. The NGI body, stage cups and throat were stored in the fridge for at least 60 min prior to start of the experiment. After nebulisation, the FP content of each stage of the NGI was washed with methanol into volumetric flasks, prefilled with water. The volumetric flasks were 100 mL, 50 mL x 7 and 250 mL, corresponding to the mouthpiece and throat, stages 1 to 7 of the NGI, and the device respectively. At the filter stage, the filter was removed carefully with a tweezer and placed into a crystalliser. Diluent (65:35 % v/v methanol: water), 50 mL, was added and the crystalliser was covered in parafilm and allowed to sonicate for 10 min. Using a syringe, 5 ml of the sample was filtered through a 0.45 µm PTFE ACRODISC CR filter for analysis by HPLC. The mass median aerodynamic diameter (MMAD) and geometric standard deviation (GSD) values were calculated using an online MMAD calculator. The fine particle fraction (FPF) was calculated using equation (27). All data were expressed as a mean of six measurements ± SD.

$$\text{FPF} = [(\text{amount of deposited particles} < 5.39\ \mu\text{m})/\text{total deposited amount}] * 100 \quad (27)$$

The work was carried out at Intertek Melbourn.

6.3.7 Assessment of the dissolution of FP microemulsion and Flixotide® suspension formulations

The dissolution method used in this study was as described and concluded in Chapter 5, whereby the optimum conditions were applied. In brief, the Transwell® dissolution system was used, with a dissolution media of 0.1% w/v SDS in PBS. 1 mL of FP microemulsion and 5 mL of Flixotide® suspension was aerosolised for 2 and 5 min respectively, and the fine particle fraction was collected by the TSI, under a vacuum flow rate of 45 L/min. Dissolution was carried out at a stirring rate of 15 rev p min and performed at 37°C. The dissolution time points were prolonged to 8 hours, whereby the time points were 2, 5, 10, 15, 30, 45, 60, 120, 240, 360 and 480 min. The recovery sample was at 540 min and treated the same way as the 180 sample was treated in previous methods. For sample collection, 100 µL of each sample at each time point was collected and diluted with 100 µL methanol prior to analysis via RP-HPLC-UV.

6.3.8 Quantification of FP by RP-HPLC-UV

For experiments carried out at King's College London, quantification of FP in the samples was carried out using the method described in Chapter 2, section 2.3.2. For experiments carried out at Intertek Melbourn, quantification was made using an assay developed by the Intertek laboratory team (Parry, 2015)

6.3.9 Statistical analysis

Data were normally distributed (Histogram; Skewness and Kurtosis). Therefore, the non-parametric paired sample T-test was applied. Statistical analysis was performed using the IBM SPSS software, version 24, (SPSS, Armonk, NY, USA). Data was regarded statistically significant when $p \leq 0.05$.

6.4 Results

6.4.1 Manufacture, nebulisation and characterisation of the physicochemical properties of FP microemulsion

Preparation of a stable microemulsion, incorporating the FP drug appeared to be successful. The final product was a visually clear and transparent yellow liquid. The solubilising capacity of the system towards FP was 100 ± 0.00%. This was confirmed further by the Raman Chemical Imaging technique, when the microemulsion was compared with the Flixotide® suspension and the pure FP powder particles (Figure 6.2). The particles present in the suspension appeared to be finer and much smaller than pure FP particles, with many agglomerated (Figure 6.2b). However, each particle presented spectrums that resembled that of pure FP, although of lower intensity (Figure 6.2d). On the contrary, for the images of the FP microemulsion, agglomerated particulate matter was only visible under high magnification (20x) and the Raman spectrum of the particle did not match that of FP (Figure 6.2c and Figure 6.2d).

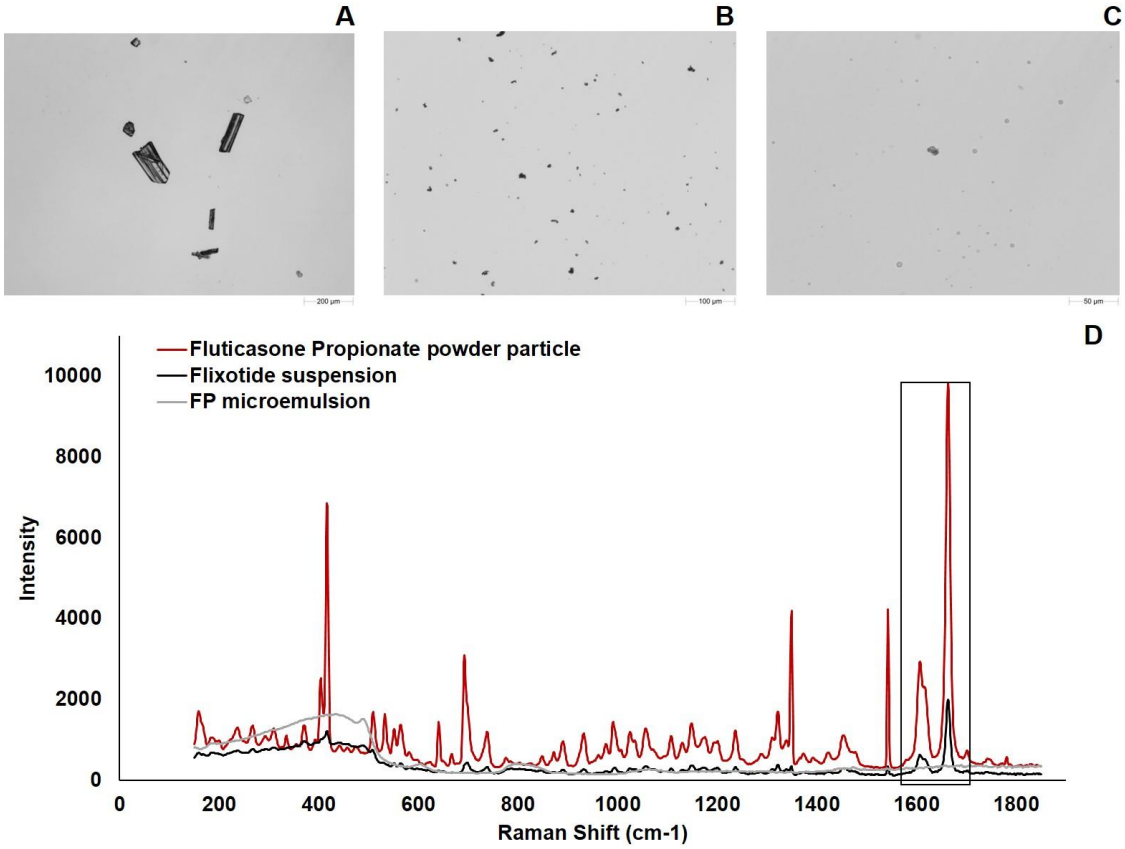

Figure 6. 2. Raman chemical imaging data. Microscopy images of a) standard fluticasone propionate (FP) powder (5x magnification), b) Flixotide® suspension (10 x magnification), c) FP microemulsion (20x magnification) and full Raman spectra for all three formulations (d).

The physicochemical properties of the FP microemulsion was identified and compared to the commercially available Flixotide® suspension (Table 6.2). The pH of the microemulsion was 6.52 ± 0.01 and this was complied with the standard for nebuliser preparations (Amani *et al.*, 2011). The pH, density and conductivity of the microemulsion was slightly higher than that of the suspension. However, the viscosity of the microemulsion was almost five times greater. According to the photon correlation spectroscopy data, although the microemulsion possessed a wider range of particle sizes than the suspension, the average diameter (z-average) of the particles in the microemulsion was 12.31 ± 1.50 d.nm and the average diameter of the particles in the suspension was 5682.67 ± 827.64 d.nm (Table 6.2).

Table 6. 2. The physicochemical properties of the Flixotide® suspension and fluticasone propionate microemulsion. Data expressed as mean ± SD (n=6).

Physicochemical property	Flixotide® suspension	FP microemulsion
pH	6.00 ± 0.00	6.52 ± 0.01
Density	1.011 ± 0.00 g/cm^3	1.019 ± 0.00 g/cm^3
Viscosity	0.946 ± 0.001 mPa.s	5.910 ± 0.014 mPa.s
Conductivity	7.01 ± 0.05 ms	7.24 ± 0.02 ms
Surface Tension	40.60 ± 0.53 mN/m	35.50 ± 0.50 mN/m
Particle size distribution	1 peak: • 100% intensity for ≈ 3000 d.nm	3 peaks: • 87% intensity for ≈ 10.4 d.nm • 7% intensity for ≈ 159.1 d.nm • 4% intensity for ≈ 1774.3 d.nm
	Z-average = 5682.67 ± 827.64 d.nm	Z-average = 12.31 ± 1.50 d.nm
	PDI = 0.32 ± 0.21	PDI = 0.28 ± 0.05

6.4.2 Characterisation of the aerosol output of the FP microemulsion and the Flixotide® suspension formulations

The FP microemulsion and Flixotide® suspension aerosol output performance was characterised in terms of its delivered rate, delivered dose, aerosol droplet size distribution and aerodynamic deposition profiles. The delivered rate and dose of the formulations is shown in Table 6.3. The delivery rate of both formulations was the same. However, the microemulsion delivered a significantly higher percentage of FP after 1 min, almost double the amount, and the amount of drug deposited on the inhalation and exhalation filters for the microemulsion were significantly larger than for the Flixotide® suspension ($p \leq 0.05$).

Table 6. 3. The delivery rate, % delivered dose and % exhaled from the Flixotide® suspension and Fluticasone propionate microemulsion. Data expressed as mean ± SD (n=6).

Formulation	Delivery rate (mg/min)	% Delivered at 1 min	% Delivered dose (Inhalation filters 1 and 2)	% Exhaled (Exhalation filter 3)
Flixotide® suspension	0.02 ± 0.01	4.51 ± 1.14*	16.69 ± 1.81*	8.04 ± 1.21*
FP microemulsion	0.03 ± 0.00	8.54 ± 0.77*	35.78 ± 1.43*	19.35 ± 1.21*

*Difference is significant (T-Test, $p \leq 0.05$)

The aerosol droplet size distribution for the formulations, obtained from the Spraytec Laser Diffraction, is shown in Figure 6.3 and Table 6.4. Both formulations appear to have produced a bimodal distribution and exhibit a wide range of particle diameters (Figure 6.3). However, this was more profound for the Flixotide® suspension, indicating a slightly less polydisperse particle size distribution for the microemulsion. The differences in the volume distributions ($Dv_{(90)}$, $Dv_{(50)}$ and $Dv_{(10)}$), the spread of the droplet size distribution (span) and % of droplets ≤ 2.15 µm were insignificant ($p \leq 0.05$), highlighting an overall similar aerosol droplet size distribution profile. However, the % of droplets ≥ 11.66 µm appeared to be significantly higher for the suspension than the microemulsion ($p \leq 0.05$) (Table 6.4).

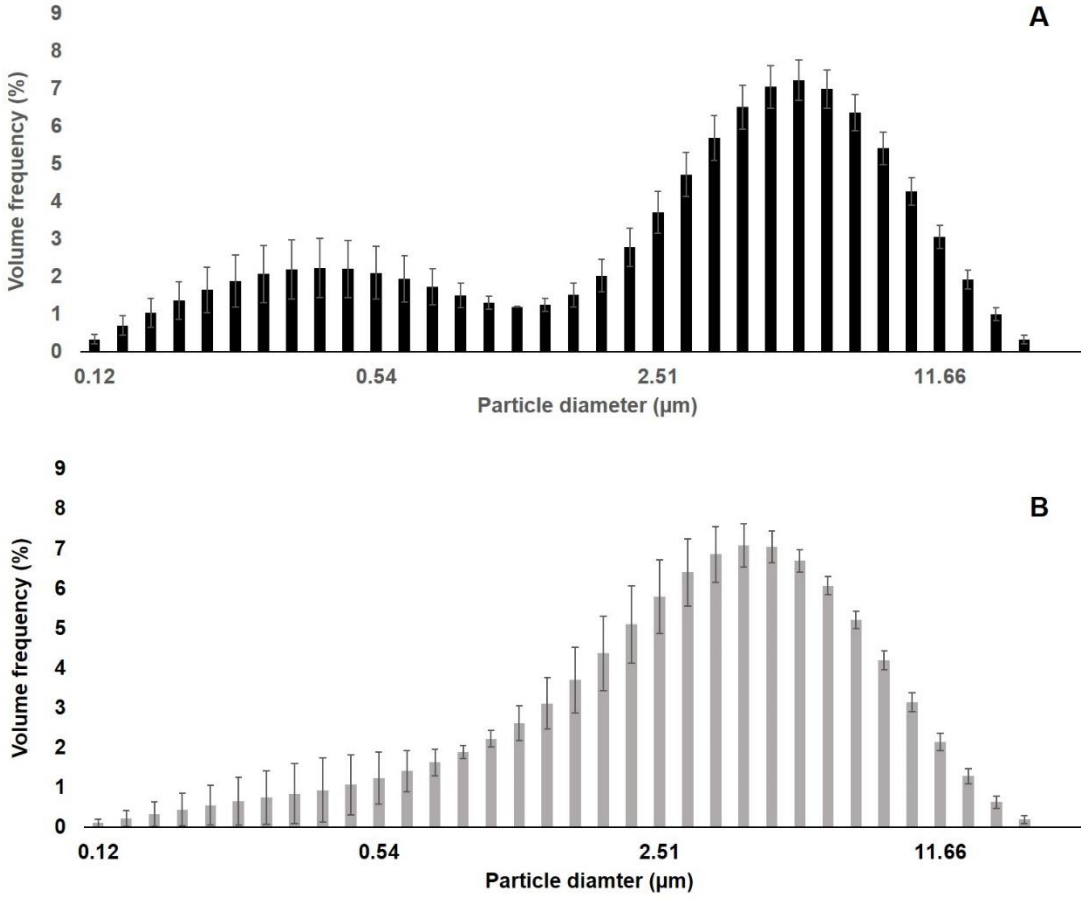

Figure 6. 3. Droplet distribution by volume of a) Flixotide® suspension and b) fluticasone propionate microemulsion, obtained from Spraytec Laser Diffraction. Data expressed as mean ± SD (n=3).

Table 6. 4. Aerosol droplet size distribution for the Flixotide® suspension and fluticasone propionate microemulsion. $Dv_{(90)}$, $Dv_{(50)}$ and $Dv_{(10)}$ represent the volume diameter of 90%, 50% and 10% of aerosol droplets respectively. Data expressed as mean ± SD (n=6).

Formulation	$Dv_{(90)}$ (µm)	$Dv_{(50)}$ (µm)	$Dv_{(10)}$ (µm)	Span	% droplets ≤ 2.15 µm	% droplets ≥ 11.66 µm
Flixotide® suspension	9.55 ± 0.57	3.63 ± 0.40	0.35 ± 0.11*	2.55 ± 0.16	33.12 ± 6.56	8.84 ± 1.47
FP microemulsion	9.15 ± 0.30	3.25 ± 0.06	0.74 ± 0.38*	2.59 ± 0.22	36.53 ± 2.89	8.28 ± 0.67

*Difference is significant (T-Test, $p \leq 0.05$)

The particle deposition pattern for both formulations is shown in Figure 6.4. The suspension evidently had a significantly higher percentage of particles than the microemulsion at stages 2 to 4. However, the microemulsion had a significantly higher percentage of particles than the suspension in stages 5 to 7 and on the filter, indicating the FP microemulsion consisted of and aerosolised more small-sized FP particles in the size range of 1-2.80 µm. It was evident that the FP microemulsion presented a significantly higher FPF, lower MMAD and higher GSD value in comparison to the Flixotide® suspension ($p \leq 0.05$) (Table 6.5).

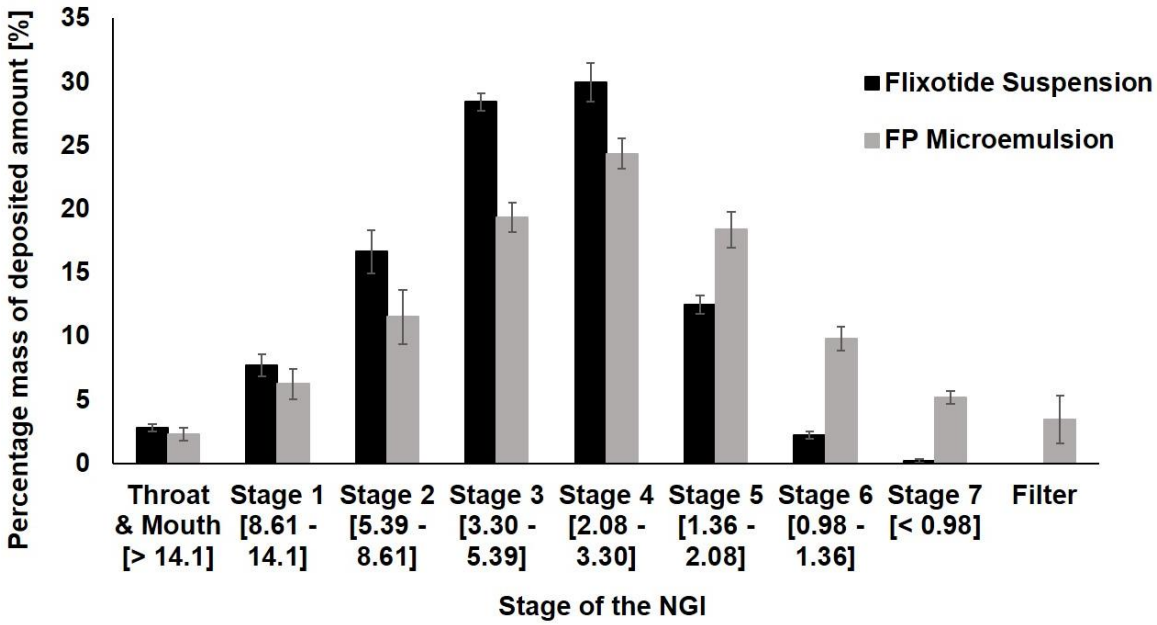

Figure 6. 4. In vitro aerodynamic deposition profile of the Flixotide® suspension and fluticasone microemulsion, obtained from the Next Generation Impactor (NGI). Data expressed as mean ± SD (n=6).

Table 6. 5. The fine particle fraction (FPF), Mass Median Aerodynamic Diameter (MMAD) and Geometric Standard Deviation (GSD) of the Flixotide® suspension and fluticasone microemulsion. Data expressed as mean ± SD (n=6).

Formulation	FPF (%)	MMAD (µm)	GSD (µm)
Flixotide® suspension	73.36 ± 2.27	5.74 ± 0.22*	1.83 ± 0.03*
FP microemulsion	80.60 ± 4.60	4.26 ± 0.37*	2.17 ± 0.05*

*Difference is significant (T-Test, $p \leq 0.05$)

6.4.3 Assessment of the dissolution of FP microemulsion and the Flixotide® suspension formulations

The dissolution profiles of the fluticasone microemulsion and the Flixotide® suspension is presented in Figure 6.5. Under the dissolution conditions, a higher percentage of FP was dissolved from the FP microemulsion compared to the suspension formulation, reaching up to approximately 70% by the end of the 8 h experiment. The FP microemulsion showed an overall improved dissolution profile over the suspension, where the % dissolved continued to increase with time, unlike the suspension, where the % dissolved appeared to reach a plateau after 60 min.

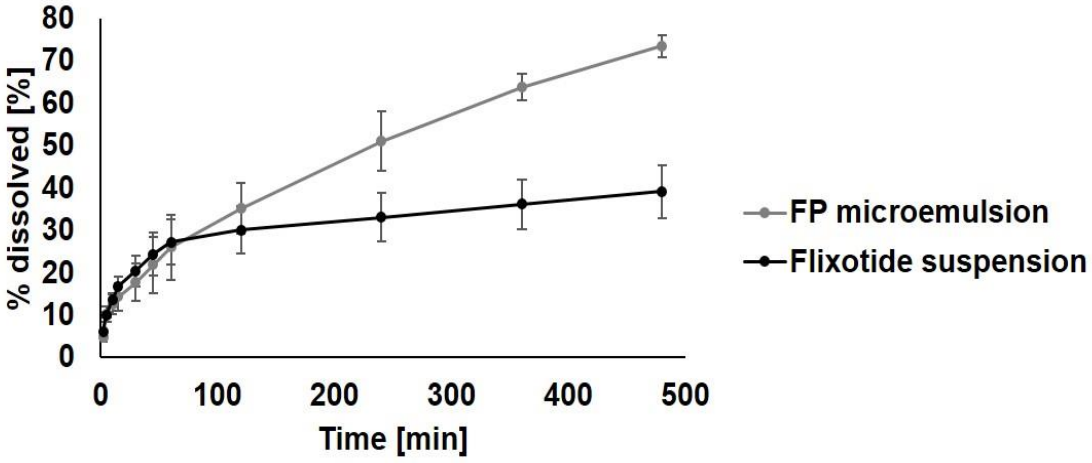

Figure 6. 5. The dissolution profiles of fluticasone microemulsion and Flixotide® suspension, obtained from the TSI/ Transwell dissolution system. Data expressed as mean ± SD (n=3).

6.5 Discussion

6.5.1 Manufacture, nebulisation and the physicochemical properties of FP microemulsion

The successful manufacture of a stable microemulsion as a drug delivery system requires the harmonious contribution of multiple factors. The choice and proportion of excipients, the order in which they are incorporated into the formulation and the physicochemical properties of the active pharmaceutical ingredient (API), all affect the final product and its characteristic properties (Lawrence and Rees, 2000; Fanun, 2012). Although microemulsions have been formulated for drug delivery via a range of administration routes, not many of these have been designed for the respiratory route. This may be due to the relatively small number of pharmaceutically acceptable excipients available for inhaled drug delivery (Tiwari *et al.*, 2012). In particular, the formulation of microemulsions of the pulmonary route is limited by the sensitivity of the respiratory tract to some of the surfactants and co-surfactants typically used to stabilise the microemulsions. The chosen excipients were selected to have good overall biocompatibility and the preparation method of the FP microemulsion specific for nebulisation was done in accordance to the methodology used in a study conducted by Amani et al (Amani *et al.*, 2010).

A particularly important consideration when formulating microemulsions for the inhaled route, is to avoid the precipitation of the API on deposition in the lung and dilution in the fluids (Thakkar *et al.*, 2011). Also, to achieve localised effects, a balance is required between completely dissolving sufficient API to have a pharmacological action and limit the clearance mechanisms so that a persistent concentration of the dissolved drug in the lung can be maintained. Therefore, the delivery system should have high solubilisation capacity for the API, hence why an experiment to identify the solubilising capacity was carried out. The assumption that formed the basis of the test, was that FP particles contained in a droplet of disperse phase or micelle with size ≤ 0.2 μm was solubilised in the microemulsion. Therefore, the amount of FP determined from the

filtrate was considered as the fraction representing 'microemulsion-encapsulated FP'. The microemulsion formulation manufactured in this study had excellent solubilising capacity towards FP. This was made more evident by the Raman imaging which showed undissolved crystalline FP particles in the suspension and none in the microemulsion. The agglomerated clump found in the FP microemulsion however may have been undissolved surfactant. For this imaging technique, although the whole spectra can be compared for the formulations, attention was made to the duplet peak at 1663 cm^{-1}, because it is the Raman band previously identified to be specifically characteristic to FP, when compared to the Raman bands of other materials often present in an FP suspension (Doub *et al.*, 2007; Ali *et al.*, 2009).

These results indicated that the microemulsion formulation does present an advantage over the suspension, since the system improved the solubility of the poorly aqueous soluble FP. FP is hydrophobic thus its solubility in a microemulsion occurs via encapsulation in the micelles or incorporation into the oil phase of a microemulsion, particularly in the oil-in-water variety (Gibaud and Attivi, 2012). Since micelles form at high surfactant concentrations, it can be concluded that the composition of the surfactants which made up the Smix in the formulation, allowed for the successful encapsulation of all the FP particles and hence its complete solubilisation. While this is advantageous from a formulation perspective, the high surfactant concentration (25% Tween 80), although this surfactant is biocompatible, presents a limitation in terms of potentially causing toxicity to the cells and tissues of the respiratory tract (Alany and Wen, 2007). Therefore, further investigations into the safety of the formulation is necessary.

In terms of the physicochemical properties, the greater viscosity was likely contributed by the thickness of the surfactant solution and the oil phase of the formulation i.e. the Tween 80 and crodamol. Presence of surfactants in the microemulsion was also responsible for its lower surface tension, as expected, although the difference was not statistically significant. According to the photon correlation spectroscopy results, the colloidal phase of the microemulsion appeared to be more polydisperse than the particle

size of the suspension, giving rise to 3 peaks of varied particle diameters/sizes unlike the suspension, which had a single 100% intensity peak at a much greater particle diameter. Consequently, for the microemulsion, the peak corresponding to 10.4 d.nm was the highest and this further confirmed the successful preparation of the microemulsion, since microemulsions often possess droplet sizes in the diameter range of 10 – 100 nm (McClements, 2012).

6.5.2 Characterisation of the aerosol output of the FP microemulsion and the Flixotide® suspension formulations

In a clinical setting, how quickly an inhaled dose is administered has major effects on patient adherence and this often presents as a disadvantage of nebuliser drug delivery in comparison to other forms of inhaled drug delivery, such as the pMDIs and DPIs. The amount of drug delivered to the lung is also a measure of the efficiency of the process and could determine the frequency of dosing of the drug. Therefore, in the context of aerosol output performance of an inhaled product, it would be ideal for the nebulised formulation to have a relatively high delivery rate and percent delivered dose so that the patient receives the maximum amount of drug over a short period of time.

In this study, the FP microemulsion exhibited a higher delivered rate and dose over the Flixotide® suspension and this indicated a major improvement in performance for the microemulsion formulation over the commercially available product. However, there was some inefficiency observed with the formulations overall and this may be attributed to drug wastage, which is common to continuously operated jet nebulisers (McCallion *et al.*, 1996). This is where FP that was nebulised during the non-inspiratory parts of the breathing cycle is released into the surrounding environment. The nebulisers also experience evaporative losses and slight temperature reduction as the air flows through the device (Cockcroft *et al.*, 1989). This causes some drug to be trapped in the nebuliser device or lost through the valve, characteristic of the 'breath assisted, open-vent' technology of the Pari LC sprint (O'Callaghan and Barry, 1997).

Another important characteristic property of an inhaled formulation is the size of the droplets produced when aerosolised. The size of the droplets is a major determinant of the lung particle deposition pattern of aerosols. The larger droplets i.e. greater than 5 µm deposit preferentially by inertial impaction in the oropharyngeal regions of the respiratory tract, droplets in sizes between 1 to 5 µm deposit by sedimentation in the lower airways in the bronchioles and droplets less than 0.5 µm are mostly removed on expiration with exhaled air (Smola *et al.,* 2008; Carvalho *et al.*, 2011). This study considered the % droplets ≤ 2.15 µm and % droplets ≥ 11.66 µm, as they represent the predicted fraction of aerosol droplets that deposit within the alveolar region and the oropharyngeal deposition respectively (Najlah *et al.*, 2014). The results indicated that although both formulations would deliver similar amount of FP to the alveoli to achieve localised effects, a lot more FP particles from the suspension would either deposit by impaction, at the back of the throat or on the upper airways where it is subject to ciliary clearance. This has been reported previously in studies on suspension (Cheng, 2014). In a clinical setting of the delivery of inhaled corticosteroids, this presents an advantage to the FP microemulsion because a slightly reduced impaction of FP in the mouth and throat, results in a reduced potential for side effects such as oral candidiasis and thus an overall improvement in patient compliance (McCallion *et al.*, 1996).

However, whilst aerosol droplet size distribution estimated by laser diffraction has been shown to correspond to favourable lung deposition pattern (Clark, 1995), the measurements correspond to the size of the droplets generated by the nebuliser and does not consider whether the droplets contain FP drug particles or not. Therefore, to obtain a more accurate prediction of the distribution of the FP particles in the respiratory tract, the NGI was used. The experiment was carried out in temperatures between 2 and 8°C to reduce the effects of evaporation which have shown to significantly affect the deposition patterns of aerosols (Abdelrahim, 2011).

In the pathology of asthma, it is well known that inflammation occurs predominantly in the lower airways thus an optimal formulation would be expected to have a high proportion of aerodynamic particle size in the range of 1 to 5 µm, quantified as the

respirable fraction or the FPF. Consequently, it is favourable for the formulation to exhibit a lower MMAD since it indicates that it consists of smaller aerodynamic droplet sizes overall, so essentially are more likely to deposit into the lower airways *in vivo*, as required. The higher FPF and lower MMAD exhibited by the FP microemulsion in comparison to the suspension highlights that it is the favourable formulation and this difference between the two types of formulations was also seen in previous studies conducted by Amani et al, who compared a nanoemulsion preparation to a suspension preparation of Budesonide (Amani *et al.*, 2010). This is likely explained by the difference in surface tension, even if only slight different. The FP microemulsion and the Flixotide® suspension had surface tensions of 35.50 ± 0.5 mN/m and 40.60 ± 0.5 mN/m respectively. Surface tension represents the energy barrier that must be overcome for a new surface to form which occurs when larger droplets collapses into smaller droplets (McCallion *et al.*, 1996). Since the microemulsion consisted of surface active agent that acts to reduce the interfacial tension between the oil and water interfaces, it likely facilitated the production of smaller droplet sizes.

6.5.3 Assessment of the dissolution of FP microemulsion and the Flixotide® suspension formulations

The conditions under which the dissolution experiment was carried out were: 0.1% w/v SDS in PBS dissolution medium, stirring rate of 15 rev per min and under a temperature of 37°C. They were the optimal and physiological conditions identified by the DOE study carried out in Chapter 5. The time points were prolonged to 8 h to allow for better discrimination between the dissolution profiles and evaluate for differences better. The volumes selected for aerosolisation and the flow rate selected for particle deposition via TSI, were based on preliminary investigations that indicated that these conditions ensure equal quantity of FP deposition on the filter paper (Appendix D, Table D.2) hence, the dissolution profiles are likely normalised to the amount deposited.

In terms of the dissolution method, upon observation, it appeared that the suspension produced a more distributed deposition within the TSI and on the filter, with

droplets depositing everywhere on the equipment. However, the microemulsion was easier to handle and the droplets deposited predominantly on the filter paper. The dissolution profiles produced were discriminatory and showed a clear difference in the dissolution rate between the formulations. This highlighted the positive benefit of applying dissolution testing to provide a more holistic evaluation of inhaled formulation performances.

The enhanced dissolution rate and improved profile is likely accounted for by the higher solubility of FP in the microemulsion formulation, in comparison to the suspension. For poorly soluble drugs, dissolution is thought to be an important determinant of their pharmacokinetics and pharmacodynamics in the lungs (Hastedt *et al.*, 2016). Therefore, the profile exhibited by the microemulsion many indicate lower non-absorptive clearance via mucociliary clearance and enhanced bioavailability.

Summary and conclusions

This study was carried out for the purpose of evaluating the application of the developed biorelevant dissolution test and assessing the dissolution of nebulised formulations. Results highlighted that formulation of an FP microemulsion for nebuliser devices is certainly a realisable approach. Although there are formulations proposed as viable alternatives to a suspension, when formulating poorly aqueous soluble drugs for pulmonary delivery, the ease and scaleup of an optimised formulation and the simplicity of manufacture make microemulsions a unique choice for the formulation of drugs for inhaled delivery.

Like previous studies that considered preparing a nebulisable microemulsion formulation for inhaled drugs, such as budesonide, a microemulsion of fluticasone propionate has been successfully prepared and can be delivered effectively to the lung via the nebulised route. The microemulsion solubilised FP sufficiently and showed an overall improved *in vitro* aerodynamic performance over the commercially available Flixotide® suspension, exhibiting larger FPF, higher alveolar deposition and significantly greater delivered dose.

Application of dissolution testing during the development of the microemulsion provided discriminatory power to distinguish the dissolution performance of the two formulations. It allowed for a better insight into the prospects of success of the microemulsion preparation and allowed the evaluation of dissolution of nebulised formulations in general. Consequently, the slightly improved dissolution demonstrated by the microemulsion indicated a potentially higher therapeutic bioavailability, making this formulation a promising prototype for drug delivery via the pulmonary route using a jet nebuliser.

Chapter 7

General Discussion

7.1 Basis for the project

This thesis reports investigations into novel dissolution systems and their fitness to evaluate the dissolution of aerosols emitted orally inhaled pharmaceutical products. Studies were based on considerations of importance regarding the dissolution of pharmaceutical aerosols from scientific, academic and industrial pharmacy perspectives.

It is appreciated that dissolution assays are widely used tests in medicines development and manufacture, not least during the early stages of product development, for the optimisation of various formulations. There are well-established dissolution methods for the evaluation of solid oral dosage forms which are used in all phases of development for characterising drug release and evaluating product performance between batches and over time. Over the past 50 years, dissolution testing has been commonly employed as a QC test in R&D, where drug release constitutes a critical product attribute and can be used to detect the impact of manufacturing variables (Chen *et al.*, 2016). The FDA guidance on dissolution testing for immediate release solid oral dosage forms has been included in the BCS guidelines, which is based upon API dose, solubility and permeability. According to the BCS guidelines, *in vitro* dissolution testing may be a useful tool to compare the performance of drug products and for BCS class API reduce the number of bioequivalence clinical studies. However, despite being already entrained in pharmaceutical and biotechnology industry, it has not been recognised as a vital test for the development of OIPs.

As mentioned previously, the EMA and FDA have issued guidelines and specific requirements for the approval of OIPs, which include the need to assess the dose content uniformity and the ASPD. However, it has been recognised that these tests come with their limitations, one of which is that they do not fully predict the *in vivo* performance of OIPs (Newman and Chan, 2008). This provided motive for scientists and researchers to attempt to develop dissolution testing as a requirement test for the development and

approval of inhaled pharmaceutical products. In 2012, a review by an IPAC-RS working group, consisting of a cross-company team evaluating the need for dissolution testing for OIP, concluded that 'dissolution testing would be a valuable tool in the development of inhaled dosage forms'. In an APS-organised symposium in 2015, there was an emphasis that dissolution was currently a neglected aerosol property, most likely because its usefulness as a QC test was unproven. For any *in vitro* test to be accepted for QC purposes, it must be at reliable, simple, discriminatory and relatively economic as a minimal requirement. Many studies have taken these considerations into account and proposed a variety of aerosol particle collection and dissolution testing methodologies, with the advantages and disadvantages of each method as documented in this thesis. It was also well recognised in a number of conference presentations and talks that in fact, the factors influencing the PK of an inhaled drug, e.g. absorptive clearance, are still poorly understood and they are not well predicted from the current *in vitro* aerosol collection tests and dissolution tests proposed. Hence, to date, there is yet no reliable, standardised nor universal pharmaceutical dissolution system present for OIPs.

For dissolution testing to be used as a predictive IVIVC tool, it was realised that the *in vitro* system must mimic the important features of the *in vivo* environment and hence, for OIPs, it must present conditions that replicate the physiology of the lungs. Although some systems have emerged that attempt to mimic aspects of the lung environment, such as the TS/Transwell® system or the Dissolv*It*® system and the various proposed simulated fluids that have been applied to them, they do not closely mimic the *in vivo* RTLF in terms of its composition and characteristics. Therefore, using fluticasone propionate as the model drug, this thesis predominantly aimed to address these drawbacks and limitations and develop a dissolution system for OIPs, that can be used universally during research and discovery and pharmaceutical manufacturing.

7.2 Conclusions from the project

The objectives in this thesis were completed successfully, providing new insights into and developing methods for dissolution testing, while opening opportunities for future work to investigate hypotheses based on the findings. The study first evaluated two dissolution systems, both of which were simple, easy to conduct and repeatable. The NGI/rotating paddle system included a novel aerosol collection technique and utilised apparatus already available for pharmacopoeial quality control testing. Using the filter-holding device and collecting particles externally from stage 2, provided a means of collecting the respirable fraction. It provided a large surface area and ensured an even distribution of particles, overcoming the recognised limitation shown in other dissolution systems that used the NGI to collect the aerosol particles, where particles collected in piles under the nozzles (Son and McConville, 2009; Son *et al.*, 2010). The system also had the advantage of using standard USP 2 dissolution apparatus, giving confidence in the reliability of the dissolution profiles generated and increasing the likelihood of the system being used universally. Whilst many published prototype systems possessed deficiencies such as poor repeatability, difficulty in handling or poor discriminatory ability, this novel system appeared to be excellent to take forward for QC purposes, proving to be robust and sensitive to experimental changes, providing greater discrimination between the dissolution profiles when experimental variables were modified, such as the composition of the dissolution media, and presenting repeatable data.

However, from the perspective of developing a dissolution test with the potential to be utilised as an IVIVC tool, the TSI/Transwell® system emerged as the preferred contender. Optimisation of the system was performed in accordance to techniques applied previously (Arora *et al.*, 2010; Rohrschneider *et al.*, 2015). The adapted system appeared to provide the best representation of lung physiology, since it was fluid-restricted, provided a thin wet layer for particles to deposit on the surface of the filter and required small volumes of fluid for the dissolution of the inhaled particles. The latter aspect meant that biorelevant fluids (some of which are expensive, such as Survanta®)

can be utilised in small volumes, making the system economic in accordance with the key requirements of the assay.

There were suggestions that due to the limited volume used in the Transwell® system and the low aqueous solubility of FP, it may be difficult to maintain sink conditions (Rohrschneider, 2012; Rohrschneider *et al.*, 2015). However, by moving the Transwell to new receiver chambers (i.e. from one well to another), each containing a fresh volume of medium, this limitation can be overcome. The modification to replace the membrane in the Transwell insert was undertaken to avoid this providing an excessive diffusion barrier and being the rate-limiting steps. This was first reported as an issue and the adaptation proposed in the study by Rohrschneider et al (Rohrschneider *et al.*, 2015). The findings in this thesis supported the findings in the study, in that the measured dissolution rate was greater when this experimental modification was applied. This becomes particularly useful when evaluating the dissolution and overall performance of poorly aqueous soluble inhaled drug compounds, in which their PK profiles are presumed to be dissolution-rate limited (Hastedt *et al.*, 2016). Therefore, the TSI/Transwell® dissolution system was selected as the system to be developed further as a more biorelevant system with the aim of providing dissolution data with relevance to PK and establishing predictive IVIVC.

Having observed the dependency of dissolution rate on the dissolution medium, the first approach in developing a biorelevant dissolution test was to devise a biorelevant medium that represents the *in vivo* RTLF, then establish a manufacturing method to provide a consistent, standard product that is readily available for use as a dissolution medium with appropriate *in vitro* systems. In this thesis, a novel SLF, of biorelevant composition was developed and manufactured, and shown to possess physicochemical properties comparable to those of the RTLF. The stability of SLF was also assessed and indicated that although it must be stored in the fridge and used within 14 days of manufacture, the SLF could also be used on the bench, at room temperature, for short period of time up to 48 h, for dissolution studies for example, and can also be used at 37^{o}C temperature, if required. The ability to freeze-dry SLF was established and meant

that it could be stored for prolonged periods, in its powder form and so can be more easily handled and transported for reconstitution at its required place and time of use, providing an added advantage.

On a wider scale, the SLF has huge applicability within the field of inhalation biopharmaceutics, besides dissolution, such as for solubility of inhaled compounds and to study the interactions of the aerosol drug or particle with lung cells. Drug solubility is a key consideration in the development of inhaled medicines, including drug design/discovery (Edwards *et al.*, 2016), formulation (Hastedt *et al.*, 2016) and toxicokinetics (Jones and Neef, 2012). Consequently, it is an essential characteristic required for the development of the BCS for OIPs. When assessing the solubility of FP in this study for example, in various proposed lung fluids, the value obtained in SLF seemed to closely support the estimated solubility of FP in lungs used as an input for mechanistic modelling of PK after inhaled administration (Boger *et al.*, 2016). The SLF can also be used to study for interactions since it has been suggested that particle-lung fluid interactions can impact on inhaled drug delivery (Das and Stewart, 2016). For example, significant interactions between inhaled nanomaterials and lung fluid have been demonstrated (Kumar *et al.*, 2016; Beck-Broichsitter *et al.*, 2017). For lung-particle interaction studies, the SLF must be biocompatible with respiratory cells and the biocompatibility of SLF with the A549 cells indicated by the MTT assay in this thesis, was followed up by exploring any morphometric or transcriptional changes induced by exposure of A549 cells to SLF, in another study conducted by collaborators (Kumar *et al.*, 2017). Both results highlighted the biocompatibility of SLF and hence maximised its utility. Studies of all these phenomena benefit from biorelevant fluids, i.e. SLF, to make meaningful *in vitro* measurements. Experimental *in vitro* data such as those obtained here, has been increasingly in demand to provide inputs to computational models that predict the drug bioavailability in the lungs or the rate and extent of absorption to the systemic circulation (Bäckman *et al.*, 2018).

In Chapter 4, experiments were designed to explore an application of SLF in dissolution experiments by incorporating the SLF onto a dissolution system and

assessing the impact on dissolution profiles and evaluating these by computational modelling that evaluate the role of dissolution rate on PK. It was hypothesised that using more physiological conditions for *in vitro* investigations may improve the accuracy of physiologically-based mechanistic modelling. The Dissolv*It*® system was utilised as a system designed to mimic the *in vivo* lung luminal environment, while incorporating transfer of dissolved drug to a flow-through perfusate where drug concentration can be measured. The system had been developed to use a simple polyethylene oxide gel as the dissolution matrix and hence, there was room to incorporate SLF to introduce a more biorelevant medium to the system. The *in-silico* model was developed by collaborators at University of Graz, Austria, to explore the impact of the dissolution rates derived from the medium on the *in vivo* PK. However, it was found that simply adding SLF to the Dissolv*It*® chamber did not significantly modify FP dissolution profiles and although the model provided reasonable estimates of PK, further work would be required to explore the impact of assay conditions on dissolution profiles and how these might influence PK.

Although studies using the Dissolv*It*® system did not support the hypothesis that using more physiological conditions for *in vitro* investigations may improve the accuracy of physiologically-based mechanistic modelling, further studies were concocted. It was rationalised that if simpler aqueous or surfactant-based solutions, such as those commonly used for OIP dissolution studies, were to be used for applications in the dissolution systems, then these should provide equivalent solubilising capacity for the API as RTLF. To enable studies to be conducted using small amounts of aerosol in the TSI/Transwell system, a novel solid phase extraction method for the assay of FP in the dissolution medium (SLF) was required. Thus, a sensitive technique with the ability to quantify picogram quantities of the drug was developed which proved to be reliable and can be used more widely, to quantify FP in a variety of biological fluids.

Based on these findings, a biorelevant dissolution test for OIPs was developed and evaluated in Chapter 5. It relied on using a surfactant-based dissolution medium, SDS in PBS, and the TSI/Transwell dissolution system. A DOE approach was used i.e. a three-level three factorial Box-Behnken experimental design was used, constructed

using Design-Expert 11, to identify assay conditions based on physiologically-relevant features that were hypothesised to impact on dissolution profiles and to investigate their impact. It was hypothesised that dissolution can be influenced by the dissolution media, temperature and stirring rate, which were all applied variably in reported dissolution methods. Although many studies have used simple aqueous solutions such as PBS alone or surfactant solutions, such as 0.5% w/v SDS in PBS, they provided an overestimation on the solubility of FP. Therefore, for the medium to be of biorelevance, the selection of the concentration of SDS in the medium that provides the same solubilising capacity towards FP as the SLF was determined. The experimental design required a quantitative measure of dissolution which was provided by mathematical modelling of the profiles. There were many theoretical and logical reasons as to why Weibull was selected, one of which it has been used to model the dissolution of FP from the Transwell system in a previous study (Kippax *et al.*, 2016). Preliminary experiments found this model to be the most appropriate for the data obtained and T25 was selected as the 'Response' parameter for the study design.

The experimental outcomes suggested interactions between the factors evaluated on dissolution rate but demonstrated the dependency of dissolution rate on the experimental conditions in the assay. A dissolution medium of 0.1% w/v SDS in PBS (the concentration of medium at which the FP solubility matches its solubility in SLF), conducting the experiment at 37°C and under a stirring rate of 15 rpm was considered as physiologically relevant. The thesis presents a TSI/Transwell® dissolution system, under these specified conditions as a biorelevant system that can explored for IVIVC purposes.

The concluding experimental chapter focused on the dissolution of nebulised dosage forms, as there appeared no data evaluating the dissolution of such formulations to date. An opportunity was taken here to develop a novel nebulised formulation in which the drug was solubilised as a comparison to FP suspension, then explore the performance of the nebuliser solutions using the biorelevant dissolution system. The study showed that formulation of a nebulisable FP microemulsion is a realisable

outcome, with advantages over some limitations of the suspension version currently on the market. The dissolution assay discriminated between the two different nebulised formulations for the same drug, highlighting how that the biorelevant system could have an important role or application in the development of novel aerosol medicines.

It is interesting to compare the dissolution of various inhaled FP products (pMDI, powder, nebuliser) in the biorelevant TSI/Transwell® system, conducted under these physiological conditions: temperature of 37°C, dissolution medium of 0.1% w/v SDS in PBS and stirring rate of 15 rpm (Figure 7.1). The dissolution profile of FP from the Flixotide® pMDI and DPI seemed to very closely overlap, providing an f2 value of 88.56%, and this was as expected according to previous findings in the thesis and in previous studies. However, dissolution from the nebuliser suspension appeared to be greater, with a higher % of FP dissolved at each time point. Although the test ensured similar amounts of FP was deposited from each formulation, the difference in profiles is likely attributed to the difference in the ingredients present in the different formulations, such as presence of surfactants in the nebulised suspension formulation In the DPI, the FP particles are formulated such that it is blended with larger lactose carrier particles, or in some cases blended with other excipients and when aerosolised, the lactose fines deposit on the filter and assist dissolution. In MDIs, the drug is dissolved or suspended in its micronized form in a propellant, HFA 134a, of ethanol composition, on the basis that FP is completely soluble in ethanol. It has been suggested that the DPI formulation increases the wetting of the FP particles, more than the MDI formulation, although the exact mechanism is not fully understood (Shur, 2016). However, this did not seem to be the case here and may be due to the fact that upon actuation of both the DPI and MDI formulations, the apparatus ensured dry solid FP powder particles, of the same physical form, to deposit for dissolution in both cases, causing similarity in the dissolution rate and profiles (Arora *et al*., 2010). However, in the case of the nebulised formulation, the FP is presented as a suspension, and is nebulised to deposit FP in the form of droplets, stabilised by surfactants, such as Polysorbate 20 and Sorbitan Laurate. Presence of surfactants have shown to hugely increase the wetting and solubility of inhaled particles

within the nebulised formulation and since the FP particles deposit in the form of droplets on the filter paper, for dissolution, they are available in a more soluble form than the dry solid particles. Upon dissolution in the 0.1% w/v SDS in PBS dissolution media, the added presence of the SDS surfactants further increases the wettability of the particles as they enter. Hence, the nebuliser suspension provides a higher initial dissolution rate, in comparison to the DPI and MDI. The impact of these formulation variables on dissolution provide opportunities for further research.

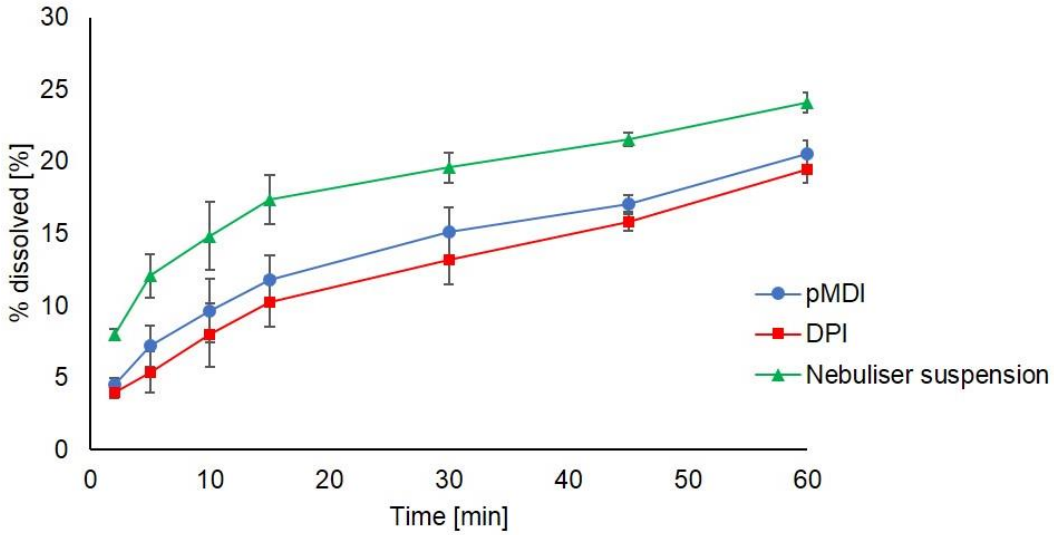

Figure 7. 1. Dissolution of fluticasone propionate from the Flixotide® 50 µg Evohaler (pMDI), Flixotide® 50 µg Accuhaler (DPI) and Flixotide® 0.5 mg/ 2 mL nebuliser suspension. Data obtained via the TSI/Transwell® dissolution system. Data expressed as mean ± SD (n=3).

7.3 Future work

In satisfying the main objectives of the thesis, a number of observations were made that should be investigated in future work. For example, a biorelevant TSI/Transwell system has been developed. Although the system demonstrated discriminatory ability between various inhaled formulation types, future work could involve assessing the sensitivity of the system to detect formulation-dependent factors such as particle size, physical stability or amorphous versus crystalline particles.

In terms of the NGI/Rotating Paddle system, which provided an excellent starting point to be utilised for QC purposes, it would be interesting to compare the novel particle collection system developed in this study with a recently emerged collection system developed by Jag Shur and Robert Price, at the University of Bath (Shur, 2016; Price, 2018). The novel UniDose collection system was developed to also overcome the limitations of previously published NGI particle-collection methods and allow for more uniformly distributed particles to deposit onto a glass microfibre filter membrane. The UniDose allows for the whole impactor stage mass i.e. below stage 2 of the NGI to deposit and the filter is then placed into a disk cassette and placed into a USP II Paddle apparatus. Data obtained from their system indicated excellent repeatability and accuracy and therefore, when the method is published, it would be interesting to compare the performance of the system against the novel system NGI/Rotating Paddle system developed in this study.

With regards to development of a biorelevant simulant, the work is yet considered to be at early stages. It provides a 'base' model reflective of the RTLF of a healthy individual. Future work would extend biorelevance of this by attempting to reflect any differences in the RTLF in lung disease states and consider making SLF specific to the lung disease being studied. For example, in the case of cystic fibrosis (CF), the disease is characterised by a build-up of mucus throughout the lung tubes, including the alveolar lining and therefore, when evaluating the performance of drugs used for the treatment of

CF *in vitro*, using a more reflective SLF of the disease state i.e. incorporating mucins may be more beneficial.

When evaluating the compatibility of SLF with respiratory cells, although findings from the MTT analysis carried out in this thesis, and morphometry transcriptomic analysis, proved biocompatibility with human epithelial A549 cells, future work would require establishment on how robust this finding is across different lung cell lines and in primary cell models. With regards to SLF applicability in inhalation biopharmaceutics studies, the solubility of a few inhaled compounds has been measured in this thesis. A list of inhaled compounds that are considered dissolution-rate limited, i.e. their predicted solubility is significantly less than their inhaled dose, has been identified and listed in Appendix A, Table A.4. Measurement of solubility of those compounds in SLF to provide inputs to computational models that require this data for PBPK modelling would be extremely useful.

Over the course of this thesis solubility measurements and dissolution data/performance of FP in SLF has been rationalised in terms of the post-deposition fate of inhaled aerosols. For example, in SLF very stable colloidal structures may form due to tight packing of the lipid components providing a sink that may sequester the lipophilic FP particles. On the contrary, it was suggested that albumin in SLF may interact with cholesterol, which is required to form stable micelles, causing the structures to break down and inhibiting its ability to solubilise the FP particles. Future work would be required, to visually see if and how efficiently, the FP interact or sequester within the micelles in SLF. This can be done via titration calorimetry, whereby a quantitative value of the binding affinity as well as the stoichiometric properties can be obtained. It would also be interesting to investigate the impact of albumin alone on the solubility and dissolution of FP in the SLF medium. This is because, it has been suggested in this study that the presence of lipids and surfactants likely impact FP solubility and dissolution, however, other studies have identified and considered the impact of albumin in increasing the solubilisation of a range of drugs (Khodor *et al*., 2016; Khodor *et al*., 2018; Leon-Ortega *et al*., 2018). An increase in drug solubility, mediated by albumin,

has been reported for a range of drugs, such as antifungal compounds and poorly aqueous-soluble drugs, and it has been thought to be through complexation mechanisms (Leon-Ortega *et al*., 2018).

With regards to the developed nebulisable microemulsion formulation for FP, although it has now been recognised as a realisable outcome, it required a large concentration of the Tween 80 surfactant to solubilise the concentration of FP. The concentration is above the typical used in inhaled formulations i.e. 15% w/v, future work on this would be to assess the toxicity of various concentrations of Tween 80 in the human lung using alveolar cell lines, such as A549 cells via MTT analysis and perform acute toxicity studies in vivo to identify the maximum concentration that can be used before detrimental effects on the cells is visualised.

7.4 Conclusions

The key conclusions drawn from the thesis are:

1. A novel NGI/Rotating paddle dissolution system has been developed that has the attributes of an assay suitable for QC purposes suitable and is available for validation and testing.
2. A biorelevant TSI/Transwell® system has been developed that provides a step closer towards establishing IVIVC for dissolution in the lungs.
3. The biorelevant TSI/Transwell® system appears to be the most ideal system to date, fulfilling the minimum requirements of a dissolution system that can be utilised universally for QC, classification and IVIVC
4. A novel biorelevant dissolution medium has been developed that has promising applicability in the field of inhalation biopharmaceutics.
5. *In silico* modelling has been applied to assess the implications of *in vitro* experimentations on the *in vivo* drug PK profile and illustrates an approach to understanding the impact of dissolution on inhaled drug delivery.

6. A novel nebuliser formulation of FP, in the form of a microemulsion, has been manufactured, providing an example of how suspension products can be reformulated for use with modern nebulisers.

References

Abdelrahim, M. E. (2011) ‘Aerodynamic characteristics of nebulized terbutaline sulphate using the Andersen Cascade Impactor compared to the Next Generation Impactor’, *Pharmaceutical Development and Technology*, 16(2), pp. 137–145.

Abramson, M. B., Colacicco, G., Curci, R and Rapport, M.M. (1968) ‘Ionic Properties of Acidic Lipids. Phosphatidylinositol’, *Biochemistry*, 7(5), pp. 1692–1698.

Ahuja, S and Scypinski, S. (2001) 'Handbook of Modern Pharmaceutical Analysis', pp.207-208

Alany, R. G. and Wen, J. (2007) ‘Microemulsions as Drug Delivery Systems’, in *Pharmaceutical Manufacturing Handbook*, pp. 769–792.

Ali, H. R. H., Edwards, H.G., Kendrick, J and Scowen, I.J. (2009) ‘Vibrational spectroscopic study of fluticasone propionate’, *Spectrochimica Acta - Part A: Molecular and Biomolecular Spectroscopy*, 72(2), pp. 244–247.

Almgren, M., Edwards, K. and Karlsson, G. (2000) ‘Cryo transmission electron microscopy of liposomes and related structures’, *Colloids and Surfaces A: Physicochemical and Engineering Aspects*, 174(1–2), pp. 3–21.

Alonso, C., Waring, A. and Zasadzinski, J. A. (2005) ‘Keeping lung surfactant where it belongs: Protein regulation of two-dimensional viscosity’, *Biophysical Journal*, 89(1), pp. 266–273.

Amani, A., York, P., Chrystyn. and Clark, B.J. (2010) ‘Evaluation of a Nanoemulsion-Based Formulation for Respiratory Delivery of Budesonide by Nebulizers’, *AAPS PharmSciTech*, 11(3), pp. 1147–1151.

Amani, A., Amini, M.A., Ali, H.S. and York, P. (2011) ‘Alternatives to conventional suspensions for pulmonary drug delivery by nebulisers: A review’, *Journal of Pharmaceutical Sciences*, pp. 4563–4570.

Amidon, G. L., Lennernas, H., Shah, V.P. and Crison, J.R. (1995) ‘A Theoretical Basis for a Biopharmaceutic Drug Classification: The Correlation of in Vitro Drug Product Dissolution and in Vivo Bioavailability’, *Pharmaceutical Research,* 12(3), pp.413-420

Amiji, A.A., Sandmann, B.J. (2003) 'Applied physical pharmacy', McGrawHill Companies, USA, pp. 312-316.

Amini, M. A., Faramarzi, M.A., Gilani, K., Moazeni, E., Esmaeilzadeh-Gharehdaghi, E. and Amani, A. (2014) ‘Production, characterisation, and in vitro nebulisation performance of budesonide-loaded PLA nanoparticles’, *Journal of Microencapsulation*, 31(5), pp. 422–429.

Anand, O., Yu, L.X., Conner, D.P. and Davit, B.M. (2011) ‘Dissolution Testing for Generic Drugs: An FDA Perspective’, *The AAPS Journal*, 13(3), pp.328-335.

Anderson, G. P. (1993) ‘Formoterol: Pharmacology, molecular basis of agonism, and mechanism of long duration of a highly potent and selective β2-adrenoceptor agonist bronchodilator’, *Life Sciences*, 52(26), pp.2145-2160

Arora, D., Shah, K.A., Halquist, M.S. and Sakagami, M. (2010) ‘In Vitro aqueous fluid-capacity-limited dissolution testing of respirable aerosol drug particles generated from

inhaler products', *Pharmaceutical Research*, 27(5), pp.786-795

Ashok, D.P. (2014) 'Theories of dissolution', *R.C. Patel Institute of Pharmaceutical Education and Research, Department of Pharmaceutics,* pp.1-18

Askal, H. F., Khedt, A.S., Darwish, I.A. and Mahmoud, R.M. (2008) 'Quantitative thin-layer chromatographic method for determination of amantadine hydrochloride.', *International journal of biomedical science*, 4(2), pp. 155–60.

Aveldaño, M. I. and Horrocks, L. (1983) 'Quantitative release of fatty acids from lipids by a simple hydrolysis procedure.', *Journal of lipid research*, 24(8), pp. 1101–1105.

Bäckman, P., Adelmann, H., Petersson, G and Jones, C.B. (2014) 'Advances in inhaled technologies: Understanding the therapeutic challenge, predicting clinical performance, and designing the optimal inhaled product', *Clinical Pharmacology and Therapeutics*, 95(5), pp.509-520.

Bäckman, P., Arora, S., Couet, W., Forbes, B., de Kruijf, W and Paudel, A. (2018) 'Advances in experimental and mechanistic computational models to understand pulmonary exposure to inhaled drugs', *European Journal of Pharmaceutical Sciences*, 113, pp. 41–52.

Bastacky, J., Lee, C.Y., Goerke, J., Koushafar, H., Yager, D., Kenaga, L., Speed, T.P., Chen, Y and Clements, J.A. (1995) 'Alveolar lining layer is thin and continuous: low-temperature scanning electron microscopy of rat lung.', *Journal of applied physiology*, 79(5), pp. 1615–1628.

Beck-Broichsitter, M., Bohr, A. and Ruge, C. A. (2017) 'Poloxamer-Decorated Polymer Nanoparticles for Lung Surfactant Compatibility', *Molecular Pharmaceutics*, 14(10), pp. 3464–3472.

Bernardino de la Serna, J., Vargas, R., Picardi, V., Cruz, A., Arranz, R., Valpuesta, J.M., Mateu, L and Perez-Gil, J. (2013) 'Segregated ordered lipid phases and protein-promoted membrane cohesivity are required for pulmonary surfactant films to stabilize and protect the respiratory surface', *Faraday Discuss.*, 161, pp. 535–548.

Berthoud, A.J. (1912) ' Theorie de la formation des faces d'un crystal', *J. Chim. Phys.*, 10, PP. 624-635

Bhagwat, S. Schilling, U., Chen, M.J., Wei, X., Delvadia, R., Absar, M., Saluja, B and Hochhaus, G. (2017) 'Predicting Pulmonary Pharmacokinetics from In Vitro Properties of Dry Powder Inhalers', *Pharmaceutical Research*, 34(12), pp. 2541–2556.

Bicer, E.M., Forbes, B., Somers, G., Blomberg, A., Behndig, A.F and Mudway, I. (2012) 'Characterizing the composition of human respiratory tract lining fluids in health and disease', *American Journal of Respiratory and Critical Care Medicine,* pp.185: A4661

Bligh, E. G. AND Dyer, W.J. (1959) 'A rapid method of total lipid extraction and purification', *Canadian Journal of Biochemistry and Physiology*, 37(8), pp. 911–917.

Boger, E., Evans, N., Chappell, M., Lundqvist, A., Ewing, P., Wigenborg, A. and Friden, M. (2016) 'Systems Pharmacology Approach for Prediction of Pulmonary and Systemic Pharmacokinetics and Receptor Occupancy of Inhaled Drugs', *CPT: Pharmacometrics and Systems Pharmacology*, 5(4), pp. 201–210.

Boni, J. E., Brickl, R.S., Dressman, J and Pfefferle, M.L. (2009) 'Instant FaSSIF and FeSSIF-Biorelevance meets practicality', *Dissolution Technologies*, 16(3), pp. 41–45.

Bozdogan, H. (1987) ‘Model selection and Akaike’s Information Criterion (AIC): The general theory and its analytical extensions’, *Psychometrika*, 52(3), pp.345-370

Brindley, C., Falcoz, C., Makie, A.E and Bye, A (2000) 'Absorption kinetics after inhalation of fluticasone propionate via the Diskhaler, Diskus, and metered-dose inhaler in healthy volunteers', *Clinical Pharmacokinetics*, 39, pp.1-8

Burmeister Getz, E. Carroll, K.J., Jones, B. and Benet, L.Z. (2016) ‘Batch-to-batch pharmacokinetic variability confounds current bioequivalence regulations: A dry powder inhaler randomized clinical trial’, *Clinical Pharmacology and Therapeutics*, 100(3), pp.223-231

Buttini, F., Colombo, G., Kwok, P.C.L. and Wui, W.T. (2013) ‘Aerodynamic Assessment for Inhalation Products: Fundamentals and Current Pharmacopoeial Methods’, in *Inhalation Drug Delivery: Techniques and Products*.

Buttini, F., Miozzi, M., Balducci, A.G., Royall, P.G., Brambilla, G., Colombo, P., Bettini, R. and Forbes, B. (2014) ‘Differences in physical chemistry and dissolution rate of solid particle aerosols from solution pressurised inhalers’, *International Journal of Pharmaceutics*, 465(1–2), pp. 42–51.

Byrro, R.M.D., Cesar, I.C., Cardoso, F.F.d.S., Mundim, I.M., Teixeira, L.d.S., Bonfim, R.R., Gomes, S.A and Pianetti, G.A. (2012) 'A rapid and sensitive HPLC-APCI-MS/MS method determination of fluticasone in human plasma: Application for a bioequivalency study in nasal spray formulations', *Journal of Pharmaceutical and Biomedical Analysis,* pp.38-43.

Caccavo, D., Lamberti, G., Cafaro, M.M.,Barba, A.A., Kazlauske, J. and Larsson, A. (2017) ‘Mathematical modelling of the drug release from an ensemble of coated pellets’, *British Journal of Pharmacology*, 174(12), pp.1797-1809.

Cardot, J. M., Beyssac, E. and Alric, M. (2007) ‘In vitro–in vivo correlation: Importance of dissolution in IVIVC’, *Dissolution Technologies*, pp.15-20.

Carvalho, T. C., Peters, J. I. and Williams, R. O. (2011) ‘Influence of particle size on regional lung deposition--what evidence is there?’, *International journal of pharmaceutics*, 406(1–2), pp. 1–10.

Cascone, S. (2017) ‘Modeling and comparison of release profiles: Effect of the dissolution method’, *European Journal of Pharmaceutical Sciences*, 106, pp.352-361.

Chen, a., L. Yarmush, M. and Maguire, T. (2012) ‘Physiologically Based Pharmacokinetic Models: Integration of In Silico Approaches with Micro Cell Culture Analogues’, *Current Drug Metabolism*, 13(6), pp.863-880

Chen, Y., Gao, Z. and Duan, J. Z. (2016) ‘Dissolution testing of solid products’, in *Developing Solid Oral Dosage Forms: Pharmaceutical Theory and Practice: Second Edition*.

Cheng, Y. S. (2014) ‘Mechanisms of Pharmaceutical Aerosol Deposition in the Respiratory Tract’, *AAPS PharmSciTech*, 15(3), pp. 630–640.

Cheng, Y. S., Dahl, A. R. and Jow, H. N. (1997) ‘Dissolution of metal tritides in a simulated lung fluid’, *Health Physics*, 73(4), pp.633-638

Choi, Y., Attwood, S.J., Hoopes, M.I., Drolle, E., Karttunen, M, and Leonenko, Z. (2014)

‘Melatonin directly interacts with cholesterol and alleviates cholesterol effects in dipalmitoylphosphatidylcholine monolayers’, *Soft Matter*, 10(1), pp. 206–213.

Clark, A. R. (1995) ‘The use of laser diffraction for the evaluation of the aerosol clouds generated by medical nebulizers’, *International Journal of Pharmaceutics*, 115(1), pp. 69–78.

Cockcroft, D. W., Hurst, T. S. and Gore, B. P. (1989) ‘Importance of evaporative water losses during standardized nebulized inhalation provocation tests’, *Chest*, 96(3), pp. 505–508.

Colombani-Dauvergne, A.C., Burrows, J.L., Humphrey, M., Mitchell, J.C. and Snowden, M.J. (2006) ' A novel measurement of the dissolution rates of low solubility compounds, *Drug Delivery to the Lungs proceedings,* pp.121-124

Coowanitwong, I., Arya, V., Kulvanich, P. and Hochhaus, G. (2008) ‘Slow Release Formulations of Inhaled Rifampin’, *The AAPS Journal*, 10(2), pp.342-348

Copley, M and Sipitanou, A. (2018) 'Demonstrating Bioequivalence', *Inhalation Technology Supplement, Orally Inhaled Products,* pp.12-15.

Costa, P. and Sousa Lobo, J. M. (2001) ‘Modeling and comparison of dissolution profiles’, *European Journal of Pharmaceutical Sciences*, 13(2), pp.123-133

Crapo, J. D., Barry, B.E., Gehr, P., Bachofen, M and Weibel, E.R. (1982) ‘Cell number and cell characteristics of the normal human lung.’, *The American review of respiratory disease*, 126(2), pp.332-337

D'Angelis, C.A JJCaRMR (2011). In: Zinimerman BPFaJJ, editor. Pediatric Critical Care, 4th Edition ed. Philadelphia, PA, USA.

Das, S. C. and Stewart, P. J. (2016) ‘The influence of lung surfactant liquid crystalline nanostructures on respiratory drug delivery’, *International Journal of Pharmaceutics*, 514(2), pp. 465–474.

Dash, S., Murthy, P.N., Nath, L. and Chowdhury, P. (2010) ‘Kinetic modeling on drug release from controlled drug delivery systems.’, *Acta poloniae pharmaceutica*, 67(3), pp.217-223

Davies, N. M. and Feddah, M. R. (2003) ‘A novel method for assessing dissolution of aerosol inhaler products’, *International Journal of Pharmaceutics*, 255(1–2), pp. 175–187.

Dean, A.M and Voss, D.T. (2000) 'Design and Analysis of Experiment', *Technometrics*, 42(3)

Di, L., Feng, B., Goosen, T.C., Lai, Y., Steyn, S.J., Varma, M.V. and Obach, R.S. (2013) ‘A perspective on the prediction of drug pharmacokinetics and disposition in drug research and development’, *Drug Metabolism and Disposition*, 41(12), pp.1975-1993

Ding, J., Takamoto, D.Y., von Nahmen, A., Lipp, M.M., Lee, K.Y., Waring, A.J. and Zasadzinski, J.A. (2001) ‘Effects of lung surfactant proteins, SP-B and SP-C, and palmitic acid on monolayer stability’, *Biophysical Journal*, 80(5), pp. 2262–2272.

Dokoumetzidis, A., Papadopoulou, V., Valsami, G. and Macheras, P. (2008) 'Development of a reaction-limited model of disoslution: Application to official dissolution tests expeirments', *Int. J. Pharm.,* 355, pp.114-125

Doub, W. H., Adams, W.P., Spencer, J.A., Buhse, L.F., Nelson, M.P. and Treado, P.J.

(2007) ‘Raman chemical imaging for ingredient-specific particle size characterization of aqueous suspension nasal spray formulations: A progress report’, *Pharmaceutical Research*, 24(5), pp. 934–945.

Dynarowicz-ŁĄtka, P. and Hąc-Wydro, K. (2004) ‘Interactions between phosphatidylcholines and cholesterol in monolayers at the air/water interface’, *Colloids and Surfaces B: Biointerfaces*, 37(1–2), pp. 21–25.

Edsbäcker, S. and Johansson, C. J. (2006) ‘Airway selectivity: An update of pharmacokinetic factors affecting local and systemic disposition of inhaled steroids’, *Basic and Clinical Pharmacology and Toxicology*, 98(6), pp.523-536

Edwards, C. D., Luscombe, C., Eddershaw, P and Hessel, E.M. (2016) ‘Development of a Novel Quantitative Structure-Activity Relationship Model to Accurately Predict Pulmonary Absorption and Replace Routine Use of the Isolated Perfused Respiring Rat Lung Model’, *Pharmaceutical Research*, 33(11), pp. 2604–2616.

Edwards, D. A., Hanes, J., Caponetti, G., Hrkach, J., Ben-Jebria, A., Eskew, M.L., Mintzes, J., Deaver, D., Lotan, N and Langer, R. (1997) ‘Large porous particles for pulmonary drug delivery’, *Science*, 276(5320), pp.1868-1871

Effros, R. M., Peterson, B., Casaburi, R., Su, J., Dunning, M., Torday, J., Biller, J. and Shaker, R. (2005) ‘Epithelial lining fluid solute concentrations in chronic obstructive lung disease patients and normal subjects.’, *Journal of applied physiology*, 99(4), pp. 1286–1292.

El-Gendy, N., Kaviratna, A., Berkland, C and Dhar, P. (2013) ‘Delivery and performance of surfactant replacement therapies to treat pulmonary disorders’, *Therapeutic Delivery*, 4(8), pp.951-980

El-Nesr, O. H., Yahiya, S. A. and El-Gazayerly, O. N. (2010) ‘Effect of formulation design and freeze-drying on properties of fluconazole multilamellar liposomes’, *Saudi Pharmaceutical Journal*, 18(4), pp. 217–224.

European Lung Foundation (2016) 'Your lungs and exercise', *Breathe (Sheff),* 12(1), pp. 97-100

European Medicines Agency (2006) 'Committee for medicinal products for human use (CHMP): Guideline on the pharmaceutical quality of inhalation and nasal products'. pp.1-27

European Pharmacopoeia, Counsil of Europe (2012) 'Dissolution test for solid dosage forms. 8th Edition, May 7. Available from: http://online6.edqm.eu/ep800/NetisUtils/srvrutil_getdoc.aspx/0L3WoCJ4tCLmoC3amCqKkQ7Hj/20903E.pdf

Fan, J and de Lannoy, I.A.M. (2014) 'Pharmacokinetics', *Biochemical Pharmacology*, pp.93-120

Fanun, M. (2012) ‘Microemulsions as delivery systems’, *Current Opinion in Colloid and Interface Science*, pp. 306–313.

Fehrenbach, H. (2001) ‘Alveolar epithelial type II cell: Defender of the alveolus revisited’, *Respiratory Research*, 2, pp.33-46

Fiegel, J., Ehrhardt, C., Schaefer, U.F., Lehr, C.M. and Hanes, J. (2003) ‘Large porous particle impingement on lung epithelial cell monolayers--toward improved particle

characterization in the lung.', *Pharmaceutical research*, 20(5), pp.788-796

Filipe, V., Hawe, A. and Jiskoot, W. (2010) 'Critical evaluation of nanoparticle tracking analysis (NTA) by NanoSight for the measurement of nanoparticles and protein aggregates', *Pharmaceutical Research*, 27(5), pp. 796–810.

Finlay, W. H. (2001) *The Mechanics of Inhaled Pharmaceutical Aerosols*

Flanner, H and Moore, J.W. (1996) 'Mathematical comparison of curves with an emphasis on dissolution profiles', *Pharmaceutical Technology,* 20 (6), p. 64-74

Forbes, B., Shah, A., Martin, G.P. and Lansley, A.B. (2003) 'The human bronchial epithelial cell line 16HBE14o- as a model system of the airways for studying drug transport', *International Journal of Pharmaceutics*, 257(1-2), pp.161-167

Forbes, B., Backman, P., Christopher, D., Dolovich, M., Li, B.V and Morgan, B. (2015) 'In Vitro Testing for Orally Inhaled Products: Developments in Science-Based Regulatory Approaches', *The AAPS Journal*, 17(4), pp. 837–852.

Forbes, B. and Ehrhardt, C. (2005) 'Human respiratory epithelial cell culture for drug delivery applications', in *European Journal of Pharmaceutics and Biopharmaceutics*, 60(2), pp.193-205

Forbes, B., Richer, N. H. and Buttini, F. (2015) 'Dissolution: A Critical Performance Characteristic of Inhaled Products?', in *Pulmonary Drug Delivery*.

Fotaki, N., Aivaliotis, A., Butler, J., Dressman, J., Fischback, M., Hempenstall, J., Klein, S and Reppas, C. (2009) 'A comparative study of different release apparatus in generating in vitro-in vivo correlations for extended release formulations', *European Journal of Pharmaceutics and Biopharmaceutics*, 73(1), pp.115-120

Fotaki, N. and Vertzoni, M. (2010) 'Biorelevant Dissolution Methods and Their Applications in In Vitro- In Vivo Correlations for Oral Formulations', *The Open Drug Delivery Journal*, 4, pp.2-13

Freiwald, M., Valotis, A., Kirschbaum, A., McClellan, M., Murdter, T., Fritz, P., Friedel, G., Thomas, M and Hogger, P. (2005) 'Monitoring the initial pulmonary absorption of two different beclomethasone dipropionate aerosols employing a human lung reperfusion model', *Respiratory Research*, 24, pp.6-21

Fröhlich, E., Mercuri, A., Wu, S and Salar-Behzadi, S. (2016) 'Measurements of deposition, lung surface area and lung fluid for simulation of inhaled compounds', *Frontiers in Pharmacology*, 7, 181

Gaohua, L., Wedagedera, J., Small, B.G., Almond, L., Romero, K., Hermann, D., Hanna, D., Jamei, M and Gardner, I. (2015) 'Development of a Multicompartment Permeability-Limited Lung PBPK Model and Its Application in Predicting Pulmonary Pharmacokinetics of Antituberculosis Drugs', *CPT: Pharmacometrics and Systems Pharmacology*, 4(10), pp.605-613

Geiser, M. and Kreyling, W. G. (2010) 'Deposition and biokinetics of inhaled nanoparticles', *Particle and Fibre Toxicology*, 7(2), pp.1-17

Gerde, P., Malmlof, M., Havsborn, L., Sjoberg, C., Ewing, P., Eirefelt, S and Ekelund, K. (2017) 'Dissolv *It* : An *In Vitro* Method for Simulating the Dissolution and Absorption of Inhaled Dry Powder Drugs in the Lungs', *ASSAY and Drug Development Technologies*, 15(2)

Gibaud, S. and Attivi, D. (2012) 'Microemulsions for oral administration and their therapeutic applications', *Expert Opinion on Drug Delivery*, 9(8), pp. 937–951.

Gittings, S., Turnbull, N., Henry, B., Roberts, C.J and Gershkovich, P. (2015) 'Characterisation of human saliva as a platform for oral dissolution medium development', *European Journal of Pharmaceutics and Biopharmaceutics*, 91, pp. 16–24.

Goerke, J. (1998) 'Pulmonary surfactant: functions and molecular composition', *Biochimica et Biophysica Acta (BBA) - Molecular Basis of Disease*, 1408(2-3), pp.79-89

Gonjari, I. D., Karmarkar, A. B. and Hosmani, A. H. (2009) 'Evaluation of in vitro dissolution profile comparison methods of sustained release tramadol hydrochloride liquisolid compact formulations with marketed sustained release tablets', *Digest Journal of Nanomaterials and Biostructures*, 4(1), pp.26-32

Gowthamarajan, K. and Singh, S. K. (2010) 'Dissolution testing for poorly soluble drugs: A continuing perspective', *Dissolution Technologies*, pp.24-32

Grainger, C. I., Greenwell, L.L., Martin, G.P and Forbes, B. (2009) 'The permeability of large molecular weight solutes following particle delivery to air-interfaced cells that model the respiratory mucosa', *European Journal of Pharmaceutics and Biopharmaceutics*, 71(2), pp.318-324

Grainger, C. I., Saunders, M., Buttini, F., Telford, R., Merolla, L.L., Martin, G.P., Jones, S.A and Forbes, B. (2012) 'Critical characteristics for corticosteroid solution metered dose inhaler bioequivalence', *Molecular Pharmaceutics*, 9(3), pp. 563–569.

Gray, V.A., Hickey, A.J., Balmer, P., Davies, N.M., Dunbar, C., Foster, T.S., Olsson, B.L., Sakagami, M., Shah, V.P., Smurthwaite, M.J., Veranth, J and Zaidi, K. (2008) 'The Inhalation Ad Hoc Advisory Panel for the USP performance tests of inhalation dosage forms', *Pharmacopeial Forum*, 34(4), pp.1068-1075

Grit, M., Zuidam, N.J., Underberg, W.J and Crommelin, D.J. (1993) 'Hydrolysis of Partially Saturated Egg Phosphatidylcholine in Aqueous Liposome Dispersions and the Effect of Cholesterol Incorporation on Hydrolysis Kinetics', *Journal of Pharmacy and Pharmacology*, 45(6), pp. 490–495.

Guan, F., Uboh, C., Soma, L., Hess, A., Luo, Y and Tsang, D.S (2003) 'Sensitive liquid chromatographic/tandem mass spectrometric method for the determination of beclomethasone dipropionate and its metabolites in equine plasma and urine', *Journal of Mass Spectrometry,* 38, p.823-838

Haddrell, A. E., Davies, J.F., Miles, R.E., Reid, J.P., Dailey, L.A and Murnane, D. (2014) 'Dynamics of aerosol size during inhalation: Hygroscopic growth of commercial nebulizer formulations', *International Journal of Pharmaceutics*, 463(1), pp. 50–61.

Hairer, E. and Wanner, G. (1991) *Solving ordinary differential equations II: Stiff and differential-algebraic problems*, *SpringerVerlag*.

Hammouda, B. (2013) 'Temperature Effect on the Nanostructure of SDS Micelles in Water', *Journal of Research of the National Institute of Standards and Technology*, 11(118), pp.151-167

Hastedt, J. E., Backman, P., Clark, A.R., Doub, W., Hickey, A., Hochhaus, G., Kuehl, P.J., Lehr, C., Mauser, P., McConville, J., Niven, R., Sakagimi and Weers, J.G. (2016) 'Scope and relevance of a pulmonary biopharmaceutical classification system

AAPS/FDA/USP Workshop March 16-17th, 2015 in Baltimore, MD', *AAPS Open*, 2(1), p. 1.

Hochhaus, G., Horhota, S., Hendeles, L., Suarez, S and Rebello, J. (2015) 'Pharmacokinetics of Orally Inhaled Drug Products', *The AAPS Journal*, 17(3), pp.769-775

Hribar, B., Southall, N.T., Vlachy, V and Dill, K.A. (2002) 'How ions affect the structure of water', *Journal of the American Chemical Society*, 124(41), pp. 12302–12311.

Hu, D., Mafi, A and Chou, K.C. (2016) 'Revisiting the thermodynamics of water surfaces and the effects of surfactant head group', *J Phys Chem B,* 120(9), p.2257-2261

Hua, T. C., Liu, B. L. and Zhang, H. (2010) *Freeze-Drying of Pharmaceutical and Food Products*.

Huang, Y. B., Xin, P., Li, J., Shao, Y., Huang, C and Pan, H. (2016) 'Room-Temperature Dissolution and Mechanistic Investigation of Cellulose in a Tetra-Butylammonium Acetate/Dimethyl Sulfoxide System', *ACS Sustainable Chemistry and Engineering*, 4(4), pp.2286-2294

ICH (1996) 'Guidance for industry: Q2B validation of analytical procedures: methodology', *International conference on harmonisation of technical requirements for registration tripartite guideline*.

Ikegami, M., Weaver, T.E., Grant, S.N and Whitsett, J.A. (2009) 'Pulmonary surfactant surface tension influences alveolar capillary shape and oxygenation', *American Journal of Respiratory Cell and Molecular Biology*, 41(4), pp. 433–439.

Ingvarsson, P. T, Yang, M., Nielsen, H.M., Rantanen, J and Foged, C. (2011) 'Stabilization of liposomes during drying', *Expert Opinion on Drug Delivery*, 8(3), pp. 375–388.

Irvin, C. G. and Bates, J. H. T. (2009) 'Physiologic Dysfunction of the Asthmatic Lung: What's Going On Down There, Anyway?', *Proceedings of the American Thoracic Society,* 6(3), pp.306-311

Janssens, J.-P., Pache, J.-C. and Nicod, L. P. (1999) 'Physiological changes in respiratory function associated with ageing.', *The European respiratory journal*, 13(1), pp.197-205

Jaspart, S, Bertholet, P., Piel, G., Dogne, J., Delattre, L and Evrard, B. (2007) 'Solid lipid microparticles as a sustained release system for pulmonary drug delivery', *European Journal of Pharmaceutics and Biopharmaceutics*.

Jeschek, D., Lhota, G., Wallner, J and Vorauer-Uhl, K. (2016) 'A versatile, quantitative analytical method for pharmaceutical relevant lipids in drug delivery systems', *Journal of Pharmaceutical and Biomedical Analysis*, 119, pp. 37–44.

Jivani, R., Patel, C. and Jivani, N. (2012) 'Statistical design of experiments on fabrication of bilayer tablet of narrow absorption window drug: Development and In vitro characterisation', *Indian Journal of Pharmaceutical Sciences*, 74(4), pp.302-311

Johns Hopkins University, 'The Mouse', *Animal Care and Use Committee.* Baltimore, Maryland. Jan 19. Accessed from:
http://web.jhu.edu/animalcare/procedures/mouse.html

Jones, H. M., Chen, Y., Gibson, C., Heimbach, T., Parrott, N., Peters, S.A., Snoeys, J.,

Upreti, V.V., Zheng, M and Hall, S.D. (2015) 'Physiologically based pharmacokinetic modeling in drug discovery and development: a pharmaceutical industry perspective', *Clinical pharmacology and therapeutics*, 97(3), pp.247-262

Jones, R. M. and Neef, N. (2012) 'Interpretation and prediction of inhaled drug particle accumulation in the lung and its associated toxicity', *Xenobiotica*, pp. 86–93.

Karnad, D. R., Mhaisekar, D. G. and Moralwar, K. V. (1990) 'Respiratory mucus pH in tracheostomized intensive care unit patients: Effects of colonization and pneumonia', *Critical Care Medicine*, 18(7), pp. 699–701.

Khadka, P., Ro, J., Kim, H., Kim, I., Kim, J.T., Kim, H., Cho, J.M., Yun, G and Lee, J. (2014) 'Pharmaceutical particle technologies: An approach to improve drug solubility, dissolution and bioavailability', *Asian Journal of Pharmaceutical Sciences*, 9(6), pp.304-316

Khodor, M., Abdelkader, H., ElShaer, A., Karam, A., Najlah, M and Alany, R.G. (2016) 'Efficient approach to enhance drug solubility by particle engineering of bovine serum albumin', *Int J Pharm*, 515(1-2), pp.740-748

Khodor, M., Abdelkader, H., ElShaer, A., Karam, A., Najlah, M and Alany, R.G. (2018) 'The use of albumin solid dispersion to enhance the solubility of unionizable drugs', *Pharm Dev Technol*, 23(7), pp. 732-738

Kholodenko, A. L. and Douglas, J. F. (1995) 'Generalized Stokes-Einstein equation for spherical particle suspensions', *Physical Review E*. 51, 1081

Kim, K., Choi, S.Q., Zell, Z.A., Squires, T.M. and Zasadzinski, J.A. (2013) 'Effect of cholesterol nanodomains on monolayer morphology and dynamics.', *Proceedings of the National Academy of Sciences of the United States of America*, 110(33), pp. E3054-60.

Kippax, P., Huck-Jones, D., Suman, J.D., Hochhaus, G and Bhagwat, S. (2016) 'Dissolution testing - Exploring the link between particle size and dissolution behavior for OINDPs', *Drug Development and Delivery*.

Klein, S. (2010) 'The Use of Biorelevant Dissolution Media to Forecast the In Vivo Performance of a Drug', *The AAPS Journal*, 12(3), pp. 397–406.

Kobzik, L. (2007) 'Lung immune defenses against environmental agents'. *In: Environmental and Occupational Medicine,* eds. Rom W., Markowitz, S., editors. (Philadelphia, PA: Lippimcott Williams & Wilkins), pp.187-199

Krishnaswami, S., Mollmann, H., Derendorf, H and Hochhaus, G. (2000) 'A sensitive LC-MS/MS method for the quantification of fluticasone propionate in human plasma.', *Journal of pharmaceutical and biomedical analysis*, 22(1), pp.123-129

Kröll, F., Karlsson, J.A., Nilsson, E., Persson, C.G and Ryrfeldt, A. (1986) 'Lung mechanics of the guinea-pig isolated perfused lung, *Acta Physiol Scand*, 128, pp.1-8.

Kulthanan, K., Nuchkull, P. and Varothai, S. (2013) 'The pH of water from various sources: an overview for recommendation for patients with atopic dermatitis', *Asia Pacific Allergy*, 3(3), pp.155.

Kumar, A., Bicer, E.M., Morgan, A.B., Pfeffer, P.E., Monopoli, M., Dawson, K.A., Eriksson, J., Edwards, K., Lynham, S., Arno, M., Behndig, A.F., Blomberg, A., Somers, G., Hassall, D., Dailey, L.A., Forbes, B and Mudway, I.S. (2016) 'Enrichment of

immunoregulatory proteins in the biomolecular corona of nanoparticles within human respiratory tract lining fluid', *Nanomedicine: Nanotechnology, Biology, and Medicine*, 12(4), pp. 1033–1043.

Kumar, A., Terakosolphan, W., Hassoun, M., Vandera, K.K., Novicky, A., Harvey, R., Royall, P.G., Bicer, E.M., Eriksson, J., Edwards, K., Valkenborg, D., Nelissen, I., Hassall, D., Mudway, I.S. and Forbes, B. (2017) 'A Biocompatible Synthetic Lung Fluid Based on Human Respiratory Tract Lining Fluid Composition', *Pharmaceutical Research*, 34(12), pp.2454-2465

Kuzuya, M., Naito, M., Funaki, C., Hayashi, T., Yamada, K., Asai, K and Kuzuya, F. (1991) 'Antioxidants stimulate endothelial cell proliferation in culture.', *Artery*, 18(3), pp. 115–124.

Labiris, N. R. and Dolovich, M. B. (2003) 'Pulmonary drug delivery. Part I: Physiological factors affecting therapeutic effectiveness of aerosolized medications', *British Journal of Clinical Pharmacology*, 56(6), pp.588-599

Lai, S. K., Wang, Y.Y., Wirtz, D and Hanes, J. (2009) 'Micro- and macrorheology of mucus', *Advanced Drug Delivery Reviews*, 61(2), pp.86-100

Lakeram, M., Lockley, D.J., Pendlington, R and Forbes, B. (2008) 'Optimisation of the Caco-2 permeability assay using experimental design methodology', *Pharmaceutical Research*, 25(7), pp.1544-1551

Langenbucher, F. (1972) 'Letters to the Editor: Linearization of dissolution rate curves by the Weibull distribution', *Journal of Pharmacy and Pharmacology*, 24(12), 979-981

Larsson, J. (2009) 'Methods for measurement of solubility and dissolution rate of sparingly soluble drugs. Master thesis. Accessed from: http://lup.lub.lu.se/luur/download?func=downloadFile&recordOId=2117470&fileOId=2117482

Lavorini, F. (2013) 'The challenge of delivering therapeutic aerosols to asthma patients.', *ISRN allergy*, pp.1-18

Lawrence, M. J. and Rees, G. D. (2000) 'Microemulsion-based media as novel drug delivery systems.', *Advanced drug delivery reviews*, 45(1), pp. 89–121.

Leach, C. L., Davidson, P. J. and Boudreau, R. J. (1998) 'Improved airway targeting with the CFC-free HFA-beclomethasone metered- dose inhaler compared with CFC-beclomethasone', *European Respiratory Journal*, 12(6), pp.1346-1353

Leblond, D., Altan, S., Novick, S., Peterson, J., Shen, Y and Yang, H. (2016) 'In vitro dissolution curve comparisons: A critique of current practice', *Dissolution Technologies*. pp.14-23

Lee, S., Lee, J. and Young, W. C. (2007) 'Characterization and evaluation of freeze-dried liposomes loaded with ascorbyl palmitate enabling anti-aging therapy of the skin', *Bulletin of the Korean Chemical Society*, 28(1), pp. 99–102.

Lennernäs, H., Aarons, L., Augustijns, P., Beato, S., Bolger, M., Box, K., Brewster, M., Butler, J., Dressman, J., Holm, R., Julia, K.F., Kendall, R., Langguth, P., Sydor, J., Lindahl, A., McAllister, M., Muenster, U., Mullertz, A., Ojala, K., Pepin, X., Reppas, C., Rostami-Hodjegan, A., Verwei, M., Weitschies, W., Wilson, C., Karlsson, C and Abrahamsson, B. (2014) 'Oral biopharmaceutics tools - Time for a new initiative - An introduction to the IMI project OrBiTo', *European Journal of Pharmaceutical Sciences*,57,

pp. 292–299.

Leon-Ortega, R.D.d., D'Arcy, D.M., Bolhuis, A and Fotaki, N. (2018) 'Investigation and simulation of dissolution with concurrent degradation under healthy and hypoalbuminaemic simulated parenteral conditions- case example Amphotericin B', *European Journal of Pharmaceutics and Biopharmaceutics*, 127, pp.423-431

Li, Y.N., Tattam, B.N., Brown, K.F and Seale, J.P. (1997) 'A sensitive method for the quantification of fluticasone propionate in human plasma by high-performance liquid chromatography/atmospheric pressure chemical ionisation mass spectroscopy', *J Pharm Biomed Anal,* 16(3), p. 447-452

Liao, X. and Wiedmann, T. S. (2003) 'Solubilization of Cationic Drugs in Lung Surfactant', *Pharmaceutical Research*, 20(11), pp. 1858–1863.

Ligório Fialho, S. and da Silva-Cunha, A. (2004) 'New vehicle based on a microemulsion for topical ocular administration of dexamethasone', *Clinical and Experimental Ophthalmology*, 32(6), pp. 626–632.

Lim, Y. H., Tiemann, K.M., Hunstad, D.A., Elsabahy, M and Wooley, K.L. (2016) 'Polymeric nanoparticles in development for treatment of pulmonary infectious diseases', *Wiley Interdisciplinary Reviews: Nanomedicine and Nanobiotechnology*, pp. 842–871.

Lokhandwala, H., Deshpande, A. and Deshpande, S. (2013) 'Kinetic modeling and dissolution profiles comparison: An overview', *International Journal of Pharma and Bio Sciences*, 4(1), pp.728-737

Lombardi, C. (2015) 'Solid phase extraction', *Chemistry in New Zealand*, 88-90

Lötvall, J. (2001) 'Pharmacological similarities and differences between beta2-agonists', *Respir Med,* 95, pp. S7-11

Lötvall, J. and Ankerst, J. (2008) 'Long duration of airway but not systemic effects of inhaled formoterol in asthmatic patients', *Respiratory Medicine*, 102(3), pp.449-456

LP, H and XL,B. (2012) 'How to choose an appropiate experimental design type (Part 1)', *Zhong Xi Yi Jie He Xue Bao,* 10(6), p.615-618

Mackie, A. E. McDowall, J.E., Ventresca, P., Bye, A., Falcoz, C and Daley-Yates, P.T. (2000) 'Systemic exposure to fluticasone propionate administered via metered-dose inhaler containing chlorofluorocarbon or hydrofluoroalkane propellant', *Clin Pharmacokinet*, 39, pp.17-22

Madelung, P., Ostergaard, J., Bertelsen, P., Jorgensen, E.V., Jacobson, J and Mullertz, A. (2014) 'Impact of sodium dodecyl sulphate on the dissolution of poorly soluble drug into biorelevant medium from drug-surfactant discs', *International Journal of Pharmaceutics,* 467(1-2), pp.1-8

Maharjan, S. (2014) ' Assignment on Mathematical models used in drug release studies', *Education*.

Mahdy, G. and Yang, T. A. (2014) 'Effect superheated steam on physical and lipid stability of reconstituted whole milk powder', *International Journal of Scientific and Research Publications*, 4(1), pp. 250–256.

Malcolmson, C., Satra, C., Kantaria, S., Sidhu, A and Lawrence, M.J. (1998) 'Effect of oil on the level of solubilization of testosterone propionate into nonionic oil-in-water

microemulsions', *Journal of Pharmaceutical Sciences*, 87(1), pp. 109–116.

Malcolmson, C. and Lawrence, M. J. (1993) 'A comparison of the incorporation of model steroids into non?ionic micellar and microemulsion systems', *Journal of Pharmacy and Pharmacology*, 45(2), pp. 141–143.

Mangal, S., Nie, H., Xu, R., Guo, R., Cavallaro, A., Zemlyanov, D and Zhou, Q.T. (2018) 'Physico-Chemical Properties, Aerosolization and Dissolution of Co-Spray Dried Azithromycin Particles with L-Leucine for Inhalation', *Pharmaceutical Research*, 35(2), pp.28

Marcolongo, J.P and Mirenda, M. (2011) 'Thermodynamics of Sodium Dodecyl Sulfate (SDS) Micellization: An Undergraduate Laboratory Experiment', *J Chem Educ,* 88(5), p.629-633

Marple, V. A., Olson, B.A., Santhanakrishnan, K., Roberts, D.L., Mitchell, J.P and Hudson-Curtis, B.L. (2003) 'Next Generation Pharmaceutical Impactor (A New Impactor for Pharmaceutical Inhaler Testing). Part I: Design', *Journal of Aerosol Medicine*, 17(4), pp.335-343

Marques, M. R. C., Loebenberg, R. and Almukainzi, M. (2011a) 'Simulated biologic fluids with possible application in dissolution testing', *Dissolution technologies*, pp. 15–28.

Martins, M. T., Paim, C. S. and Steppe, M. (2010) 'Development of a dissolution test for lamotrigine in tablet form using an ultraviolet method', *Brazilian Journal of Pharmaceutical Sciences*, 46(2), pp.179-186

Martonen, T. B. and Katz, I. M. (1993) 'Deposition Patterns of Aerosolized Drugs Within Human Lungs: Effects of Ventilatory Parameters', *Pharmaceutical Research: An Official Journal of the American Association of Pharmaceutical Scientists*, 10(6), pp.871-878

Matuszewski, B. K., Constanzer, M. L. and Chavez-Eng, C. M. (2003) 'Strategies for the assessment of matrix effect in quantitative bioanalytical methods based on HPLC-MS/MS', *Analytical Chemistry*, 75(13), pp.3019-3030

May, S., Jensen, B., Wolkenhauer, M., Schneider, M and Lehr, C.M. (2012) 'Dissolution techniques for in vitro testing of dry powders for inhalation', *Pharmaceutical Research*, 29(8), pp.2157-2166

May, S. (2013) 'Dissolution testing of powders for inhalation', Dissertation, pp.1-162

May, S., Jensen, B., Weiler, C., Wolkenhauer, M., Schneider, M and Lehr, C.M. (2014) 'Dissolution testing of powders for inhalation: Influence of particle deposition and modeling of dissolution profiles', *Pharmaceutical Research*, 31(11), pp.3211-3224

McCallion, O. N. M., Taylor, K.M.G., Bridges, P.A., Thomas, M and Taylor, A.J. (1996) 'Jet nebulisers for pulmonary drug delivery', *International Journal of Pharmaceutics*, 130(1), pp. 1–11.

McClements, D. J. (2012) 'Nanoemulsions versus microemulsions: Terminology, differences, and similarities', *Soft Matter*, pp. 1719–1729.

McConville, J. T., Patel, N., Ditchburn, N., Tobyn, M.J., Staniforth, J.N and Woodcock, P. (2000) 'Use of a novel modified TSI for the evaluation of controlled-release aerosol formulations. I', *Drug Development and Industrial Pharmacy*, 26(11), pp.1191-1198

Mees, J., Fulton, C., Wilson, S., Bramwell, N., Lucius, M and Cooper, A. (2011) ' Development of dissolution methodology for dry powder inhalation aerosols,

International Pharmaceutical Aerosol Consortium on Regulation & Science, Accessed from: http://ipacrs.com/posters2011.html.

Meindl, C., Stranzinger, S., Dzidic, N., Salar-Behzadi, S., Mohr, S., Zimmer, A and Frohlich, E. (2015) 'Permeation of therapeutic drugs in different formulations across the airway epithelium in vitro', *PLoS ONE*.

Messina, M. S., O'Riordan, T. G. and Smaldone, G. C. (1991) 'Changes in mucociliary clearance during acute exacerbations of asthma.', *The American review of respiratory disease*, 143(5 part 1), pp.993-997

Mitchell, J. P. and Roberts, D. L. (2012) 'Current approaches to APSD measurements of OIPs based on inertial impaction', in *Good Cascade Impactor Practices, AIM and EDA for Orally Inhaled Products*, pp.15-55

Mogal, P and Derle, D. (2017) 'Optimization and Formulation Development of Cefixime Complex Using Spray Drying Technique: DOE Approach', *J Appl Pharm,* 9(3), pp.1-8

Möllmann, H., Wagner, M., Meibohm, B., Hochhaus, G., Barth, J., Stockmann, R., Krieg, M., Weisser, H., Falcoz, C and Derendorf, H. (1998) 'Pharmacokinetic and pharmacodynamic evaluation of fluticasone propionate after inhaled administration', *European Journal of Clinical Pharmacology*, 53(6), pp.459-467

Morris, R. H. K., Tonks, A.J., Jones, K.P., Ahluwalia, M.K, Thomas, A.W., Tonks, A and Jackson, S.K. (2008) 'DPPC regulates COX-2 expression in monocytes via phosphorylation of CREB', *Biochemical and Biophysical Research Communications*, 370(1), pp. 174–178.

Mosharraf, M. and Nyström, C. (1995) 'The effect of particle size and shape on the surface specific dissolution rate of microsized practically insoluble drugs', *International Journal of Pharmaceutics*, pp.35-47

Mujumdar, A. S. and Devahastin, S. (2008) 'Fundamental Principles of Drying', *Freeze Drying*, pp. 1–22.

Munkholm, M. and Mortensen, J. (2014) 'Mucociliary clearance: Pathophysiological aspects', *Clinical Physiology and Functional Imaging*, 34(3), pp.171-177

Murnane, D., Marriott, C. and Martin, G. P. (2008) 'Crystallization and crystallinity of fluticasone propionate', *Crystal Growth and Design*, 8(8), pp. 2753–2764.

Murnane, D., Martin, G. P. and Marriott, C. (2006) 'Validation of a reverse-phase high performance liquid chromatographic method for concurrent assay of a weak base (salmeterol xinafoate) and a pharmacologically active steroid (fluticasone propionate)', *Journal of Pharmaceutical and Biomedical Analysis*, 40(5), pp.1149-1154

Najlah, M., Parveen, I., Alhnan, M.A., Ahmed, W., Faheem, A., Phoenix, D.A., Taylor, K.M and Elhissi, A. (2014) 'The effects of suspension particle size on the performance of air-jet, ultrasonic and vibrating-mesh nebulisers', *International Journal of Pharmaceutics*, 461(1–2), pp. 234–241.

National Research Council (US) Panel (1991) on 'Dosimetric assumptions affecting the application of radon risk estimates. Comparative dosimetry of radon in mines and homes', *National Academies Press, US.*

Nawar, W. W. (1969) 'Thermal degradation of lipids', *Journal of Agricultural and Food Chemistry*, 17(1), pp. 18–21.

Newman, S. P. and Chan, H.-K. (2008) 'In vitro/in vivo comparisons in pulmonary drug delivery.', *Journal of aerosol medicine and pulmonary drug delivery*, 21(1), pp.77-84

Nikander, K., Turpeinen, M. and Wollmer, P. (1999) 'The conventional ultrasonic nebulizer proved inefficient in nebulizing a suspension', *Journal of Aerosol Medicine-Deposition Clearance and Effects in the Lung*, 12(2), pp. 47–53.

Noriega, B., Costa, E and Maia, F. (2017) 'Disoslution of orally inhaled drugs using DissolvIt - Influence of a newly designed pre-seperator for particle collection', *Drug Delivery to the Lungs*

Nounou, M. and El-Khordagui, L. (2005) 'Influence of different sugar cryoprotectants on the stability and physico-chemical characteristics of freeze-dried 5-fluorouracil plurilamellar vesicles', *DARU Journal of Pharmaceutical Sciences*, 13(4), pp. 133–142.

O'Callaghan, C. and Barry, P. W. (1997) 'The science of nebulised drug delivery', *Thorax*, 52(Supplement 2), pp. S31–S44.

O'Callaghan, C., White, J. A. and Kantar, A. (2014) 'Nebulization of corticosteroids to asthmatic children: Large variation in dose inhaled', *Respirology*, 19(2), pp. 276–279.

Okumu, A., DiMaso, M. and Löbenberg, R. (2008) 'Dynamic dissolution testing to establish in vitro/in vivo correlations for montelukast sodium, a poorly soluble drug', in *Pharmaceutical Research*.

Olsson, B., DiMaso, M and Lobenberg, R. (2011) *Pulmonary drug metabolism, clearance and absorption*, *Controlled Pulmonary Drug Delivery: Advances in Delivery Science and Technology*, 25(12), pp.2778-2785

Olsson, B. and Bäckman, P. (2014) 'Mouth-Throat Models for Realistic In Vitro Testing – A Proposal for Debate', *Respiratory Drug Delivery*, 1, pp.287-294

Otero, G.C.F., Lucangioli, S.E and Carducci, C.N. (2001) 'Adsorption of drugs in high-performance liquid chromatography injector loops', *Journal of Chromatography A,* 654(1), pp.87-91

Parry, M. (2015) 'Determination of assay, uniformity of content, particle size distribution by NGI, uniformity of delivered dose and blend homogeneity of Fluticasone/Salmeterol 100/50, 250/50, 500/50 ug DPI capsules and blend', *Internal Analytical Mathod, Melbourn Scientific,* pp.1-10

Patel, N., Forbes, B., Eskola, S and Murray, J. (2006) 'Use of Simulated Intestinal Fluids with Caco-2 Cells and Rat Ileum.', *Drug Development & Industrial Pharmacy*, 32(2), pp. 151–161.

Patel, N., Chotai, N., Patel, J., Soni, T., Desai, J and Patel, R. (2008) 'Comparison of in vitro dissolution profiles of oxcarbazepine-HP β-CD tablet formulations with marketed oxcarbazepine tablets', *Dissolution Technologies*, pp.28-34

Patel, R.P., Baria, A.H and Patel, N.A. (2008) 'An overview of size reduction technologies in the field of pharmaceutical manufacturing', *Asia Journal of Pharmaceutics,* p.216-220

Patton, J. S., Brain, J.D., Davies, L.A., Fiegel, J., Gumbleton, M., Kim, K.J., Sakagami, M., Vanbever, R and Ehrhardt, C. (2010) 'The Particle has Landed—Characterizing the Fate of Inhaled Pharmaceuticals', *Journal of Aerosol Medicine and Pulmonary Drug Delivery*, 23(suppl 2), pp.S71-S87

Payton, N. M. *et al.* (2014) ‘Long-term storage of lyophilized liposomal formulations’, *Journal of Pharmaceutical Sciences*, 103(12), pp. 3869–3878.

Peck, T., Hill, S. and Williams, M. (2008) ‘Drug passage across the cell membrane’, *Pharmacology for Anaesthesia and Intensive Care, third edition*, pp.1-10

Pérez-Gil, J. and Keough, K. M. W. (1998) ‘Interfacial properties of surfactant proteins’, *Biochimica et Biophysica Acta - Molecular Basis of Disease*, pp. 203–217.

Petersson, J. and Glenny, R. W. (2014) ‘Gas exchange and ventilation-perfusion relationships in the lung’, *European Respiratory Journal*, 44(4), pp.1023-1041

Pham, S. and Wiedmann, T. S. (2001) ‘Note: Dissolution of aerosol particles of budesonide in Survanta™, a model lung surfactant’, *Journal of Pharmaceutical Sciences*, 90(1), pp. 98–104.

Price, R. (2015) 'The API matters-studying appropriate drug dissolution and deposition', *APS.Aerosol Society-Bioequivalence of Orally Inhaled Drug Products.*

Price, R. (2018) 'Developing alternative *in vitro* approaches for bioequivalence testing of orally inhaled drug products', *7th Medicon Valley Inhalation Symposium, Medicon Valley Inhalation Consortium, Lund, Sweden.*

Pritchard, J. N., Hatley, R.H., Denyer, J and Hollen, D.V. (2018) ‘Mesh nebulizers have become the first choice for new nebulized pharmaceutical drug developments’, *Therapeutic Delivery*, 9(2), pp. 121–136.

Puchelle, E., Zahm, J.M., Girard, F., Bertrand, A., Polu, J.M., Aug, F and Sadoul, P. (1980) ‘Mucociliary transport in vivo and in vitro. Relations to sputum properties in chronic bronchitis’, *Eur J Respir Dis*, 61(5), pp.254-264

Ramteke, K. H., Dighe, P.A., Kharat, A.R., Patil, S.V. (2014) ‘Review Article Mathematical Models of Drug Dissolution : A Review’, *Scholars Academic Journal of Pharmacy*, 3 (5), p.388-396

Rangel-Yagui, C.O., Pessoa-Jr, A and Tavares, L.C. (2005) 'Micellar solubilisation of drugs', *J Pharm Pharmaceut Sci,* 8(2), p.147-163

Reis, A. and Spickett, C. M. (2012) ‘Chemistry of phospholipid oxidation’, *Biochimica et Biophysica Acta - Biomembranes*, pp. 2374–2387.

Rickard, D.T and Sjoberg, E.L. (1983) 'Mixed kinetic control of calcite dissolution rates', *Am. J. Sci,* 283, pp.815-830

Riethorst, D., Baatsen, P., Remijn, C., Mitra, A., Tack, J., Brouwers, J and Augustijns, P. (2016) ‘An In-Depth View into Human Intestinal Fluid Colloids: Intersubject Variability in Relation to Composition’, *Molecular Pharmaceutics*, 13(10), pp. 3484–3493.

Riley, T., Christopher, D., Arp, J., Casazza, A., Colombani, A., Cooper, A., Dey, M., Maas, J., Mitchell, J., Reiners, M., Sigari, N., Tougas, T and Lyapustina, S. (2012) ‘Challenges with Developing In Vitro Dissolution Tests for Orally Inhaled Products (OIPs)’, *AAPS PharmSciTech*, 13(3), pp. 978–989.

Rogueda, P. G. and Traini, D. (2007) ‘The nanoscale in pulmonary delivery. Part 2: formulation platforms’, *Expert Opinion on Drug Delivery*, 4(6), pp. 607–620.

Rohrs, B. R. (2001) ‘Dissolution method development for poorly soluble compounds’,

Dissolution Technologies, pp.1-5

Rohrschneider, M. (2012) 'Correlation of ICS in vitro dissolution and pulmonary absorption', Dissertation, p. 1-115

Rohrschneider, M., Bhagwat, S., Krampe, R., Michler, V., Breitkreutz, J and Hochhaus, G. (2015) 'Evaluation of the Transwell System for Characterization of Dissolution Behavior of Inhalation Drugs: Effects of Membrane and Surfactant', *Molecular Pharmaceutics*, 12(8), pp.2618-2624

Rubin, B. K. (2014) 'Secretion properties, clearance, and therapy in airway disease', *Translational Respiratory Medicine*, 1, pp.1-7

Sahib, M. N.,, Abdulameer, S.A., Darwis, Y., Peh, K.K. and Tan, Y.T. (2012) 'Solubilization of beclomethasone dipropionate in sterically stabilized phospholipid nanomicelles (SSMs): Physicochemical and in vitro evaluations', *Drug Design, Development and Therapy*, 6, pp. 29–42.

Sakagami, M. (2014) 'Fluticasone pharmacokinetics: meta-analysis and models. In: Dalby, R., Byron, P., Peart J et al. eds.', Repsiratory Drug Delivery, Puerto Rico. DHI Publishing, LLC, River Grove, IL, P. 143-153

Salama, R. O., Traini, D., Chan, H.K., Sung, A., Ammit, A.J. and Young, P.M. (2009) 'Preparation and evaluation of controlled release microparticles for respiratory protein therapy', *Journal of Pharmaceutical Sciences*, 98(8), pp.2709-2717

Salar-Behzadi, S., Wu, S., Mercuri, A., Meindl, C., Stranzinger, S and Frohlich, E. (2017) 'Effect of the pulmonary deposition and in vitro permeability on the prediction of plasma levels of inhaled budesonide formulation', *International Journal of Pharmaceutics*, 532(2), pp.337-344

Scano, G., Gorini, M., Duranti, R., Misuri, G., Landelli, I and Gigliotti, F. (1999) 'Physiological changes during severe airflow obstruction in chronic obstructive pulmonary disease.', *Monaldi archives for chest disease,* 54(5), pp.413-416

Schürch, S., Goerke, J. and Clements, J. A. (1976) 'Direct determination of surface tension in the lung.', *Proceedings of the National Academy of Sciences of the United States of America*, 73(12), pp. 4698–702.

Shur, J. (2016) 'The development of predictive dissolution methods for orally inhaled drug products', *University of Bath, Department of Pharmacy and Pharmacology*

Siebert, T. A. and Rugonyi, S. (2008) 'Influence of liquid-layer thickness on pulmonary surfactant spreading and collapse', *Biophysical Journal*, 95(10), pp. 4549–4559.

Sikorska, E., Wyrzykowski, D., Szutkowski, K., Greber, K, Lubecka, E.A., and Zhukov, I. (2016) 'Thermodynamics, size, and dynamics of zwitteronic dodecylphosphocholine and anionic sodium dodecyl sulfate mixed micelles', *Journal of Thermal Analysis and Calorimetry*, 123(1), pp.511-523

Simionato, L. D., Petrone, L., Baldut, M., Bonafede, S.L. and Segall, A. (2018) 'Comparison between the dissolution profiles of nine meloxicam tablet brands commercially available in Buenos Aires, Argentina', *Saudi Pharmaceutical Journal*, 26(4), pp.578-584

Singh, S. K., Reddy, I. K. and Khan, M. A. (1996) 'Optimization and characterization of controlled release pellets coated with an experimental latex. II. Cationic drug',

International Journal of Pharmaceutics, 141(1-2), pp.179-195

Smola, M., Vandamme, T. and Sokolowski, A. (2008) 'Nanocarriers as pulmonary drug delivery systems to treat and to diagnose respiratory and non respiratory diseases', *International Journal of Nanomedicine*, pp. 1–19.

Soares, S., Fonte, P., Costa, A., Andrade, J., Seabra, V., Ferreira, D., Reis, S and Sarmento, B. (2013) 'Effect of freeze-drying, cryoprotectants and storage conditions on the stability of secondary structure of insulin-loaded solid lipid nanoparticles', *International Journal of Pharmaceutics*, 456(2), pp. 370–381.

Solid, R. and Dosage, O. (1997) 'Guidance for Industry Guidance for Industry Dissolution Testing of Immediate', *Evaluation*.

Son, Y.-J. and McConville, J. T. (2009) 'Development of a standardized dissolution test method for inhaled pharmaceutical formulations', *International Journal of Pharmaceutics*, 382(1), pp. 15–22.

Son, Y. J., Horng, M., Copley, M and McConville, J.T. (2010) 'Optimization of an in vitro dissolution test method for inhalation formulations', *Dissolution Technologies*, pp.6-13

Sul, B., Wallqvist, A., Morris, M.J., Reifman, J and Rakesh, V. (2014) 'A computational study of the respiratory airflow characteristics in normal and obstructed human airways', *Computers in Biology and Medicine*, 52, pp.130-143

Sundstrom, E., Lastbom, L., Ryrfeldt, A and Dahlen, S.E. (2003) 'Interactions among three classes of mediators explain antigen-induced bronchoconstriction in the isolated perfused and ventilated guinea pig lung', *Journal of Pharmacology and Experimental Therapeutics*, 307(1), pp.408-418

Sunesen, V. H., Vedelsdal, R., Kristensen, H.G., Christrup, L and Mullertz, A. (2005) 'Effect of liquid volume and food intake on the absolute bioavailability of danazol, a poorly soluble drug', *European Journal of Pharmaceutical Sciences*, 24(4), pp.297-303

Szczuka, A., Wennerberg, M., Packeu, A and Vauquelin, G. (2009) 'Molecular mechanisms for the persistent bronchodilatory effect of the β2-adrenoceptor agonist salmeterol', *Br J Pharmacol,* 158(1), pp.183-194

Takaya, M., Shinohara, Y., Serita, F., Ono-Ogasaware, M., Otaki, N., Toya, T., Takata, A, Yoshida, K and Kohyama, N. (2006) 'Dissolution of functional materials and rare earth oxides into pseudo alveolar fluid.', *Industrial health*, 44(4), pp.639-644

Tang, X. and Pikal, M. J. (2004) 'Design of Freeze-Drying Processes for Pharmaceuticals: Practical Advice', *Pharmaceutical Research*, pp. 191–200.

Tashkin, D. P. (2016) 'A review of nebulized drug delivery in COPD', *International Journal of COPD*, pp. 2585–2596.

Tayab, Z. R. and Hochhaus, G. (2005) 'Pharmacokinetic/pharmacodynamic evaluation of inhalation drugs: application to targeted pulmonary delivery systems.', *Expert opinion on drug delivery*, 2(3), pp.519-532

Telko, M. J. and Hickey, A. J. (2005) 'Dry powder inhaler formulation', *Respiratory care*, 50(9), pp.1209-1227

Thakkar, H., Nangesh, J., Parmar, M and Patel, D. (2011) 'Formulation and characterization of lipid-based drug delivery system of raloxifene-microemulsion and

self-microemulsifying drug delivery system', *Journal of Pharmacy and Bioallied Sciences*, 3(3), p. 442.

Thompson AJHaDC (1996). 'Inhalation Aerosols: Physical and Biological Basis for Therapy', New York, NY, USA, p.83

Thompson AJHaDC (2004). In: A.J. Hickey MD edition. 'Pharmaceutical Inhalation Aerosol Technology'. 2nd Edition ed. New York, NY, USA, p.1

Thorsson, L., Edsbacker, S., Kallen, A and LofdahL, C.G. (2001) 'Pharmacokinetics and systemic activity of fluticasone via Diskus and pMDI, and of budesonide via Turbuhaler', *British journal of clinical pharmacology*, 52(5), pp.529-538

Tiwari, G., Tiwari, R., Sriwastawa, B., Bhati, L., Pandey, S., Pandey, P and Bannerjee, S.K. (2012) 'Drug delivery systems: An updated review.', *International journal of pharmaceutical investigation*, 2(1), pp. 2–11.

Tiwari, G., Tiwari, R. and Rai, A. K. (2010) 'Cyclodextrins in delivery systems: Applications.', *Journal of pharmacy & bioallied sciences*, 2(2), pp.72–79.

Tolman, J. A. and Williams, R. O. (2010) 'Advances in the pulmonary delivery of poorly water-soluble drugs: Influence of solubilization on pharmacokinetic properties', *Drug Development and Industrial Pharmacy*, 36(1), pp.1-30

US FDA CDER. (1997) 'Guidance for Industry: Disoslution testing of immediate release solid oral dosage forms, May 15. Accessed from: http://www.fda.gov/downloads/drugs/guidancecomplianceregulatoryinformation/guidances/ucm070237.pdf.

US FDA CDER, (1998) 'Draft guidance: Metered dose inhaler (MDI) and dry powder inhaler (DPI) drug products chemistry, manufacturing and controls documentation', May 15. Accessed from: http://www.fda.gov/downloads/Drugs/GuidanceComplianceRegulatoryInformation/Guidances/ucm070573.pdf.

US FDA CDER, (2001) 'Guidance for industry: bioanalytical method validation', June 16. Accessed from: http://www.fda.gov/downloads/Drugs/Guidances/ucm070107.pdf

V.N, L., Leterme, P., Gayot, A and Flament, M.P. *et al.* (2006) 'Aerosolization potential of cyclodextrins - Influence of the operating conditions', *PDA Journal of Pharmaceutical Science and Technology*, 60(5), pp. 314–322.

Vaughan, W. J. and Vaughan, B. E. (1969) 'Deposition of inhaled particles in lungs', *Nature*, 221, pp.661-662

Vertzoni, M., Fotaki, N., Kostewicz, E., Stippler, E., Leuner, C., Nicolaides, E., Dressman, J and Reppas, C. (2004) 'Dissolution media simulating the intralumenal composition of the small intestine: physiological issues and practical aspects', *Journal of Pharmacy and Pharmacology*, 56(4), pp.453-462

Vollhardt, D. and Fainerman, V. B. (2006) 'Progress in characterization of Langmuir monolayers by consideration of compressibility', *Advances in Colloid and Interface Science*, pp. 83–97.

Wagner, A., Platzgummer, M., Kreismayr, G., Quendler, H., Stiegler, G., Ferko, B., Vecera, G., Vorauer-Uhl, K and Katinger, H. (2006) 'GMP Production of Liposomes—A New Industrial Approach', *Journal of Liposome Research*, 16(3), pp. 311–319.

Wang, J. and Flanagan, D. R. (1999) 'General solution for diffusion-controlled dissolution of spherical particles. 1. Theory', *Journal of Pharmaceutical Sciences*, 88(7), pp.731-738

Wang, W., Chen, M. and Chen, G. (2012) 'Issues in freeze drying of aqueous solutions', *Chinese Journal of Chemical Engineering*, 20(3), pp. 551–559.

Warisnoicharoen, W., Lansley, A. B. and Lawrence, M. J. (2000) 'Nonionic oil-in-water microemulsions: The effect of oil type on phase behaviour', *International Journal of Pharmaceutics*, 198(1), pp. 7–27.

Washington, N., Steele, R.J., Jackson, S.J., Bush, D., Mason, J., Gill, D.A., Pitt, K and Rawlins, D.A. (2000) 'Determination of baseline human nasal pH and the effect of intranasally administered buffers', *International Journal of Pharmaceutics*, 198(2), pp. 139–146.

Weber, B. and Hochhaus, G. (2013) 'A Pharmacokinetic Simulation Tool for Inhaled Corticosteroids', *The AAPS Journal*, 15(1), 159-171

West, J. B. (2013) 'Pulmonary Pathophysiology: the essentials', Shock, *Baltimore, Williams and Wilkins, Eigth edition*, pp.20-48

Wiedmann, T. S., Bhatia, R. and Wattenberg, L. W. (2000) 'Drug solubilization in lung surfactant', *Journal of Controlled Release*, 65(1–2), pp. 43–47.

Wu, S.Q., Salar-Behzadi, S and Froehlich, E. (2014) 'Comparison of in silico and in vivo pharmacokinetic data for inhalation products'., *Journal of Aerosol Medicine and Pulmonary Drug Delivery*, 27(4), pp. A19-A19

Wuyts, B., Riethorst, D., Brouwers, J., Tack, J., Annaert, P and Augustijns, P. (2015) 'Evaluation of fasted and fed state simulated and human intestinal fluids as solvent system in the Ussing chambers model to explore food effects on intestinal permeability', *International Journal of Pharmaceutics*, 478(2), pp. 736–744.

Xu, Y. Y., Howes, T., Adhikari, B and Bhandari, B. (2013) 'Effects of Emulsification of Fat on the Surface Tension of Protein Solutions and Surface Properties of the Resultant Spray-Dried Particles', *Drying Technology*, 31(16), pp. 1939–1950.

Yeh, H. C. and Schum, G. M. (1980) 'Models of human lung airways and their application to inhaled particle deposition', *Bulletin of Mathematical Biology*, 42(3), pp.461-480

Yu, J. and Chien, Y. W. (1997) 'Pulmonary drug delivery: physiologic and mechanistic aspects.', *Critical reviews in therapeutic drug carrier systems,* 14(4), pp.395-453

Yu, L. X., Lipka, E., Crison, J.R and Amidon, G.L. (1996) 'Transport approaches to the biopharmaceutical design of oral drug delivery systems: Prediction of intestinal absorption', *Advanced Drug Delivery Reviews*, 19(3), pp.359-376

Zhang, J. A., Xuan, T., Parmer, M., Mal, L., Ugwu, S., Ali, S and Ahmad, I. (2004) 'Development and characterization of a novel liposome-based formulation of SN-38', *International Journal of Pharmaceutics*, 270(1–2), pp. 93–107.

Zhang, Y., Huo, M., Zhou, J., Zou, A., Li, W., Yao, C and Xie, S. (2010) 'DDSolver: An Add-In Program for Modeling and Comparison of Drug Dissolution Profiles', *The AAPS Journal*., 12(3), pp.263-271

Zhuang, X. and Lu, C. (2016) 'PBPK modeling and simulation in drug research and

development', *Acta Pharmaceutica Sinica B*, 6(5), pp.430-440

Zhou, M., Shen, L., Lin, X., Hong, Y and Feng, Y. (2017) 'Design and pharmaceutical applications of porous particles'. *RSC Adv,* 7, p. 39490 - 39501

Zuo, J., Gao, Y., Bou-Chacra, N and Lobenberg, R. (2014) 'Evaluation of the DDSolver software applications', *BioMed Research International*, pp.1-10

Zwir-Ferene, A and Biziuk, M. (2006) 'Solid Phase Extraction Technique - Trends, Opportunities and Applications', *Polish Journal of Environmental Studies,* 15(5), pp. 677-690

APPENDIX A

Appendix A Table A. 1. Cryo-TEM images of human respiratory tract lining fluid. Data obtained from Dr. Abhinav Kumar, 2015.

Physicochemical property	Human RTLF
Particle morphology (via Cryo-TEM)	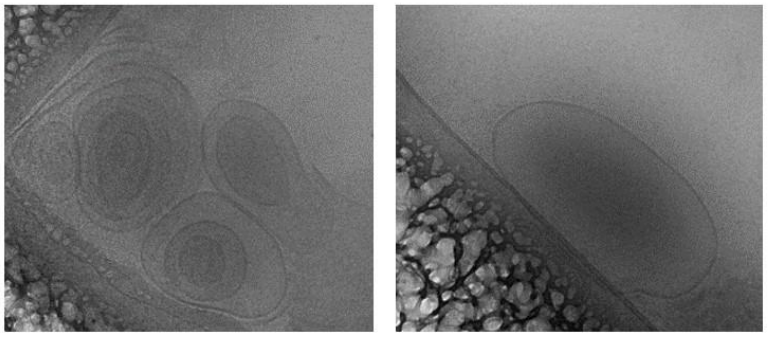

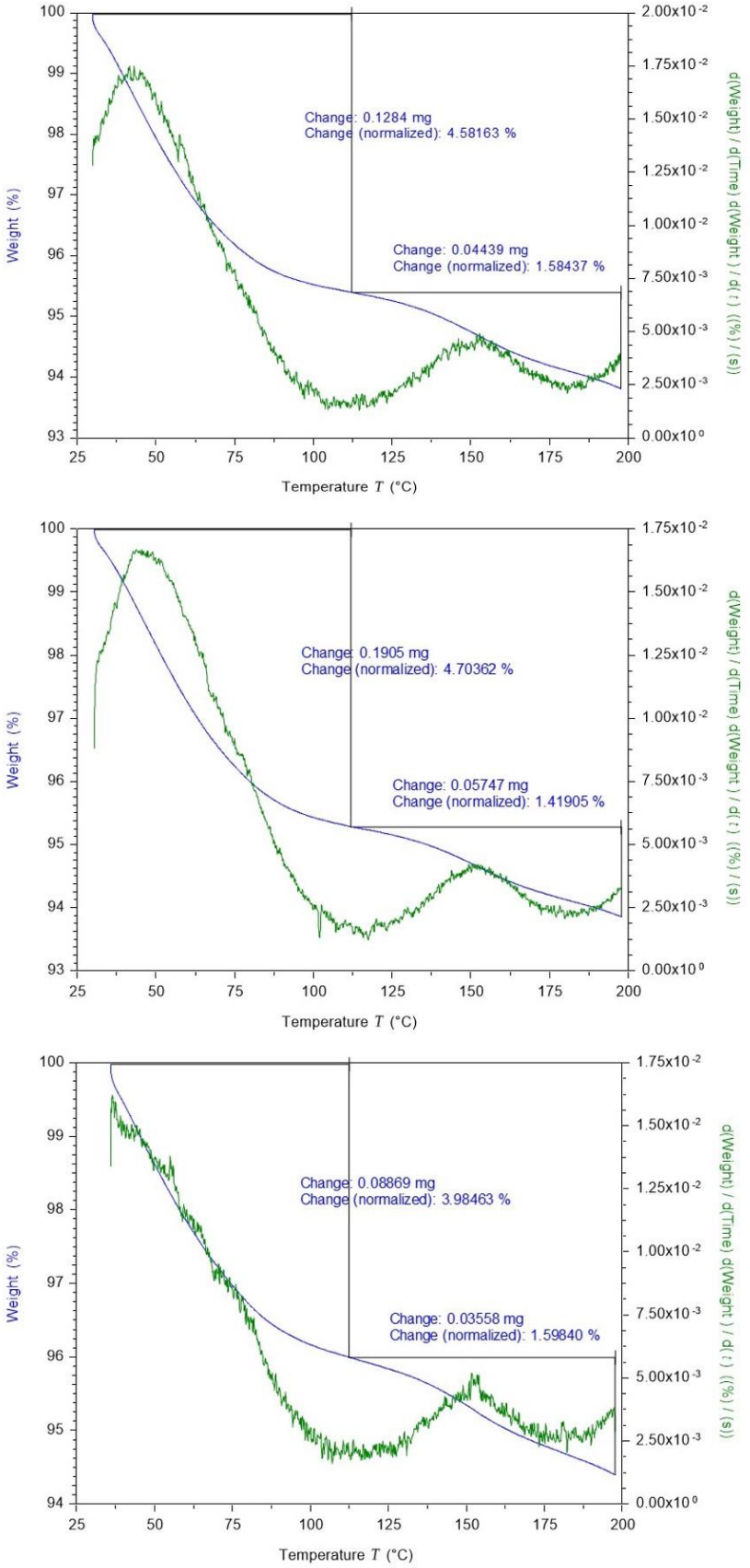

Appendix A Figure A.1. Thermogravimetric graphs of the simulated lung fluid (SLF) to identify the amount of moisture retained in the freeze-dried powder.

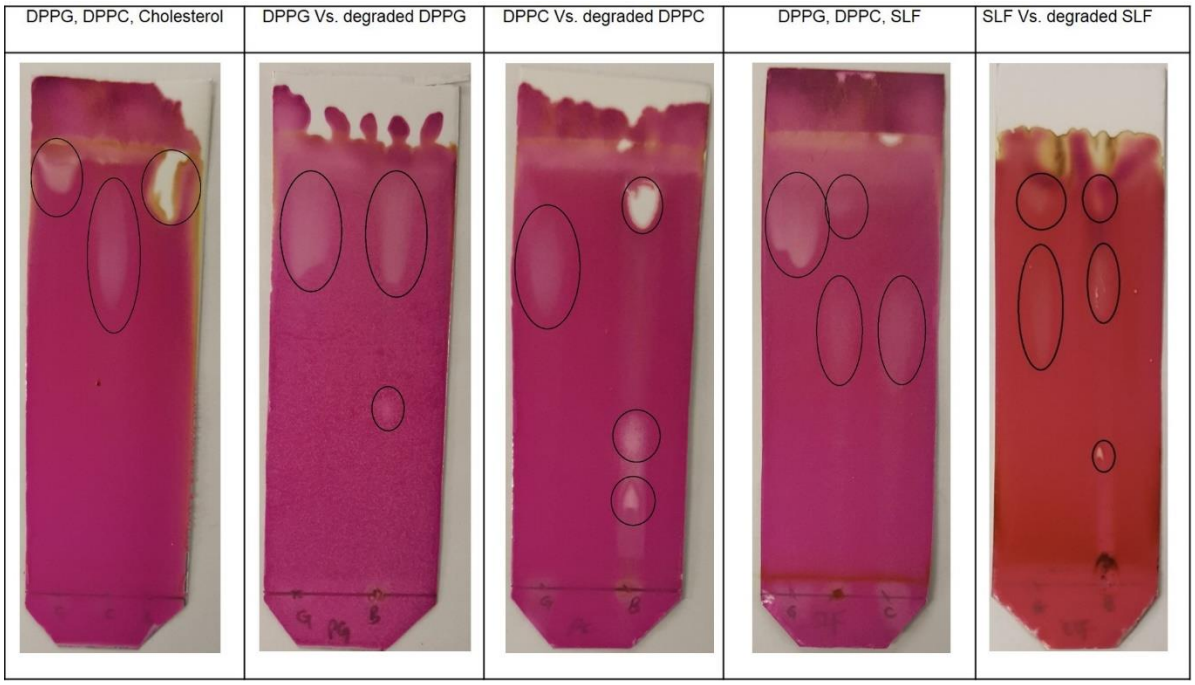

Appendix A Figure A.2. Thin Layer Chromatography (TLC) preliminary study. TLC plate runs of DPPG, DPPC, cholesterol, simulated lung fluid and their force-degraded solutions. Potassium permanganate staining was used to detect the phospholipids present.

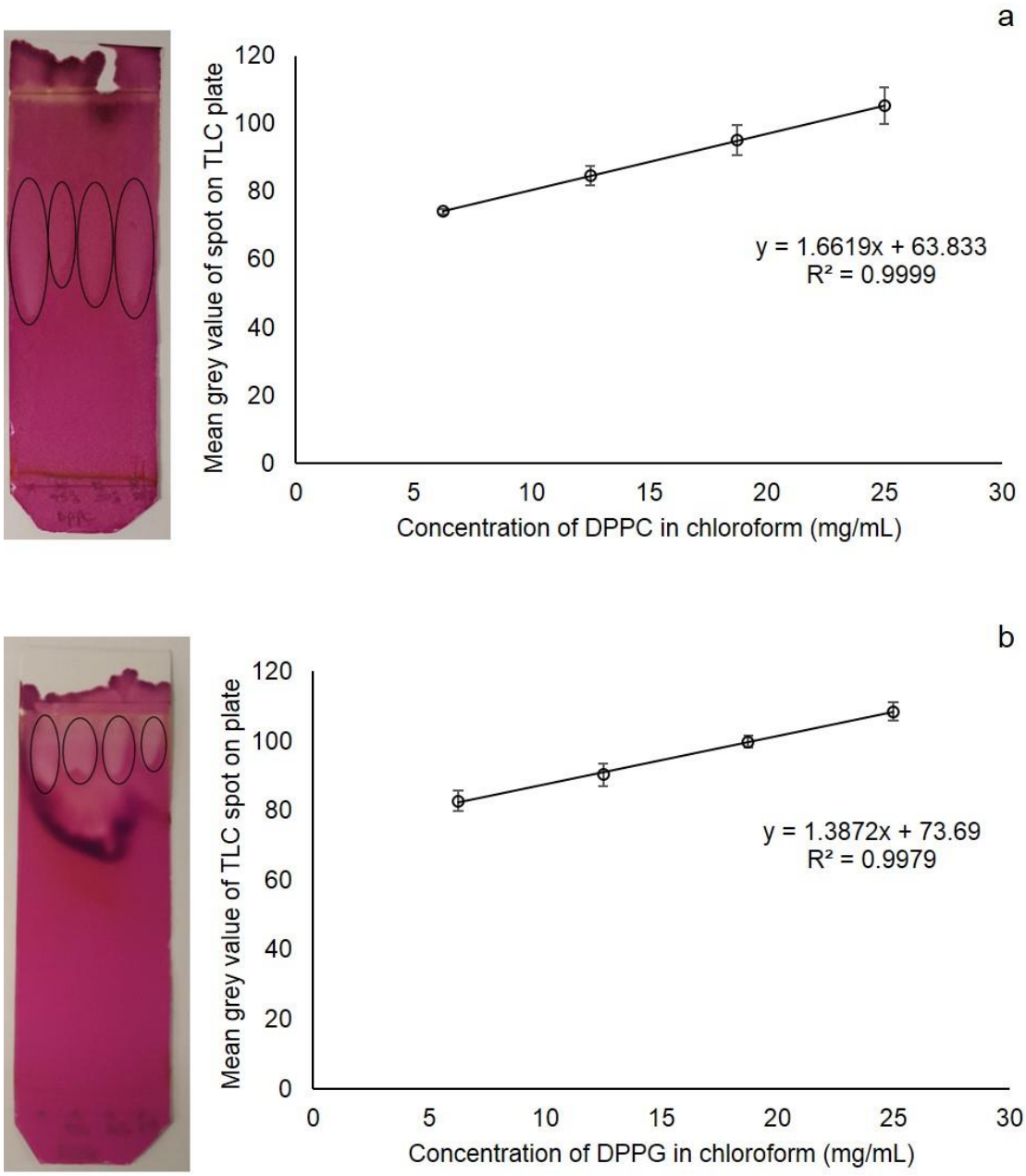

Appendix A Figure A.3. Thin layer chromatography runs of 100, 75, 50 and 25% v/v concentrations, and a plot of the mean grey value of TLC spot/spot intensity as a function of the concentration of a) DPPC and b) DPPG.

***Appendix A Table A.2. The salt components of Gamble's solution and their relative concentrations. The components were added in that specific order to avoid precipitation of salts. Citrate was used in place of proteins and acetate to replace organic acids, adapted from method by Marques et al* (Marques *et al*., 2011)**

Components of Gamble's solution	Concentration [g/L]
Magnesium chloride ($MgCl_2$)	0.095
Sodium chloride (NaCl)	6.019
Potassium chloride (KCl)	0.298
Sodium phosphate dibasic ($Na_2HPO_{4)}$	0.126
Sodium sulphate ($Na_2SO_{4)}$	0.063
Calcium chloride dihydrate ($CaCl_2 \cdot 2H_2O$)	0.368
Sodium acetate ($C_2H_3O_2Na$)	0.574
Sodium bicarbonate ($NaHCO_3$)	2.604
Trisodium citrate dihydrate ($C_6H_5Na_3O_7 \cdot 2H_2O$)	0.097

Appendix A Table A.3. The components of Survanta® and their relative concentrations.

Components of Survanta®	Concentration [mg/mL]
Phospholipids	25
Disaturated phosphatidylcholine	11.0 – 15.5
Triglycerides	0.5-1.75
Free fatty acids	1.4-3.5
Protein	< 1.0

Appendix A Table A.4. List of inhaled drug compounds currently available, their drug class, chemical classification, inhaled dose, melting point, molecular weight, Log P, polar surface area, reported aqueous solubility and their measured solubility in Gamble's solution, SLF, 0.5% w/v SDS in PBS and Survanta®. Melting point and solubility data expressed as mean ± SD (n=3).

Drug	Drug class	Chemical structure/classification	Inhaled dose (µg/mL) *	Melting Point (°C)**	MW (g/mol)***	log P***	PSA (Å^2)***	Reported/predicted aqueous solubility (µg/mL)***	Solubility (µg/mL)			
									Gamble's	SLF	0.5% SDS	Survanta®
Formoterol Fumarate [a]	β2- adrenoceptor agonist	Aryl, hydroxy-ethylamine	0.80		344.41	2.20	90.82	41.60				
Indacaterol Maleate	β2- adrenoceptor agonist	Aryl, hydroxy-ethylamine	10.00		392.49	3.31	81.59	7.98				
Olodaterol [a]	β2- adrenoceptor agonist	Aryl, hydroxy-ethylamine	0.17		386.44	2.02	100.05	70.30				
Salbutamol Sulphate [a]	β2- adrenoceptor agonist	Aryl, hydroxy-ethylamine	1666.67		239.31	1.40	72.72	14100.00				
Salmeterol Xinafoate	β2- adrenoceptor agonist	Aryl, hydroxy-ethylamine	3.33		415.57	3.82	81.95	2.26				
Terbutaline Sulphate [a]	β2- adrenoceptor agonist	Aryl, hydroxy-ethylamine	3333.33		225.28	0.55	72.72	213000.00				
Vilanterol Trifenatate	β2- adrenoceptor agonist	Aryl, hydroxy-ethylamine	0.83		774.78	3.39	91.18	1.18				
Tobramycin [a]	Antibiotic	Aminoglycoside	3733.33		467.52	-6.50	268.17	53700.00				
Aztreonam Lysine	Antibiotic	Monocyclic β-lactam	2500.00		435.43	0.04	206.03	42.90				
Aclidinium Bromide	Antimuscarinic bronchodilator	Quarternary ammonium	12.5		564.56	3.07	55.76	1.52				
Glycopyrronium Bromide	Antimuscarinic bronchodilator	Quarternary ammonium	1.67		318.43	-1.20	46.53	0.94				
Ipratropium Bromide	Antimuscarinic bronchodilator	Quarternary ammonium	16.66		412.37	0.21	46.53	0.70				
Tiotropium Bromide [a]	Antimuscarinic bronchodilator	Quarternary ammonium	0.60		472.42	-0.55	59.06	15.60				
Umeclidinium	Antimuscarinic bronchodilator	Quarternary ammonium	1.83		508.49	0.68	29.46	0.02				
Pentamidine Isethionate	Antiprotazoal	Amidine, Di-base	10,000		340.42	2.32	118.20	23.60				
Ribavirin [a]	Antiviral	Guanosine nucleoside	66.67		244.21	-1.90	143.72	33200.00				
Zanamivir [a]	Antiviral	Guanido-neuraminic acid	333.33		332.31	-2.30	200.72	7310.00				
Beclometasone Dipropionate	Corticosteroid	Steroid	13.33	85.69 ± 0.22	521.04	3.69	106.97	0.2	1.03 ± 0.12	16.79 ± 0.17	64.36 ± 1.38	37.16 ± 0.89
Budesonide	Corticosteroid	Steroid	26.67	244.28 ± 0.59	430.53	2.42	93.06	45.70	12.84 ± 0.21	26.24 ± 0.56	379.36 ± 3.09	18.79 ± 0.44
Ciclesonide	Corticosteroid	Steroid	5.33		540.70	4.08	99.13	1.57				
Fluticasone Propionate	Corticosteroid	Steroid	16.66	280.71 ± 0.19	444.51	3.69	80.67	0.1	0.74 ± 0.03	2.04 ± 0.09	13.08 ± 0.26	20.28 ± 1.51
Fluticasone Furoate [a]	Corticosteroid	Steroid	6.67		538.58	3.73	93.81	43.40				
Mometasone Furoate	Corticosteroid	Steroid	13.33	225.17 ± 0.69	521.43	2.81	74.60	5.23	0.59 ± 0.03	0.80 ± 0.15	87.89 ± 1.70	2.30 ± 0.03
Sodium cromoglicate	Cromoglicate	Salt	333.33		512.33	1.84	165.89	35.80				
Nedocromil Sodium	Cromoglicate	Pyranoquinolone	133.33		371.34	2.18	121.21	45.90				

* Calculated by max dose per inhalation divided by lung fluid volume (30 mL) ; derived from: Hastedt, J.E., Backman, P., Clark, A.R., Doub, W., Hickey, A., Hochhaus, G., Kuehl, P.J., Lehr, C., Mauser, P., McConville, J., Niven, R., Sakagimi, M., Weers, J.G. Scope and relevance of a pulmonary biopharmaceutical classification system AAPS/FDA/USP Workshop March 16-17th, 2015 in Baltimore, MD. AAPS Open, 2:1, 1-20

**Measured by Differential Scanning Calorimetry (DSC)

*** Data obtained from Drugbank database version 5.0 (https://www.drugbank.ca/) or Pubchem open chemistry database (https://pubchem.ncbi.nlm.nih.gov/search/)

[a] Predicted solubility >> inhaled dose therefore, drug is not dissolution-limited

APPENDIX B

***Appendix B Table B.5. System-specific input parameters for humans (table adapted from Boger et al* (Boger *et al.*, 2016).**

Tissue	Volume (fraction of BW)	Blood flow (fraction of Q_{CO})[a]
Adipose	0.12	0.050
Gut	0.017	0.17
Liver	0.026	0.060
Lung	0.0076	0.025[c)]/1
Poorly perfused[**]	1-(the rest)	1-(the rest)
Richly perfused[***]	0.029	0.35
Spleen	0.0026	0.020
Arterial blood	0.026	NA
Venous blood	0.051	NA

[*]Poorly perfused = 1 – other organs; [***]Richly perfused = heart + brain + kidney from Brown *et al*; *BW* = body weight; Q_{CO} = cardiac output, 5.2 L/min.

References: [a]Brown, R.P., Delp, M.D., Lindstedt, S.L., Rhomberg, L.R. & Beliles, R.P. (1997) ''Physiological parameter values for physiologically based pharmacokinetic models'', *Toxicology and industrial health,* 13, 407-484

Appendix B Table B.6. System-specific input parameters for the central lung and peripheral lung in human (adapted from Boger et al **(Boger *et al.*, 2016)***.*

Parameter	Central lung	Peripheral lung
Blood flow		
(fraction of Q_{CO})*	0.025	1
Surface area (dm^2/kg)	48.0	8410
Lining fluid volume (mL/kg)	3.84	5.89
Fraction of tissue volume	0.27	0.73
k_{mcc} (h^{-1})**	0.0792	NA

*Q_{CO}=Cardiac output; **k_{mcc}=rate constant for mucociliary clearance

Appendix B Table B.7. Drug and formulation specific input parameters for fluticasone propionate (adapted from Boger et al **(Boger *et al.*, 2016)***.*

Parameter	Value
Molecular weight	500.6
P_{app} (cm/s)	$46.9*10^{-6}$
Particle density ($nmol/dm^3$)	$1.430*10^{9}$
$logD_{7.4}$	4.2
Blood/Plasma Ratio	0.95
CLp (L/h/kg)	0.9368[a]
Diffusion Coefficient (m^2/s)	$2.27*10^{-11}$
$f_0,\ldots,f_6$	0.096, 0.086, 0.203, 0.343, 0.213, 0.053, 0.006
$r_0,\ldots,r_6$ (µm)	13.17, 8.14, 5.04, 3.13, 2.01, 1.38, 1.17
f_u	0.016
$f_{u,fluid}$	1
F	0[b]
C_s ($nmol/dm^3$)	4530

P_{app} = apparent permeability; Cl_p = plasma clearance, $f_0,\ldots,f_6$ = mass fractions for particle size classes; $r_0,\ldots,r_6$ = initial geometric radius of particle size classes 0,…,8; f_u = fraction unbound in plasma; $f_{u,fluid}$ = fraction unbound in epithelial lining fluid; Cs = solubility of FP in epithelial lining fluid

References: [a]https://www.drugbank.ca/drugs/DB00588; [b]Harding S.M. (1990) ''The human pharmacology of fluticasone propionate'', *Respir Med,* 84, Suppl A, pp. 25-29.

Appendix B Table B.8. Concentration of fluticasone propionate (FP) in the perfusate over time following dissolution in 1.5% w/v Polyethylene oxide + 0.4% w/v L-alphaphosphatidyl choline (PEO), simulated lung lining fluid (SLF) and diluted Survanta®. Data represent mean ± SD (n=3).

Time point (min)	Concentration of FP in the perfusate (%/s)		
	PEO	SLF	Survanta®
0	0.00000 ± 0.00000	0.00006 ± 0.00007	0.00006 ± 0.00011
3	0.00031 ± 0.00012	0.00022 ± 0.00008	0.00030 ± 0.00021
6	0.00080 ± 0.00017	0.00057 ± 0.00024	0.00060 ± 0.00033
9	0.00102 ± 0.00003	0.00072 ± 0.00032	0.00078 ± 0.00034
12	0.00137 ± 0.00011	0.00062 ± 0.00006	0.00106 ± 0.00059
15	0.00133 ± 0.00013	0.00065 ± 0.00010	0.00120 ± 0.00053
30	0.00152 ± 0.00074	0.00070 ± 0.00002	0.00109 ± 0.00065
60	0.00114 ± 0.00047	0.00074 ± 0.00016	0.00099 ± 0.00043
120	0.00093 ± 0.00040	0.00057 ± 0.00014	0.00082 ± 0.00050

Appendix B Table B.9. Concentration of fluticasone propionate (FP) in the perfusate over time following dissolution in rat isolated perfused lung (IPL). Data represent mean ± SD (n=3).

Time point (min)	Concentration of FP in the perfusate (%/s)
0	0.00000 ± 0.00000
4.5	0.00063 ± 0.00010
6	0.00160 ± 0.00028
7.5	0.00200 ± 0.00030
9	0.00210 ± 0.00037
12	0.00210 ± 0.00042
15	0.00214 ± 0.00045
30	0.00216 ± 0.00047
60	0.00216 ± 0.00037
120	0.00212 ± 0.00031

APPENDIX C

Appendix C Table C.1. The cumulative amount of fluticasone propionate dissolved (FP) at each time point, for experiments 1 to 45 and the total amount of FP deposited on the Transwell® insert filter, from the TSI/Transwell® dissolution method.

Experiment number	Cumulative amount dissolved at each time (µg)							Total amount deposited (µg)
	2	5	10	15	30	45	60	
1	0.10	0.20	0.32	0.42	0.52	0.62	0.74	7.64
2	0.10	0.20	0.34	0.48	0.61	0.75	0.87	4.67
3	0.22	0.41	0.54	0.66	0.81	0.94	1.10	5.50
4	0.19	0.38	0.54	0.68	0.82	0.96	1.07	5.29
5	0.29	0.59	0.82	1.02	1.19	1.42	1.60	6.74
6	0.10	0.20	0.28	0.38	0.49	0.60	0.71	4.51
7	0.16	0.32	0.48	0.61	0.75	0.86	0.98	4.90
8	0.22	0.39	0.56	0.69	0.84	0.98	1.11	5.27
9	0.11	0.22	0.32	0.44	0.56	0.67	0.75	6.05
10	0.09	0.19	0.29	0.38	0.48	0.57	0.69	4.87
11	0.09	0.22	0.33	0.43	0.54	0.63	0.75	5.31
12	0.19	0.42	0.57	0.70	0.85	0.99	1.14	5.40
13	0.07	0.16	0.26	0.35	0.44	0.53	0.63	7.18
14	0.09	0.20	0.30	0.40	0.52	0.63	0.75	7.29
15	0.10	0.21	0.31	0.42	0.55	0.68	0.86	6.04
16	0.10	0.20	0.30	0.40	0.52	0.62	0.72	5.37
17	0.32	0.49	0.63	0.77	0.90	1.03	1.17	5.97
18	0.32	0.54	0.70	0.85	0.99	1.13	1.26	6.29
19	0.16	0.36	0.58	0.79	0.99	1.17	1.39	11.50
20	0.19	0.43	0.67	0.90	1.18	1.44	1.75	9.69
21	0.21	0.53	0.83	1.11	1.37	1.64	1.91	9.30
22	0.56	0.99	1.38	1.71	2.04	2.36	2.72	13.96
23	0.19	0.42	0.68	0.93	1.13	1.36	1.58	17.00
24	0.32	0.64	0.94	1.27	1.63	1.94	2.31	12.79
25	0.25	0.53	0.79	1.03	1.31	1.55	1.78	8.93
26	0.20	0.47	0.72	0.99	1.24	1.47	1.72	13.58
27	0.59	0.99	1.41	1.81	2.13	2.49	2.85	13.10
28	0.09	0.17	0.26	0.34	0.45	0.54	0.65	5.29
29	0.07	0.17	0.25	0.35	0.45	0.54	0.65	3.79
30	0.11	0.24	0.35	0.51	0.64	0.76	0.92	4.41
31	0.23	0.39	0.56	0.73	0.85	0.98	1.18	5.31
32	0.10	0.21	0.32	0.45	0.55	0.65	0.74	3.83
33	0.08	0.17	0.27	0.38	0.49	0.59	0.69	5.34
34	0.11	0.20	0.28	0.36	0.45	0.55	0.63	4.16
35	0.29	0.52	0.75	0.92	1.04	1.19	1.46	6.09
36	0.17	0.32	0.44	0.55	0.68	0.81	0.92	4.49
37	0.15	0.33	0.48	0.61	0.75	0.90	1.07	5.91
38	0.18	0.42	0.57	0.71	0.86	1.04	1.21	5.76
39	0.12	0.29	0.49	0.69	0.89	1.06	1.32	9.49
40	0.25	0.44	0.71	0.90	1.30	1.60	2.16	14.49
41	0.15	0.27	0.49	0.65	0.87	1.03	1.25	12.30
42	0.10	0.26	0.39	0.48	0.62	0.75	0.85	10.47
43	0.17	0.36	0.59	0.80	0.92	1.13	1.35	10.26
44	0.19	0.36	0.52	0.71	0.93	1.04	1.13	5.60
45	0.44	0.82	1.14	1.40	1.81	2.10	2.48	13.65

Appendix C Table C.2. The cumulative percent of fluticasone propionate dissolved (FP) at each time point, for experiments 1 to 45, via the TSI/Transwell® dissolution method.

Experiment number	Cumulative % of FP dissolved at each time (%)						
	2	5	10	15	30	45	60
1	1.34	2.61	4.23	5.53	6.83	8.14	9.71
2	2.19	4.33	7.19	10.28	13.10	15.98	18.64
3	3.93	7.40	9.75	11.97	14.71	17.18	20.02
4	3.52	7.18	10.17	12.85	15.43	18.15	20.31
5	4.37	8.68	12.15	15.11	17.61	21.09	23.77
6	2.28	4.37	6.12	8.35	10.80	13.31	15.76
7	3.23	6.47	9.73	12.42	15.36	17.63	20.04
8	4.09	7.39	10.61	13.10	15.86	18.56	21.12
9	1.88	3.56	5.25	7.26	9.25	10.86	12.38
10	1.94	3.95	5.94	7.83	9.84	11.72	14.22
11	1.76	4.08	6.13	8.13	10.09	11.90	14.17
12	3.45	7.73	10.48	12.90	15.67	18.37	21.06
13	0.97	2.30	3.69	4.86	6.09	7.45	8.75
14	1.22	2.69	4.10	5.51	7.16	8.69	10.25
15	1.70	3.45	5.10	6.88	9.09	11.26	14.20
16	1.94	3.80	5.59	7.51	9.73	11.51	13.50
17	5.41	8.27	10.59	12.94	15.08	17.24	19.57
18	5.04	8.66	11.19	13.48	15.69	17.91	19.97
19	1.41	3.15	5.07	6.87	8.62	10.18	12.11
20	1.97	4.39	6.97	9.25	12.19	14.83	18.04
21	2.22	5.68	8.97	11.91	14.68	17.65	20.52
22	4.01	7.08	9.91	12.24	14.62	16.92	19.51
23	1.11	2.44	3.97	5.48	6.67	8.03	9.32
24	2.49	4.99	7.36	9.91	12.72	15.17	18.05
25	2.80	5.91	8.80	11.55	14.72	17.41	19.97
26	1.48	3.50	5.33	7.31	9.13	10.83	12.67
27	4.52	7.55	10.73	13.81	16.27	19.00	21.79
28	1.65	3.25	4.87	6.40	8.55	10.29	12.35
29	1.84	4.44	6.69	9.31	11.97	14.37	17.16
30	2.57	5.49	8.02	11.52	14.49	17.15	20.86
31	4.25	7.40	10.57	13.79	16.08	18.43	22.16
32	2.61	5.57	8.23	11.67	14.32	17.06	19.38
33	1.58	3.25	5.13	7.11	9.09	11.13	12.94
34	2.64	4.76	6.83	8.58	10.72	13.10	15.06
35	4.82	8.45	12.28	15.14	17.01	19.53	23.99
36	3.89	7.02	9.72	12.15	15.05	18.06	20.45
37	2.59	5.62	8.06	10.26	12.74	15.30	18.07
38	3.21	7.30	9.96	12.30	15.00	18.00	21.09
39	1.30	3.09	5.14	7.30	9.42	11.20	13.90
40	1.72	3.01	4.90	6.25	8.99	11.02	14.94
41	1.25	2.18	3.98	5.25	7.06	8.34	10.13
42	0.94	2.46	3.76	4.60	5.90	7.13	8.14
43	1.64	3.52	5.74	7.80	8.97	11.04	13.18
44	3.37	6.46	9.34	12.75	16.68	18.55	20.14
45	3.24	6.02	8.36	10.28	13.24	15.37	18.14

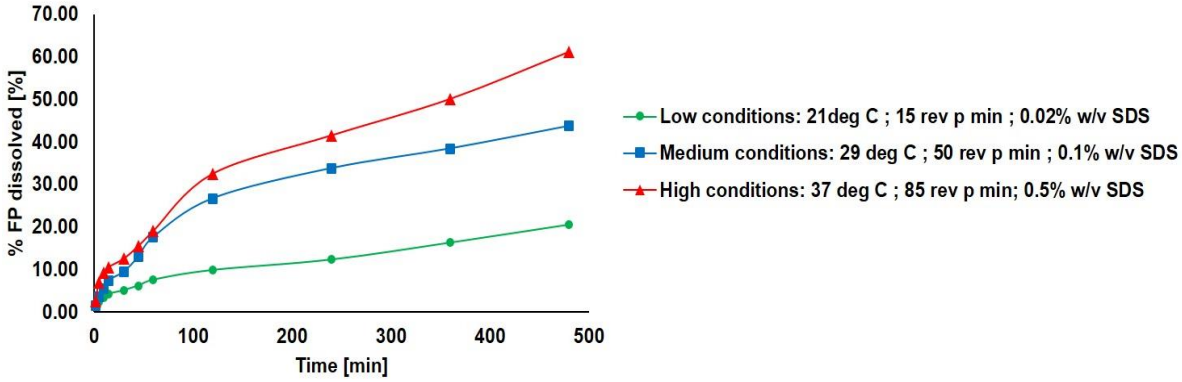

Appendix C Figure C.1. Dissolution of fluticasone propionate from the TSI/Transwell method, over 8 h, under the lowest, medium and highest conditions.

APPENDIX D

Appendix D Table D.10. List of the components of the Budesonide nanoemulsion and their concentrations, prepared by Amani et al (Amani et al, 2010).

Ingredient	Nanoemulsion component	Concentration (% w/v)
Budesonide	API	1.5
Polysorbate 80	Surfactant	10
Ethanol	Co-surfactant	1
Crodamol	Oil phase / inner phase	1
Normal saline (0.9% NaCL w/v)	Aqueous phase	To the required volume

Appendix D Table D.11. Preliminary investigations for dissolution testing. The flow rate, volume of solution in the nebuliser, time for nebulisation and the amount of fluticasone propionate deposited on the Transwell® filter paper, for the Flixotide suspension and fluticasone microemulsion formulations.

Sample	Flow rate (L/min)	Volume in nebuliser (mL)	Time for nebulisation (min)	Amount of FP deposited (µg)
Flixotide® Suspension	60	2	2	2.14 ± 0.08
	60	5	5	3.19 ± 0.16
	45	2	2	4.97 ± 0.70
	45	5	5	9.73 ± 0.54
FP Microemulsion	60	2.5	5	14.45 ± 0 .55
	45	1	2	9.72 ± 0.15
	45	2	1	13.09 ± 0.66

APPENDIX E

Published articles related to my PhD

(1) **Hassoun M**, Malmlöf M, Scheibelhofer O, Kumar A, Bansal S, Selg E, Nowenwik M, Gerde P, Radivojev S, Paudel A, Arora S, Forbes B. Use of PBPK modelling to evaluate the performance of DissolvIt, a biorelevant dissolution assay for orally inhaled drug products. Molecular Pharmaceutics: A-J (2019)

vnd00 | ACSJCA | JCA11.14300/W Library-x64 | research.3f (R4.1.3 HF01:4938 | 2.1) 2018/08/24 11:08:00 | PROD-WS-120 | rq_874985 | 1/25/2019 09:09:06 | 10 | JCA-DEFAULT

molecular pharmaceutics

Article

pubs.acs.org/molecularpharmaceutics

Use of PBPK Modeling To Evaluate the Performance of Dissolv*It*, a Biorelevant Dissolution Assay for Orally Inhaled Drug Products

Mireille Hassoun,[†,#] Maria Malmlöf,[‡,§,#] Otto Scheibelhofer,[∥] Abhinav Kumar,[†] Sukhi Bansal,[†] Ewa Selg,[‡] Mattias Nowenwik,[‡] Per Gerde,[‡,§] Snezana Radivojev,[∥] Amrit Paudel,[∥,⊥] Sumit Arora,[∥,○,▽] and Ben Forbes*[,†,○]

[†]King's College London, Institute of Pharmaceutical Science, London SE1 9NH, U.K.

[‡]Inhalation Sciences Sweden AB, Hälsovägen 7-9, 141 57 Huddinge, Sweden

[§]Institute of Environmental Medicine, Karolinska Institutet, 171 77 Stockholm, Sweden

[∥]Research Centre Pharmaceutical Engineering GmbH, Inffeldgasse 13, Graz 8010, Austria

[⊥]Institute of Process and Particle Engineering, Graz University of Technology, Inffeldgasse 13, Graz, 8010, Austria

Supporting Information

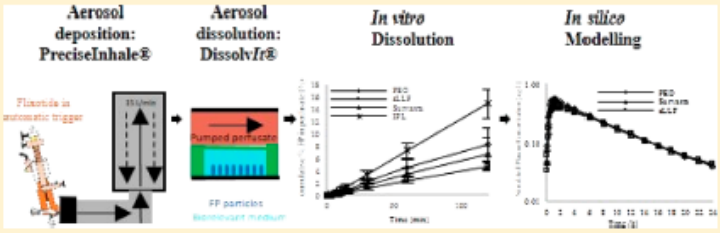

ABSTRACT: The dissolution of inhaled drug particles in the lungs is a challenge to model using biorelevant methods in terms of (i) collecting a respirable emitted aerosol fraction and dose, (ii) presenting this to a small volume of medium that is representative of lung lining fluid, and (iii) measuring the low concentrations of drug released. We report developments in methodology for each of these steps and utilize mechanistic *in silico* modeling to evaluate the *in vitro* dissolution profiles in the context of plasma concentration−time profiles. The PreciseInhale aerosol delivery system was used to deliver Flixotide aerosol particles to Dissolv*It* apparatus for measurement of dissolution. Different media were used in the Dissolv*It* chamber to investigate their effect on dissolution profiles, these were (i) 1.5% poly(ethylene oxide) with 0.4% L-alphaphosphatidyl choline, (ii) Survanta, and (iii) a synthetic simulated lung lining fluid (SLF) based on human lung fluid composition. For fluticasone proprionate (FP) quantification, solid phase extraction was used for sample preparation with LC−MS/MS analysis to provide an assay that was fit for purpose with a limit of quantification for FP of 312 pg/mL. FP concentration−time profiles in the flow-past perfusate were similar irrespective of the medium used in the Dissolv*It* chamber (~0.04−0.07%/min), but these were significantly lower than transfer of drug from air-to-perfusate in isolated perfused lungs (0.12%/min). This difference was attributed to the Dissolv*It* system representing slower dissolution in the central region of the lungs (which feature nonsink conditions) compared to the peripheral regions that are represented in the isolated lung preparation. Pharmacokinetic parameters (C_{max}, T_{max} and $AUC_{0-\infty}$) were estimated from the profiles for dissolution in the different lung fluid simulants and were predicted by the simulation within 2-fold of the values reported for inhaled FP (1000 μg dose) administered via Flixotide Evohaler 250 μg strength inhaler in man. In conclusion, we report methods for performing biorelevant dissolution studies for orally inhaled products and illustrate how they can provide inputs parameters for physiologically based pharmacokinetic (PBPK) modeling of inhaled medicines.

KEYWORDS: *Flixotide Evohaler, fluticasone, PreciseInhale, isolated perfused lungs, simulated lung fluid, Survanta*

1. INTRODUCTION

In vitro dissolution testing is well established for enteral solid dosage forms for quality control purposes, for comparing products under drug classification frameworks, and for predicting drug pharmacokinetics *in vivo*.[1−4] The therapeutic effect of an inhaled particulate aerosol is only realized after

Received: November 14, 2018
Revised: December 27, 2018
Accepted: January 14, 2019
Published: January 14, 2019

DOI: 10.1021/acs.molpharmaceut.8b01200
Mol. Pharmaceutics XXXX, XXX, XXX−XXX

drug release into solution; thus, investigating the dissolution of solid particle aerosol dosage forms has attracted interest.[5−8] Dissolution testing for orally inhaled products (OIP) is currently a "hot topic" with research groups adapting a panoply of adaptations of pharmacopoeial apparatus for aerosol collection and dissolution to function as *in vitro* tests for discerning the quality attributes of inhaled medicines. The latest developments in oral biopharmaceutics demonstrate convincingly that biorelevant methods are important if dissolution testing is to be used as an *in vivo* predictive tool and realize its full potential in a regulatory context and to predict clinically relevant performance.[3,4]

The complexity of biorelevant dissolution for inhaled products derives from the need to capture representative aerosol particles in a dispersed manner that reflects their deposition in the lungs, to present the particles to low volumes of lung fluid-like dissolution medium, and to measure reliably the low mass of drug delivered by aerosol medicines. Of the systems reported to date,[5−11] none accommodates all these features. The disparate OIP dissolution methods that have been studied tend to be nonintegrated and utilize large volumes of dissolution medium, which precludes the use of a dissolution medium that represents human lung lining fluid.[12,13] For some studies of poorly soluble drugs, the medium has been supplemented by addition of protein or phospholipid components, e.g., surfactants such as DPPC[6,14] or lung surfactant preparations such as Survanta.[15] However, biorelevant media are either expensive or difficult to prepare, and often represent only the surfactant component of distal respiratory tract lining fluid, with the highly abundant proteins absent.

Recently, an integrated apparatus has been developed by Inhalation Sciences for depositing aerosols to a flow past dissolution cell,[16] comprising the PreciseInhale and DissolvIt systems, respectively. The PreciseInhale can deliver carefully controlled doses of aerosols from powder inhalers or pressurized metered dose inhalers to the DissolvIt system, in which particle dissolution can be followed by simultaneous observation of aerosol particles using microscopy and measurement of dissolved drug transferred to a flow-past perfusate. Although DissolvIt addresses various limitation of dissolution systems used for OIP, the dissolution vessel contains 5.7 μL of a poly(ethylene oxide) (PEO) gel as the dissolution matrix rather than a biorelevant medium. Due to the novelty of the system, there is little reported data on the performance of the system in predicting dissolution.[16,17]

To study clinically relevant scenarios, dissolution studies to date have focused on the dissolution of poorly soluble inhaled drugs, in particular fluticasone proprionate (FP).[10,11,18] Delivery of FP to the DissolvIt with different biorelevant media in the chamber permits comparison to FP dissolution−absorption profiles in other systems, e.g., isolated perfused lungs (IPL). To perform these experiments requires accurate quantification of submicromolar concentrations of FP using a sensitive assay and an efficient extraction method.[19,20] Liquid-chromatography with tandem mass spectrometric detection (LC−MS/MS) provides selective and sensitive analysis of glucocorticoids in biological fluids.[21−23] However, poor repeatability using reported methods[21−23] required development of a new solid phase extraction (SPE) method, which was reliable and quick and required minimal sample preparation and solvent use.

The value of *in vitro* systems is in providing decision-making data, e.g., dissolution measurements for predicting and modeling impacts on drug pharmacokinetics in the early stages of the drug development process. Such data can expedite drug development and prevent unexpected toxico-kinetics and ultimately avoid costly end-stage failures.[24] Reliable predictive models for pharmacokinetics depend on selecting appropriate mathematical approaches, and more current studies tend to utilize *in silico* techniques.[25−27] For modeling dissolution, Backman et al. have described how mechanistic models may aid in obtaining a better understanding of dissolution, which can be used to predict systemic exposure (AUC) and hence its influence on drug therapeutic effect.[28] For this study, a mechanistic model was developed to evaluate the dissolution data derived from the biorelevant approach using the DissolvIt system.

In summary, the aim of the present study was to develop a biorelevant dissolution method by utilizing simulated lung fluid in the DissolvIt system. To measure the dissolution of FP, a LC−MS/MS method was validated for measurement of low drug concentrations. The effect of dissolution medium on FP aerosol particle dissolution was investigated using three different media: (i) 1.5% poly(ethylene oxide) + 0.4% L-alphaphosphatidyl choline, (ii) Survanta , and (iii) a synthetic simulated lung lining fluid (SLF), synthesized based on human lung fluid composition.[29,30] Finally, an *in silico* model based on the method of Boger et al.[31] was adapted to explore the impact of the dissolution rates derived on pharmacokinetics.

2. EXPERIMENTAL SECTION

2.1. Materials. Flixotide 50 μg Evohaler (GSK), poly(ethylene oxide) (PEO), and L-alphaphosphatidyl choline were supplied by Sigma-Aldrich Limited (Dorset, UK), whereas Survanta was obtained from Abbvie Ltd. (Berkshire, UK). The chemicals required for the production of SLF and the preparation of SLF were carried out according to a recently published method.[30] For solid phase extraction validation, the chemicals included were micronized FP (USP grade, purity 98%) supplied by LGM Pharma Inc. (Boca Raton, USA), pentadeuterated FP (FP-d5; USP grade, purity 97%) by Insight Biotechnology Limited (Wembley, UK), and rabbit serum, purchased from Sigma-Aldrich Company Limited (Dorset, UK). Chemicals needed for the extraction procedure were zinc sulfate powder, supplied by VWR International Limited (Lutterworth, UK), HPLC-gradient grade acetonitrile, 35% v/v ammonium hydroxide solution, and Analytical-Reagent grade dichloromethane, which were all purchased from Fischer Chemical (Loughborough, UK). The materials required for aerosolization, deposition, and dissolution of FP were provided by Inhalation Sciences, Sweden. For FP dissolution in rat IPL, female CD IGS (Sprague−Dawley) rats were obtained from Charles River (Sulzfeld, Germany), and the necessary equipment was provided by Inhalation Sciences, Sweden.

2.2. Preparation of Calibration Curve and Validation of Assay. Primary stock solutions of FP and FP-d5 were prepared by adding 1 mg of FP or FP-d5 into a 10 mL volumetric flask and filled to the volume with pure acetonitrile, producing 100 μg/mL solutions, and stored at −20 °C. A 1 μg/mL FP working solution was prepared by the appropriate dilution of the stock with pure acetonitrile. The calibration standards (156, 313, 625, 1250, 2500, 5000, and 10,000 pg/mL) were prepared from serial dilution of the working solution

DOI: 10.1021/acs.molpharmaceut.8b01200
Mol. Pharmaceutics XXXX, XXX, XXX−XXX

with pure acetonitrile. Method validation was conducted in terms of linearity, precision (intraday and interday), accuracy, limit of detection, and limit of quantification. Linearity was evaluated by plotting a calibration curve of mean peak area ratio of FP/FP-d5 ($n = 9$) against the concentrations of seven standards, using a weighted ($1/x$) linear regression model. The coefficient of variation (%CV) was calculated across three calibration sets prepared on the same day for intraday precision. For interday precision, another three fresh series of calibration standards prepared on days 2 and 3 were analyzed. Accuracy of the data was also evaluated across nine determinants of each standard, ensuring it was within 15% of each standard concentration. The limit of detection (LOD) and limit of quantification (LOQ) were calculated based on eqs 1 and 2, respectively.[19]

$$\mathrm{LOD} = 3.3[\mathrm{SD}/\mathrm{slope}] \quad (1)$$

$$\mathrm{LOQ} = 10[\mathrm{SD}/\mathrm{slope}] \quad (2)$$

where SD is the standard deviation of the y estimate (peak area ratio) and slope is the gradient of the line.

2.3. Deposition and Dissolution of FP Aerosol in the DissolvIt System. The aerosolization of Flixotide was carried out by connecting the Flixotide pMDI canister to the US Pharmacopeia Induction Port No. 1 (standardized simulation of the throat) of the PreciseInhale aerosol system from Inhalation Sciences (Stockholm, Sweden) (Figure 1). The

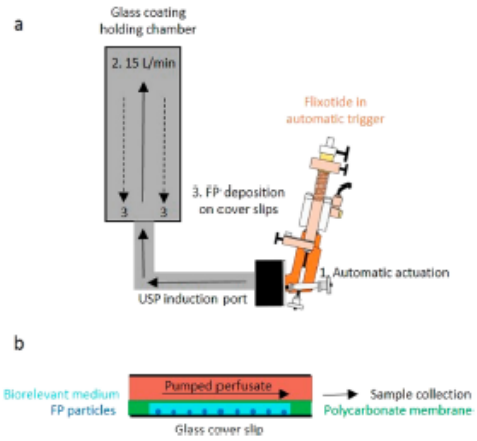

Figure 1. Schematic diagram of (a) fluticasone propionate aerosolization and particle deposition and (b) the dissolution system.

aerosol particles were deposited on nine circular microscope glass coverslips, 13 mm in diameter, and the dissolution of the deposited particles was investigated by interfacing the particles with the dissolution medium in the DissolvIt dissolution system from Inhalation Sciences (Stockholm, Sweden),[16] thermostated to 37 °C. Prewarmed dissolution medium, 5.7 μL of PEO, Survanta, or SLF, was applied to the polycarbonate membrane (pore size 0.03 μm) of each DissolvIt dissolution chamber, with the perfusate buffer streaming on the other side. The flow past perfusate consisted of 0.1 M phosphate buffer containing 4% w/v albumin solution, mixed using a magnetic stirrer. The perfusate was degassed using helium to remove excess bubbles and streamed at a flow rate of 0.4 mL/min over a period of 4 h with samples collected by an automated fraction collector at 0, 3, 6, 9, 12, 15, 20, 25, 30, 40, 50, 60, 120, and 240 min.

2.4. Dissolution of FP Aerosol in Rat Isolated Perfused Lungs. Female rats with body weight 279 ± 20 g were euthanized with phenobarbital sodium (100 mg/kg, i.p.), and their whole lungs were maintained *ex vivo* as described in other reports.[32,33] The lungs were placed in the artificial thoracic chamber. They were ventilated with room air at 75 breaths/min by creating an alternating negative pressure (−0.2 to −0.8 kPa)[3] inside the chamber, using an Ugo Basile model 7025 animal respirator (Varese, Italy), with a stroke volume of 6 mL, superimposed on a constant vacuum source connected to the chamber. The tracheal air flow velocity and pressure inside the chamber were measured with a heated Hans Rudolph 8430 series pneumotachograph (Kansas City, USA) at 0−3 L/min and a differential pressure transducer from EMKA Technologies (Paris, France), respectively. The physiological lung-function variables: tidal volume (V_t), dynamic lung compliance (C_{dyn}),[34] and lung conductance (G_{aw}), which is inversely proportional to lung resistance (RL),[34] were calculated from each breath in real time and logged by a data acquisition system using the EMKA Technologies software IOX v. 6.1a. The lungs were perfused via the pulmonary artery in a single-pass mode, at a constant hydrostatic pressure of approximately 12 cm H_2O, and the perfusate reservoir was continually overflowing into a recirculation drain pipe, in order to keep a constant liquid pressure head. Throughout the experiments, the perfusate flow rate after the passage through the lungs (Q_{perf}) was measured gravimetrically using a custom-made fraction collector with a balance. The perfusion medium consisted of Krebs−Henseleit buffer, 5.5 mM glucose, 12.6 mM HEPES, and 4% w/v bovine serum albumin. The temperature of the perfusate and the artificial thoracic chamber were maintained at 37 °C. The lungs were left to stabilize for 30 min prior to aerosol exposures, and only the lung preparations with stable baseline values for V_t, C_{dyn}, G_{aw}, and Q_{perf} during at least a 15 min period were used. The measured values were $V_t = 1.8 \pm 0.2$ mL, $C_{dyn} = 6.6 \pm 1.0$ mL/kPa; $G_{aw} = 279 \pm 20$ mL/s/kPa, and $Q_{perf} = 32 \pm 2$ mL/min ($n = 6$). Administration of Flixotide aerosol to the IPL was carried out using the PreciseInhale system as described above, where the aerosol was delivered to the lungs by the active dosing system, and the system automatically terminated the exposure when the inhaled target dose was reached. The perfusate was sampled using an automatic fraction collector over a 2 h period from the start of the aerosol exposure with sampling intervals of 4.5, 6, 7.5, 9, 12, 15, 30, 60, and 120 min. After the end of the perfusion period, the lungs and trachea were harvested for analysis of the amount of FP retained in the tissues after the perfusion period to enable mass balance calculations. The experiments were approved by a local ethical review board in Stockholm.

2.5. Sample Extraction. Samples were prepared for analysis following a new solid phase extraction method. Each sample, 325 μL, was loaded into a deep-well sample plate from Thermo-Scientific (Surrey, UK) followed by 50 μL of internal standard (0.1 μg/mL FP-D5). Zinc sulfate 0.1 M, 300 μL, followed by 75 μL of 10% ammonium hydroxide were added and mixed using a multichannel pipet. The SPE plate was placed on an orbital shaker for 30 min followed by

DOI: 10.1021/acs.molpharmaceut.8b01200
Mol. Pharmaceutics XXXX, XXX, XXX−XXX

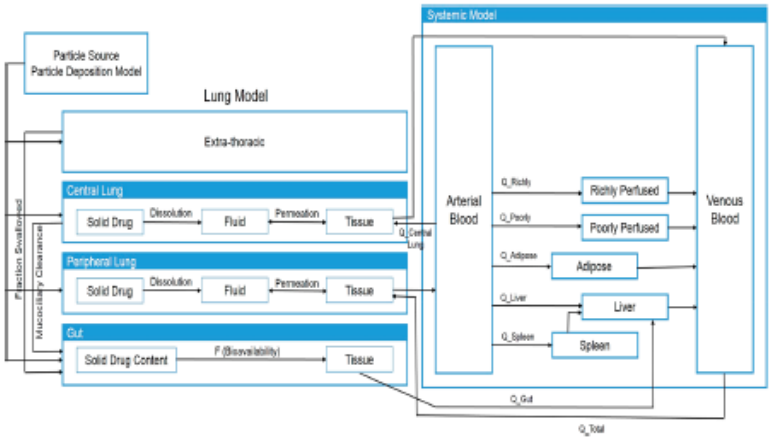

Figure 2. Schematic diagram representing the whole body physiologically based pharmacokinetic (PBPK) model.

centrifugation at 3700 rpm for 5 min. The samples were then transferred to a preconditioned Evolute Express ABN 10 mg SPE 96-well plate by Biotage (Uppsala, Sweden) and washed by applying low vacuum with 200 μL HPLC-grade water followed by 200 μL of 25% v/v methanol in water. The analytes were eluted twice with 200 μL of pure acetonitrile, once with 100 μL of dichloromethane then vacuum centrifuged to dryness. Samples were reconstituted with 30 μL of 55% v/v acetonitrile in water and sonicated rapidly for 10 min. Finally, an aliquot of the sample (20 μL) was injected into the LC−MS/MS system.

2.6. FP Quantification Using LC−MS/MS. Quantification of FP was carried out by Waters Xevo TQ tandem quadrupole mass spectrometer by Waters (Elstree, UK) equipped with an ESI interface, coupled with a Waters Acquity Ultra High Performance LC system (UPLC), equipped with a binary solvent delivery system. Chromatographic separations were carried out on a Waters Acquity UPLC BEH C18 column 130 Å, 1.7 μm, 2.1 × 50 mm. The mobile phase was a mix of mobile phase A and mobile phase B, which were 0.1% ammonium hydroxide in water and 1:1 v/v acetonitrile in water, respectively. The flow rate of the mobile phase was 0.2 mL/min with a 2 min gradient from 50% to 95% B. Argon was used as the collision gas and the collision energy was set at 12 V. The LC−MS/MS operations were controlled by the computer software, MassLynx 4.1, and analyte quantification was performed with multiple reaction monitoring using the following transitions: m/z 501.4 > 313.1 for FP and m/z 506.4 > 313.1 for FP-d5.

2.7. Data Analysis. For the validation process, peak integrations and data analysis were performed using the MassLynx 4.1 computer software. The relationship between peak area ratio and FP concentration (pg/mL) was calculated using the LINEST function in Microsoft Excel. Data was expressed as the mean ± standard deviation of replicate determinations, where $n \geq 3$. For the DissolvIt system, the FP transferred to the perfusate was expressed as a percent of the deposited amount on the glass slide. For statistical analysis, one-way ANOVA was applied to the data followed by Tukey post-hoc analysis, using the IBM SPSS version 22 software. Data was identified as statistically significant when $p \leq 0.05$.

2.8. Mechanistic Modeling. *2.8.1. Simulation of Plasma Concentration−Time Profiles of Fluticasone.* A mechanistic physiologically based pharmacokinetic (PBPK) model for predicting the fate of inhaled FP (as illustrated in Figure 2) was developed using Java (version 1.8.0_111, Oracle, Redwood City, US). The integration of the system of ordinary differential equations was performed via the 8(5,3) Dormand−Prince integrator[35] as realized in the Apache Commons Math library version 3.6.1 from Apache Software Foundation (Forest Hill, US). The model was adapted from that published by Boger et al.[31] Briefly, the model was based on the respiratory physiology divided into three compartments; extra-thoracic, tracheobronchial (central lung), and alveolar (peripheral lung) region (Figure 2). The particles deposited in the extra thoracic region were swallowed and transferred to gut, where they were subjected to systemic absorption, based on their bioavailable fraction (F). Particles deposited in the central and peripheral lung regions were modeled for their dissolution in epithelial lung lining fluid, using input from the *in vitro* dissolution experiments in DissolvIt system. The *in vitro* data were fitted to a Weibull function to extract the shape and time scale parameters that were then used to model the dissolution of particles in the model. FP permeation in lung tissues and mucociliary clearance of particles deposited in the central lung were modeled as described by Boger et al.[31] The central and peripheral lung areas were perfused by the bronchial blood flow (Q_central lung) and entire cardiac output (Q_cardiac output), respectively. Perfusion-rate limited distribution was assumed to apply for all tissues. System-specific input parameters for central lung, peripheral lung, blood flows, and volume of the tissue compartments are provided as Supporting Information (Tables S1 and S2).

For regional lung deposition modeling, the particle size distribution of the tested formulations was determined using next generation impactor (NGI), resulting in a discrete distribution of seven particle sizes with corresponding mass fraction deposited (f_0, ..., f_6). Multiple-Path Particle Dosimetry model MPPD V2.11 2009 from Applied Research Associates

DOI: 10.1021/acs.molpharmaceut.8b01200
Mol. Pharmaceutics XXXX, XXX, XXX−XXX

Inc. (Albuquerque, US) was used to calculate the regional deposition of particles from the tested formulations. A breathing pattern with 2 s inspiration, 1 s expiration, 10 s breath hold, and a tidal volume of 625 mL was used.[36] The Yeh-Shum 5-lobe lung model was chosen for the calculations of regional deposition fraction.[37] The drug and formulation specific parameters for FP inhaled in the model are provided as Supporting Information (Table S3).

2.8.2. Sensitivity Analysis of Dissolution Kinetics. A sensitivity analysis of the pharmacokinetic parameters to the *in vitro* dissolution kinetics of FP was performed using the mechanistic PBPK model (described in section 2.8.1). Hypothetical *in vitro* dissolution profiles of FP were created by means of numerical approximation with maximum cumulative percent dissolved fixed to mimic the cumulative percent of FP in SLF. The numerical approximations were selected in order to probe three different possible *in vitro* dissolution scenarios: a profile where release greatly exceeded that observed experimentally in SLF (case 1) and two profiles that are similar to SLF but initially more rapid (case 2) or slower (case 3). The data was fitted to a Weibull function to extract the shape (b) and time scale (a) parameters of these profiles (Table 1). The Weibull eq (eq 3) was applied to describe the hypothetical dissolution curves and used as an input to the PBPK model. It describes the accumulated fraction of the drug (m) in solution at time t. The location parameter (T_i) is the lag time before the onset of the dissolution and, in all investigated cases, was zero.

$$m = 1 - \exp\left[\frac{-(t - T_i)^b}{a}\right] \quad (3)$$

Table 1. Fitted Weibull Shape Factor (b) Together with Pharmacokinetic Data of FP Following Its Dissolution in SLF and Artificial Dissolution Profiles (Cases 1−3)[a]

parameter	SLF*	case 1**	case 2**	case 3**
Weibull shape parameter	1.5285 ± 0.08	3.0204	1.1508	1.8716
C_{max} (μg/L)	0.74 ± 0.05	4.61	1.44	0.53
T_{max} (h)	3.01 ± 0.58	0.50	0.75	6.00
$AUC_{0-\infty}$ (μg/L·h)	6.46 ± 0.08	6.92	6.87	6.04

[a]*n = 3; **n = 1.

3. RESULTS

3.1. Extraction and Quantification of Fluticasone Propionate Using LC−MS/MS. As published methods for FP analysis[21−23] proved difficult to replicate with adequate reproducibility and sensitivity, a new SPE method for sample preparation was developed for use with LC−MS/MS for the assay of FP in biorelevant media. The methodology was easy to perform, and the relationship between the mean peak area ratio of FP/FP-d5 and the concentration of FP in the samples was linear (R^2 value = 0.999) with interday and intraday precision (CV) being <20% (in according to ICH guidelines), except for 156 pg/mL. The accuracy for all FP standard concentrations was within 85−115% (Figure 3). The LOD and LOQ were 106 and 312 pg/mL, respectively. Since the FP concentrations in all dissolution experiments fell within the upper range of the assay, the method was fit for purpose.

3.2. Dissolution of FP in Dissolv*it* and IPL. The penetration of FP, manifested as perfusate concentration, was higher at all time points when the dissolution medium was PEO or Survanta with lipid content lower than that of SLF (Figure 4), in good agreement with the theoretical models. However, overall the influence of medium on FP dissolution was limited since the difference in the FP perfusate concentration values were not statistically significant (one-way ANOVA, $p > 0.05$) between dissolution in any of three lung fluids at most time points, except the difference in FP concentration for PEO and SLF at 20 min. The FP concentration−time profile in perfusate was also similar between PEO and Survanta, both reaching a C_{max} at approximately 20 min. The cumulative percent of FP transferred into the perfusate over time in the Dissolv*it* system showed similar profiles in each dissolution medium reflecting

a

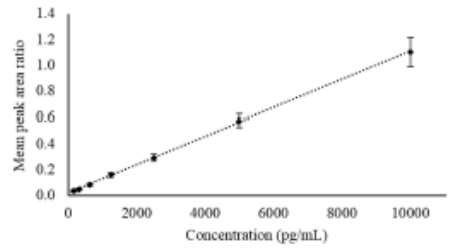

b

FP (pg/mL)							
Theoretical concentration	156	313	625	1250	2500	5000	10000
Mean measured concentration[a]	142.6 ± 66.5	288.1 ± 57.8	645.6 ± 93.3	1404.1 ± 166.9	2732.2 ± 277.3	5557.4 ± 493.7	10808.5 ± 1110.2
CV (%)	46.6	20.0	14.5	11.9	10.2	8.8	10.3
Accuracy[b] (%)	91.4	92.0	103.3	112.3	109.3	111.1	108.1

Figure 3. Validation of the solid phase extraction and LC−MS/MS assay of fluticasone propionate (FP): (a) linearity of the mean peak area ratio vs concentration; (b) FP concentration, precision, and accuracy. Data expressed as mean ± SD ($n = 9$).

DOI: 10.1021/acs.molpharmaceut.8b01200
Mol. Pharmaceutics XXXX, XXX, XXX−XXX

a

Simulant	Protein concentration (mg/mL)	Lipid concentration (mg/mL)
PEO	-	4.0
SLF	12.9	5.4
Survanta®[a]	0.01-0.16	4.0

[a]Diluted with water to obtain a lipid concentration of 4.0 mg/mL

b

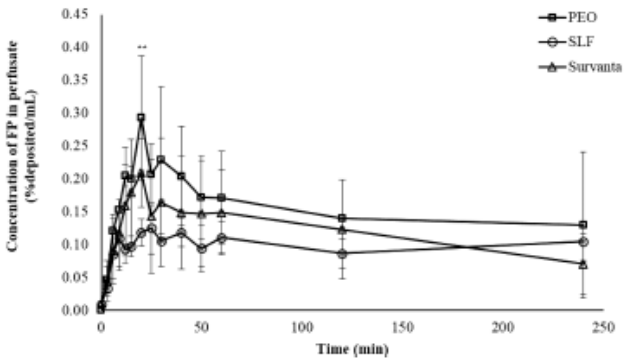

Figure 4. (a) Protein and lipid concentration in poly(ethylene oxide) in phosphate buffer solution (PEO), simulated lung lining fluid (SLF), and Survanta and (b) concentration of FP in the perfusate over time following dissolution in PEO, SLF, and Survanta normalized to mass deposited on the glass coverslips. **Difference in FP concentration in PEO and SLF is statistically significant (one-way ANOVA, $p < 0.05$). Data expressed as mean ± SD ($n = 3$).

the ranking observed in the perfusate concentrations, whereas administration to the rat IPL resulted in concentrations of FP and cumulative % of FP in the perfusate that were significantly higher at nearly all time points (Figure 5).

3.3. *In Silico* Modeling of FP Dissolution. Pharmacokinetic parameters (C_{max}, T_{max}, and $AUC_{0-\infty}$), calculated from the simulated plasma concentration time profiles for the different lung fluid simulants, predicted within two-folds the observed pharmacokinetic parameters of inhaled FP (1000 μg dose) administered via Flixotide Evohaler 250 μg strength inhaler[38] (Figure 6). No significant difference was found between the clinically observed and simulated pharmacokinetic parameters when *in vitro* dissolution input from PEO and Survanta was used in the developed PBPK model. However, differences ($p > 0.05$) in C_{max} and $AUC_{0-\infty}$ compared to the clinical data were found when the slower *in vitro* dissolution of FP in SLF was modeled. The $AUC_{0-\infty}$ predicted by the model for all three media were slightly underestimated owing to the underestimation of terminal time points of plasma concentration−time profile of inhaled FP suggesting that FP is retained for longer in the airways, which if incorporated into the model would improve the simulation.

To understand the sensitivity of the predicted PK parameters toward the dissolution profiles of FP, different hypothetical dissolution profiles were created (Figure 7). In the cases where the dissolution−time curves differed from the SLF profile only in terms of faster or slower initial rate (cases two and three), a similar shape parameter described the exponential curves ($b \approx 1$). Fitting of an immediate release type hypothetical dissolution profile (case one) resulted in a value describing a sigmoidal curve ($b \gg 1$). Calculated values of AUC for the cases were similar to the values generated for SLF, which reflect the fixing of the cumulative percentage of dissolved FP to 9.34% in 4 h. Differences were observed in terms of C_{max} and T_{max} with profiles when drug dissolution was faster/slower than *in vitro* dissolution profile of FP in SLF. Dissolution profiles mimicking the faster dissolution rates (case one and case two) predicted higher values of C_{max} (6- and 2-fold), and lower values of T_{max} (6- and 4-fold) compared to the values observed in SLF.

4. DISCUSSION

The use of different dissolution media in the DissolvIt dissolution assay was investigated. A PEO-based medium is used as the "standard" solvent for the DissolvIt system and possesses a lipid content of 4 mg/mL, which was lower than that of SLF (5.4 mg/mL; Figure 4a). Survanta is a lung surfactant extract concentrate and was diluted (1:5 with water) to normalize the lipid concentration to that of PEO. PEO has no biological relevance beyond providing a viscosity that could be regarded as analogous to that provided by respiratory mucus in the airways.[39] The slower appearance of FP in the perfusate when using SLF compared to PEO or Survanta may reflect slower dissolution or greater retention of FP as a result of the drug preferentially residing or becoming trapped within the more abundant lipid/lamellar structures in SLF, which also contains cholesterol. Cholesterol can form tight nanodomain complexes with DPPC, stabilizing DPPC in lipid structures in which FP can be solubilized and retained.[40]

Appearance of a low-soluble inhalant in perfusate or plasma is a serial process of dissolution in lung lining fluid followed by diffusion through the air-to-blood barrier. The second step is

DOI: 10.1021/acs.molpharmaceut.8b01200
Mol. Pharmaceutics XXXX, XXX, XXX−XXX

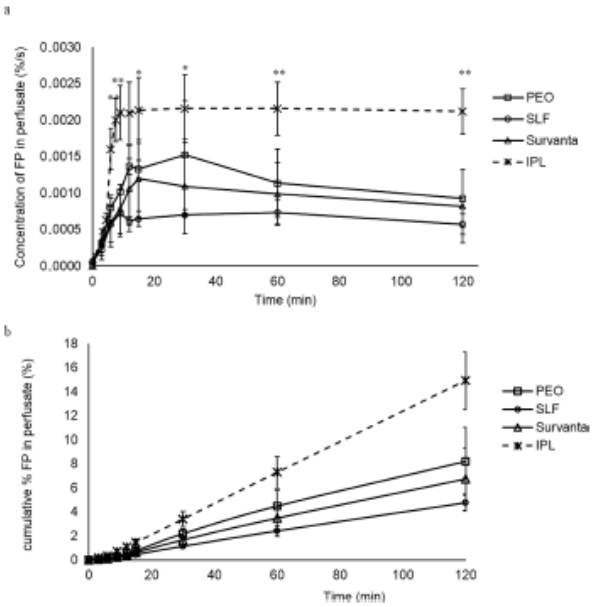

Figure 5. (a) Concentration of FP in the perfusate over time following dissolution in poly(ethylene oxide) in buffer solution (PEO), simulated lung lining fluid (SLF), Survanta, and rat isolated perfused lung (IPL). *Difference in FP concentration in IPL and SLF is statistically significant (one-way ANOVA, $p < 0.05$). **Difference in FP concentration in IPL and the remaining three lung fluids, PEO, SLF, and Survanta is statistically significant (one-way ANOVA, $p < 0.05$). (b) Cumulative % of FP transferred into the perfusate over time, following its dissolution in PEO, SLF, Survanta, and IPL. Data expressed as mean ± SD ($n = 3$).

controlled by barrier thickness and lipid content and distribution within the barrier. While the mathematics of transport in such two-phase heterogeneous barriers was established decades ago,[41,42] the concept was later investigated for lipophilic toxicants in the airway lining layer.[43] By adding a small amount of surfactant to an aqueous model of the airway lining layer, the penetration of lipophilic benzo(a)pyrene through the experimental barrier was greatly reduced.[44] Thus, a higher content of disperse lipids SLF would be expected to reduce penetration of lipophilic drugs.

Although the simulations in this study were based entirely on human parameters, including the ratio of central/peripheral aerosol deposition, the *ex vivo* rat IPL model was used as a comparator for experimentally determined dissolution−permeation profiles. The PreciseInhale system provides the advantage of a common delivery platform that can be used to deliver accurate dose and identical respirable aerosol fractions from the pMDI to the *in vitro* dissolution apparatus and *ex vivo* model. The concentration of FP and cumulative proportion of FP in the perfusate was significantly higher at nearly all time points following administration to the rat IPL compared to DissolvIt. The higher rate of absorptive clearance was attributed to the IPL possessing a comparatively rapid peripheral (alveolar) dissolution−permeation component in addition to slower central (airway) dissolution−permeation. In contrast, the DissolvIt system is hypothesized to model better the dissolution and absorptive clearance mechanisms in the central airways. In the central regions of the lungs, nonsink conditions may be expected as the dose is distributed over a smaller area compared to the alveolar region, and dissolved FP molecules are required to diffuse across the 5−20 μm pseudostratified epithelium, compared to 1−2 μm in the alveoli of the lungs, to reach the perfusate.[17] The DissolvIt system possesses an effective dissolution area of 0.95 cm^2, and the penetration distance is approximately 60 μm. Despite being an *ex vivo* nonhuman model, the IPL is an adaptable tool for teasing out the contributions of dissolution and permeation in different regions of the lungs to drug absorption and local exposure.

As FP exhibits dissolution rate-limited absorption from the lungs of humans,[31,45] modeling was carried out to understand the sensitivity of simulated plasma concentration−time profiles of inhaled FP to dissolution profiles. When faster dissolution rates compared to the values observed in SLF were modeled (Figure 7), the higher predicted higher values of C_{max} and lower values of T_{max} were obtained as a result of higher drug concentration in solution during the early stages of the dissolution process. Where the initial rate of *in vitro* dissolution was lower than that in SLF, a lower C_{max} and higher T_{max} value were predicted. This showed clearly the ability of the developed PBPK model to respond to the differences in the *in vitro* dissolution profiles and translate the differences to the respective PK parameters despite the rapid peripheral dissolution and absorption implied by the IPL studies being unaccounted. These results illustrate how dissolution profiles can have significant impact on the PK parameters of a poorly

DOI: 10.1021/acs.molpharmaceut.8b01200
Mol. Pharmaceutics XXXX, XXX, XXX−XXX

a

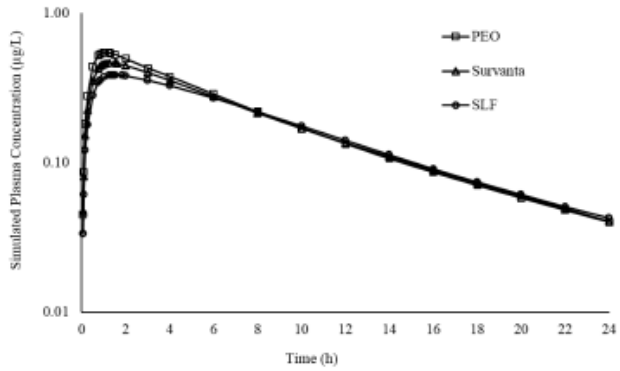

b

Pharmacokinetic parameter	In-vivo profile*	PEO**	SLF**	Survanta®**
Cmax (µg/L)	0.54	0.54 ± 0.08	0.39 ± 0.03	0.47 ± 0.10
Tmax (h)	0.80	1.11 ± 0.15	1.55 ± 0.26	1.22 ± 0.36
AUC0-∞ (µg/L.h)	6.54	4.97 ± 0.10	4.61 ± 0.09	4.74 ± 0.40

Figure 6. *In silico* modeling. (a) Simulated plasma concentration of FP over time, following its dissolution in poly(ethylene oxide) in buffer solution (PEO), simulated lung lining fluid (SLF), and Survanta. (b) Pharmacokinetic data of FP absorbed in plasma from healthy volunteers, after inhalation of FP pMDI (*in vivo*) and of FP absorbed in perfusate, following its dissolution in PEO, SLF, and Survanta. Data expressed as mean ± SD (n = 3 or 9).

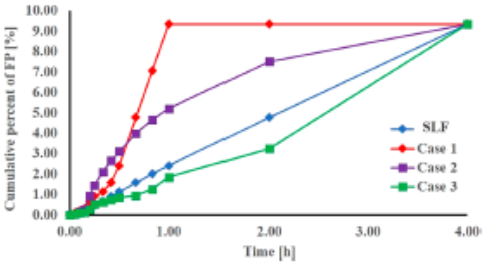

Figure 7. Sensitivity testing using numerical approximation to derive three dissolution profiles that vary from the experimental observations for dissolution of fluticasone in SLF (observed): a profile where release greatly exceeded that observed experimentally in SLF (case 1) and two profiles that are similar to dissolution SLF but initially more rapid (case 2) or slower (case 3).

soluble inhaled drug and demonstrate the application of biorelevant *in vitro* assays together with PBPK modeling.

5. CONCLUSION

We report the development of experimental methods for performing biorelevant dissolution studies for orally inhaled products illustrated by a study into the impact of the dissolution of FP, an archetypal poorly soluble inhaled drug, on plasma pharmacokinetics when the drug was delivered using Flixotide. The *in silico* model was able to translate the *in vitro* data for FP dissolution in the lungs into impacts on physiologically relevant simulated plasma concentration−time profiles. This approach can lead to enhanced understanding regarding how dissolution processes of inhaled poorly soluble drugs may influence absorptive clearance from the lungs.

■ ASSOCIATED CONTENT

Supporting Information

The Supporting Information is available free of charge on the ACS Publications website at DOI: 10.1021/acs.molpharmaceut.8b01200.

System-specific input parameters for humans; system-specific input parameters for the central lung and peripheral lung in humans; drug and formulation specific input parameters for fluticasone propionate; data obtained from FP absorption and concentration profile in the perfusate (PDF)

■ AUTHOR INFORMATION

Corresponding Author

*E-mail: ben.forbes@kcl.ac.uk. Tel: +44 (0)207 848 4823.

ORCID

Amrit Paudel: 0000-0002-3325-7828

Ben Forbes: 0000-0001-8193-6107

Present Address

[V]Certara UK, Simcyp Division, Level-2 Acero, 1 Concourse Way, Sheffield S1 2BJ, U.K.

Author Contributions

[#]Denotes equal contribution to authorship.

Author Contributions

[○]Denotes joint senior authors.

Notes

The authors declare no competing financial interest.

DOI: 10.1021/acs.molpharmaceut.8b01200
Mol. Pharmaceutics XXXX, XXX, XXX−XXX

■ ACKNOWLEDGMENTS

M.H. was supported by a BBSRC-CASE studentship (BB/K012762/1) hosted at King's College London.

■ REFERENCES

(1) US FDA CDER. Guidance for Industry: Dissolution Testing of Immediate Release Solid Oral Dosage Forms. http://www.fda.gov/downloads/drugs/guidancecomplianceregulatoryinformation/guidances/ucm070237.pdf.

(2) Cardot, J. M.; Davit, B. M. *In vitro-In Vivo Correlations*: Tricks and Traps. *AAPS J.* **2012**, *14* (3), 491−499.

(3) Grady, H.; Elder, D.; Webster, G. K.; Mao, Y.; Lin, Y.; Flanagan, T.; Mann, J.; Blanchard, A.; Cohen, M. J.; Lin, J.; Kesisoglou, F.; Hermans, A.; Abend, A.; Zhang, L.; Curran, D. Industry's View on Using Quality Control, Biorelevant, and Clinically Relevant Dissolution Tests for Pharmaceutical Development, Registration, and Commercialization. *J. Pharm. Sci.* **2018**, *107*, 34−41.

(4) Lennernas, H.; Lindahl, A.; Peer, A. V.; Olier, C.; Flanagan, T.; Lionberger, R.; Nordmark, A.; Yamashita, S.; Yu, L.; Amidon, G. L.; Fischer, V.; Sjögren, E.; Zane, P.; McAllister, M.; Abrahamsson, B. Vivo Predictive Dissolution (IPD) and Biopharmaceutical Modelling and Simulation: Future Use of Modern Approaches and Methodologies in a Regulatory Context. *Mol. Pharmaceutics* **2017**, *14* (4), 1307−1314.

(5) Arora, D.; Shah, K. A.; Halquist, M. S.; Sakagami, M. In vitro aqueous fluid-capacity-limited dissolution testing of respirable aerosol drug particles generated from inhaler products. *Pharm. Res.* **2010**, *27*, 786−795.

(6) Son, Y. J.; Horng, M.; Copley, M.; McConville, J. T. Optimization of an in vitro dissolution test method for inhalation formulations. *Dissolution Technol.* **2010**, *17*, 6.

(7) May, S.; Jensen, B.; Wolkenhauer, M.; Schneider, M.; Lehr, C. M. Dissolution techniques for in vitro testing of dry powders for inhalation. *Pharm. Res.* **2012**, *29*, 2157−2166.

(8) Rohrschneider, M.; Bhagwat, S.; Krampe, R.; Michler, V.; Breitkreutz, J.; Hochhaus, G. Evaluation of the transwell system for characterisation of dissolution behaviour of inhalation drugs: effects of membrane and surfactant. *Mol. Pharmaceutics* **2015**, *12*, 2618.

(9) Riley, T.; Christopher, D.; Arp, J.; Casazza, A.; Colombani, A.; Cooper, A.; Dey, M.; Maas, J.; Mitchell, J.; Reiners, M.; Sigari, N.; Tougas, T.; Lyapustina, S. Challenges with developing in vitro dissolution tests for orally inhaled products (OIPs). *AAPS PharmSciTech* **2012**, *13* (3), 978−989.

(10) Franek, F.; Fransson, R.; Thörn, H.; Backman, P.; Andersson, P. U.; Tehler, U. Ranking *in vitro* dissolution of inhaled micronized drug powders including a candidate drug with two different particle sizes. *Mol. Pharmaceutics* **2018**, *15*, 5319−5326.

(11) Bhagwat, S.; Schilling, U.; Chen, M. J.; Wei, X.; Delvadia, R.; Absar, M.; Saluja, B.; Hochhaus, G. Predicting Pulmonary Pharmacokinetics from In Vitro Properties of Dry Powder Inhalers. *Pharm. Res.* **2017**, *34*, 2541−2556.

(12) Hatch, G. Comparative biochemistry of airway lining fluid. *Treatise on pulmonary toxicology* **1992**, *1*, 617−632.

(13) Meyer, K. C.; Sharma, A.; Brown, R.; Weatherly, M.; Moya, F. R.; Lewandoski, J.; Zimmerman, J. J. Function and composition of pulmonary surfactant and surfactant-derived fatty acid profiles are altered in young adults with cystic fibrosis. *Chest* **2000**, *118* (1), 164−174.

(14) Marques, M. R. C.; Loebenberg, R.; Almukainzi, M. Simulated biological fluids with possible application in dissolution testing. *Dissolution Technol.* **2011**, *18*, 15−28.

(15) Davies, N. M.; Feddah, M. R. A novel method for assessing dissolution of aerosol inhaler products. *Int. J. Pharm.* **2003**, *255*, 175−187.

(16) Gerde, P.; Malmlöf, M.; Havsborn, L.; Sjöberg, C.; Ewing, P.; Eirefelt, S.; Ekelund, K. DissolvIt: An *in vitro* method for simulating the dissolution and absorption of inhaled dry powder drugs in the lungs. *Assay Drug Dev. Technol.* **2017**, *15* (2), 77.

(17) Börjel, M.; Selg, E.; Gerde, P. *In Vitro- Ex Vivo Correlation of Fluticasone Propionate Pharmacokinetic Profiles*; DDL: Edinburgh, 2015.

(18) Hastedt, J.; Bäckman, P.; Clark, A.; Doub, W.; Hickey, A.; Hochhaus, G.; Kuehl, P.; Lehr, C.; Mauser, P.; McConville, J.; Niven, R.; Sakagimi, M.; Weers, J. Scope and relevance of a pulmonary biopharmaceutical classification system AAPS/FDA/USP Workshop March 16−17th, 2015 in Baltimore, MD. *AAPS open* **2016**, *2*, 1.

(19) US FDA CDER. Guidance for Industry: Bioanalytical Method Validation. http://www.fda.gov/downloads/Drugs/Guidances/ucm070107.pdf.

(20) Lombardi, C. Solid phase extraction. *Chemistry in New Zealand* **2015**, 88−90.

(21) Krishnaswami, S.; Mollmann, H.; Derendorf, H.; Hochhaus, G. A sensitive LC-MS/MS method for the quantification of fluticasone propionate in human plasma. *J. Pharm. Biomed. Anal.* **2000**, *20*, 123−129.

(22) Matuszewski, B. K.; Constanzer, M. L.; Chavez-Eng, C. M. Strategies for the assessment of matrix effect in quantitative bioanalytical methods based on HPLC-MS/MS. *Anal. Chem.* **2003**, *75*, 3019−3030.

(23) Li, Y. N.; Tattam, B. N.; Brown, K. F.; Seale, J. P. A sensitive method for the quantification of fluticasone propionate in human plasma by high-performance liquid chromatography/atmospheric pressure chemical ionisation mass spectrometry. *J. Pharm. Biomed. Anal.* **1997**, *16* (3), 447−452.

(24) Di, L.; Goosen, T. C.; Lai, Y.; Steyn, S. J.; Varma, M. V.; Obach, S.; Feng, B. A Perspective on the Prediction of Drug Pharmacokinetics and Disposition in Drug Research and Development. *Drug Metab. Dispos.* **2013**, *41* (12), 1975−1993.

(25) Frohlich, E.; Mercuri, A.; Wu, S.; Salar-Behzadi, S. Measurements of Deposition, Lung Surface Area and Lung Fluid for Simulation of Inhaled Compounds. *Front. Pharmacol.* **2016**, *7*, 181.

(26) Gaohua, L.; Wedagedera, J.; Small, B. G.; Almond, L.; Romero, K.; Hermann, D.; Hanna, D.; Jamei, M.; Gardner, I. Development of a Multicompartment Permeability-Limited Lung PBPK Model and Its Application in Predicting Pulmonary Pharmacokinetics of Anti-tuberculosis Drugs. *CPT: Pharmacometrics Syst. Pharmacol.* **2015**, *4* (10), 605−613.

(27) Chen, A.; Yarmush, M. L.; Maguire, T. Physiologically Based Pharmacokinetic Models: Integration of In Silico Approaches with Micro Cell Culture Analogues. *Curr. Drug Metab.* **2014**, *13* (6), 863−880.

(28) Bäckman, P.; Adelman, H.; Petersson, G.; Jones, C. B. Advances in inhaled technologies: understanding the therapeutic challenge, predicting clinical performance, and designing the optimal inhaled product. *Clin. Pharmacol. Ther.* **2014**, *95* (5), 509−20.

(29) Kumar, A.; Terakosolphan, W.; Hassoun, M.; Vandera, K.; Novicky, A.; Harvey, R.; Royall, P.; Bicer, E. M.; Eriksson, J.; Edwards, K.; Hollanders, K.; Valkenborg, D.; Nelissen, I.; Hassall, D.; Mudway, I. S.; Forbes, B. A biocompatible synthetic lung fluid based on human respiratory tract lining fluid composition. *Pharm. Res.* **2017**, *34* (12), 2454−2465.

(30) Hassoun, M.; Royall, P. G.; Harvey, R. D.; Forbes, B. Design and development of a biorelevant simulated human lung fluid. *J. Drug Delivery Sci. Technol.* **2018**, *47*, 485−491.

(31) Boger, E.; Evans, N.; Chappell, M.; Lundqvist, A.; Ewing, P.; Wigenborg, A.; Friden, M. Systems Pharmacology Approach for Prediction of Pulmonary and Systemic Pharmacokinetics and Receptor Occupancy of Inhaled Drugs. *CPT: Pharmacometrics Syst. Pharmacol.* **2016**, *5* (4), 201−10.

(32) Kröll, F.; Karlsson, J. A.; Nilsson, E.; Persson, C. G.; Ryrfeldt, A. Lung mechanics of the guinea-pig isolated perfused lung. *Acta Physiol. Scand.* **1986**, *128*, 1−8.

(33) Sundström, E.; Lästbom, L.; Ryrfeldt, Å.; Dahlén, S. E. Interactions among three classes of mediators explain antigen-induced bronchoconstriction in the isolated perfused and ventilated guinea pig lung. *J. Pharmacol. Exp. Ther.* **2003**, *307*, 408−418.

DOI: 10.1021/acs.molpharmaceut.8b01200
Mol. Pharmaceutics XXXX, XXX, XXX−XXX

(34) Uhlig, S.; Wollin, L. An improved setup for the isolated perfused rat lung. *J. Pharmacol. Toxicol. Methods* **1994**, *31* (2), 85−94.
(35) Hairer, E.; Norsett, S. P.; Wanner, G. *Solving Ordinary Differential Equations I*, 2nd ed.; Springer-Verlag: Berlin, 1993.
(36) Ibrahim, M.; Verma, R.; Garcia-Contreras, L. Inhalation drug delivery devices: technology update. *Med. Devices: Evidence Res.* **2015**, *12* (8), 131−139.
(37) Yeh, H. C.; Schum, G. M. Models of Human-Lung Airways and Their Application to Inhaled Particle Deposition. *Bull. Math. Biophys.* **1980**, *42*, 461−480.
(38) Macklie, A. E.; et al. Systemic Exposure to Fluticasone Propionate Administered via Metered-Dose Inhaler Containing Chlorofluorocarbon or Hydrofluoroalkane Propellant. *Clin. Pharmacokinet.* **2000**, 39 (1), 17−22.
(39) Shah, S.; Fung, K.; Brim, S.; Rubin, B. K. An in vitro evaluation of the effectiveness of endotracheal suction cathetars. *Chest* **2005**, *128* (5), 3699−3704.
(40) Kim, K.; Choi, S. Q.; Zell, Z. A.; Squires, T. M.; Zasadzinski, J. A. Effect of cholesterol nanodomains on monolayer morphology and dynamics. *Proc. Natl. Acad. Sci. U. S. A.* **2013**, *110*, E3054−E3060.
(41) Higuchi, W. I.; Higuchi, T. Theoretical analysis of diffusional movement through heterogeneous barriers. *J. Am. Pharm. Assoc., Sci. Ed.* **1960**, *49* (9), 598−606.
(42) Ash, R.; Barrer, R. M.; Petropoulos, J. H. Diffusion in heterogeneous media: properties of the laminated slab. *Br. J. Appl. Phys.* **1963**, *14*, 854−862.
(43) Gerde, P.; Scholander, P. A mathematical model of the penetration of polycyclic aromatic hydrocarbons through the bronchial lining layer. *Environ. Res.* **1987**, *44*, 321−334.
(44) Gerde, P.; Scholander, P. An experimental study on the penetration of polycyclic aromatic hydrocarbons through a model of the bronchial lining layer. *Environ. Res.* **1989**, *48*, 287−295.
(45) Edsbacker.; et al. Airway Selectivity: An Update of Pharmacokinetic Factors Affecting Local and Systemic Disposition of Inhaled Steroids. *Basic Clin. Pharmacol. Toxicol.* **2006**, *98*, 523−536.

DOI: 10.1021/acs.molpharmaceut.8b01200
Mol. Pharmaceutics XXXX, XXX, XXX−XXX

(2) **Hassoun M**, Royall P.G, Parry M, Harvey R.D, Forbes B. Design and development of a biorelevant simulated human lung fluid. Journal of Drug Delivery Science and Technology 47: 485-491 (2018)

Journal of Drug Delivery Science and Technology 47 (2018) 485–491

Contents lists available at ScienceDirect

Journal of Drug Delivery Science and Technology

journal homepage: www.elsevier.com/locate/jddst

Design and development of a biorelevant simulated human lung fluid

Mireille Hassoun[a], Paul G. Royall[a], Mark Parry[b], Richard D. Harvey[c], Ben Forbes[a,*]

[a] King's College London, Institute of Pharmaceutical Science, London, SE1 9NH, UK
[b] Intertek-Melbourn Scientific Limited, Melbourn, SG8 6DN, UK
[c] Institute of Pharmacy, Martin-Luther-Universität Halle-Wittenberg, 06108, Halle (Saale), Germany

ARTICLE INFO

Keywords:
Respiratory
Simulated lung fluid (SLF)
Surfactant
Dissolution
Solubility
Inhalation biopharmaceutics

ABSTRACT

Biorelevant fluids are required to enable meaningful *in vitro* experimental determinations of the biopharmaceutical properties of inhaled medicines, e.g. drug solubility, particle dissolution, cellular uptake. Our aim was to develop a biorelevant simulated lung fluid (SLF) with a well-defined composition and evidence-based directions for use. The SLF contained dipalmitoylphosphotidylcholine, dipalmitoylphosphatidylglycerol, cholesterol, albumin, IgG, transferrin and antioxidants. Freshly made SLF had pH 7.2, viscosity 1.138×10^{-3} Pa s, conductivity 14.5 mS/m, surface tension 54.9 mN/m and density 0.999 g/cm^3. Colour, surface tension and conductivity were the most sensitive indicators of product deterioration. The simulant was stable for 24 h and 48 h at 37 °C and 21 °C, respectively, (in-use stability) and for 14 days when stored in a refrigerator (storage stability). To extend stability, the SLF was vacuum freeze-dried in batches to produce lyophilised powder that can be reconstituted readily when needed at the point of use. In conclusion, we have reported the composition and manufacture of a biorelevant, synthetic SLF, provided a detailed physico-chemical characterisation and recommendations for how to store and use a product that can be used to generate experimental data to provide inputs to computational models that predict drug bioavailability in the lungs.

1. Introduction

The factors that govern respiratory and systemic exposure to drugs delivered as inhaled medicines define their 'inhalation biopharmaceutics' [1]. The major factors determining the bioavailability of drugs delivered as inhaled medicines are lung dose and aerodynamic particle size distribution, which determines regional deposition [2]. Following deposition, the interactions of aerosol particles or drug with competing lung clearance mechanisms determine (i) drug bioavailability in the lungs; (ii) the rate and extent of absorption to the systemic circulation [3]. Drug solubility is a key consideration in the development of inhaled medicines, including drug design/discovery [4,5], formulation [6] and toxicokinetics [7]. The importance of solubility and dissolution in predicting the pharmacokinetics of some orally inhaled drug products has been demonstrated convincingly [8] and particle-lung fluid interactions have been suggested to impact on inhaled drug delivery [9]. For example, excipients such as glycerol in licenced inhaled medicines have been shown to influence aerosol particle dissolution [10,11] and interactions between inhaled nanomaterials and lung fluid have been investigated [12,13]. Study of all these phenomena require biorelevant fluids in which to make meaningful *in vitro* experimental measurements.

Since the first biological destination of inhaled medicinal aerosols is the respiratory tract lining fluid (RTLF) in which they deposit, it is surprising how little is published about models of RTLF in which to study interactions with particles, e.g. requirements for fluid composition or critical attributes. A variety of approaches have been adopted to simulate RTLF, including use of surfactant solutions, e.g. Tween 80 or sodium dodecyl sulphate in phosphate buffered saline [8,10], phospholipid-containing fluids [14,15] or diluted surfactant replacement products, such as Alveofact, Exosurf, Curosurf or Survanta [16,17]. Recently, a synthetic simulated lung fluid (SLF) based on human lung fluid composition has been characterised in terms of its vesicular structure and particle size, surface pressure and assessed for biocompatibility with A549 alveolar epithelial cells [18]. A similar SLF has been reported for applications in environmental toxicology [19], but here we provide a more detailed validation and characterisation of a 'base' SLF that reflects human lung fluid composition and can be incorporated into *in vitro* experimental models or adapted for specific applications in pharmaceutical science, e.g. if particular surfactant proteins, specific metabolic activities or model inflammatory disease states are of interest.

If a simulant is to prove useful, it must be readily available, convenient, economic and have well defined conditions for storage and use.

* Corresponding author. Department of Pharmacy King's College London, 150 Stamford Street, London, SE1 9NH, UK
E-mail address: ben.forbes@kcl.ac.uk (B. Forbes).

https://doi.org/10.1016/j.jddst.2018.08.006
Received 6 July 2018; Received in revised form 6 August 2018; Accepted 8 August 2018
Available online 09 August 2018

Abbreviation section

RTLF	Respiratory Tract Lining Fluid
SLF	Simulated Lung Fluid
DPPC	1,2-dipalmitoyl-*sn*-glycero-3-phosphocholine
DPPG	1,2-dipalmitoyl-*sn*-glycero-3-phospho-(1′-*rac*-glycerol) sodium salt
IgG	Immunoglobulin G
HBSS	Hank's Balanced Salt Solution
TLC	Thin Layer Chromatography
TGA	Thermogravimetric Analysis

For a complex aqueous fluid with components susceptible to chemical degradation, physical instability or microbial spoilage, freeze-drying provides an excellent means of preservation. Desiccation will protect the SLF since it minimises chemical reactions, e.g. the rate of lipid hydrolysis during storage [20], and deters microbiological growth. Accordingly, freeze-drying the SLF would allow batch manufacture in a form that has an extended use-by date and is easily handled and transported for reconstitution at its place and time of use [21,22].

This study provides a complete description of the design and manufacture of the biorelevant SLF of Kumar and co-workers [18] and reports a suite of physicochemical parameters that characterise the product and can be used as sensitive indicators of SLF stability. The stability of SLF was investigated to define appropriate conditions for its storage and use. We also investigated freeze-drying the lung fluid simulant to produce a lyophilised powder with long term stability that can be reconstituted when required at the point of use.

2. Materials and methods

The 25 mg/mL stock solutions of 1,2-dipalmitoyl-*sn*-glycero-3-phosphocholine (DPPC) and 1,2-dipalmitoyl-*sn*-glycero-3-phospho-(1′-*rac*-glycerol) sodium salt (DPPG), both > 99% purity, were obtained from Avanti Polar Lipids, Inc. (Alabama, USA). Reagent-grade purified human immunoglobulin (IgG), lyophilised human serum albumin, Bioreagent-grade transferrin, cholesterol, ascorbate, urate, certified reference material-grade glutathione and BioReagent grade gentamicin solution were supplied by Sigma-Aldrich Company Limited (Dorset, UK). Hanks' Balanced Salt Solution (HBSS), phenol red-free, was also supplied by Sigma-Aldrich and consisted of: 0.19 g/L calcium chloride dihydrate, 0.09 g/L magnesium sulphate anhydrous, 0.40 g/L

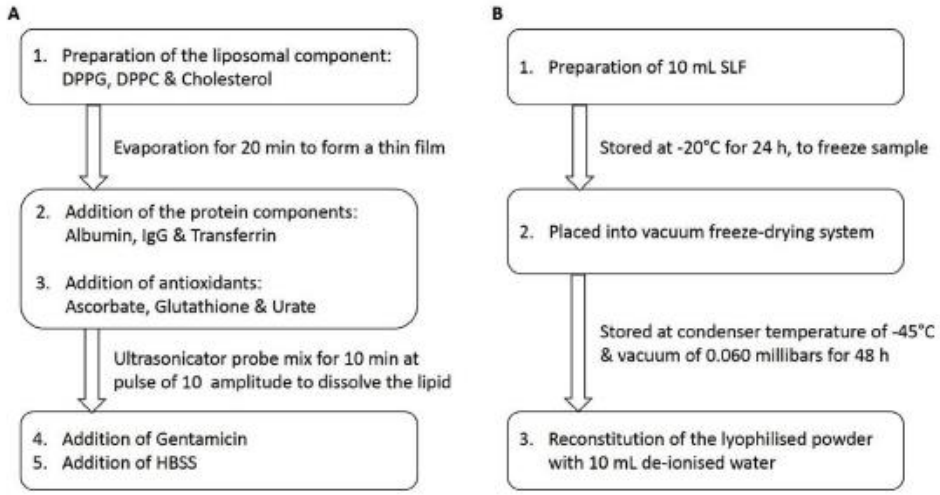

C

Ingredient	Concentration in 10mL SLF	
DPPG	0.5	mg/mL
DPPC	4.8	mg/mL
Cholesterol	0.1	mg/mL
Albumin	8.8	mg/mL
IgG	2.6	mg/mL
Transferrin	1.5	mg/mL
Ascorbate	122.14	µM
Urate	95.47	µM
Glutathione	161.61	µM
Gentamicin	10	µL
HBSS	775	µL

D

Fig. 1. A) Manufacturing steps of simulated lung fluid (SLF), B) Freeze-drying and reconstitution steps of SLF, C) Composition of SLF and D) Images of the original and the reconstituted SLF.

potassium chloride, 0.06 g/L potassium phosphate, 0.35 g/L sodium bicarbonate, 8.00 g/L sodium chloride, 0.05 g/L sodium phosphate dibasic, and 1.00 g/L D-Glucose. HPLC-grade chloroform and methanol was supplied by Fischer Chemicals (Loughborough, UK). 25% ammonium hydroxide, sodium chloride and 2 M hydrochloric acid solutions were obtained from Sigma-Aldrich Company Limited (Dorset, UK).

2.1. Preparation of SLF

SLF consisted of the key components found in healthy human RTLF, the major soluble proteins, the abundant lipids and the antioxidants that were identified in a study by Bicer [23]. The proteins were albumin, IgG and transferrin, and the lipids were DPPC, DPPG and cholesterol. The preparation method was optimised into two stages, with the manufacture of a liposomal dispersion followed by addition of the proteins (Fig. 1). To prepare the liposomal component, 1.92 mL DPPC and 0.2 mL DPPG, from 25 mg/mL stock solutions in chloroform were combined in a bijou bottle, with 5 µL of cholesterol from a 200 mg/mL stock solution in chloroform also added. The mixture was stirred gently and the chloroform evaporated under a stream of nitrogen gas for 30 min (sufficient to ensure that the lipid film was solvent free) to produce a thin film of lipids. The proteins were added to the lipid film in aliquots of aqueous stock solutions: 4 mL of albumin (88 mg/mL), 4 mL of IgG (26 mg/mL) and 1 mL of transferrin (15 mg/mL). To represent lung antioxidant levels, 88.5 µL of the following antioxidant stock solutions were added: 10 mM ascorbate, 10 mM glutathione, and 5 mM urate in the HPLC-grade water. The mixture was vortexed for 5 min. Using an ultrasonicator/probe for 10 min at a pulse of 10 amplitude, the lipids were dispersed into the solution in the form of polydisperse multilamellar liposomes. Finally, 10 µL of 50 mg/mL gentamicin was added, followed by 775 µL of HBSS under gentle agitation.

2.2. Characterisation of SLF

The SLF was characterised in this study in terms of its pH, density, viscosity, conductivity and surface tension. The pH was measured using a pH probe (pH level 2 InoLab, WTW, Germany). The density of SLF was measured using a density meter (DMA 35, Anton Paar, UK) whereby the inverted capillary cell was filled with approximately 5 mL of SLF. Distilled water was used as the reference. The viscosity was measured using the Automated Micro Viscometer (AMVn 320, Anton Paar, UK). A 1.6 mm diameter capillary, containing a 1.5 mm diameter ball was filled with 400 µL SLF, sealed with a luer cap and measurements made with the capillary tilted at 50°, 60° and 70°. The conductivity of SLF was measured using a conductivity probe and meter (Jenway A520, Cole-Parmer, UK), calibrated using 0.01 M potassium chloride solution, providing a value of 1413 ± 1 µS/cm. The surface tension of SLF was measured using a torsion balance (Model OS, TBS, UK), using distilled water as the reference sample which gave a surface tension value of 72.5 ± 0.5 mN/m. A 4 cm circumference platinum ring was immersed approximately 0.5 cm into SLF ring and the force required for withdrawal of the platinum ring from the surface of the fluid was recorded as the surface tension. All measurements were conducted in triplicate at ambient temperature.

2.3. Freeze-drying of SLF

SLF, 10 mL solution, was prepared in a SCHOTT tubular glass freeze drying vial. Samples were frozen overnight at −20 °C and then placed into a vacuum freeze-drying system (Lyotrap, LTE Scientific Ltd, UK) with condenser temperature −45 °C and a vacuum of 0.060 mbars for 48 h. Thermogravimetric analysis (Discovery TGA, TA Instruments, UK) was used to analyse the residual moisture content in the freeze-dried SLF powder, heating the sample at a heating rate of 10 °C/min to a maximum of 200 °C. The powder was reconstituted with 10 mL deionised water and compared to fresh SLF using the physico-chemical parameters described in section 2.2.

2.4. Stability of SLF

SLF stability was determined for samples stored in the fridge (at 4 °C), at room temperature (20 °C) and at human physiological temperature (37 °C). The stability was assessed by analysing pH, viscosity, conductivity and surface tension after their storage for 0, 1, 2, 3, 4, 7, 14 and 28 days using the methods described above. The appearance and colour of SLF were also analysed visually and via measurements of the mean grey value, using the Image J software (Java 1.8.0–25, version 1.51p). Using the software, the images captured were first converted to '8-bit' prior to obtaining the mean grey value. All data were recorded as the mean of three measurements ± SD.

Lipid degradation was evaluated using one-dimension thin layer chromatography (TLC). The lipid components were extracted from the SLF fluid, using an adapted version of the method detailed by Bligh and Dyer [24]. Briefly, 1 mL SLF sample was centrifuged at 13,000 rpm for 10 min to sediment out the lipids and proteins. To the pellet obtained, 1 mL of a mix consisting of chloroform: methanol [2:1] and 0.26 mL, was added and mixed to form a single phase. The sample was left to incubate with gentle agitation for 90 min at 37 °C. Acidified saline (150 mM sodium chloride adjusted to pH 2 with hydrochloric acid), 0.5 mL, was added and vortex mixed for 5 min followed by centrifugation at 2000 rpm for 15 min (Biofuge Pico, Jencons-PLS Scientific, UK). The aqueous phase was removed and 0.25 mL methanol and 0.25 mL acidified saline was added to the remaining organic phase. This was vortex mixed and centrifuged again at 2000 rpm for 15 min, then the aqueous layer was removed and the organic solvent evaporated to concentrate the lipids.

To analyse the isolated lipids by TLC, the sample was spotted approximately 1 cm from the bottom of a plain silica gel 60 TLC plate. The plate was transferred to a glass TLC tank containing 1 cm depth of the mobile phase, consisting of chloroform, methanol and 25% ammonium hydroxide solution at a ratio of 65:25:10. When the mobile phase reached three-quarters way up the plate the lipids were visualised as yellow spots using potassium permanganate stain. The retardation factor (RF) was calculated as the distance travelled by centre of the spot divided by the distance travelled by the solvent front. A calibration between spot intensity (using the mean grey value) and concentration of DPPC and DPPG was established and used to estimate the content of lipid in the SLF.

2.5. Statistical analysis

The physicochemical properties were derived from three independent batches; the data for the stability study was for 3 vials from a single batch of SLF. One-way ANOVA or paired sample T-test was applied, using the IBM SPSS version 24 software, to determine the statistical significance of results. Data was statistically significant when $p \leq 0.05$.

3. Results and discussion

3.1. Composition and characterisation of SLF

The composition of the simulated lung fluid was identical to that reported previously [18] and was designed to provide a simulant that trades off the biorelevance of featuring the full complexity of lung lining fluid with the pragmatic need for a simulant that can be manufactured economically, reproducibly and is fit for the majority of applications in inhaled medicines biopharmaceutics. Although DPPC, which contributes approximately 80% w/v of surfactant phospholipids, is often used as a sole representative phospholipid component in model lung fluids, for physiological relevance other lipid components were

incorporated including DPPG which represents approximately 10% of total phospholipids, and cholesterol which accounts for 5–10% lipids and has been shown to have a stabilising role in bilayer structures. Although lung fluid contains a mixture of saturated and unsaturated lipid, the unsaturated species were avoided as being more susceptible to oxidation. Urea corrected total protein concentration measured in human lavage samples is in the range 17.9 ± 8.6 mg/mL [23], but due to the limited commercial availability and consistency of some human protein components, e.g. SP-A, SP-B, SP-C, IgA and A1TA, the total proteins used in the preparation of SLF was 12.9 mg/mL. Biorelevant concentrations of antioxidants were included to promote the reported biocompatibility of the SLF with respiratory epithelial cells [18].

Appearance and four physicochemical properties were used to characterise SLF: colour, pH, conductivity, viscosity and surface tension (Table 1). The pH of SLF was pH 7.2, buffered by the use of HBSS as a base medium. The pH the human respiratory tract is subject to some variability, e.g. pH 6.3 (range 5.2–8.1) in the nasal cavity [25], pH 6.9–9.0 in the trachea [26] and suggested to be more acidic in inflammation and infection [26]. The essential inorganic ions of the HBSS provide a physiological salt composition, tonicity (280 mOsM) and are responsible for the high conductivity in comparison to de-ionised water matching the properties of lung lining fluid in healthy subjects [27]. The surface tension of SLF, 55 mN/m, was lower than that of water which was measured to be 72 mN/m. DPPC is the most surface-active molecule in the pulmonary surfactant mix and significantly reduces surface tension [28]. Pulmonary surfactants in the epithelial lung lining form a lipid-rich film with a significantly reduced surface tension from 70 mN/m at the upper airways to near 0 mN/m at the alveoli [29,30]. The absence of surfactant proteins in SLF (particularly surfactant protein B), which are present in epithelial lung lining fluid result in the higher surface tension value than would otherwise be anticipated for a lung fluid simulant [29,31]. Surfactant proteins also play a role in fluid viscosity, whereby surfactant protein-C (SP-C) interacts with the lipids to produce high surface viscosity [32]. Despite the absence of SP-C in SLF, the viscosity of SLF was higher than that of simple aqueous solutions, which was attributed to the presence of protein macromolecules and complex lipids in their physiological concentrations. The absence of specialist surfactant proteins (SP) limits the application of the SLF for some specialist immunological applications, e.g. where SP A and D are important in host-defence or biophysical studies where SP C and B have important roles in the complex membrane network in the lung lining fluid sub-phase.

3.2. Freeze-dried SLF

For freeze drying to be successful, a dry fluffy lyophilised powder should be produced which can easily be reconstituted to possess physiochemical properties that match the original sample [33]. Without addition of cryoprotectants, lyophilised liposomal powders are often compact, clumpy and difficult to reconstitute [20,34,35]. SLF was freeze-dried successfully without the need for additional formulation components to act as cryoprotectants; the powder produced was fluffy and easy to reconstitute with water to restore the appearance and physicochemical properties of the SLF (Table 1). The reconstituted freeze-dried formulation was identical to the freshly made solution except for a small statistically significant increase in pH (one-way ANOVA, $p \leq 0.05$), which can be readily corrected. Although water is predominantly neutral in pH, the use of different grades for reconstitution, e.g. distilled water, de-ionised water, HPLC-grade water or ultrapure water, may result in variations in pH [36].

While freeze-drying can improve the storage stability of liposomal formulations, it has been recognised that the process can also cause damage to the liposome structures which are exposed to stress conditions, e.g. excessive dryness, which can pierce the liposomes or predispose them to aggregation [20,37,38]. TGA indicated that 4.42 ± 0.15% moisture was retained in the lyophilised powder produced. In combination, the avoidance of excessive dryness, the likelihood that formulation components provide a degree of cryoprotection and the polydisperse multivesicular nature of the liposomes rendered the SLF resistant to destabilising stress factors under the freeze-drying process parameters employed, i.e. freezing rate, freezing temperature and processing time.

3.3. Stability of SLF

Preliminary studies showed that appearance and four physicochemical properties were stability-indicating; these were used to evaluate SLF over 28 days at three temperatures, 4, 20 and 37 °C (Fig. 2). The assays were congruous in detecting the conditions and time at which SLF began to degrade and in profiling temporal stability at each storage temperature. Although the use of dynamic light scattering was considered as a means to study any changes in the polydispersity and the size distribution of the structures in SLF, in previous studies [18] the extent of background scattering by the multi-molecular protein aggregates present in the fluid has complicated interpretation of results and we found it was not suitable as a stability test.

In terms of appearance, SLF was peach coloured when freshly made. This was quantified using Image J as a mean grey value on a scale where 0 corresponds to black and a value of 255 corresponds to white (Fig. 2A). SLF lightened in colour visibly, becoming whiter by day 2, with the mean grey value rising from 168.5 ± 0.4 to 174.5 ± 0.1 at 20 °C and 169.7 ± 0.3 to 175.3 ± 0.3 at 37 °C. At 4 °C, the mean grey value was unchanged at day 14 and the only increased from 168.9 ± 0.3 to 175.9 ± 0.3 at day 28. The pH and viscosity of the SLF samples stored at 20 and 37 °C also began to decrease after day 2 of storage (Fig. 2B and C). Conductivity and surface tension were affected similarly (Fig. 2D and E), at 37 °C there was a reduction of surface tension from 54.6 ± 0.5 mN/m to 53.0 ± 0.2 mN/m at day 2, which continued to decrease until 28 days (One-way ANOVA, $p \leq 0.05$).

Liposomes in aqueous dispersions tend to be relatively unstable and these results were consistent with changes that occur to lipids at elevated temperature or over periods of time, e.g. hydrolysis or lipid peroxidation [39–41]. Although antioxidants are present in SLF in small quantities, they are not fully protective and ascorbate may even catalyse the oxidation of phospholipids in solvent systems [42]. Degradation of the phospholipids can reduce pH as lipids dissociate into their constituent fatty acids [43]. Metal cations, such as the sodium ion present in DPPG and the quaternary ammonium ion in DPPC, can participate in reactions that produce a sharp decrease in viscosity [43]. Hydrolysis of phospholipids produces two main lysoforms, with the 1-acyl lysoform being predominant [44]. Higher levels of lipids reduce the surface tension of protein-containing solutions [45] and the electrical conductivity of aqueous solutions [46].

TLC analysis was used to probe lipid stability further. Potassium permanganate was used to detect phospholipids by oxidising the phosphorus groups giving a distinctive colour change from pink to yellow. At day 0, TLC of SLF revealed two spots with RF values of 0.66 ± 0.01 and 0.85 ± 0.01, which were identified as DPPC and DPPG, respectively, by comparison to reference standards (data not

Table 1
Physicochemical properties of simulated lung fluid (SLF) when freshly manufactured and when reconstituted after freeze-drying. All measurements made at 25 °C, data represent mean ± SD (n = 3).

Physicochemical property	SLF before freeze-dried	SLF after freeze-dried
Appearance [mean grey value]	168.6 ± 0.4	168.6 ± 0.1
pH	7.2 ± 0.0[a]	7.7 ± 0.1[a]
Conductivity [mS/m]	14.5 ± 0.1	14.6 ± 0.2
Viscosity [Pa.s x 10^{-3}]	1.138 ± 0.008	1.111 ± 0.015
Surface Tension [mN/m]	54.9 ± 0.3	55.6 ± 0.7

[a] Difference is significant (T-test, $p \leq 0.05$).

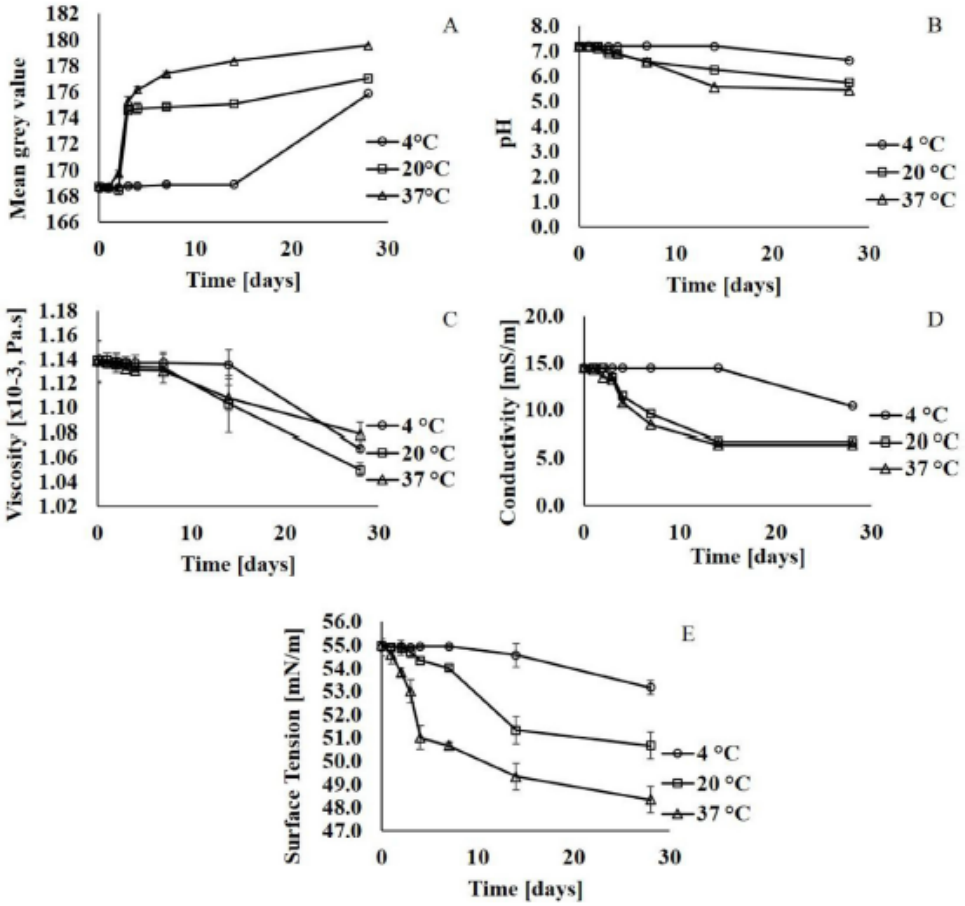

Fig. 2. Stability assessment of simulated lung fluid (SLF) after its storage at 4, 20 and 37 °C for 0, 1, 2, 3, 4, 7, 14 and 28 days: A) Colour, B) pH, C) viscosity, D) conductivity, and E) surface tension. Data expressed as mean ± SD (n = 3).

shown). From day 3 and day 2, SLF stored at 20 °C and 37 °C exhibited an additional spot with RF value of 0.48 ± 0.01, indicating presence of a lipid hydrolysis product. The lipidomic analysis which would be needed to identify the lipid species is beyond the scope of this study, but TLC was used for quantitative determination [47] using image analysis to provide a semi-quantitative measure of spot intensity for DPPC and DPPG. For SLF stored at 20 °C, DPPC concentration fell by approximately 15% and DPPG concentration fell by 25% by day 3. For SLF stored at 37 °C, both DPPC and DPPG concentrations decreased by approximately 20% by day 2. In contrast, less than 10% loss of DPPC and DPPG was measured in SLF stored at 4 °C.

3.4. Recommendations for use of SLF

SLF can be stored in a refrigerator for 2 weeks based on observations that the appearance, pH, viscosity, conductivity and surface tension remained constant for 14 days at 4 °C, and significant changes in SLF characteristic do not become evident until day 28 (One-Way ANOVA, $p < 0.05$) (Table 2). At 20 °C, changes in the SLF characteristics only became significant after 3–4 days of storage, indicating that SLF is stable for 48 h and can be used in laboratory experiments, e.g. solubility or dissolution tests, carried out at room temperature. At 37 °C, changes in SLF characteristics became significant at day 2, indicating that *in vitro* experiments which involve cell culture or the use of physiological temperature should be restricted to 24 h. Deteriorated SLF can influence *in vitro* assay results, for example FP solubility increases from 2.20 ± 0.29 μg/mL in freshly prepared SLF to 6.80 ± 0.55 μg/mL in SLF stored at 37 °C for 7 days. In contrast, FP solubility was identical in freshly prepared compared to freeze dried and reconstituted SLF.

The stability of the lyophilised powder is currently under

Table 2
The day at which the simulated lung fluid (SLF) changed with regards to its appearance and physicochemical properties (tested at days 1, 2, 3, 4, 7, 14, 28) under storage at 4, 20 and 37 °C.

Physicochemical property	Day at which there is a significant difference[a] from day 0 [day]		
	4 °C	20 °C	37 °C
Appearance [mean grey value]	28	3	2
pH	28	3	3
Conductivity [mS/m]	28	3	2
Viscosity [Pa.s x 10^{-3}]	28	4	3
Surface Tension [mN/m]	28	4	2
Stability	**14 days**	**2 days**	**1 day**

[a] Significance determined by One-way ANOVA, $p \leq 0.05$.

investigation using the assays described herein. In an ongoing stability study of the lyophilised powder stored at 4, 20 and 37 °C, the appearance, pH, viscosity, conductivity and surface tension in the reconstituted fluid are unchanged after 6 months of storage (Fig. 3) with no chemical changes to the lipids detected by TLC. Thus, improved stability of lyophilised liposomal formulations in contrast to the aqueous formulations and thus allows for a longer-term storage of material. Lyophilisation clearly increases the shelf-life of liposomes, preserving it in a dry form that can easily be reconstituted with water immediately prior to use.

4. Conclusion

A SLF of biorelevant composition was characterised and shown to possess physicochemical properties comparable to those of RTLF. The simulant was determined to be stable for 24 and 48 h at 37 and 20 °C, respectively (in-use stability) and for 14 days when stored in a refrigerator (storage stability). Colour, surface tension and conductivity were the most sensitive indicators of product deterioration. The SLF can be freeze-dried which provides a means of prolonged storage. Initial data indicates the stability of the freeze-dried preparation at room temperature for up to 3 months, with studies ongoing. This work describes a readily available, biorelevant SLF that can be used for *in vitro* investigations in the field of inhalation biopharmaceutics, e.g. the solubility of inhaled compounds, the dissolution of inhaled medicines and the interaction of aerosol drugs or particles with lung cells. Experimental *in vitro* data such as this is increasingly in demand to provide inputs to computational models that predict (i) drug bioavailability in the lungs; (ii) the rate and extent of absorption to the systemic circulation [3].

Conflict of Interest

There are no known conflicts of interest associated with this publication and there has been no significant financial support for this work that could have influenced its outcome.

Acknowledgement

Mireille Hassoun was supported by a BBSRC-CASE studentship (BB/K012762/1) hosted at King's College London, and Orchid numbers for Ben Forbes 0000-0001-8193-6107, Richard D. Harvey 0000-0003-

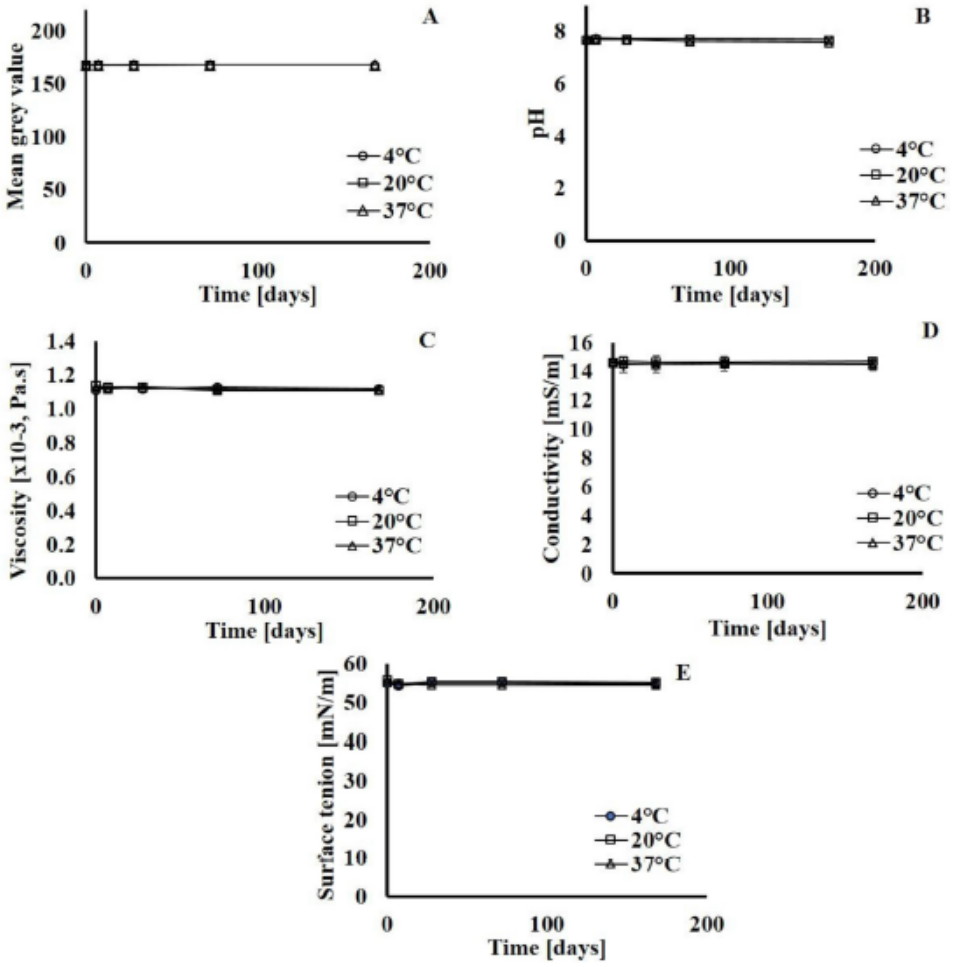

Fig. 3. Stability assessment of freeze-dried simulated lung fluid (SLF) after its storage at 4, 20 and 37 °C for 0, 7, 28, 72 and 168 days: A) Colour, B) pH, C) viscosity, D) conductivity, and E) surface tension. Data expressed as mean ± SD (n = 3).

3625-4654, and Paul Royall 0000-0002-7101-2776.

References

[1] C. Ehrhardt, Inhalation biopharmaceutics: progress towards comprehending the fate of inhaled medicines, Pharm. Res. (N. Y.) 34 (2017) 2451–2453.
[2] B. Forbes, P. Backman, D. Christopher, M. Dolovich, L. Bing, B. Morgan, In vitro testing for orally inhaled products: developments in science-based regulatory approaches, AAPS J. 17 (2015) 837–852.
[3] P. Bäckman, A. Sumit, W. Couet, B. Forbes, W. Kruijf, A. Paudel, Advances in experimental and mechanistic computational models to understand pulmonary exposure to inhaled drugs, Eur. J. Pharmaceut. Sci. 113 (2018) 41–52.
[4] C.D. Edwards, C. Lusconbe, P. Eddershaw, E.M. Hessel, Development of a novel quantitative structure-activity relationship model to accurately predict pulmonary absorption and replace routine use of the isolated perfused respiring rat lung model, Pharmaceut. Res. 33 (11) (2016) 2604–2616.
[5] J.G. Weers, Enhanced design of inhaled therapeutics: what does the future hold? Ther. Deliv. 7 (2016) 145–148.
[6] J.E. Hastedt, P. Bäckman, A.R. Clark, W. Doub, A. Hickey, G. Hochhaus, P.J. Kuehl, C. Lehr, P. Mauser, J. McConville, R. Niven, M. Sakagimi, J.G. Weers, Scope and relevance of a pulmonary biopharmaceutical classification system AAPS/FDA/USP Workshop March 16-17th, 2015 in Baltimore, MD, AAPS Open 2 (1) (2016) 1.
[7] R.M. Jones, N. Neef, Interpretation and prediction of inhaled drug particle accumulation in the lung and its associated toxicity, Xenobiotica 42 (1) (2012) 86–93.
[8] S. Bhagwat, U. Schilling, M. Chen, X. Wei, R. Delvadia, M. Absar, B. Saluja, G. Hochhaus, Predicting pulmonary pharmacokinetics from in vitro properties of dry powder inhalers, Pharmaceut. Res. 34 (12) (2017) 2541–2556.
[9] S.C. Das, P.J. Stewart, The influence of lung surfactant liquid crystalline nanostructures on respiratory drug delivery, Int. J. Pharm. 514 (2) (2016) 465–474.
[10] F. Buttini, M. Miozzi, A.G. Balducci, P.G. Royall, G. Brambilla, P. Colombo, R. Bettini, B. Forbes, Differences in physical chemistry and dissolution rate of solid particle aerosols from solution pressurised inhalers, Int. J. Pharm. 465 (1–2) (2014) 42–51.
[11] C.I. Grainger, M. Saunders, F. Buttini, R. Telford, G.P. Martin, S.A. Jones, B. Forbes, Critical characteristics for corticosteroid solution metered dose inhaler bioequivalence, Mol. Pharm. 9 (2012) 563–569.
[12] M. Beck-Broichsitter, A. Bohr, C.A. Ruge, Poloxamer-decorated polymer nanoparticles for lung surfactant compatibility, Mol. Pharm. 14 (10) (2017) 3464–3472.
[13] A. Kumar, E.M. Bicer, A.B. Morgan, P.E. Pfeffer, M. Monopoli, K.A. Dawson, J. Eriksson, K. Edwards, S. Lynham, M. Arno, A.F. Behndig, A. Blomberg, G. Somers, D. Hassall, L.A. Dailey, B. Forbes, I.S. Mudway, Enrichment of immunoregulatory proteins in the biomolecular corona of nanoparticles within human respiratory tract lining fluid, Nanomed. Nanotechnol. Biol. Med. 12 (4) (2016) 1033–1043.
[14] N.M. Davies, M.R. Feddah, A novel method for assessing dissolution of aerosol inhaler products, Int. J. Pharm. 255 (1–2) (2003) 175–187.
[15] Y.J. Son, J.T. McConville, Development of a standardized dissolution test method for inhaled pharmaceutical formulations, Int. J. Pharm. 382 (1–2) (2009) 15–22.
[16] W. Bernhard, J. Mottaghian, A. Gebert, G.A. Rau, H. Hardt, C. Poets, Commercial versus native surfactants: surface activity, molecular components, and the effect of calcium, Am. J. Respir. Crit. Care Med. 162 (4) (2000) 1524–1533.
[17] S. Pham, T. Wiedmann, Dissolution of aerosol particles of budesonide in Survanta (TM), a model lung surfactant, J. Pharmaceut. Sci. 90 (1) (2001) 98–104.
[18] A. Kumar, W. Terakosolphan, M. Hassoun, V. Kalliopi-Kelli, A. Novicky, R. Harvey, P.G. Royall, E.M. Bicer, J. Eriksson, K. Edwards, D. Valkenborg, I. Nelissen, D. Hassall, I.S. Mudway, B. Forbes, A biocompatible synthetic lung fluid based on human respiratory tract lining fluid composition, Pharmaceut. Res. 34 (12) (2017) 2454–2465.
[19] N. Boisa, N. Elom, J.R. Dean, M.E. Deary, G. Bird, Entwistle, Development and application of an inhalation bio-accessibility method (IBM) for lead in the PM10 size fraction of soil, Environ. Int. 70 (2014) 132–142.
[20] M.M. Nounou, L. El-Khordagui, N. Khalla fallah, S. Khalil, Influence of different sugar cryoprotectants on the stability and physico-chemical characteristics of freeze-dried 5-fluorouracil plurilamellar vesicles, Daru 13 (4) (2005) 133–142.
[21] S. Lee, J. Lee, Y.W. Choi, Characterisation and evaluation of freeze-dried liposomes loaded with ascorbyl palmitate enabling anti-aging therapy of the skin, Bull. Kor. Chem. Soc. 28 (1) (2007) 99–102.
[22] X. Tang, M.J. Pikal, Design of freeze-drying processes for pharmaceuticals practical advice, Pharmaceut. Res. 21 (2) (2004) 191–200.
[23] E.M. Bicer, Compositional Characterisation of Human Respiratory Tract Lining Fluids for the Design of Disease Specific Simulants, PhD Thesis King's College London, 2015, pp. 1–428.
[24] E.G. Bligh, W.J. Dyer, A rapid method of total lipid extraction and purification, Can. J. Biochem. Physiol. 37 (8) (2011) 911–917.
[25] N. Washington, R.J.C. Steele, S.J. Jackson, D. Bush, J. Mason, D.A. Gill, K. Pitt, D.A. Rawlins, Determination of baseline human nasal pH and the effect of intranasally administered buffers, Int. J. Pharm. (Amst.) 198 (2000) 139–146.
[26] D.R. Kamad, D.G. Mhaisekar, K.V. Moralwar, Respiraotry mucus pH in tracheotomised intensive care unit patients: effects of colonisation and pneumonia, Crit. Care Med. 18 (1990) 699–701.
[27] R.M. Effros, B. Peterson, R. Csaburi, J. Su, M. Dunning, J. Torday, J. Biller, R. Shaker, Epithelial lining fluid solute concencntrations in chronic obstructive lung disease patients and normal subjects, J. Appl. Physiol. 99 (4) (2005) 1286–1292.
[28] J. Perez-Gil, K.M. Keough, Interfacial properties of surfactant proteins, Biochim. Biophys. Acta Biomembr. 1408 (2–3) (1998) 203–217.
[29] M. Ikegamic, T.E. Weaver, S.N. Grant, J.A. Whitsett, Pulmoary surfactant surface tension influences alveolar capillary shape and oxygenation, Am. J. Respir. Cell Mol. Biol. 41 (4) (2009) 433–439.
[30] T.A. Siebert, S. Rugonyi, Influence of liquid-layer thickness on pulmonary surfactant spreading and collapse, Biophys. J. 95 (10) (2008) 4549–4559.
[31] R. Veldhuizen, K. Nag, S. Orgeig, F. Possmayer, The role of lipids in pulmonary surfactant, Biochim. Biophys. Acta (BBA) - Mol. Basis Dis. 1408 (2–3) (1998) 90–108.
[32] C. Alonso, A. Waring, J.A. Zasadzinski, Keeping lung surfactant where it belongs: protein regulation of two-dimensional viscosity, Biophys. J. 89 (1) (2005) 266–273.
[33] L. Rey, J.C. May, third ed., Freeze Drying/lyophilisation of Pharmaceutical and Biological products., Drugs and the Pharmaceutical Sciences vol. 206, Informa Healthcare, UK, 2010.
[34] O.H. El-Nesr, A.S. Yahiya, O.N. El-Gazayerly, Effect of formulation design and freeze-drying on properties of fluconazole multilamellar liposomes, Saudi Pharmaceut. J. 18 (4) (2010) 217–224.
[35] S. Soares, P. Fonte, A. Costa, J. Andrade, V. Seabra, D. Ferreira, S. Reis, B. Sarmento, Effect of freeze-drying, cryoprotectants and storage conditions on the stability of secondary structure of insulin-loaded solid lipid nanoparticles, Int. J. Pharm. (Amst.) 456 (2) (2013) 370–381.
[36] K. Kulthanan, P. Nuchkull, S. Varothai, The pH of water from various sources: an overview for recommendation for patients with atopic dermatitis, Asia Pac Allergy 3 (3) (2013) 155–160.
[37] P.T. Ingvarsson, M. Yang, H.M. Nielsen, J. Rantanen, C. Foged, Stabilization of liposomes during drying, Expet Opin. Drug Deliv. 8 (3) (2011) 375–388.
[38] E.C.A. Van Winden, Freeze-drying of liposomes: theory and practice, in: D. Nejat (Ed.), Methods Enzyme, Academic Press, 2003, pp. 99–110.
[39] G. Mahdy, T.A. Yang, Effect superheated stam on physical and lipid stability of reconstituted whole milk powder, International Journal of Science and Research Publications 4 (11) (2014) 1–6.
[40] W.W. Nawar, Thermal degradation of lipids, J. Agric. Food Chem. 17 (1) (1969) 18–21.
[41] A. Reis, C.M. Spickett, Chemistry of phospholipid oxidation, Biochim. Biophys. Acta Biomembr. 1818 (10) (2012) 2374–2387.
[42] H.F. Deutsch, B.E. Kline, P. Rusch, The oxidation of phospholipids in the presence of ascorbic acid and carcinogenic chemicals, J. Biol. Chem. 141 (1941) 529–538.
[43] M.B. Abramson, G. Colacicco, R. Curci, M.M. Rapport, Ionic properties of acidic lipids, Phosphatidylinositol. Biochemistry 7 (5) (1968) 1692–1698.
[44] D. Jeschek, G. Lhota, J. Wallner, K. Vorauer-Uhl, A versatile, quantitative analytical method for pharmaceutical relevant lipids in drug delivery systems, J. Pharmaceut. Biomed. Anal. 119 (2016) 37–44.
[45] Y.Y. Xu, T. Howes, B. Adhikari, B. Bhandari, Effects of emulsification of fat on the surface tension of protein solutions and surface properties of the resultant spray-dried particles, Dry. Technol. 31 (16) (2013) 1939–1950.
[46] D.J. McClements, Food Emulsions: Principles, Practice and Techniques, second ed., CRC Press, Boca Raton, FL, 2005.
[47] H.F. Askal, A.S. Khedr, I.A. Darwich, R.M. Mahmoud, Quantitative thin-layer chromatographic method for determination of amantadine hydrochloride, Int. J. Biomed. Sci. 4 (2) (2008) 155–160.

(3) Kumar A, Terakosolphan W, **Hassoun M**, Vandera K, Novicky A, Harvey R, Royall P.G, Bicer, E.M, Eriksson J, Edwards K. Valkenborg D, Nelissen I, Hassall D, Mudway I.S, Forbes B. A biocompatible synthetic lung fluid based on human respiratory tract lining fluid composition: 2454-2465 (2017)

Pharm Res
DOI 10.1007/s11095-017-2169-4

RESEARCH PAPER

A Biocompatible Synthetic Lung Fluid Based on Human Respiratory Tract Lining Fluid Composition

Abhinav Kumar[1] · Wachirun Terakosolphan[1] · Mireille Hassoun[1] · Kalliopi-Kelli Vandera[1] · Astrid Novicky[1] · Richard Harvey[1,2] · Paul G. Royall[1] · Elif Melis Bicer[3] · Jonny Eriksson[4] · Katarina Edwards[4] · Dirk Valkenborg[5,6,7] · Inge Nelissen[5] · Dave Hassall[8] · Ian S. Mudway[3] · Ben Forbes[1]

Received: 7 February 2017 / Accepted: 27 April 2017

ABSTRACT

Purpose To characterise a biorelevant simulated lung fluid (SLF) based on the composition of human respiratory tract lining fluid. SLF was compared to other media which have been utilized as lung fluid simulants in terms of fluid structure, biocompatibility and performance in inhalation biopharmaceutical assays.

Methods The structure of SLF was investigated using cryo-transmission electron microscopy, photon correlation spectroscopy and Langmuir isotherms. Biocompatibility with A549 alveolar epithelial cells was determined by MTT assay, morphometric observations and transcriptomic analysis. Biopharmaceutical applicability was evaluated by measuring the solubility and dissolution of beclomethasone dipropionate (BDP) and fluticasone propionate (FP), in SLF.

Results SLF exhibited a colloidal structure, possessing vesicles similar in nature to those found in lung fluid extracts. No adverse effect on A549 cells was apparent after exposure to the SLF for 24 h, although some metabolic changes were identified consistent with the change of culture medium to a more lung-like composition. The solubility and dissolution of BDP and FP in SLF were enhanced compared to Gamble's solution.

Conclusion The SLF reported herein constitutes a biorelevant synthetic simulant which is suitable to study biopharmaceutical properties of inhalation medicines such as those being proposed for an inhaled biopharmaceutics classification system.

KEY WORDS aerosol · beclomethasone dipropionate · biopharmaceutics · dissolution · fluticasone propionate · inhalation · solubility

Abhinav Kumar and Wachirun Terakosolphan contributed equally to this work.

✉ Ben Forbes
ben.forbes@kcl.ac.uk

[1] Institute of Pharmaceutical Science, Faculty of Life Sciences and Medicine King's College London, London SE1 9NH, UK

[2] Institute of Pharmacy, Martin-Luther-Universität Halle-Wittenberg, 06108 Halle (Saale), Germany

[3] MRC-PHE Centre for Environment and Health and NIHR-HPRU in Health Impact of Environmental Hazards, Environmental and Analytical Research Division, Faculty of Life Sciences and Medicine King's College London, London SE1 9NH, UK

[4] Department of Chemistry – BMC, Uppsala University, Uppsala, Sweden

[5] Health Unit, VITO NV, 2400 Mol, Belgium

[6] Interuniversity Institute for Biostatistics and statistical Bioinformatics Hasselt University, 3500 Hasselt, Belgium

[7] Centre for Proteomics, University of Antwerp, 2000 Antwerp, Belgium

[8] GSK Medicines Research Centre, Gunnels Wood Road, Stevenage Hertfordshire SG1 2NY, UK

ABBREVIATIONS

BDP	Beclomethasone dipropionate
CCM	Cell culture medium
DPPC	1,2-dipalmitoyl-sn-glycero-3-phosphocholine
DPPG	1,2-dipalmitoyl-sn-glycerol-3-phosphot-rac(1-glycerol)
FDR	False discovery rate
FP	Fluticasone propionate
GO	Gene ontology
HBBS	Hank's balanced salt solution
KEGG	Kyoto Encyclopedia of Genes and Genomes
MTT	3-(4,5-dimethylthiazol-2-yl)-2,5-diphenyltetrazolium bromide
pAcc	The total perturbation accumulation
pORA	The over-representation
pMDI	Pressurised metered dose inhaler
RTLF	Respiratory tract lining fluid
SDS	Sodium dodecyl sulfate
SLF	Simulant lung lining fluid
TEM	Transmission electron microscopy

Published online: 30 May 2017

INTRODUCTION

Drug solubility in lung fluid is an important determinant of the fate of inhaled aerosol medicines. Persistence in the form of a solid particle slows drug availability for target engagement, systemic absorption or metabolism [1–4]. Particles that dissolve slowly provide a sustained release mechanism, but are also susceptible to mucociliary clearance [5] and uptake by macrophages [6], or may lead to drug accumulation [7] or toxicity [8]. These factors, together with recent interest in developing a biopharmaceutical classification system for inhaled medicines [9], have focused attention on drug solubility in the lungs and the need to measure solubility in a medium that is representative of human respiratory tract lining fluid (RTLF). In contrast to intestinal fluid in which drug solubility and dissolution has been investigated extensively [10], the development of lung fluid simulants is in its infancy. Human intestinal fluids have been characterised thoroughly in terms of their composition and structure [11–13]. Simulants have been designed to represent fed and fasted conditions [13,14], studied for their biocompatibility [15] and made available as commercial products [16].

When drug solubility or dissolution in the lungs has been studied, the fluid used to represent RTLF has been water or physiological salt solutions [17] (archetypically Gamble's solution), often supplemented with phospholipids [18–20] or a surfactant such as sodium dodecyl sulphate (SDS) [21,22]. Alternatively, products based on lung surfactant extracts such as Survanta® or Curosurf® have been used [23]. The tendency to refer to all these fluids as 'simulated lung fluid' reflects a confusion regarding how best to simulate RTLF *in vitro*. Emerging data regarding the composition of healthy human lung lining fluid in different regions of the lungs [24] provides an opportunity to design a synthetic lung fluid that incorporates the major or critical components of the fluid that lines the human lungs. For maximum utility, such a simulant should be biocompatible with respiratory cells so that it can be used in models to study lung-particle interactions *in vitro*.

The aim of this study was to characterize a synthetic simulated lung fluid (SLF) that has been developed based on the composition of human RTLF [25]. SLF was manufactured and compared to other fluids which have been used as simulants for RTLF in terms of structure and biocompatibility with A549 alveolar epithelial cells and inhaled drug solubility and dissolution.

MATERIAL AND METHODS

Materials

The 25 mg/mL stock solutions of 1,2-dipalmitoyl-sn-glycero-3-phosphocholine (DPPC) and 1,2-dipalmitoyl-sn-glycerol-3-phosphot-rac(1-glycerol) ammonium salt (DPPG) were obtained from Avanti Polar Lipids, Inc. (Alabama, USA). Reagent-grade purified human immunoglobulin (IgG), lyophilized human albumin, Bioreagent-grade transferrin, Sigma-grade cholesterol, ascorbate, urate, certified reference material-grade glutathione and Hank's Balanced Salt Solution (HBSS) were supplied by Sigma-Aldrich Company Limited (Dorset, UK). HPLC-grade chloroform and water were supplied by Fischer Chemicals (Loughborough, UK). 6α,9-Difluoro-17-[[(fluoromethyl)sulfanyl]carbonyl]-11β-hydroxy-16α-methyl-3-oxo androsta-1,4-dien-17α-yl propanoate (fluticasone propionate: FP) was purchased from Adooq Bioscience (Irwin, CA), 9-Chloro-11β-hydroxy-16β-methyl-3,20-dioxopregna-1,4-diene-17,21-diyl dipropanoate (beclomethasone dipropionate; BDP) was purchased from Medchem Express (US), and Survanta® from AbbVie Ltd. (UK).

Preparation of Simulated Lung Fluid (SLF)

The SLF was formulated to contain the most abundant components of healthy human alveolar RTLF in the concentrations that they manifest *in vivo* as determined recently by Bicer [24] and was prepared as described previously [25] (Table I). Briefly, to prepare the liposomal content, 1.92 mL DPPC and 0.2 mL DPPG, from 25 mg/mL stock solutions in chloroform were combined and 5 µL of cholesterol from a 200 mg/mL stock solution in chloroform was added. The mixture was stirred gently in a round bottom flask and the chloroform evaporated under streamed nitrogen gas, to produce a thin layer of lipids at the base of the flask. The proteins were added into the lipid flask in aliquots of aqueous stock solutions: 4 mL of albumin (88 mg/mL), 4 mL of IgG (26 mg/mL) and 1 mL of transferrin (15 mg/mL). In order to represent lung antioxidant levels 88.5 µL of the following antioxidant stock solutions were added: 10 mM ascorbate, 10 mM glutathione, and 5 mM urate in the HPLC-grade water. The mixture was vortexed

Table I The Composition of Survanta and Simulated Lung Fluid (SLF)

Survanta®	SLF
- Phospholipids 25 mg/mL (including 11.0–15.5 mg/mL disaturated phosphatidylcholine) - Triglycerides 0.5–1.75 mg/mL - Free fatty acids 1.4–3.5 mg/mL - Protein less than 1.0 mg/mL	- DPPC 4.8 mg/mL - DPPG 0.5 mg/mL - Cholesterol 0.1 mg/mL - Albumin 8.8 mg/mL - IgG 2.6 mg/mL - Transferrin 1.5 mg/mL - Ascorbate 140 µM - Urate 95 µM - Glutathione 170 µM

for 5 min, then gently mixed using a vibrating probe for 10 min at an amplitude of 10 to dissolve the lipids into the solution. Finally, 10 µL of gentamicin was added, followed by 775 µL of HBSS under gentle mixing.

Characterisation of the SLF

Cryo-transmission electron microscopy (cryo-TEM) of SLF and Survanta was performed using a Zeiss Libra 120 Transmission Electron Microscope (Carl Zeiss NTS, Oberkochen, Germany). The microscope operated at 80 kV in zero loss bright-field mode under cryo conditions. Digital images were recorded under low dose conditions, with a slow-scan CCD camera (TRS GmbH, Moorenweis, Germany) and iTEM software (Olympus Soft Imaging System GmbH, Münster, Germany). An under focus of 1–2 µm was used to enhance the image contrast. Thinly spread samples were prepared in a 100% humidity chamber to avoid dehydration, then quickly vitrified in liquid ethane held at a temperature just above its freezing point (−182°C). After vitrification, the samples were transferred to the microscope using a Gatan CT3500 cryo-transfer (Gatan, Oxon, UK), to maintain samples below −165°C.

Photon correlation spectroscopy (Nanosizer, Malvern Instruments, UK) at a scattered angle of 173° was used to measure the hydrodynamic diameter of structures in SLF and Survanta. Suspensions (1 mL) of both fluids were analysed using instrument parameters: refractive index 1.330, temperature 25°C, dynamic viscosity 0.8882×10^{-3} Pa s. Zetasizer Software 6.20 was used to analyze the data.

A Langmuir trough (Model 602A; Nima Technologies Ltd., Coventry, UK) was used to make surface pressure-area measurements at 23°C using a PS4 surface pressure microbalance (0–240 mN/m range, 0.1 mN/m resolution) fitted with a Wilhelmy plate (1 cm width Whatman Grade 1 chromatographic paper, GE Healthcare life sciences, Little Chalfont, UK) and controlled by Nima IU4 computer interface unit software. Suspensions of freeze dried SLF and Survanta, 1 mg/mL, were prepared in chloroform, vortexed for 10 min, then bath sonicated at 37 kHz, 25°C, for 10 min. For each isotherm, the test fluid was deposited dropwise onto a 0.9% *w/v* NaCl subphase surface using a Hamilton syringe and spreads rapidly to cover the available area of the trough until the surface pressure reached 20 mN/m, with the barriers open at their maximum. The solvent was allowed to evaporate for 10 min before the barriers were compressed at 35 cm^2/min. The mean molecular weights of the surface-active components of SLF (38,760.9 g/mol) and Survanta (843.5 g/mol) were calculated from their defined compositions and together with the known masses of the deposited monolayers, were used to determine the mean molecular area for each sample. The isotonic saline subphase was used to simulate the influence of normal lung fluid counter-ions on the behavior of the monolayer components [26].

Individual compressions were used to determine the collapse pressure, which was 50 and 60 mN/m for SLF and Survanta, respectively. Subsequently, each film was compressed to a surface pressure 5 mN/m below their collapse pressures and then expanded to reach the initial surface pressure, 20 mN/m. Triplicate experiments of ten isotherm cycles were performed for each simulant without an equilibration period between the expansion and re-compression. Each individual compression-expansion cycle took 10–25 min to complete. The degree of hysteresis was determined from differences between the compression and expansion isotherms for each cycle. The surface compressional modulus (K) [27], was calculated using eq. 1:

$$K = \frac{1}{C} = -A \times \left(\frac{d\Pi}{dA}\right)_T \quad (1)$$

where C is compressibility, A is the mean area per molecule and $\left(\frac{d\Pi}{dA}\right)_T$ is the slope of the isotherm at a defined surface pressure. Compressibility is characterized by high surface elasticity and low interfacial stiffness [28]. K ranges between 12.5 and 50 mN/m for the liquid expanded phase, 50–100 mN/m liquid intermediate phase and 100–250 mN/m for the liquid condensed phase [29], whilst the condensed state has K values >250 mN/m.

Biocompatibility with the Human A549 Cell Line

Human alveolar epithelial A549 cells (passage 38–46) were cultured in a humidified atmosphere at 37°C, 5% CO_2 using a cell culture medium (CCM) composed of RPMI-1640 medium supplemented with 10% *v/v* fetal bovine serum (FBS), 1% *v/v* L-glutamine and 0.1% *v/v* gentamicin. For the 3-(4,5-dimethylthiazol-2-yl)-2,5-diphenyltetrazolium bromide (MTT) assay A549 cells were seeded in 96-well plates at 30,000 cells/cm^2 using reduced serum (2% FBS) CCM for 48 h before exposure to SLF or Survanta for 24 h. After 24 h, cells were washed with PBS and 200 µL of fresh CCM containing 50 µL of MTT solution (2.5 mg/mL in PBS) was added to each well and the plate was incubated for 4 h in a humidified incubator, after which the solution was discarded. The cells were lysed and formazan crystals formed were solubilised with 100 µL of a solution of 10% SDS in dimethylformamide:water (1:1). Cells were incubated with lysis solution overnight at 37°C before the absorbance of solubilised formazan was measured at

570 nm using a SpectraMax microplate reader (Molecular Devices, UK). SLF was non-toxic to A549 cells and was evaluated further using TEM and transcriptomics.

For TEM, A549 cells on glass coverslips were fixed using 2.5% (*v*/v) glutaraldehyde in 0.1 M phosphate buffer for 2 h at 4°C. Following fixation the cells were rinsed with 0.1 M phosphate buffer and treated with 1% (*w*/*v*) osmium tetroxide in 0.1 M phosphate buffer (pH 7.3) for 20 min at 4°C. The coverslips were washed for 10 min in phosphate buffer and dehydrated in a graded ethanol dilution series 0 to 100%. Finally, the cells were infiltrated with TAAB epoxy resin for 4 h at room temperature. To section in the plane of the monolayers, the coverslips were embedded in resin and polymerized for 24 h at 70°C. Ultrathin sections (70–90 nm) were prepared using a Reichert-Jung Ultracut E ultramicrotome, mounted on 150 mesh copper grids, contrasted using uranyl acetate and lead citrate, and examined on an FEI Tecnai 12 transmission microscope operated at 120 kV. Images were acquired with an AMT 16000 M digital camera. Images ($n \geq 6$ for each sample) were acquired and analysed using ImageJ 1.47 software. Effects on cell health was assessed based on morphometry; cellular, nuclear and mitochondrial area.

For transcriptomic analysis, RNA was isolated from the A549 cells in 6-well plates (30,000 cells/cm^2 in 2 mL CCM) after 24 h exposure to with SLF or CCM (control). The cells were washed 3 times with PBS, then lysed with RLT buffer (Qiagen). Total RNA was isolated using an RNeasy mini kit (Qiagen) following the manufactures guidelines. The RNA concentration was determined using a NanoDrop spectrophotometer (NanoDrop Technologies, ThermoFisher, USA). RNA integrity was analysed using the Agilent 2100 Bioanalyzer (Agilent Technologies). Only samples demonstrating high RNA Integrity Number value (>9) were qualified for microarray analysis.

RNA was amplified and labeled using the one-colour LowInput QuickAmp Labeling Kit (Agilent Technologies). Briefly, 200 ng of total RNA was reverse transcribed into complementary DNA (cDNA) using a T7-promoter primer and MMLV reverse transcriptase. The cDNA was transcribed into complementary RNA (cRNA), during which it was fluorescently labeled by incorporation of cyanine(Cy)3-CTP. After purification using the RNeasy mini kit (Qiagen), cRNA yield and specific activity were determined using a NanoDrop spectrophotometer. Only labeled cRNAs showing a specific activity above 8 pmol dye/µg RNA were analysed. Labeled cRNA, 1.65 µg, was competitively hybridized onto Whole Human Genome 4 x 44 K oligonucleotide arrays (G4112F, Agilent Technologies) for 17 h in a Tecan HS 4800 Pro Hybridization Station (Tecan Benelux BVBA, Belgium). The arrays were scanned on an Agilent G2565BA microarray scanner and further processed using Agilent Feature Extraction Software (version 10.7.3.1). Data processing steps used to generate the Agilent one-color output was performed as indicated in the Agilent protocol GE1–107-Sep09. For each feature (spot) on the array, gProcessedSignal (normalized values for Cy3 fluorescence), feature quality and gene information were analysed. Normalization included linear scaling and Quantile normalization; data were filtered with regard to reliability including signal strength (only features with signal values 3x the background standard deviation were considered valid features).

Solubility and Dissolution of Poorly Soluble Inhaled Drugs

The solubility of fluticasone propionate (FP) and beclomethasone dipropionate (BDP) was measured in Gamble's solution, SLF, Survanta and 0.5% sodium dodecyl sulphate (SDS) by mixing excess drug powder (approximately 0.5 mg) with 0.5 mL of the solvent in a microcentrifuge tube. The sealed tubes were vortex mixed for 5 min before sonication at 37°C for 30 min before transfer to a shaking water-bath at 37°C. After 48 h, the drug suspensions were centrifuged at 13000 rpm for 10 min, then the supernatant (0.2 mL) was centrifuged for a second time before 0.1 mL of supernatant was diluted 10 times with methanol. This sample was analysed for drug concentration by HPLC.

For dissolution experiments Flixotide® 50 µg pMDI or QVAR® 50 µg pMDI were actuated 10 times to deliver aerosol to the surface of 0.45 µm pore polyester membrane Transwell inserts (membrane pre-wetted with dissolution medium) using a twin stage impinge as described previously [30]. The inserts were transferred to wells in 24-well base-plates containing 600 µL dissolution medium (Gambles solution, SLF, or water with 0.5% SDS). At intervals, the insert was moved to a new well containing fresh dissolution medium. The drug transferred to each receiver chamber was measured at the end of the experiment using HPLC as described previously [30]. The test was performed at room temperature, with each result measured in triplicate.

RESULTS AND DISCUSSION

Characterisation of SLF

Uni-, bi-, and oligolamellar liposomes were visualised in the SLF and Survanta using CryoTEM (Fig. 1a and b).

The vesicles in SLF and Survanta samples had similar appearance despite their different origins and processing; SLF has a defined compositions and is fabricated from defined individual components, whereas Survanta is an enriched surfactant extract from bovine lungs. Both fluids showed irregular electron-dense structures, which may be protein aggregates. Dynamic light scattering also detected structures in the fluids; SLF showed a strong signal for structures with a size of 57 nm corresponding to the size of liposomes and a weaker signal for 946 nm. Further interpretation was not possible due to background scattering by multi-molecular protein agglomerates, which is a recognized limitation of dynamic light scattering size analysis in media with high protein content [31].

Langmuir isotherms (pressure-area relationships) were explored to determine whether the apparent similarities in structures observed in the lung fluids extended to the physicochemical behavior of monolayers formed on water. The mean molecular area of SLF was greater than that of Survanta (668–800 $Å^2$ and 48–26 $Å^2$, respectively, over the 10 cycles), possibly due to the albumin (which was present in SLF, but not Survanta) affecting DPPC packing. SLF formed a stable monolayer after the first compression-expansion cycle (Fig. 1b). During compression it underwent transitions from a liquid expanded to intermediate phase, followed by a liquid condensed phase. A large hysteresis loop and shift towards lower molecular area was observed between the first and second compression cycle. The isotherms of the

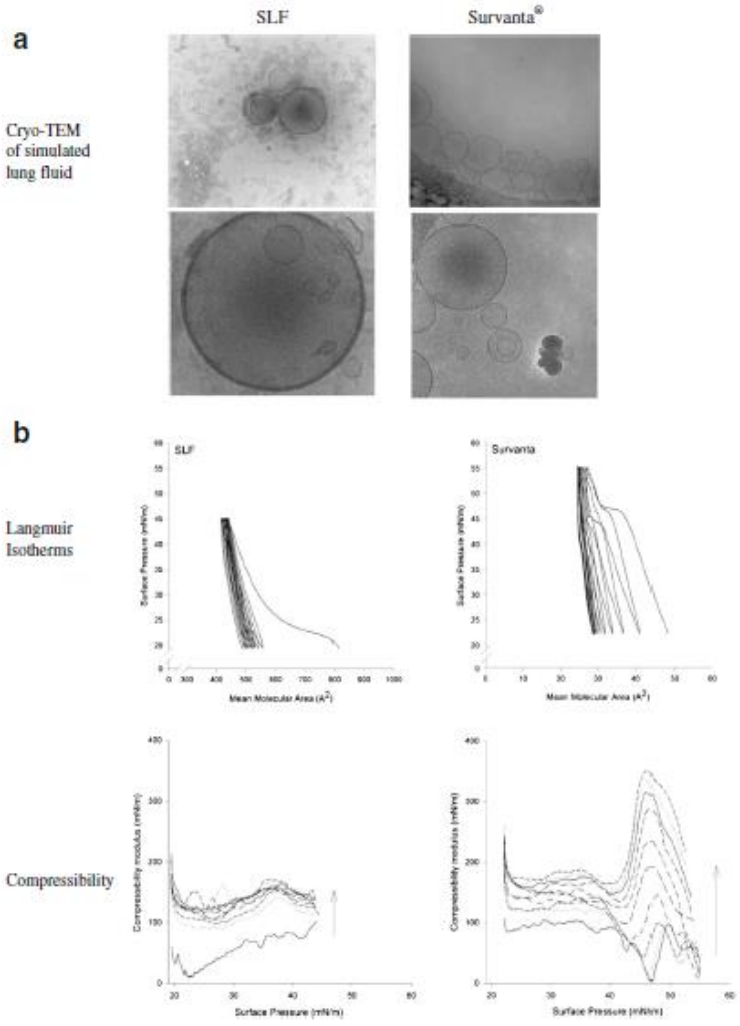

Fig. 1 (**a**) CryoTEM. Microstructures in synthetic lung fluid (SLF) and Survanta®. Microstructures imaged in the suspension of SLF and Survanta showing the presence of bilamellar and oligolamellar liposomal vesicles. (**b**) Isotherms. Isotherm cycles and changes in compressibility modulus over 10 consecutive compressions for SLF and Survanta films measured by Langmuir-Blodgett trough.

remaining cycles were identical indicating the formation of a stable monolayer.

Three phase transitions were observed in the Survanta isotherm during the first few cycles which disappeared during the later cycles (Fig. 1b). At the initial surface pressure (20 mN/m) Survanta formed an intermediate phase (K < 100 mN/m), in which liquid expanded and liquid condensed phases are assumed to coexist. Upon compression a plateau phase appeared at around 47 mN/m, which occurred at progressively lower surface pressures over the course of subsequent cycles, followed by an intermediate phase when further compression was applied. Over the course of 10 cycles, hysteresis occurred and the isotherm cycles underwent an inward shift. The systematic shift of hysteresis loops implied that there was an irreversible loss of material from the surface due to the irreversible desorption into the subphase over the course of a compression cycle. The reduced hysteresis after the 7th cycle indicates the formation of a stable monolayer at this point from which no further loss of material occurred.

The reduction of Survanta compressibility observed over the sequence of compression cycles has been reported previously and attributed to the extrusion of hydrophobic proteins and associated lipids into the subphase [32]. The hydrophobic SP-B and SP-C proteins present in Survanta are thought to facilitate this extrusion, which is normally reversed upon expansion [33]. However, the speed at which the compression/expansion cycles were repeated may have led to the increasing hysteresis observed in the Survanta isotherms because re-compression began before the monolayer had completed re-spreading. Compared to Survanta, SLF underwent the composition-refining process during the first isotherm cycle when excess material was removed from the interface during the first cycle, indicating a simpler stable colloidal system. These data characterize the structural and mechanical properties of RTLF simulants which may affect drug solubility and dissolution. *In vivo*, a monolayer depleted in hydrophobic proteins during breathing-cycle related compression will show different wetting characteristics for drug particles settling on its surface compared to the expanded system. Thus the first stages of the particle dissolution process will be affected by compression-dependent monolayer composition, whereas changes in the micellar sub phase will influence bulk solubility. *In vitro*, the lower stability of the Survanta monolayer indicates a high propensity to form micellar aggregates which are likely to sequester poorly soluble drugs. In contrast, the stability of colloidal structures in SLF make them less likely to sequester drugs in micelles, however its high albumin content will provide a reservoir for poorly-soluble compounds.

Biocompatibility of SLF

Survanta had a catastrophic effect on A549 cells in the MTT assay, reducing viability by >90% after 24 h exposure. In contrast, SLF and Gamble's solution indicated mitochondrial activity comparable to that observed in HBSS with cellular metabolism remaining within 20% of that in reduced-serum CCM control (data not shown). The adverse effects of Survanta were mitigated fully by dilution to 21% Survanta in HBSS (i.e. Survanta diluted to match the phospholipid content of SLF/human RLTF). The apparent biocompatibility of SLF with A549 cells indicated by MTT assay was followed up by exploring any morphometric or transcriptional changes induced by exposure of A549 cells to SLF.

TEM analysis following incubation of SLF with A549 cells revealed no effect compared to control on cellular, nuclear and mitochondrial areas (Fig. 2). Nor were other morphological signs of cell distress observed, e.g. nuclear condensation, crescent shaped condensed chromatin abnormal lamellar bodies or epithelial projections (Fig. 2a). Interestingly, cytoplasmic and membrane-bound vacuole inclusions (vacuoles at the apical surface of the plasma membrane) were observed, which it is tempting to attribute to uptake of DPPC liposomes following exposure to with SLF (Fig. 2b).

Using microarray analysis, 116 differentially expressed genes ($p < 0.05$; 2 log-fold change in expression) were identified out of 10,705 genes with measured expression. The data was analysed using iPathwayGuide (Advaita Corporation, 2015) within the context of pathways in the Kyoto Encyclopedia of Genes and Genomes (KEGG) database and gene ontologies (GO) from the Gene Ontology Consortium database. After correction for the false discovery rate, 5 KEGG pathways were found to be affected significantly (Table II). After elim pruning to favour more significant terms, 5 GO terms with a threshold above 10 genes per term were impacted significantly (Table III). The perturbation (pAcc) provides a perturbation factor for each gene and the over-representation (pORA) describes the probability of changes to the number of genes affected in a certain pathway (Fig. 3).

Pathway analysis showed that steroid biosynthesis, including biosynthesis of cholesterol, steroid hormones and vitamin D, was significantly induced. This was corroborated by the GO analysis which confirmed induction of the cholesterol, sterol and steroid biosynthetic pathways ($p < 0.05$). This may be the consequence of exogenous cholesterol in SLF. An increase in oxidation-reduction processes may also be related to the increase in cholesterol synthesis, which involves many redox enzymes. As

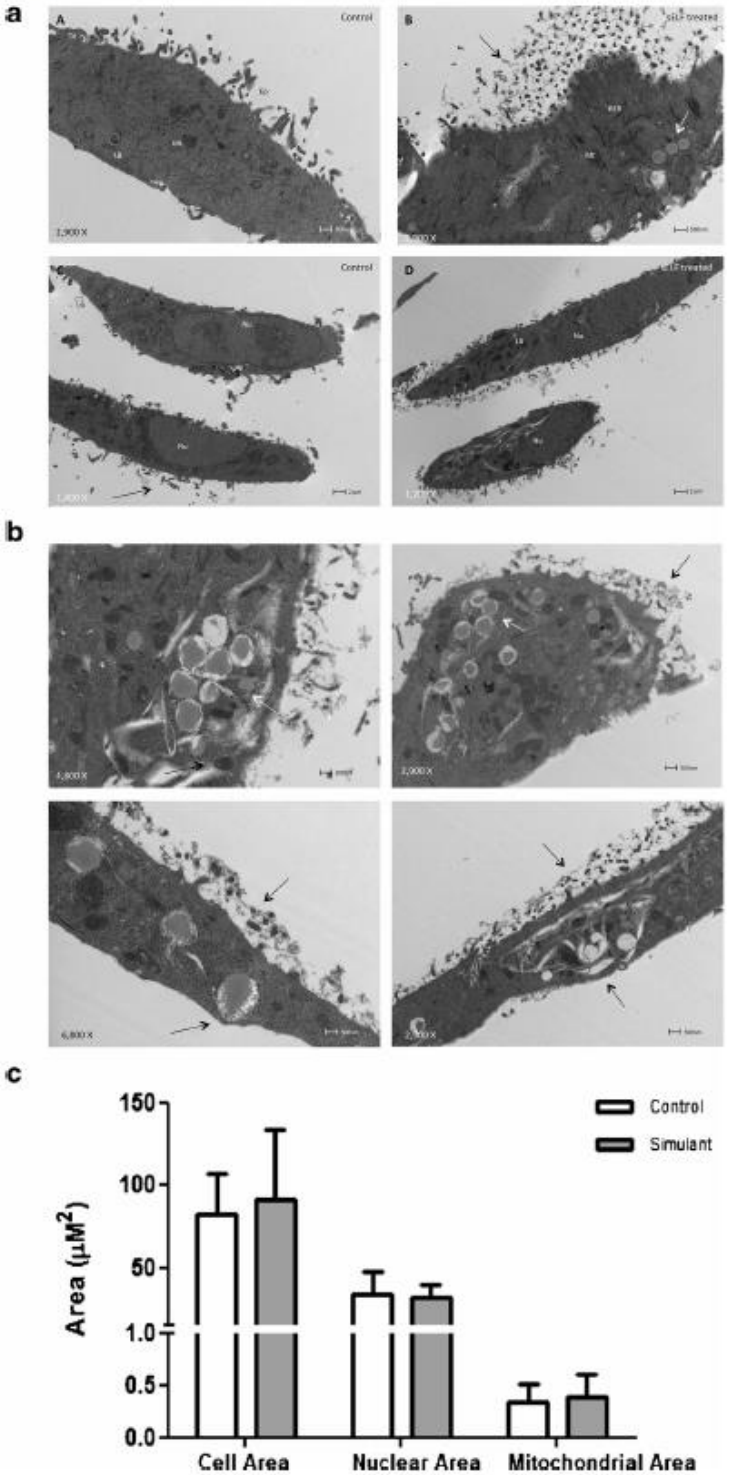

Fig. 2 Morphological characterisation of A549 cells cultured in cell culture medium and SLF for 24 h. (**a**) Cell morphology. A549 control cells incubated with cell culture medium (left) compared to A549 cell incubated with SLF (right). Scale bar: 2 μm. (**b**) Cellular uptake. SLF interaction with A549 cells indicated with arrows. Scale bar: 500 nm (**c**) Cell dimensions. Culture medium compared to SLF showing no differences. Data represent mean ± sd, $n = 6$ images.

Table II The Top (Strongest Signal) Pathways in Rank Order with their *p*-values: *p*-values in Bold Represent Significance

Pathway name	Pathway id	*p*-value	*p*-value (FDR)	*p*-value (Bonferroni)
Steroid biosynthesis	00100	**2.599e-10**	**3.015e-8**	**3.015e-8**
DNA replication	03030	**1.493e-6**	**8.658e-5**	**1.732e-4**
Terpenoid backbone biosynthesis	00900	**5.547e-5**	**0.002**	**0.006**
Metabolic pathways	01100	**2.810e-4**	**0.008**	**0.033**
Tryptophan metabolism	00380	**0.002**	**0.038**	0.191
Cell cycle	04110	**0.002**	**0.040**	0.240

many activators of the NfkB pathway are oxidants, the observed up-regulation in the oxidative-reductive process in this study might indicate that incubation with SLF has immunomodulatory roles [34]. This would be consistent with previous findings demonstrating that DPPC can exert anti-inflammatory effects through the inhibition of the NFkB-pathway [35]. Reduced DNA replication was also identified robustly by pathway and GO analysis, i.e. negative regulation of transcription from RNA polymerase II promotor. This may be explained by the effect of change of culture environment which stalls cell replication *in vitro*.

Taken together, the MTT, morphometry transcriptomic analyses demonstrate that SLF is biocompatible with A549 cells, though clearly further work will be required to establish how robust this finding is across cell lines and in primary cell models.

Solubility and Dissolution of FP and BDP in SLF

FP and BDP are poorly water soluble drugs, reported to have concentrations of approximately 0.1–0.2 μg/mL in water [9,36,37]. In Gamble's solution, FP and BDP solubility was 0.7 and 1.0 μg/mL, respectively (Fig. 4). In surfactant-containing media, the solubility of FP increased in the rank order: SLF (2.0 μg/mL) < 0.5% SDS (13.1 μg/mL) < Survanta (20.3 μg/mL). The BDP rank order of solubility in the different media was changed, but BDP solubility was higher than that of FP in each medium: SLF (16.8 μg/mL), < Survanta (37.2 μg/mL) and <0.5% SDS (64.4 μg/mL). Lung surfactants enhance the solubility of small, lipophilic drug molecules, such as corticosteroids and cationic compounds because they form structures with lipid domains [38,39]. Unexpectedly, FP solubility in SLF was much closer to that in Gamble's solution than Survanta. Solubilisation may be determined not only by lipid content but also the interaction of components, including the drug, which affect liposomal structures. For example, cholesterol may form tight nanodomain complexes with DPPC stabilising the lamellar structures formed [40], whereas albumin may solubilise the cholesterol [41] and reduce the stability of the lamellar phase and the extent to which drug is solubilised in such structures. A recent review by Das *et al.* speculates how lung surfactant may form different liquid crystalline phases with potential roles in defining dissolution mechanism and rate [42].

The dissolution of FP and BDP aerosols from licenced inhaler products correlated with drug solubility in the dissolution medium. BDP dissolved more readily

Table III Top Gene Outology (GO) Terms and their *p*-values: *p* values in Bold Represent Significance

No pruning				Elim pruning		Weight pruning	
GO Term	*p*-value	*p*-value (FDR)	*p*-value (Bonferroni)	GO Term	*p*-value	GO Term	*p*-value
Sterol biosynthesis process	**2.000e-14**	**5.018e-11**	**5.018e-11**	Cholesterol biosynthesis process	**1.900e-9**	Sterol biosynthesis process	**2.000e-14**
Cholesterol biosynthesis process	**2.300e-13**	**1.924e-10**	**5.771e-10**	Negative regulation of transcription from RNA polymerase II promoter	**0.008**	Cell cycle phase transition	**6.100e-5**
Secondary biosynthesis process	**2.300e-13**	**1.924e-10**	**5.771e-10**	Oxidation-reduction process	**0.013**	Oxidation-reduction process	**0.003**
Steroid biosynthesis process	**1.400e-12**	**8.782e-10**	**3.513e-9**	Sterol biosynthesis process	**0.039**	Negative regulation of transcription from RNA polymerase II promoter	**0.008**
Sterol metabolic process	**1.300e-10**	**6.523e-8**	**3.262e-7**	Steroid biosynthesis process	**0.044**		

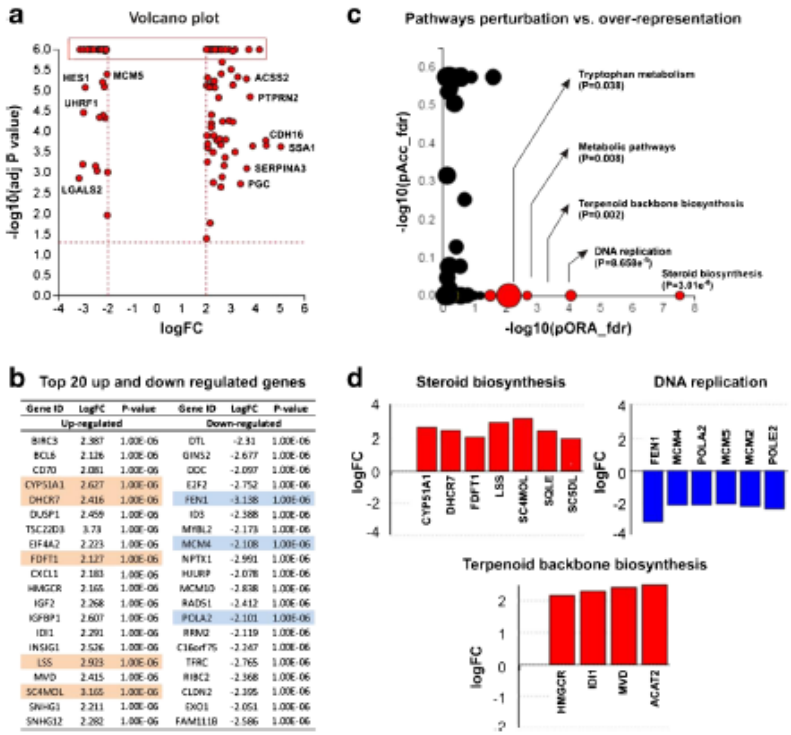

Gene ID	LogFC	P-value	Gene ID	LogFC	P-value
Up-regulated			Down-regulated		
BIRC3	2.387	1.00E-06	DTL	-2.31	1.00E-06
BCL6	2.126	1.00E-06	GINS2	-2.677	1.00E-06
CD70	2.081	1.00E-06	DDC	-2.097	1.00E-06
CYP51A1	2.627	1.00E-06	E2F2	-2.752	1.00E-06
DHCR7	2.416	1.00E-06	FEN1	-3.138	1.00E-06
DUSP1	2.459	1.00E-06	ID3	-2.388	1.00E-06
TSC22D3	3.73	1.00E-06	MYBL2	-2.173	1.00E-06
EIF4A2	2.223	1.00E-06	MCM4	-2.108	1.00E-06
FDFT1	2.127	1.00E-06	NPTX1	-2.991	1.00E-06
CXCL1	2.183	1.00E-06	HURP	-2.078	1.00E-06
HMGCR	2.165	1.00E-06	MCM10	-2.838	1.00E-06
IGF2	2.268	1.00E-06	RAD51	-2.412	1.00E-06
IGFBP1	2.607	1.00E-06	POLA2	-2.101	1.00E-06
IDI1	2.291	1.00E-06	RRM2	-2.119	1.00E-06
INSIG1	2.526	1.00E-06	C16orf75	-2.247	1.00E-06
LSS	2.923	1.00E-06	TFRC	-2.765	1.00E-06
MVD	2.415	1.00E-06	RIBC2	-2.368	1.00E-06
SC4MOL	3.165	1.00E-06	CLDN2	-2.195	1.00E-06
SNHG1	2.211	1.00E-06	DIO1	-2.051	1.00E-06
SNHG12	2.282	1.00E-06	FAM111B	-2.586	1.00E-06

Fig. 3 Whole human genome microarray analysis of A549 cells incubated for 24 h with simulated lung fluid (SLF) or standard tissue culture media. Panel (**a**) - Volcano plot: All 116 significantly differentially expressed (DE) genes are displayed according to their measured expression change (x-axis) and negative log (base 10) of the *p*-value (y-axis). The higher the gene is plotted on the y-axis, the more significant it is. The dotted line shows the thresholds for expression change; $p < 0.05$. The top 20 up and down regulated genes, reflecting the highlighted section in panel A are provided in panel (**b**). Panel (**c**) - Pathways perturbation vs over-representation: The most disrupted pathways are plotted in terms of the two types of evidence: over-representation on the x-axis (pORA) and the total perturbation accumulation on the y-axis (pAcc). Red spots indicate significantly perturbed pathways, with the size of the spot reflecting the number of DE genes within the identified pathways. Panel (**d**) illustrates the DE genes within the three most significant pathways identified as perturbed following incubation with the SLF.

than FP and for both drugs the dissolution rate in SLF was greater than in Gamble's solution, but lower than the rate in 0.5% SDS. An estimate for the solubility of FP in the lungs using mechanistic modelling [43] appears to support the value obtained with SLF, supporting the hypothesis that the salt solution is likely to underestimate the dissolution of hydrophobic drugs, while 0.5% SDS may overestimate solubility and hence dissolution in the lungs. FP and BDP were selected to represent inhaled drugs that have poor aqueous solubility and may be dissolution limited, accounting for their relatively slow dissolution profiles which appear to contrast with the rapid onset of action that can be observed for some inhaled molecules, e.g. many bronchodilators. However, it is important to appreciate that oral inhaled product dissolution methods are at an early stage of development and are not optimised for *in vitro-in vivo* correlation. Furthermore, PK-PD relationships to link the potency of inhaled drugs, physicochemical properties, drug formulation, dose interval, temporal profiles of free (unbound) drug concentration at the effect site and pharmacological response are at a nascent stage of development (43, 44).

Using more physiological conditions for *in vitro* investigations into inhalation biopharmaceutics may improve the accuracy of physiologically-based mechanistic modeling and in the future biorelevence may be extended to reflect any differences in RTLF in lung disease and the influence of less abundant components that are recognized to have functional significance, e.g. surfactant proteins that are concentrated in the corona that forms on the surface of biopersistent nanoparticles and influences their uptake [45,46].

CONCLUSIONS

We report a synthetic simulated lung fluid based on human RTLF that can be used for the *in vitro* studies

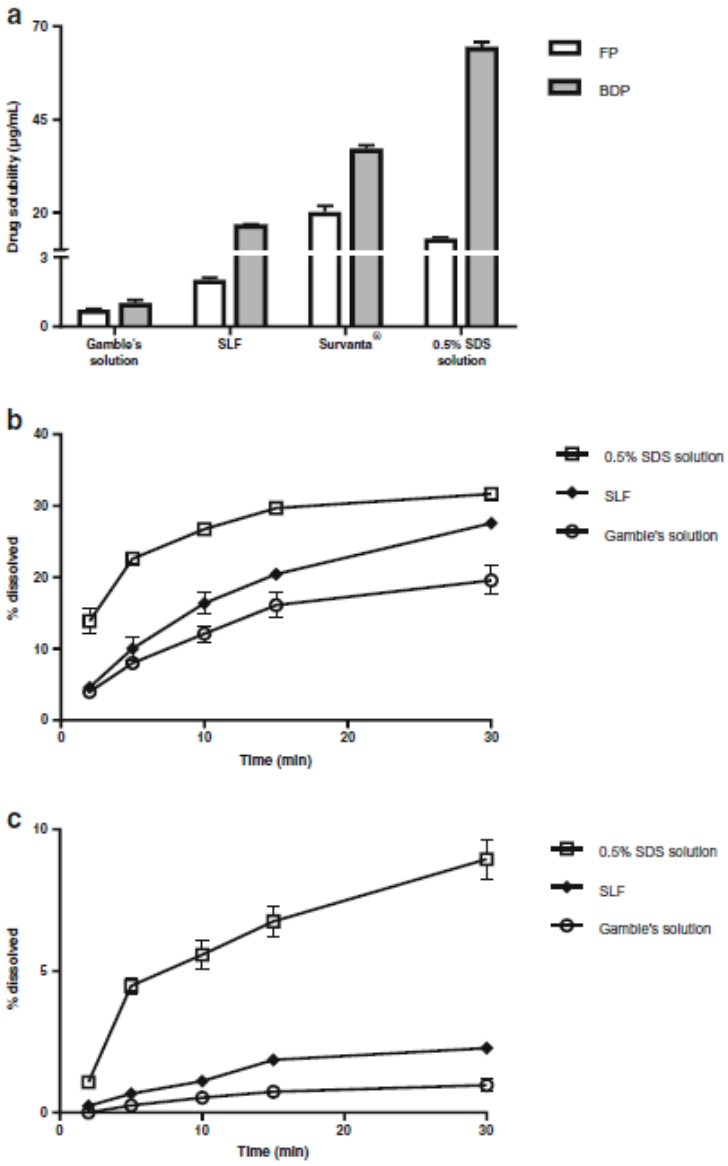

Fig. 4 (**a**) Solubility Beclomethasone dipropionate (BDP) and fluticasone propionate (FP) solubility in media used to represent lung fluid: Gamble's solution, the biorelevant simulated lung fluid, SLF, Survanta® and 0.5% SDS. (**b**) Dissolution of BDP Aerosol from QVAR® 50 µg pressurised metered dose inhalers, (**c**) Dissolution of FP Aerosol from Flixotide® 50 µg pressurised metered dose inhalers. Data represent mean ± sd, $n = 3$.

into inhalation biopharmaceutics, e.g. the solubility of inhaled drugs, dissolution of aerosol particles and particle-lung cell interactions. The SLF has a stable colloidal structure, possessing vesicles that are similar in nature to those found in lung extracts. No adverse effects on A549 cells were observed after exposure to the simulant for 24 h, although some metabolic changes were indicated that are consistent with the change of culture medium to a more physiologic composition. Based on preliminary results, we hypothesize that the use of biorelevant medium provides realistic estimates of the solubility and dissolution of hydrophobic drugs *in vivo*. Whilst the present SLF was based on the composition of RTLF from the alveolar region of healthy subjects, we acknowledge that further work is still required to develop simulants reflective of different regions of the airway, as well as variation in composition associated with established respiratory disease.

ACKNOWLEDGEMENTS AND DISCLOSURES

This research received support from the QualityNano project http://www.qualitynano.eu which is financed by the European Community Research Infrastructures under the FP7 Capacities Programme (Grant No. INFRA-2010-262,163), and its partners VITO (for transcriptomics) and Uppsala University (for CryoTEM). Elif Melis Bicer was supported by a BBSRC-CASE studentship (BB/1532696/1) in association with GlaxoSmithKline Research & Development. Mireille Hassoun was supported by a BBSRC-CASE studentship (BB/K012762/1), in association with Intertek-Melbourn.

REFERENCES

1. Bäckman P, Adelmann H, Petersson G, Jones CB. Advances in inhaled Technologies: understanding the therapeutic challenge, predicting clinical performance, and designing the optimal inhaled product. Clin Pharmacol Ther. 2014;95:509–20.
2. Borghardt JM, Weber B, Staab A, Kloft C. Pharmacometric models for characterizing the pharmacokinetics of orally inhaled drugs. AAPS J. 2015;17:853–70.
3. Edsbacker S, Wollmer P, Selroos O, Borgstrom L, Olsson B, Ingelf J. Do airway clearance mechanisms influence the local and systemic effects of inhaled corticosteroids? Pulm Pharmacol Ther. 2008;21:247–58.
4. Patton JS, Brain JD, Davies LA, Fiegel J, Gumbleton M, Kim K-J, *et al.* The particle has landed–characterizing the fate of inhaled pharmaceuticals. J. Aerosol Med. Pulm. Drug Deliv. 2010;23(Suppl 2):S71–87.
5. Foster WM, Langenback E, Bergofsky EH. Measurement of tracheal and bronchial mucus velocities in man : relation to lung clearance. J Appl Physiol. 1980;48:965–71.
6. Stöber WKW. A simple pulmonary retention model accounting for dissolution and macrophage-mediated removal of deposited polydisperse particles. Inhal. Toxicol. 2001;13:129–48.
7. Jones RM, Neef N. Interpretation and prediction of inhaled drug particle accumulation in the lung and its associated toxicity. Xenobiotica. 2012;42:86–93.
8. Forbes B, O'Lone R, Allen PP, Cahn A, Clarke C, Collinge M, *et al.* Challenges for inhaled drug discovery and development: Induced alveolar macrophage responses. Adv. Drug Deliv. Rev. Elsevier B.V. 2014;71:15–33.
9. Hastedt JE, Bäckman P, Clark AR, Doub W, Hickey A, Hochhaus G, *et al.* Scope and relevance of a pulmonary biopharmaceutical classification system AAPS/FDA/USP workshop march 16-17th, 2015 in Baltimore, MD AAPS Open AAPS Open. 2016;2:1–20.
10. Lennernäs H, Aarons L, Augustijns P, Beato S, Bolger M, Box K, *et al.* Oral biopharmaceutics tools - time for a new initiative - an introduction to the IMI project OrBiTo. Eur J Pharm Sci. 2014;57:292–9.
11. Augustijns P, Wuyts B, Hens B, Annaert P, Butler J, Brouwers J, *et al.* Eur. J. Pharm. Sci. Elsevier B.V. 2014;57:322–32.
12. Riethorst D, Baatsen P, Remijn C, Mitra A, Tack J, Brouwers J, *et al.* An in-depth view into human intestinal fluid colloids: intersubject variability in relation to composition. Mol. Pharm. 2016;13:3484–93.
13. Wuyts B, Riethorst D, Brouwers J, Tack J, Annaert P, Augustijns P. Evaluation of fasted and fed state simulated and human intestinal fluids as solvent system in the Ussing chambers model to explore food effects on intestinal permeability. Int. J. Pharm. Elsevier B.V. 2015;478:736–44.
14. Marques MRC, Loebenberg R, Almukainzi M. Simulated biological fluids with possible application in dissolution testing. Dissolution Technol. 2011;18:15–28.
15. Patel N, Forbes B, Eskola S, Murray J. Use of simulated intestinal fluids with Caco-2 cells and rat ileum. Drug Dev Ind Pharm. 2006;32:151–61.
16. Klein S. The use of biorelevant dissolution media to forecast the in vivo performance of a drug. AAPS J. 2010;12:397–406.
17. Arora D, Shah KA, Halquist MS, Sakagami M. In vitro aqueous fluid-capacity-limited dissolution testing of respirable aerosol drug particles generated from inhaler products. Pharm Res. 2010;27:786–95.
18. Davies NM, Feddah MR. A novel method for assessing dissolution of aerosol inhaler products. Int J Pharm. 2003;255:175–87.
19. Son YJ, McConville JT. Development of a standardized dissolution test method for inhaled pharmaceutical formulations. Int J Pharm. 2009;382:15–22.
20. May S, Jensen B, Weiler C, Wolkenhauer M, Schneider M, Lehr CM. Dissolution testing of powders for inhalation: influence of particle deposition and modeling of dissolution profiles. Pharm Res. 2014;31:3211–24.
21. Buttini F, Miozzi M, Balducci AG, Royall PG, Brambilla G, Colombo P, *et al.* Differences in physical chemistry and dissolution rate of solid particle aerosols from solution pressurised inhalers. Int. J. Pharm. Elsevier B.V. 2014;465:42–51.
22. Rohrschneider M, Bhagwat S, Krampe R, Michler V, Breitkreutz J, Hochhaus G. Evaluation of the Transwell system for characterization of dissolution behavior of inhalation drugs: effects of membrane and surfactant. Mol Pharm. 2015;12:2618–24.
23. Pham S, Wiedmann TS. Dissolution of aerosol particles of budesonide in Survanta, a model lung surfactant. J Pharm Sci. 2001;90:98–104.
24. Bicer EM. Compositional characterisation of human respiratory tract lining fluids for the design of disease specific simulants. King's College London 2015.
25. Kumar A, Bicer EM, Morgan AB, Pfeffer PE, Monopoli M, Dawson KA, *et al.* Enrichment of immunoregulatory proteins in the biomolecular corona of nanoparticles within human respiratory tract lining fluid. Nanomed Nanotechnol Biol. Med. Elsevier B.V. 2016;12:1033–43.
26. Scarpelli EM, Gabbay KH, Kochen JA. Lung surfactants, Counterions, and hysteresis. Science. 1965;148:1607–9.
27. Vollhardt D, Fainerman VB. Progress in characterization of Langmuir monolayers by consideration of compressibility. Adv Colloid Interf Sci. 2006;127:83–97.
28. Choi Y, Attwood SJ, Hoopes MI, Drolle E, Karttunen M, Leonenko Z. Melatonin directly interacts with cholesterol and alleviates cholesterol effects in dipalmitoylphosphatidylcholine monolayers. Soft Matter. 2014;10:206–13.
29. Dynarowicz-Latka P, Hac-Wydro K. Interactions between phosphatidylcholines and cholesterol in monolayers at the air/water interface. Colloids Surfaces B Biointerfaces. 2004;37:21–5.

30. Grainger CI, Saunders M, Buttini F, Telford R, Merolla LI, Martin GP, *et al.* Critical characteristics for corticosteroid solution metered dose inhaler bioequivalence. Mol Pharm. 2012;9:563–9.
31. Filipe V, Hawe A, Jiskoot W. Critical evaluation of nanoparticle tracking analysis (NTA) by NanoSight for the measurement of nanoparticles and protein aggregates. Pharm Res. 2010;27:796–810.
32. Lee KYC, Gopal A, von Nahmen A, Zasadzinski JA, Majewski J, Smith GS, *et al.* Influence of palmitic acid and hexadecanol on the phase transition temperature and molecular packing of dipalmitoylphosphatidyl-choline monolayers at the air–water interface. J Chem Phys. 2002;116:774.
33. Pérez-Gil J, Keough KMW. Interfacial properties of surfactant proteins. Biochim. Biophys. Acta - Mol. Basis Dis. 1998;1408:203–17.
34. Antal JM, Divis LT, Erzurum SC, Wiedemann HP, Thomassen MJ. Surfactant suppresses NF-KB activation in human Monocytic cells. Am J Respir Cell Mol Biol. 1996;14:374–9.
35. Morris RHK, Tonks AJ, Jones KP, Ahluwalia MK, Thomas AW, Tonks A, *et al.* DPPC regulates COX-2 expression in monocytes via phosphorylation of CREB. Biochem Biophys Res Commun. 2008;370:174–8.
36. Tokumura T, Miyazaki E, Isaka H, Kaneko N, Kanou M. Solubility of fluticasone propionate in aqueous solutions measured by a method avoiding its adsorption to experimental tools. Int Res J Pharm Appl Sci. 2014;4:19–24.
37. Sahib MN, Abdalwahed S, Abdulameer DY, Peh KK, YTF T. Solubilization of beclomethasone dipropionate in sterically stabilized phospholipid nanomicelles (SSMs): Physicochemical and in vitro evaluations. Drug Des. Devel. Ther. 2012;6:29–42.
38. Wiedmann TS, Bhatia R, Wattenberg LW. Drug solubilization in lung surfactant. J Control Release. 2000;65:43–7.
39. Liao X, Wiedmann TS. Solubilization of cationic drugs in lung surfactant. Pharm Res. 2003;20:1858–63.
40. Kim K, Choi SQ, Zell ZA, Squires TM, Zasadzinski JA. Effect of cholesterol nanodomains on monolayer morphology and dynamics. Proc Natl Acad Sci U S A. 2013;110:E3054–60.
41. Kim SH. Adsorption and interactions of lung surfactant lipids and proteins at air/aqueous interfaces and in aqueous solution. Purdue University; 2007.
42. Das SC, Stewart PJ. The influence of lung surfactant liquid crystalline nanostructures on respiratory drug delivery. Int J Pharm. 2016;514:465–74.
43. Boger E, Evans N, Chappell M, Lundqvist A, Ewing P, Wigenborg A, *et al.* Systems pharmacology approach for prediction of pulmonary and systemic pharmacokinetics and receptor occupancy of inhaled drugs. CPT Pharmacometrics Syst Pharmacol. 2016;5:201–10.
44. Cooper AE, Ferguson D, Grime K. Optimisation of DMPK by the inhaled route: challenges and approaches. Curr Drug Metab. 2012;13:457–73.
45. Shaw CA, Mortimer GM, Deng ZJ, Carter ES, Connell SP, Miller MR, Duffin R, Newby DE, Hadoke PWF, Minchin RF. Protein corona formation in bronchoalveolar fluidenhances diesel exhaust nanoparticle uptake and pro-inflammatory responses in macrophages. Nanotoxicology. 2016;10:981–91.
46. Wohlleben W, Driessen MD, Raesch S, Schaefer UF, Schulze C, von Vacano B, Vennemann A, Wiemann M, Ruge CA, Platsch H, Mues S, Ossig R, Tomm JM, Schnekenburger J, Kuhlbusch TAJ, Luch A, Lehr C-M, Haase A. Influence of agglomeration and specific lung lining lipid/protein interaction on short-term inhalation toxicity. Nanotoxicology. 2016;10:970–80.

Articles in Progress:

(1) **Hassoun M**, Akhuemokhan P, Parry M, Forbes B. Formulation and evaluation of a fluticasone propionate microemulsion for nebulised inhaled delivery. Intended Journal: International Journal of Pharmaceutics (2019)

Other published articles:

(1) **Hassoun M**, Ho S, Muddle J, Buttini F, Parry M, Hammond M, Forbes B. Formulating powder–device combinations for salmeterol xinafoate dry powder inhalers. International Journal of Pharmaceutics 490: 360–367 (2015)

(2) Jawad R, Drake A.F, Elleman C, Martin G.P, Warren F.J, Perston B.B, Ellis P.R, **Hassoun M**, Royall P.G. The stability of sugar solutions: A novel study of the epimerisation kinetics of lactose in water. Molecular Pharmaceutics 11(7): 2224-2238 (2014)

APPENDIX F

Conference poster abstracts

(1) **Hassoun M**, Royall P.G., Harvey R.D., Parry M, Forbes B. Development of a synthetic human lung fluid simulant for applications in inhalation biopharmaceutics. Drug Delivery to the Lungs 28: 424-427 (2017)

(2) **Hassoun M**, Copley M, Royall P.G., Parry M, Forbes B. Comparison of TSI/Transwell and NGI/Rotating paddle as dissolution methods for orally inhaled products. Drug Delivery to the Lungs 28: 347-350 (2017)

(3) **Hassoun M**, Malmof M, Kumar A, Bansal S, Nowenwik M, Gerde P, Forbes B. Effect of using bio-relevant media in the DissolveIT system to measure dissolution of fluticasone propionate from Flixotide 50 µg Evohaler. Drug Delivery to the Lungs 27: 328-332 (2016)

(4) Terakosolphan W, **Hassoun M**, Kumar A, Forbes B. Solubility of fluticasone propionate and beclomethasone dipropionate in simulated lung lining fluids. Drug Delivery to the Lungs 27: 333-336 (2016)

(5) Akhuemokhan P, Parry M, **Hassoun M**, Hammond M, Forbes B. Formulation and evaluation of fluticasone propionate microemulsions for nebuliser devices. Drug Delivery to the Lungs 26: 287-291 (2015)